UNIVERSITÉ FRANÇOIS – RABELAIS DE TOURS

ÉCOLE DOCTORALE SSBCV

UMR Inserm 1069, Nutrition, Croissance et Cancer

THÈSE présentée par :

Emeline BON

Soutenue le : **07 décembre 2015**

pour obtenir le grade de : **Docteur de l'université François – Rabelais de Tours**

Discipline/ Spécialité : Sciences de la vie

Implication de la sous-unité β4 des canaux sodiques dépendants du voltage dans l'invasivité des cellules cancéreuses mammaires et régulation de son expression par l'acide docosahexaènoïque

THÈSE dirigée par :

M. CHEVALIER Stéphan	Professeur des Universités, Université François-Rabelais de Tours
M. ROGER Sébastien	Maître de Conférences, HDR, Université François-Rabelais de Tours

RAPPORTEURS :

M. CHAVRIER Philippe	Directeur de Recherche CNRS, Institut Curie, Paris
M. SORIANI Olivier	Maître de Conférences, HDR, Université de Nice Sophia-Antipolis

---

JURY :

M. CHAVRIER Philippe	Directeur de Recherche CNRS, Institut Curie, Paris
M. CHEVALIER Stéphan	Professeur des Universités, Université François-Rabelais de Tours
Mme NEYROUD Nathalie	Chargée de Recherche Inserm, Université Pierre et Marie Curie, Paris
M. ROGER Sébastien	Maître de Conférences, HDR, Université François-Rabelais de Tours
M. SORIANI Olivier	Maître de Conférences, HDR, Université de Nice Sophia-Antipolis
M. VAN COPPENOLLE Fabien	Professeur des Universités, Université Claude Bernard Lyon1

MEMBRE INVITE :

M. BRACKENBURY William	Lecturer, Université de York, Grande Bretagne

UNIVERSITÉ FRANÇOIS – RABELAIS DE TOURS

ÉCOLE DOCTORALE SSBCV

UMR Inserm 1069, Nutrition, Growth and Cancer

THESIS presented by :

Emeline BON

Defended on: **December 7th, 2015**

To obtain the rank of : **Docteur de l'université François – Rabelais de Tours**

Discipline/ Profession : Health Science

Involvement of voltage-gated sodium channel β4 subunit in breast cancer cell invasiveness and regulation by docosahexaenoic acid

THÈSIS supervised by :

M. CHEVALIER Stéphan	Full Professor, University François-Rabelais of Tours
M. ROGER Sébastien	Lecturer, HDR, University François-Rabelais of Tours

REVIEWERS :

M. CHAVRIER Philippe	Research Director CNRS, Curie Institute, Paris
M. SORIANI Olivier	Lecturer, HDR, University of Nice Sophia-Antipolis

---

JURY :

M. CHAVRIER Philippe	Research Director CNRS, Curie Institute, Paris
M. CHEVALIER Stéphan	Full Professor, University François-Rabelais of Tours
Mme NEYROUD Nathalie	Research Fellow Inserm, University Pierre and Marie Curie, Paris
M. ROGER Sébastien	Lecturer, HDR, University François-Rabelais of Tours
M. SORIANI Olivier	Lecturer, HDR, University of Nice Sophia-Antipolis
M. VAN COPPENOLLE Fabien	Full Professor, University Claude Bernard Lyon1

GUEST MEMBER:

M. BRACKENBURY William	Lecturer, York University, Great Britain

Remerciements

En premier lieu, j'adresse mes remerciements au Dr Nathalie Neyroud, au Dr Olivier Soriani, au Dr Philippe Chavrier, au Pr Fabien Van Coppenolle, et au Dr William Brackenbury d'avoir accepté de participer à mon jury de thèse, de me faire l'honneur de juger ce travail.

Je remercie le Pr Philippe Bougnoux et le Pr Stéphan Chevalier, directeurs successifs du laboratoire, qui m'ont accueillie au sein de l'unité de recherche « Nutrition, Croissance et Cancer ».

Je souhaite remercier mes directeurs de thèse : le Pr Stéphan Chevalier et le Dr Sébastien Roger, qui m'ont permis de réaliser cette thèse. Merci pour vos conseils, votre soutien et le temps qe vous m'avez accordé tout au long de ces trois années de travail. Stéphan, te voici libéré et délivré de ton étudiante, prêt à recommencer avec une nouvelle recrue ? Puisque nous en parlions ce midi du 04 novembre 2015, :-P. Seb, chef colocataire de bureau, merci de m'avoir fait connaître les canaux ioniques, même si je ne suis toujours pas contaminée par ta passion pour l'électrophy. Je te remercie aussi de m'avoir encouragée, notamment à coup de barres chocolatées ! Merci à tous les deux de m'avoir accordé votre confiance et d'avoir partagé vos connaissances pour que je puisse en arriver là.

Je remercie Gunther pour l'analyse MatInsperctor du promoteur *SCN4B* sauvage et muté.

Je remercie Maria-Luisa Cayuela, qui m'a accueillie dans son laboratoire et m'a permis d'apprendre la manipulation des embryons de poisson zèbre. Je remercie plus particulièrement Manolo et Monique, qui étaient à la paillasse avec moi.

Je remercie Julien Burlaud-Gaillard pour sa disponibilité et son expertise en microscopie, grâce à qui nous avons notamment réalisée les images de MEB.

Merci à Dylan Manceau et Alexandre Launay, stagiaires de dernière minute qui ont fortement avancé les perspectives de l'étude DHA.

Vient désormais l'espace réservé aux remerciements moins formels mais tout aussi importants.

Tout d'abord, merci à tous les membres du N2C qui ont participé, de près ou de loin, à la réalisation de cette thèse et au bon déroulement de ces trois années. Ces remerciements ne sont pas complets et ne le seront jamais assez, mais vous m'en excuserez, vous savez bien que déblatérer (…) n'est pas mon point fort.

Merci,
à Catherine et Isa pour votre aide et vos bons petits plats ; Pierre, pour l'aide que tu m'as apportée et les nombreuses discussions ; à Jean-François, qui ne dit rien mais n'en pense pas moins ; à Aurélie pour tes conseils clonage ; à Marie pour ta bonne humeur et ton soutien dans mon « admiration » pour Gojira ; à Christophe, notamment pour la minute philosophique « la méthode scientifique en philosophie » ; à Roseline pour ton aide précieuse et ton franc-parler plein de réconfort ; à Romain, toujours prêt à aider ; à Gunther pour tes conseils et tes gâteaux à l'Allemande.

Je remercie les « thésards d'avant », à savoir Fabio, Lucie -la petite, Ludo, Alban et Joan rencontrés au cours de mon stage de licence pro, qui m'ont donné l'envie de poursuivre jusqu'en thèse. Merci à Virginie, qui a initié et bien engagé les travaux sur β4, merci à Ramez, pour tes travaux sur les PPARs, et aussi de m'avoir grandement aidée pendant mon stage de M1.

Merci à mes co-thésards de l'année d'avant et de l'année d'après, toujours présents, dans les bons et les mauvais moments. Merci à Audrey, complice de nombreux fou-rires inexpliqués et inexplicables, avec qui j'ai bétonné mes abdos. Tu vois, on l'aura fait ! Merci à Péepou, plus connue sous le nom de Laure, la boite à parole du Sud-Ouest, pour les nombreux moments passés ensemble, à se fendre la poire et à se péter la panse en buvant du bon vin, et qui s'est fait une joie de m'expliquer les règles du dada et commenter les match de rugby. Maxime, bien que m'avoir fait découvrir un nouvel univers grammatical, je te remercie, malgré. Merci à JD ou Julie, d'avoir stoïquement assisté à mes variations d'état et pour tes petites attentions réconfortantes. Fred, on avait dit que je te remercierai par apposition d'une virgule, mais je te dis encore une fois merci pour l'aide que tu m'as apportée et les multiples parties de rigolade. Luluchocho, merci pour les bons moments passés ensemble.

Merci à Karine, Caro, Stéphane, Philippe F, Bruno, Ana, Cyril, Elsa, Michelle, Jorge, Yann, ainsi que ceux que j'aurai malencontreusement oubliés de citer, et les nouvelles que je n'ai pas eu le temps de connaître davantage : Sandy, Céline et Adeline. Bon courage pour vos thèses !

Au sortir du labo, la vie continue, c'est pourquoi je tiens à remercier les « non-N2Céens » qui m'ont soutenue jusque-là.

Merci à mon « garagiste en or », qui a suivi tant bien que mal mes discours et les rebondissements relatifs aux « pipares et beta quat' », et qui a vaillamment supporté mes humeurs instables et fragiles.
Merci à Julien, mon prof de batterie, à qui j'ai déchaussé les dents plus d'une fois en tapant sans retenue sur la batterie (« t'as vu le morceau !?! »), de m'avoir permis de m'évader chaque semaine dans son univers musical. Merci également à Julien « de la microscopie », pour nos nombreuses discussions musicales et instrumentales.
Merci à mes ami(e)s, Marion Copine, présente depuis le BTS (9 ans déjà ! ça vieillit tout ça!!), Cécilia, d'encore plus longue date, Joubi ou Hélène, et Mani. Merci d'avoir été là.

Enfin je tiens à remercier de tout mon cœur ma famille, à savoir Maman, Sœurette et Roland, qui ont toujours cru en moi et m'ont toujours dit que j'y arriverai. A ce jour, c'est presque chose faite ! Papa, merci.

Résumé

Le développement des métastases et l'apparition de résistances aux chimiothérapies sont à l'origine de la majorité des décès dans le cancer du sein. Or, il n'existe à ce jour aucun traitement ciblant spécifiquement les métastases ou leur développement. Leur apparition dans un tissu distant de la tumeur primaire repose en partie sur l'acquisition par les cellules cancéreuses de la capacité à envahir les matrices extracellulaires. L'efficacité de la chimiothérapie chez des patientes ayant un cancer du sein métastasé (étude de Phase II) peut être améliorée par une supplémentation en acide docosahexaènoïque (DHA, 22:6n-3), un acide gras polyinsaturés de la série n-3, connu pour diminuer l'invasivité des cellules cancéreuses mammaires *in vitro* et *in vivo* sans que les modes d'action soient bien identifiés.

Les canaux sodiques dépendants du voltage (Na_V) sont des complexes protéiques transmembranaires composés d'une sous-unité principale $Na_V\alpha$ formant le pore du canal, associée à une ou plusieurs sous-unités β (β1, β2, β3 ou β4) dites « auxiliaires ». Les sous-unités β ont initialement été décrites dans les cellules excitables comme régulatrices des propriétés électrophysiologiques des sous-unités $Na_V\alpha$. La sous-unité α $Na_V1.5$ est anormalement exprimée dans les cellules cancéreuses mammaires. Elle favorise l'invasivité mésenchymateuse en augmentant la dégradation de la matrice extracellulaire. L'expression et l'activité de $Na_V1.5$ sont inhibées par le DHA.

L'implication des sous-unités auxiliaires β dans l'invasivité cancéreuse et le développement des métastases est mal connue. Une étude préliminaire du laboratoire a montré que la diminution de l'expression de la sous-unité β4 (gène *SCN4B)* augmente l'invasivité de lignées cancéreuses. Les objectifs de cette thèse ont été *i*) de caractériser l'expression de β4 dans les tumeurs mammaires de différents grades et dans les tissus non tumoraux *ii*) d'identifier les mécanismes par lesquels β4 régule l'invasivité des cellules cancéreuses et *iii*) d'étudier les effets du DHA sur l'expression de β4 et l'invasivité dépendante de β4.

Notre étude immunohistochimique réalisée sur des biopsies mammaires humaines montre que la protéine β4 est fortement exprimée dans les tissus mammaires non pathologiques. Son expression est diminuée dans les tissus cancéreux, particulièrement dans les tumeurs de grade élevé ainsi que dans les métastases. Dans un modèle *in vivo* d'invasivité sur embryons de poisson zèbre, l'extinction de l'expression de β4 dans les cellules cancéreuses mammaires MDA-MB-231 augmente l'invasion des tissus par ces cellules de près de 40%. L'invasion des

tissus diminue d'environ 50% si les cellules cancéreuses contrôles sont prétraitées avec le DHA, qui stimule l'expression de β4.

L'extinction de l'expression de β4 dans les cellules cancéreuses mammaires MDA-MB-231 augmente d'environ 150% leur invasivité à travers une matrice extracellulaire, tandis que la surexpression de β4 diminue l'invasivité de 50%. L'augmentation de l'invasivité induite par la sous-expression de β4 semble indépendante de celle modulée par l'activité des canaux sodiques $Na_V1.5$ car elle est également observée dans des lignées qui n'expriment pas de sous-unité $Na_V\alpha$. D'ailleurs, l'invasion associée à la diminution de l'expression de β4 n'est pas due à une augmentation de la dégradation de la matrice extracellulaire, comme c'est le cas pour l'invasion dépendante de $Na_V1.5$, mais à une augmentation de la migration. Enfin, la perte de l'expression de β4 est associée à un changement de phénotype caractérisé par l'acquisition d'une morphologie de type amoeboïde par les cellules cancéreuses mammaires, ainsi que d'une augmentation de l'activité de la RhoA GTPase, caractéristique de ce phénotype.

Comme le DHA diminue l'invasivité des cellules cancéreuses mammaires, et augmente l'expression de la sous-unité β4 (ARNm et protéine), nous avons fait l'hypothèse que la régulation transcriptionnelle de l'expression de β4, pourrait dépendre des récepteurs nucléaires PPAR (récepteurs activés par les prolifférateurs de péroxysomes), dont l'expression est elle-même inhibée par le DHA. Nous avons identifié sur le promoteur du gène *SCN4B*, codant pour la sous-unité β4, quatre éléments de réponse aux PPAR (PPRE) parmi 10 dont la mutation inhibe l'induction transcriptionnelle par le DHA. D'une part, la surexpression et l'activation de PPARα diminue l'activité du promoteur du gène *SCN4B*. D'autre part, la sous-expression de PPARα, qui réduit l'invasivité des cellules cancéreuses, augmente l'expression de β4, suggérant une régulation dépendante de PPARα. La mutation des 4 PPRE n'impacte pas cette diminution de l'activité du promoteur par PPARα, impliquant un autre mécanisme de régulation, tandis que la régulation par le DHA est dépendante des PPRE. Enfin, le co-traitement des cellules MDA-MB-231 par le DHA et un siPPARα augmente l'expression de β4 de façon additionnelle. Cette étude met en évidence l'importance de β4 dans le contrôle de l'invasivité cancéreuse et l'intérêt que pourraient représenter de nouvelles stratégies nutritionnelles modulant son expression pour améliorer les traitements anticancéreux.

Résumé en anglais

Metastasis development, and appearance of resistance to chemotherapies, are responsible for the majority of breast cancer-associated death. Yet, no specific anti-metastatic therapy is currently available. Metastasis appearance at a site distant from the primary tumor relies in part on the acquisition by cancer cell of the capacity to invade extracellular matrices. A phase II trial showed that Chemotherapy efficacy in metastatic breast patients could be improved by supplementation with docosahexaenoic acid (DHA, 22:6n-3), a long chain polyunsaturated fatty acid, known to decrease breast cancer cell invasiveness *in vitro* and *in vivo*, although its modes of actions are not well identified.

Voltage gated-sodium channels (Na_V) are transmembrane protein complexes composed of one $Na_V\alpha$ pore-forming subunit associated with one or two "auxiliary" β subunits, among the four known subunits β1, β2, β3 and β4. Beta subunits have been initially described in excitable cells as regulators of $Na_V\alpha$ electrophysiological properties. $Na_V1.5$ pore-forming subunit is abnormally expressed in breast cancer cells and promotes mesenchymal invasion, thereby enhancing extracellular matrix degradation. Its expression and activity are inhibited by DHA.

Beta subunit involvement in invasiveness and metastatic spread is not well known. In a preliminary study, we showed that β4 (*SCN4B* gene) underexpression was associated with an increased in cancer cell invasiveness. The objectives of this thesis were *i*) to characterize β4 expression in mammary tumors, as a function of their grade, and in non-cancerous tissues *ii*) to identify the mechanisms of modulation of cancer cell invasiveness by β4 and *iii*) to study the effects of DHA on β4-dependent invasiveness.

The immunohistological study performed on human mammary biopsies revealed that β4 is strongly expressed in non-pathological breast tissues. β4 expression is decreased in cancerous tissues, particularly in high grade tumors and metastases. In an *in vivo* model of organ colonization in zebrafish embryos, the loss of β4 expression in MDA-MB-231 breast cancer cells increased invasion about 40%. Organ colonization was decreased by 50 % when control cells were pretreated with DHA, which enhances β4 expression.

In vitro, β4 underexpression in MDA-MB-231 breast cancer cell line increased extracellular matrix invasion by 150%, while β4 overexpression decreased cancer cells invasiveness by 50%. β4 underexpression-induced invasiveness seems to be sodium channel $Na_V1.5$-independent since it is observed in $Na_V\alpha$–lacking cancerous cell lines. Invasiveness associated to β4 knockdown is not due to an increase in extracellular matrix degradation, unlike $Na_V1.5$-

dependent invasiveness, but rather to an increase in cell migration. The loss of β4 expression is associated with the acquisition of features described in the amoeboid phenotype such as amoeboid-like morphology and an increase in RhoA GTPase activity.

Since DHA decreases breast cancer cells invasiveness and increases β4 subunit expression (mRNA and protein), we hypothesized that the transcription of the *SCN4B* gene could depend on PPAR (peroxisome proliferator-activated receptors) nuclear receptors. DHA decreases PPAR expression. We identified four PPAR response elements (PPRE) out of 10 putative PPRE on the *SCN4B* gene promoter, the mutations of which inhibited DHA-induced transcription. On the one hand, PPARα overexpression and activation decreased *SCN4B* promoter activity. On the other hand, PPARα underexpression reduced cancer cell invasiveness and increased β4 expression, suggesting a PPARα-dependent regulation. Mutation of the four PPRE did not impact the decrease of the promoter activity induced by PPARα, involving another mechanism of regulation while regulation by DHA is PPRE-dependent. Finally, co-treatment of MDA-MB-231 cells with DHA and siPPARα additionally increased β4 mRNA expression.

This study highlights the importance of β4 in the control of cancer cell invasiveness and the benefit of novel nutritional strategies modulating its expression for the improvement of cancer treatment.

Table des matières

Liste des publications et communications

Publication intégrée à la thèse

Besson P, Driffort V, **Bon E**, Gradek F, Chevalier S, Roger S. *How do voltage-gated sodium channels enhance migration and invasiveness in cancer cells ?* Biochim Biophys Acta. 2015 Apr 20

Publications non intégrées à la thèse

Driffort V, Gillet L, **Bon E**, Marionneau-Lambot S, Oullier T, Joulin V, Collin C, Pagès JC, Jourdan ML, Chevalier S, Bougnoux P, Le Guennec JY, Besson P, Roger S. *Ranolazine inhibits NaV1.5-mediated breast cancer cell invasiveness and lung colonization.* Mol Cancer. 2014 Dec 11;13(1):264.

Wannous R, **Bon E**, Gillet L, Chamouton J, Weber G, Brisson L, Goré J, Bougnoux P, Besson P, Roger S, Chevalier S. *Suppression of PPARβ, and DHA treatment, inhibit NaV1.5 and NHE-1 pro-invasive activities.*Pflugers Arch. 2014 Jul 15. (2015) 467:1249-1259.

Wannous R, **Bon E**, Mahéo K, Goupille C, Chamouton J, Bougnoux P, Roger S, Besson P, Chevalier S. *PPARβ mRNA expression, reduced by n-3 PUFA diet in mammary tumor, controls breast cancer cell growth*. Biochim Biophys Acta. 2013 Nov;1831(11):1618-25.

Communications orales

Bon E, Wannous R, Gillet L, Besson P, Roger S, Chevalier S. Inhibition de l'invasivité des cellules cancéreuses mammaires via la surexpression de la protéine β4 par l'acide docosahexaènoïque. Mai 2015. 11ème congrès de l'axe valorisation des produits de la mer en cancérlogie, Cancéropôle Grand Ouest, Brest, France.

Bon E, Driffort V, Martines-Caceres C, Pelegrin P, Cayuela ML, Marionneau-Lambot S, Ouiller T, Piver E, Moreau A, Burlaud-Gaillard J, Chevalier S, Besson P, Roger S. Le gène *SCN4B* est-il un gèe suppresseur de tumeur dans le cancer du sein ? Décembre 2014, Journée Recherche Tours Poitiers Limoges, Tours, France.

Communications affichées

Bon E, Driffort V, Gradek F, Martines-Caceres C, Pelegrin P, Cayuela ML, Ouiller T, Marionneau-Lambot S, Besson P, Chevalier S, Roger S. The loss of β4 expression in breast

cancer cells promotes cell invasiveness. Octobre 2015, Integrated mechano-chemical signals in invasion, Invadosome Consortium, Saint Paul de Vence, France.

Driffort V, Gillet L, **Bon E**, Marioneau-Lambot S, Ouiller T, Joulin V, Pagès JC, Chevalier S, Besson P, Roger S. Ranolazine inhibits $Na_V1.5$ mediated breast cancer cell invasiveness and lung colonisation. Juin 2015. EACR-AACR-SIC Special Conference 2015, Florence, Italie.

Wannous R, **Bon E**, Gillet L, Chamouton J, Weber G, Brisson L, Goré J, Bougnoux P, Besson P, Roger S, Chevalier S. Suppression of PPARβ, and DHA treatment, inhibit Nav1.5 and NHE-1 pro-invasive activities. Octobre 2014. 1st Meeting of the International Society for Cancer Metabolism (ISCAM)/5th Meeting of the International Society for Proton Dynamics in Cancer (ISPDC) in Smolenice, Slovakia, Oct 2014.1 pro-invasive activities1st Meeting of the International Society for Cancer Metabolism (ISCAM)/5th Meeting of the International Society for Proton Dynamics in Cancer (ISPDC) in Smolenice, Slovakia.

Liste des tables

Liste des figures

Liste des annexes

Liste des abréviations

AA : arachidonic acid/acide arachidonique
Abl : Abelson non-receptor tyrosine protein kinase
ABP : actin-binding protein/protéine se liant à l'actine
ACOX : acylcoA oxydase
ADN : acide désoxyribonucléique
AGPI : acides gras polyinsaturés
ALA : Alpha linolenic acid/acid α-linolénique
AMT : amoeboid to mesenchymal transition/transition amoeboïde-mésenchymateuse
ARNm : acide ribonucléique messager
aPKC : atypical protein kinase C

BAC : bacterial artifical chromosome/chromosome artificiel bactérien
BACE1 : β-site amyloid precursor protein cleaving enzyme 1

CAM : cell adhesion molecule/molécule d'adhésion cellulaire
Cdc42 : cell division control protein 42/protéine de contrôle de la division cellulaire 42
CMV : cytomegalovirus
CRIB : Cdc42/Rac-interactive binding/liaison interactive à Cdc42/Rac

DHA : docosahexaenoic acid/acide docosahexaènoïque (22:6n-3)
DOCK : dedicator of cytokinesis

EGF : epidermal growth factor/facteur de croissance de l'épiderme
ELMO1 : engulfment and cell motility 1
EPA : eicopentaenoic acid/acide eicosapentaènoïque (20:5n-3)
ERK : extracellular signal-regulated kinase

FAK : focal adhesion kinase/kinase d'adhésion focale
FGF : fibroblast growth factor/facteur de croissance des fibroblastes
FSP-1 : fibroblast-specific protein 1
FT : facteur de transcription

GAP : GTPases activating proteins/protéines activatrices des GTPases
GDI : guanine nucleotide dissociation inhibitor/inhibiteur de dissociation du nucleotide guanine
GDP : guanosine triphosphate
GEF : guanine exchange factor/facteur d'échange de guanine
GSK3β : glycogen synthase kinase 3 β/inase de synthèse du glycogène 3 β
GTP : guanosine diphosphate

Hh : HedgeHog
HGF : hepatocyte growth factor/facteur de croissance des hépatocytes
HIF1α : hypoxia inducible factor 1α/facteur inductible par l'hypoxie 1α

IGF : insulin-like growth factor/facteur de croissance analogue à l'insuline
ILK : integrin-linked kinase/kinase liée aux intégrines

LEF-1 : lymphoid enhancer factor 1/facteur activateur lymphoïde 1
LIMK : LIM kinase
Luc : luciférase

MAPK : mitogen activated protein kinase/protéine kinase activé par les mitogènes
MAT : mesenchymal to amoeboid transition/transition mésechymato-amoeboïde
mDia : diaphanous related formin
ECM/MEC : extracellular matrix/matrice extracellulaire
MLC : myosin light chain/chaine légère de la myosine
MLCK : myosin light chain kinase/kinase de la chaine légère de la myosine
MMP : matrix metalloprotease/métalloprotéase matricielle
MT1-MMP : membrane type 1-MMP/MMP membranaire de type 1
MTOC : microtubule-organizing center/centre d'organisation des microtubules

NF-κB : nuclear factor-kappa B/facteur nucléaire kappa B
NHE : sodium-proton exchanger/echangeur sodium-proton

PAK : p21-activated kinase
PDGF : platelet-derived growth factor/facteur de croissance dérivé des plaquettes
PI(3.4)P_3 : Phosphatidylinositol-4,5-triphosphate

PIP_2 : Phosphatidylinositol-4,5-diphosphate

PKC : protein kinase C/protéine kinase C

PI3K : phosphoinositide 3 kinase

PMA : Phorbol-12-Myristate-13-Acetate

PPAR : peroxisome proliferator-activated receptor/récepteur activé par les proliférateurs de peroxysomes

PPRE : PPAR response element/élément de réponse aux PPAR

PUFA : polyunsaturated fatty acids/acides gras polyinsaturés

Rac : Ras-related C3 botulinum toxin substrate

Rho : Ras Homolog gene family

RPTPβ : récepteur phosphotyrosine phosphatase β

ROCK : Rho associated protein kinase/protéine kinase associée à Rho

RTK : récepteur aux Tyrosine Kinases/Tyrosine Kinase Receptor

TEM : transition épithélio-mésenchymateuse

TK : tyrosine kinase

TGFβ/TGFβ-R : transforming growth factor β/transforming growth factor β receptor

SMAD : Sma and Mad related proteins

Src : Sarcoma Rous chicken

uPA/uPAR : urokinase-type plasminogen activator/-receptor

VASP: vasodilatator-stimulated protein

VEGF : vascular endothelial growth factor/facteur de croissance de l'endothélium vasculaire

WASP/N-WASP : Wiskott-Aldrich syndrome protein/neural-WASP

WAVE : WASP family Verprolin-homologous protein

Wnt : wingless type

ZF : zebrafish/poisson zèbre

Revue bibliographique

I. Dynamique de la dissémination métastatique des cellules cancéreuses mammaires

Le cancer du sein reste un problème majeur de santé publique puisqu'il représente le cancer le plus fréquent chez la femme. Chez des patientes atteintes d'un cancer du sein métastasé, la survie à 5 ans est fortement diminuée (http://www.e-cancer.fr/) (Bougnoux *et al.*, 2010). Comme il n'existe aucun traitement spécifique à ce jour et l'un des objectifs majeurs de la recherche sur le cancer du sein est de comprendre les mécanismes moléculaires du développement de métastases pour chercher à les inhiber. Si le développement des métastases est classiquement décrit comme une phase tardive de la croissance tumorale (Rocken, 2010), il a été aussi proposé que la dissémination des cellules cancéreuses dans d'autres organes pourrait être un phénomène précoce du développement tumoral (Rocken, 2010, Casar *et al.*, 2014).

Dans le cancer du sein, les cellules cancéreuses mammaires originelles prolifèrent de façon anarchique et forment un carcinome *in situ*. La croissance de ce carcinome est favorisée par la sécrétion de VEGF (Vascular Endothelial Growth Factor) qui stimule l'angiogenèse tumorale, la perméabilité vasculaire, la dédifférenciation des cellules épithéliales tumorales et la transition épithélio-mésenchymateuse (TEM) de ces cellules (Goel and Mercurio, 2013). Au cours de cette transition, les cellules épithéliales perdent leur polarité apico-basale, leurs jonctions intercellulaires et acquièrent des propriétés invasives. Elles sont alors capables de dégrader la lame basale sous-jacente à l'épithélium ainsi que d'autres matrices extracellulaires. Après avoir ainsi envahi les tissus environnants, les cellules cancéreuses rejoignent le système circulatoire par intravasation dans les vaisseaux sanguins et lymphatiques. Les cellules cancéreuses circulantes sortent de la circulation générale par extravasation, et s'implantent dans les organes cibles pour former de nouveaux foyers cancéreux nommés métastases ou tumeurs secondaires. Au cours de ces différentes étapes, seules les cellules les plus agressives résistent à la mort cellulaire (Lindsey and Langhans, 2014).

I.1. Transition épithélio-mésenchymateuse (TEM)

I.1.1. Modifications cellulaires associées à la TEM

La transition épithélio–mésenchymateuse (TEM) est un processus physiologique réversible et transitoire initialement identifié au cours de l'embryogénèse, de la régénération tissulaire et de la cicatrisation (Lim and Thiery, 2012). Elle est caractérisée par l'acquisition de propriétés dites « mésenchymateuses » par les cellules épithéliales, comme le remodelage du cytosquelette d'actine, des modifications des interactions cellule-cellule et cellule-matrice extracellulaire (MEC), et la capacité à dégrader cette dernière. La TEM est également associée à certaines pathologies telles que la fibrose et le cancer (Kalluri and Weinberg, 2009). La TEM constitue alors un marqueur d'agressivité tumorale de mauvais pronostic puisqu'elle est associée à une désorganisation tissulaire qui favorise la dissémination métastatique (Takai *et al.*, 2014, Nahm *et al.*, 2015, Zhang *et al.*, 2015).

L'épithélium mammaire est un tissu non vascularisé constitué de cellules épithéliales organisées et caractérisées par une polarisation apico-basale et des jonctions intercellulaires structurées par des molécules d'adhésion localisées comme l'E-cadhérine, la β-caténine membranaire et les occludines. L'épithélium repose sur une matrice extracellulaire appelée lame basale, constituée de protéines sécrétées par les cellules épithéliales. Dans un tissu sain, la lame basale est principalement constituée de collagène IV et de laminine (Halfter *et al.*, 2015). Les cellules épithéliales ayant acquis un phénotype mésenchymateux sont désorganisées au sein du tissu car elles ont perdu leur polarité apico-basale et ont peu de contacts focaux avec les cellules adjacentes. *In vitro*, les cellules mésenchymateuses sont très mobiles et elles ont une morphologie de type fibroblastique. Cette mobilité est conférée par une forte plasticité cellulaire, permettant l'enchainement des phases de la migration cellulaire : élongation, adhésion, rétraction et mouvement vers l'avant (Ladoux and Nicolas, 2012, Bravo-Cordero *et al.*, 2013). Les cellules mésenchymateuses sont également capables de sécréter des enzymes protéolytiques, impliquées dans la dégradation de la matrice extracellulaire. Ces caractéristiques des cellules mésenchymateuses favorisent la migration cellulaire et l'invasion des tissus. Les cellules ayant acquis des propriétés invasives peuvent franchir la lame basale. Le phénotype mésenchymateux des cellules cancéreuses désigne donc des cellules capables de dégrader les matrices extracellulaires Les modifications cellulaires associées à la TEM sont présentées dans la Table 1.

Table 1 : Modifications cellulaires associées à la transition épithélio-mésenchymateuse.

Phénotype épithélial	Phénotype mésenchymateux
Adhésion cellulaire par des jonctions adhérentes et des jonctions serrées	Perte des jonctions cellulaires
Polarité apico-basale	Polarité "avant-arrière"
Non migratoires	Capacités migratoires, invasion de la MEC
Marqueurs : E-cadhérine, occludines, collagène IV, β-caténine membranaire	Marqueurs : vimentine, FSP-1, N-cadhérine, β-caténine nucléaire, Zeb, Twist, Snail
Lame basale composée de collagène IV et laminine	Expression de collagène I et III, fibronectine et métalloprotéases

I.1.2. Voies de signalisation impliquées dans la TEM

L'induction de la TEM résulte de la combinaison de signaux intra- et extracellulaires. D'une part, ces signaux favorisent la perte de marqueurs épithéliaux régulateurs de l'adhésion (E-cadhérine, caténines, molécules d'adhésion cellulaire), la perte de la polarité cellulaire, de la survie et de la résistance à l'anoïkis (mort cellulaire déclenchée par le détachement de la cellule à la matrice). D'autre part, les signaux intra- et extracellulaires favorisent le gain de marqueurs mésenchymateux impliqués dans les interactions avec la matrice extracellulaire, la sécrétion d'enzymes protéolytiques telles que des métalloprotéases matricielles (Bonnans *et al.*, 2014) ou des cathepsines (Gillet *et al.*, 2009), le remodelage du cytosquelette d'actine, la migration et l'invasion (Gonzalez and Medici, 2014). Au niveau intracellulaire, les voies de signalisation du TGFβ (Transforming Growth Factor β), des récepteurs aux tyrosines kinases (RTK), Wnt, Notch et Hedgehog (Hh) sont suractivées. L'hypoxie influence également la TEM (Gonzalez and Medici, 2014). Les différentes voies intervenant dans la TEM sont résumées dans la Figure 1.

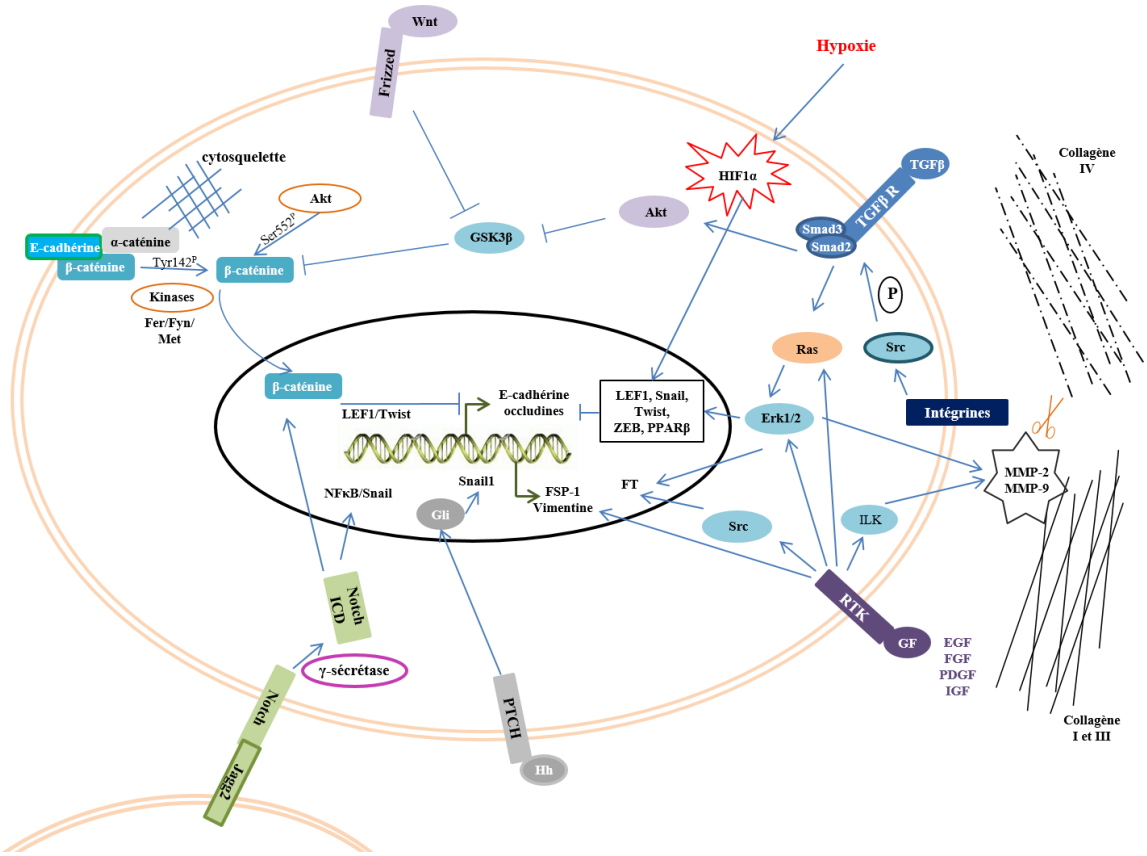

Figure 1 : Principales voies de signalisation impliquées dans la TEM.

Les voies de signalisation du TGFβ (en haut à droite), des RTK (en bas à droite), Hh (en bas au centre), Notch (en bas à gauche) et Wnt (en haut à gauche) sont représentées. Leur suractivation favorise la TEM via l'activation de facteurs de transcriptions (FT) et de gènes codant pour des FT (au centre). Les FT activés permettent la répression des gènes codant pour des marqueurs épithéliaux (E-cadhérine, occludines). La présence de collagène I et III dans la matrice extracellulaire favorise le phénotype mésenchymateux, alors que MMP2 et MMP9 sécrétées clivent le collagène IV (à droite).

- <u>E-cadhérine/β-caténine, marqueurs de la TEM</u>

L'E-cadhérine et la β-caténine membranaire constituent des marqueurs du caractère épithélial des cellules. Dans les cellules épithéliales normales, le complexe β-caténine/E-cadhérine est situé à la membrane plasmique au niveau des jonctions adhérentes. Ce complexe recrute l'α-caténine qui permet sa liaison au cytosquelette d'actine. Dans les cellules cancéreuses, la phosphorylation de la β-caténine sur la tyrosine 142 par des tyrosines kinases du type Fyn (Piedra *et al.*, 2003) ou sur la sérine 552 par Akt (Fang *et al.*, 2007) diminue son affinité pour ses deux partenaires, déstabilise le complexe β-caténine/E-cadhérine/α-caténine et augmente l'affinité de la β-caténine pour des coactivateurs transcriptionnels. Ces coativateurs induisent la translocation nucléaire de la β-caténine (Couffinhal *et al.*, 2006). Elle peut alors activer la transcription d'oncogènes cibles de la voie Wnt/β-caténine tels que le facteur de

transcription PPARβ (récepteur nucléaire activé par les prolifférateurs de péroxysomes (He *et al.*, 1999), Snail1 (ten Berge *et al.*, 2008) et LEF1 (Hovanes *et al.*, 2001). Par ailleurs, la relocalisation nucléaire de la β-caténine entraine la déstabilisation du complexe β-caténine/E-cadhérine/α-caténine et l'altération des jonctions adhérentes qui, en retour, favorise la désorganisation du tissu épithélial. Les métalloprotéases matricielles sont responsables de la dégradation de l'E-cadhérine, déstabilisant les jonctions intercellulaires (Pasca di Magliano and Hebrok, 2003) ainsi que du clivage de molécules d'adhésion cellulaire (Gavert and Ben-Ze'ev, 2008).

- Voie du TGFβ

Au cours de la TEM, la suractivation de la voie du TGFβ induit l'activation des voies PI3K/Akt et MAPK impliquées dans la survie cellulaire dans diverses lignées cancéreuses dont celles du cancer du sein (Kim *et al.*, 2015), du mélanome (Schlegel *et al.*, 2015) et du cancer du poumon (Chen *et al.*, 2012). Le TGFβ active également les récepteurs TGF-βRII et TGF-βRIII permettant le recrutement et la phosphorylation de TGFβ-RI. L'activation de ce récepteur phosphoryle les facteurs de transcription SMAD2 et SMAD3 (de SMA small body size et MAD mothers against decapentaplegic homologs 2 and 3). La phosphorylation du complexe SMAD2/3 favorise son oligomérisation avec le coactivateur SMAD4 et leur translocation nucléaire. L'activation du récepteur TGFβ-R1 soutient également l'importation du complexe R-SMAD/SMAD4 (Récepteurs aux SMADs) dans le noyau (Xu *et al.*, 2000, Kurisaki *et al.*, 2001, Yao *et al.*, 2008). Au niveau nucléaire, les complexes SMADs régulent et induisent la transcription de gènes codant des facteurs clefs de la TEM comme Snail1. La formation d'un complexe Snail1/R-SMAD peut conduire à l'inhibition de la transcription des gènes codant l'E-cadhérine et l'occludine (Peinado *et al.*, 2003, Vincent *et al.*, 2009). L'expression des facteurs de transcription ZEB, Snail2 et Twist (Peinado *et al.*, 2003, Thuault *et al.*, 2008) est également activée par le complexe Snail1/R-SMAD et par l'hypoxie, qui stabilise le facteur de transcription HIF1α (Hypoxia Inducible Factor α) (Tsai and Wu, 2012) au niveau des zones tumorales non vascularisées.

- Voie des récepteurs aux tyrosines kinases

La voie des récepteurs aux tyrosines kinases (RTK) est activée par plusieurs facteurs de croissance tels que l'EGF (Epidermal Growth Factor), le FGF (Fibroblast Growth Factor), le PDGF (Platelet-Derived Growth Factor) et l'IGF (Insulin-like Growth Factor). L'activation des RTK module les voies de signalisation Ras, PI3K (phosphoinositide 3 kinase), Src (sarcoma

rous chicken) et ILK (integrin-linked kinase) (Murillo *et al.*, 2005, Jechlinger *et al.*, 2006, Kim *et al.*, 2007b, Katoh and Katoh, 2009). Les cascades de signalisation induites par l'activation des RTK permettent d'activer divers facteurs de transcription tels que Snail1/2, ZEB1/2 et Twist, responsables de l'induction de la TEM. En effet, ces facteurs de transcription répriment la transcription de gènes codant des molécules d'adhésion cellulaire (Gonzalez and Medici, 2014). Le FGF, permettant l'activation des RTK est également responsable de l'induction de l'EMT via l'augmentation de l'expression des gènes *S100A4* et *VIM* codant respectivement pour FSP-1 (Fibroblast Specific Protein 1) et la vimentine. Ces deux protéines sont caractéristiques du phénotype mésenchymateux (Table 1). L'EGF est responsable de l'activation des voies de signalisation ERK (extracellular signal-regulated kinase) et ILK, ainsi que de la production et la sécrétion des métalloprotéases matricielles MMP-2 et MMP-9 par les cellules cancéreuses (Ahmed *et al.*, 2006).

- Voies Wnt, Notch et Hedgehog

Les voies de signalisation Wnt, Notch et Hedgehog sont, elles aussi, responsables de l'activation de facteurs de transcription favorisant la TEM. Les ligands Wnt activent les récepteurs Frizzled, favorisant la liaison de GSK-3β avec l'axine. GSK-3β est responsable de la dégradation de la β-caténine cytoplasmique. La liaison de l'axine à GSK-3β empêche la phosphorylation de la β-caténine. Ainsi, cette dernière est accumulée dans le noyau et active le facteur de transcription LEF-1, favorisant l'expression de nombreux gènes associés à la TEM. La voie Notch est activée par la fixation de JAG2 au récepteur Notch, induisant le clivage et le relargage du domaine intracellulaire du récepteur par la γ-sécrétase. Le domaine intracellulaire de Notch peut jouer directement le rôle de facteurs de transcription ou celui de stabilisateur de la β-caténine cytoplasmique. Ce deuxième rôle est responsable de l'activation des voies ERK et NF-κB induisant la transcription des gènes codant Snail1/2 et LEF-1. La voie Hedgehog induit quant à elle l'expression de gènes associés à la TEM tel que Snail1 via l'activation des facteurs de transcription Gli (Gonzalez and Medici, 2014).

I.2. Régulation de la motilité des cellules cancéreuses

La formation des métastases résulte de la capacité des cellules cancéreuses à migrer pour envahir les MECs environnant la tumeur primaire, à rejoindre la circulation sanguine et/ou lymphatique, à y survivre et à s'implanter dans d'autres organes distants. Dans ce contexte, les cellules les plus agressives possèdent plusieurs phénotypes migratoires et invasifs leur permettant de traverser des matrices extracellulaires de compositions et de densités différentes. La mise en route de la machinerie migratoire, initiée en réponse à des facteurs environnementaux (gradient de concentration de chimiokines, de nutriments ou de facteurs de croissance), requiert un certain nombre d'évènements cellulaires tels que l'adhésion, la polarisation des cellules, la polymérisation de l'actine au front de migration et la contraction du complexe acto-myosine à l'arrière. Classiquement, la migration cellulaire est décrite en 4 étapes : *i*) extension de protrusions (riches en actine) au front de migration (lamellipodes), *ii*) adhésion à la matrice (via les filopodes), *iii*) contraction du complexe acto-myosine, *iv*) rétraction du corps cellulaire (à l'arrière) en direction du front de migration. Les protrusions cellulaires sont formées à partir de la polymérisation des filaments d'actine au front de migration (Small *et al.*, 2002, Pollard and Borisy, 2003). Ces protrusions cellulaires sont ensuite stabilisées par des adhésions focales (au front de migration) médiées par les intégrines permettant de lier les protéines de la matrice extracellulaire au cytosquelette. La contraction de l'acto-myosine permet la dissociation des adhésions focales à l'arrière de la cellule, entrainant le mouvement du corps cellulaire vers l'avant de la cellule (Ridley *et al.*, 2003). Les intégrines jouent un rôle important dans la migration cellulaire car elles sont responsables d'une part de l'adhésion à la matrice extracellulaire et d'autre part à la régulation de la signalisation intracellulaire. L'activation des petites Rho GTPases permettent la transduction du signal extracellulaire modulé par les intégrines vers le milieu intracellulaire et la réorganisation du cytosquelette d'actine.

Les Rho GTPases sont des protéines régulatrices majeures des différents modes d'invasivité cellulaire. Ceux-ci sont définis en fonction de la morphologie cellulaire, des mécanismes de génération des forces de contraction, de l'organisation du cytosquelette et des interactions cellule-substrat. Succinctement, le mode « mésenchymateux » est caractérisé par des cellules ayant une morphologie allongée et capables de dégrader la matrice extracellulaire. Un autre mode d'invasivité cellulaire est connu sous le terme d'invasion « amoeboïde », pour lequel les cellules sont caractérisées par une morphologie plus sphérique, la formation de blebs

(protrusions membranaires sphériques) et l'aptitude particulière des cellules à se déformer pour passer au travers, ou entre les matrices, sans nécessité de les dégrader.

I.2.1. Les Rho GTPases

Les Ras homologous (Rho) GTPases sont des petites protéines de la superfamille Ras qui contrôlent de nombreux processus cellulaires tels que le réarrangement du cytosquelette d'actine, l'adhésion et la polarité cellulaire, le cycle cellulaire, l'apoptose, ou encore la migration cellulaire. La famille des Rho GTPases contient 22 membres répartis en 8 groupes : Cdc42 (Cdc42, TC10 ou RhoQ, TCL ou RhoJ, Chp, Wrch-1), Rac (Rac1, Rac2, Rac3, RhoG), Rho (RhoA, RhoB, RhoC), Rnd (Rnd1, Rnd2,Rnd3/RhoE), RhoD (RhoDet Rif), RhoH/TTF, RhoBTB (RhoBTB1 and RhoBTB2) et Miro (Miro-1 et Miro-2) (Aspenström *et al.*, 2004).

Les Rho GTPases sont impliquées à différents stades de la progression tumorale. Dans l'épithélium non-tumoral, elles participent au maintien de la polarité des cellules épithéliales. Une fois la tumeur initiée, Rac1, RhoA et RhoC sont capables de stimuler la dédifférenciation, la croissance cellulaire ainsi que la perte de la polarité apico-basale. Dans les tumeurs invasives, RhoA, Rac1 et ROCK (Rho-associated containing coiled-coil kinase, effecteur de RhoA) sont responsables de l'altération des adhésions cellule-cellule et cellule-MEC, ce qui contribue au développement tumoral. Enfin, au site de développement des métastases, Rho et ROCK permettent aux cellules cancéreuses de franchir la barrière endothéliale. RhoC est capable de promouvoir l'expression de facteurs pro-angiogéniques, conduisant à la vascularisation tumorale (Parri and Chiarugi, 2010).

Les GTPases RhoA (Ras homolog gene family, member A), Rac1 (Ras-related C3 botulinum toxin substrate 1) et Cdc42 (Cell division control protein 42) sont surexprimées dans de nombreux cancers (Jiang *et al.*, 2003) dont le cancer du sein (Fritz *et al.*, 1999, Jiang *et al.*, 2003). Elles sont donc des cibles thérapeutiques potentielles pour inhiber le développement métastatique. Ce sont des acteurs permettant la transduction du signal des récepteurs membranaires au cytosquelette d'actine. La Table 2 résume la régulation des Rho GTPases dans différentes tumeurs.

Table 2 : Régulation anormale de l'expression et de l'activité des Rho GTPases dans différentes tumeurs
D'après Parri and Chiarugi, 2010.

Rho	Dérégulation	Tumeurs
RhoA	Protéine ++, Activité ++	Sein, foie, peau, colon, ovaires, vessie, gastrique, testicules
RhoC	Protéine ++, Activité ++	Sein, métastases de mélanome, pancréas, foie, ovaire, prostate, gastrique
Rac1	Protéine ++, Activité ++	Sein, testicule, gastrique

I.2.1.1. Structure des Rho GTPases

Les Rho GTPases sont des petites protéines cytosoliques d'environ 21 kDa structurées en trois domaines : le domaine G, ou GTPasique, impliqué dans la fixation et l'hydrolyse du GTP, le domaine d'insertion Rho, impliqué dans la liaison aux protéines régulatrices RhoGEF (Rho Guanine Exchange Factor) et le domaine C-terminal hypervariable contenant une séquence CAAX, permettant la liaison de la GTPase aux membranes cellulaires (plasmique ou endosomale) (voir Figure 2) (Schaefer *et al.*, 2014).

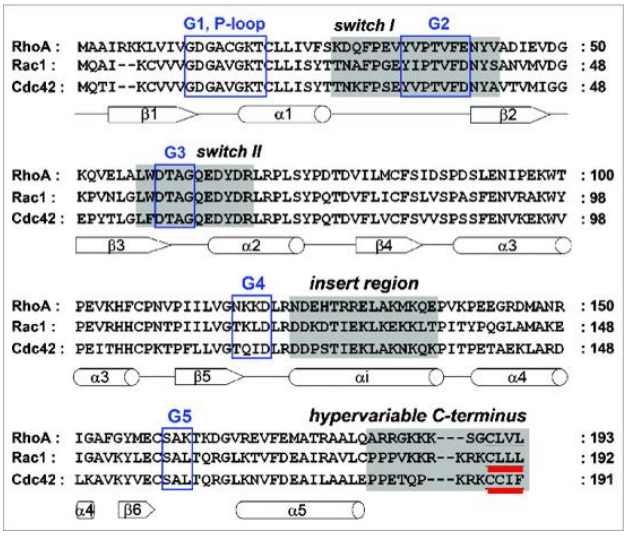

Figure 2 : Alignement des séquences humaines de RhoA, Rac1 et Cdc42.
Les domaines G sont représentés par des cadres bleus, les domaines « switch », les régions d'insertion de Rho et C-terminal hypervariable sont indiquées en gris. Les domaines « switch » servent de senseurs de liaison au GDP ou au GTP. Les sites de modification lipidique (farnésylation ou géranylgéranylation) permettant l'ancrage à la membrane sont soulignés en rouge (en C-terminal), les feuillets β sont représentés par des flèches et les hélices α par des cylindres. D'après Schaefer *et al.*, 2014.

Le domaine G, composé de 6 feuillets β et 5 hélices α, module la liaison des Rho GTPases à la guanine du GTP. Il est divisé en cinq séquences (G1-5) hautement conservées dans la superfamille de Ras-like GTPases. Le domaine G1 (aussi dénommé P-loop), engage la liaison entre le magnésium de la petite protéine G, indispensable à la liaison du nucléotide, et le β-phosphate du nucléotide. Les régions G2 et G3 contiennent des acides aminés établissant le caractère plus hydrophile ou plus hydrophobe des protéines, et déterminent la liaison spécifique à leurs effecteurs ou aux protéines régulatrices RhoGEF. La région switch II (incluant le domaine G3), contient une glutamine en position 63 nécessaire à l'hydrolyse du GTP catalysée par les protéines régulatrices RhoGAP (Rho GTPase Activating Protein). La liaison des GTPases à leurs effecteurs se fait grâce à la région d'insertion de Rho située entre les motifs G4 et G5. Cette région intervient également dans la liaison des petites protéines G à la protéine activatrice RhoGEF. Le domaine hypervariable C-terminal des Rho GTPases contient une boite CAAX qui subit des modifications post-traductionnelles permettant la prénylation de la protéine (farnésylation ou géranylgéranylation), ce qui influence sa localisation au niveau de la membrane plasmique (Ridley, 2006). Outre l'ancrage dans les membranes, ce domaine module également la liaison des Rho GTPases à leurs effecteurs spécifiques (Schaefer *et al.*, 2014).

I.2.1.2. Cycle de régulation des Rho GTPases

Les Rho GTPases subissent des changements conformationels permettant leur liaison au GTP ou au GDP, induisant respectivement leur activation ou leur inactivation. L'activation ou l'inactivation de ces protéines dépend de signaux extracellulaires tels que les œstrogènes (Azios *et al.*, 2007), l'EGF et les intégrines (Leabu *et al.*, 2005). La liaison au GDP ou au GTP est régulée par trois classes de protéines : les GDIs (Guanine nucleotide Dissociation Inhibitor), les GAPs (GTPases Activating Proteins) et les GEFs (Guanine Exchange Factor). La GTPase inactive (liée au GDP) est séquestrée dans le cytoplasme, complexée à une RhoGDI. La dissociation de ce complexe permet la liaison de la Rho GTPase à une RhoGEF induisant le relargage du GDP, remplacé par le GTP. La protéine activée (liée au GTP) pourra ainsi interagir avec ses effecteurs pour initier différentes voies de signalisation. Après inactivation par les GAPs, les Rho GTPases sont extraites de la membrane plasmique par les RhoGDI et à nouveau séquestrées dans le cytoplasme, ce qui les protège de la dégradation par le protéasome (Ridley, 2006, Garcia-Mata *et al.*, 2011). Le cycle de régulation des Rho GTPases est présenté dans la Figure 3.

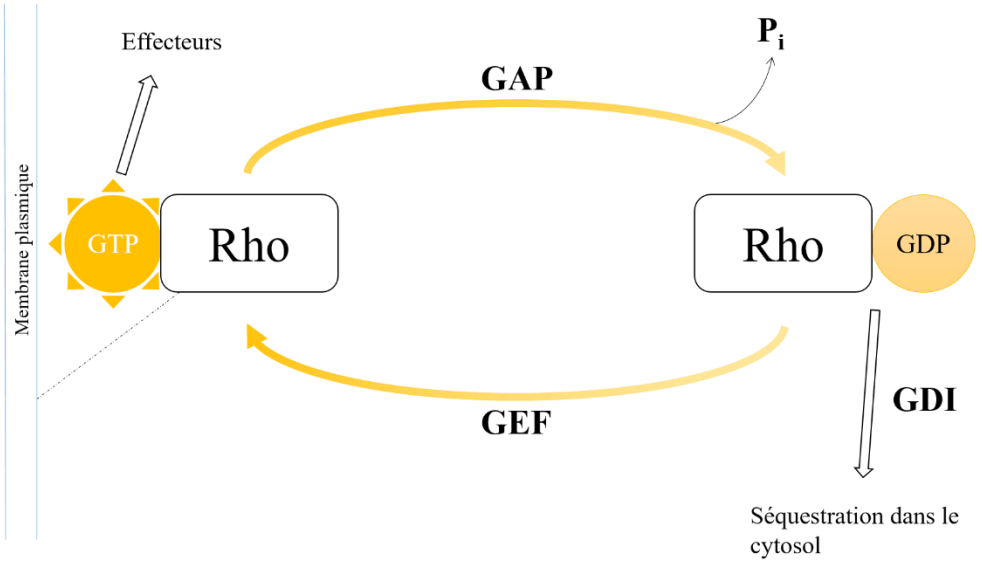

Figure 3 : Régulation des Rho GTPases.

Les Rho GTPases inactives (RhoGDP) sont activées par les RhoGEF (Guanine Exchange Factor) à la membrane plasmique. Les RhoGTP sont alors capables d'activer ses effecteurs puis elles sont inactivées par déphosphorylation par les RhoGAP (GTPases Activating Protein). Les RhoGDP peuvent être séquestrées dans le cytosol par les RhoGDI (Guanine nucleotide Dissociation Inhibitor**).**

I.2.2. Caractéristiques phénotypiques des cellules invasives

I.2.2.1. Motilité cellulaire

Le cytosquelette des cellules cancéreuses peut être remodelé, pour leur conférer des capacités migratoires et invasives via la formation de protrusions cellulaires. Le cytosquelette est constitué de trois catégories de polymères protéiques : les filaments d'actine (ou microfilaments), les filaments intermédiaires et les microtubules.

Les microfilaments (actine fibrillaire F) sont constitués de polymères d'actine G (globulaire) capables de lier l'ATP. La polymérisation de l'actine F est régulée par des protéines de la famille des ABP (Actin-Binding Protein). Les monomères d'actine G s'assemblent en double hélice polarisée, générant une extrémité « barbée » (positive) et une extrémité « effilée » ou pointue (négative). La polymérisation d'un filament d'actine est présentée dans la Figure 4.

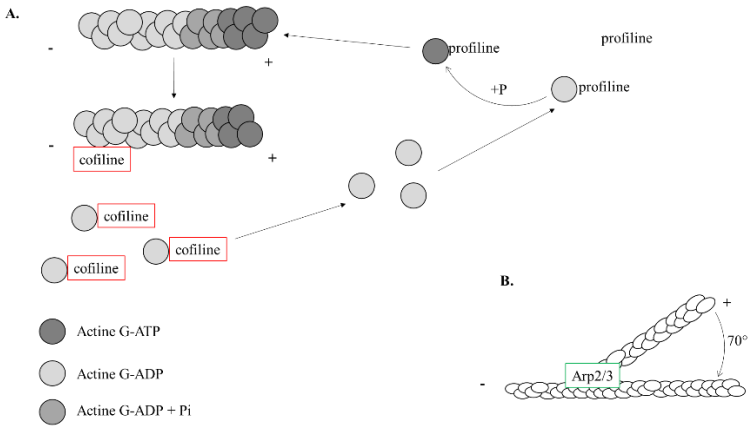

Figure 4 : Polymérisation et dépolymérisation de l'actine.

A. La nucléation de l'actine G en actine F est caractérisée par l'assemblage spontané de plusieurs monomères d'actine G. La profiline favorise l'élongation de l'actine F par ajout d'actine G liée à l'ATP sur l'extrémité barbée (+) du filament. Une fois l'actine G-ATP ajoutée au filament d'actine, la molécule est hydrolysée en ADP+Pi. Le Pi sera ensuite libéré. A l'extrémité pointue (-), la cofiline (protéine de la famille des ADF, actin depolymerizing factor ou facteur de dépolymérisation de l'actine), se fixe sur l'actine F et favorise sa dépolymérisation. Les monomères d'actine G-ADP ainsi libérés sont pris en charge par la profiline et recyclés. B. Le complexe Arp2/3 se lie aux filaments d'actine et permet leur élongation par ajout d'actine G-ATP à l'extrémité barbée du nouveau filament.

Le cytosquelette d'actine est impliqué dans l'organisation membranaire, la cytodiérèse (partage du cytoplasme), la différenciation cellulaire et la motilité (Fife *et al.*, 2014). Les filaments d'actine F sont essentiels à la formation de structures impliquées dans la migration cellulaire situées à l'avant de la cellule, appelées lamellipodes. L'orientation des microfilaments permet de pousser en avant le front de migration, augmentant la mobilité cellulaire. Les microtubules sont composés d'hétérodimères de tubuline α/β qui s'associent en polymères. L'hydrolyse du GTP de la sous-unité tubuline β détermine l'assemblage et la dépolymérisation des hétérodimères tubuline α/β, régulant la caryodiérèse (division du noyau cellulaire). L'assemblage et la dépolymérisation des hétérodimères par hydrolyse du GTP de la sous-unité tubuline sont essentielles pendant la mitose. Le réseau de microtubule est également impliqué dans le transport vésiculaire et la croissance cellulaire (Fife *et al.*, 2014). Les kératines, les neurofilaments, la desmine, la laminine et la vimentine constituent les filaments intermédiaires. Ils sont responsables de la liaison du cytosquelette aux protéines de la MEC (Fife *et al.*, 2014). Les protrusions cellulaires riches en actine situées à l'avant de la cellule, participent à la motilité cellulaire. Les Rho GTPases sont des protéines régulatrices majeures de cette motilité. Un schéma récapitulatif des voies de signalisation associées à RhoA, Rac1 et Cdc42 dans la régulation du cytosquelette est présenté en Figure 5.

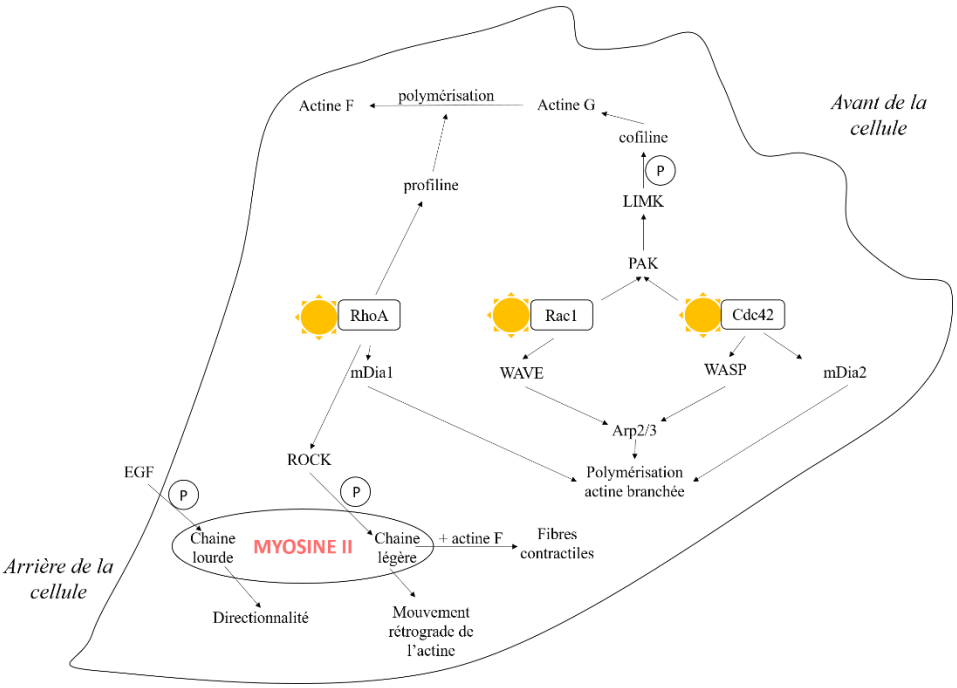

Figure 5 : Principaux acteurs de la régulation du cytosquelette d'actine.

Les Rho GTPases liées au GTP activent diverses protéines conduisant à la polymérisation de l'actine F. Rac1 et Cdc42 activent LIMK via PAK. LIMK inactive la cofiline par phosphorylation sur le résidu sérine 3. La cofiline libère l'actine G dont la polymérisation en actine F est favorisée par la profiline activée par RhoA. Cette dernière active mDia2, qui favorise la polymérisation de l'actine. RhoA est aussi responsable de l'activation de son effecteur ROCK, qui phosphoryle la chaine légère de la myosine II, induisant le mouvement rétrograde de l'actine et la formation de fibres contractiles lorsqu'elle est associée à l'actine F. La phosphorylation de la chaine lourde de la myosine II (en rouge) contrôle quant à elle la directionnalité cellulaire sous l'influence de l'EGF. Rac1, coactivateur de WAVE, et Cdc42, activateur de WASP, favorisent la polymérisation de l'actine via l'activation du complexe Arp2/3. La formine mDia2, activée par Cdc42, favorise également la polymérisation de l'actine à son extrémité barbée.

A l'avant de la cellule, la polymérisation et la dépolymérisation de l'actine est régulée par les formines et le complexe Arp2/3. Les formines (mDia1 et mDia2) sont des protéines impliquées dans la polymérisation de l'actine, notamment à l'extrémité branchée (+) de l'actine F. Ce sont des effecteurs des Rho GTPases, (mDia1 effecteur de RhoA et mDia2 effecteur de Cdc42) responsables de la formation de fibres de stress (Evangelista *et al.*, 2003) et de la régulation de la croissance des filaments d'actine (Goode and Eck, 2007). Les formines sont activées par un changement conformationnel et sont constituées de plusieurs domaines (voir Figure 6. Le domaine RBD (Rho binding domain), situé en position N-terminale de la protéine, permet l'activation de la formine lors de la fixation d'une Rho GTPase. Le domaine FH2 (formin homology 2) leur confère le rôle de nucléateur en leur permettant de se lier à l'actine

G et F. Le domaine FH1 (formin homology 1) riche en proline permet la liaison à la profiline qui recrute l'actine G, favorisant ainsi sa polymérisation. Le domaine FH3, situé en position N-terminale du domaine FH1 et en C-terminal du domaine RBD, permet le repliement de la formine en assurant la liaison avec le domaine DAD (Diaphanous autoregulatory domain) en position C-terminale. La fixation de la RhoGTPase sur le domaine RBD permet de dissocier les domaines FH3 et DAD, permettant l'activation de la protéine (Kuhn and Geyer, 2014).

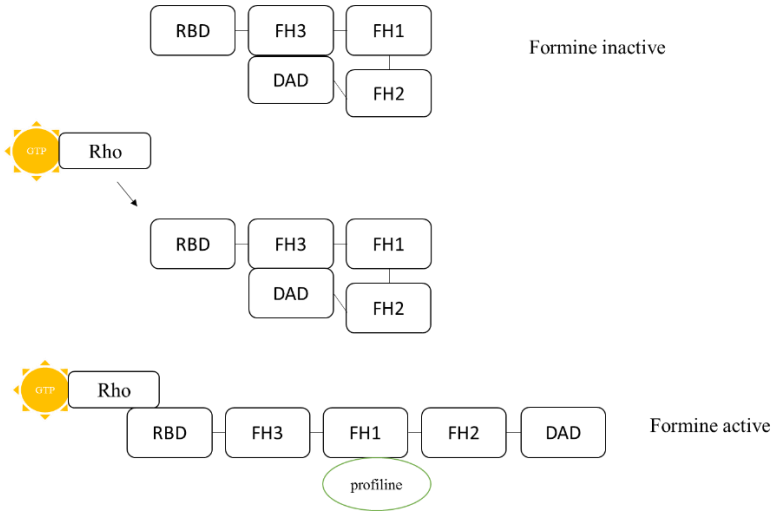

Figure 6 : Activation des formines.

La formine est inactive lorsque le domaine DAD est lié au domain FH3. La fixation d'une RhoGTPase sur le domaine RBD induit le dépliement de la formine, et la fixation de la profiline sur le domaine FH1. Le domaine FH2 est ainsi accessible et permet la liaison à l'actine pour favoriser sa polymérisation.

Rac1 et Cdc42 activent les complexes WAVE (aussi dénommé Scar) et WASP respectivement, tous deux membres de la famille des Wiskott-Aldrich Syndrome Proteins (WASP). Ces complexes sont responsables de l'activation du complexe Arp2/3 qui est constitué de 7 protéines : Arp2 et Arp3, qui servent de sites de nucléation de nouveau filament d'actine et de ArpC1, ArpC2, ArpC3, ArpC4, ArpC5, qui sont des protéines structurales. Arp2/3 stimule la formation de microfilaments et du réseau d'actine. Dans le cancer du sein, les protéines Arp2 et WAVE2 sont surexprimées et semblent participer à la dissémination des cellules cancéreuses au niveau des ganglions lymphatiques (Iwaya *et al.*, 2007). Rac et Cdc42 activent également PAK (p21-associated kinase), qui active par phosphorylation LIMK (LIM kinase). La phosphorylation de la cofiline (Ser3) par la LIMK la rend inactive. Cette modification augmente la vitesse de dissociation entre l'actine G et la cofiline. La cofiline se fixe à l'extrémité négative de l'actine F et favorise la dépolymérisation et le recyclage des anciens filaments d'actine (Devreotes and Horwitz, 2015). Au cours de la motilité cellulaire, les filaments d'actine sont

sujets à un mouvement dit de « tapis roulant ». Les filaments d'actine sont polymérisés au front de migration tandis que les extrémités pointues sont dépolymérisées et recyclées. Dans le lamellipode, le complexe Arp2/3 génère des extrémités barbées et favorise la nucléation de nouveaux filaments d'actine et la cofiline permet la dépolymérisation des extrémités pointues (Ponti *et al*., 2004). Dans la lamelle, structure située à l'arrière du lamellipode, le tapis roulant d'actine est maintenu par l'activité de la myosine II (Ponti *et al.*, 2004).

La myosine II est également responsable de la rétraction de l'arrière de la cellule en direction du front de migration en générant des forces de contraction. La myosine II est une grosse protéine composée de deux chaines lourdes associées à deux paires de chaines légères. L'activité de la protéine est régulée par la phosphorylation de la chaine légère MLC (Myosin Light Chain) ciblée par MLCK (Myosin Light Chain Kinase), ROCK (Rho Associated Protein Kinase), et la myosine phosphatase. L'assemblage de la myosine en filaments est quant à elle régulée par la phosphorylation des chaines lourdes. Dans les cellules cancéreuses mammaires MDA-MB-231, il a été montré que la phosphorylation de la chaine lourde de la myosine induite par la voie de signalisation de l'EGF régule la directionnalité de la migration et la stabilité des adhésions focales (Dulyaninova *et al.*, 2007). La pression générée par les forces de contraction de la myosine à l'arrière de la cellule conduit à la formation de « blebs » (protrusions membranaires sphériques) dans les régions pauvres en actine F. (Devreotes and Horwitz, 2015).

I.2.2.2. Adhésion à la matrice extracellulaire

Il existe deux types d'adhésion, définies en fonction de leur localisation cellulaire, de leur taille et de leur composition : le complexe focal et l'adhésion focale. Le complexe focal, régulé par l'activation de Rac et Cdc42 est situé en périphérie de la cellule et sa mise en place précède généralement la formation de l'adhésion focale, régulée par l'activité de Rho. Cette adhésion focale est associée aux fibres de stress (Wozniak *et al.*, 2004), qui sont composées de filaments d'actine (Cramer *et al.*, 1997), de myosine II (Fujiwara and Pollard, 1976) et de nombreuses protéines se liant à l'actine (ABP) dont l'α-actinine (Lazarides and Burridge, 1975). Ces fibres sont initiées à partir des adhésions focales, et l'augmentation de la tension générée par ces fibres favorise les adhésions. RhoA-GTP active ROCK qui active par phosphorylation la chaine légère de la myosine II (pMLCII). La myosine II activée s'assemble en filaments qui s'associent à l'actine F pour former les fibres contractiles (Kimura *et al.*, 1996).

L'efficacité de la migration et l'invasion cellulaire au travers des barrières tissulaires est dépendante des interactions entre les cellules et la matrice extracellulaire. Ces interactions sont

orchestrées au sein des adhésions focales, formées de GTPases, de clusters d'intégrines, et de diverses enzymes telles que des kinases, des phosphatases, des protéases et des lipases. Les intégrines sont des récepteurs transmembranaires hétérodimèriques pour des molécules extracellulaires telles que la fibronectine (Ruoslahti, 1996), le collagène, la vitronectine et la laminine (Zaidel-Bar *et al.*, 2007a). Les intégrines sont constituées de deux chaines α et β organisées en un domaine de liaison au ligand en extracellulaire et d'un court domaine intracellulaire impliqué dans la transduction du signal de l'extérieur de la cellule vers l'intérieur dit « outside-in ». La liaison du ligand sur le domaine extracellulaire des intégrines induit une modification de la conformation du domaine intracellulaire C-terminal et le regroupement de plusieurs intégrines en « cluster » (Emsley *et al.*, 2000). Les acteurs de l'adhésion cellulaire à la matrice via les intégrines sont présentés en Figure 7.

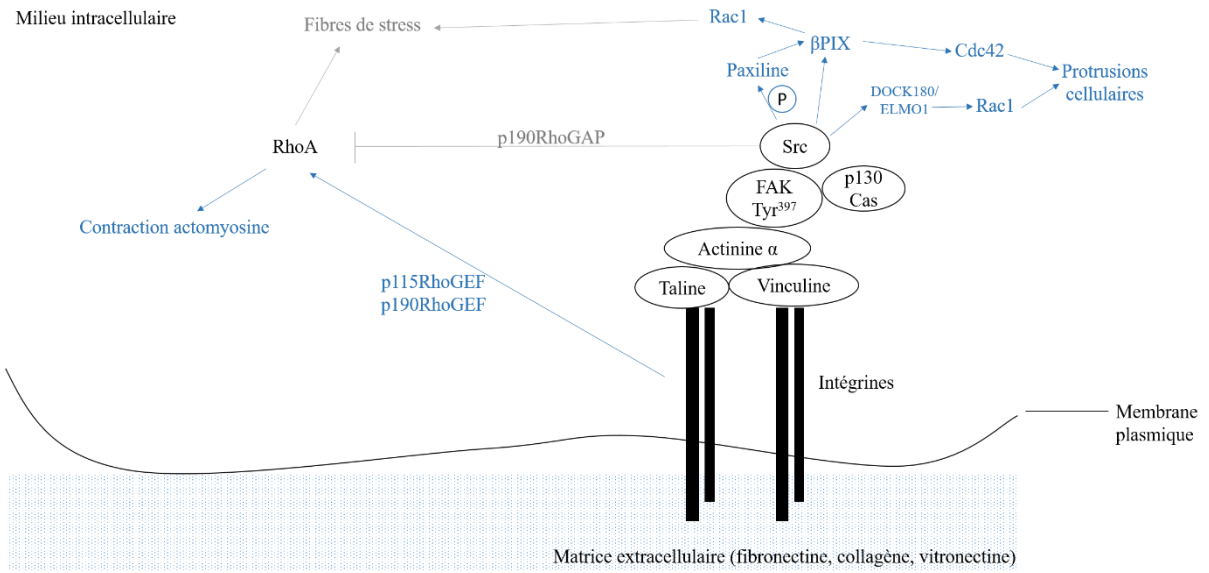

Figure 7 : Adhésion à la matrice extracellulaire.

Les intégrines permettent la liaison entre la MEC et le cytosquelette d'actine. En bleu sont représentés les régulateurs des complexes focaux, en gris les régulateurs des adhésions focales et en noir les acteurs communs aux deux types d'adhésion.

Les intégrines sont reliées au cytosquelette d'actine par leur domaine C-terminal intracellulaire via la taline, la vinculine et l'α-actinine (Zamir and Geiger, 2001, Selhuber-Unkel *et al.*, 2010, Abbey and Bayless, 2014). L'activation des intégrines par des protéines de la matrice extracellulaire permet la transduction de divers signaux intracellulaires via la phosphorylation de protéines de signalisation. C'est le cas de la FAK (focal adhesion kinase) sur la tyrosine 397 qui recrute les kinases de la famille Src (Sarcoma Rous Chicken kinase et

Fyn kinase) pour phosphoryler la paxilline (Le Clainche and Carlier, 2008), nécessaire à la formation de complexes d'adhésion (Zaidel-Bar *et al.,* 2007b). Le complexe FAK/Src permet d'activer diverses Rho GTPases telles que Rac1 et Cdc42 via l'activation des RhoGEF Dock180-ELMO1 (Dedicator of cytokinesis-Engulfment and cell motility 1, GEF de Rac1) et β-PIX (GEF de Rac1 et Cdc42), favorisant la formation de protrusions cellulaires impliquées dans la migration (Brugnera *et al.,* 2002, ten Klooster *et al.,* 2006). Dans les cellules cancéreuses mammaires MDA-MB-231, la formation d'un complexe FAK/intégrine β4, sous la dépendance de la voie EGFR/Src induit l'activation de voies de signalisation responsables de la prolifération, la migration, l'invasion cellulaire et le développement des métastases (Tai *et al.,* 2015).

La protéine p130Cas est une protéine d'échafaudage des adhésions focales qui peut interagir avec Src, tout comme la paxilline. Cette dernière peut également se lier à FAK et aux intégrines. La paxilline peut activer Rac, via l'interaction avec la RhoGEF βPIX et stimuler la migration cellulaire (Wozniak *et al.,* 2004).

L'assemblage du complexe focal au front de migration permet de stabiliser les structures néoformées telles les filopodes et les lamellipodes. La formation des adhésions focales résulte de l'accumulation de paxilline, organisée avec l'α-actinine, la taline, la vinculine, l'ILK et les intégrines (Laukaitis *et al.,* 2001, Zaidel-Bar *et al.,* 2003). Les intégrines sont transportées jusqu'au site d'adhésion par le trafic vésiculaire (Laukaitis *et al.,* 2001), régulé par les Rho GTPases (Symons and Rusk, 2003). Un modèle de régulation des adhésions focales a été récemment proposé. Au niveau du lamellipode, les intégrines sont activées par l'initiation du tapis roulant d'actine modulé par la taline. Les tensions exercées sur les intégrines engagées favorisent le recrutement et l'activation par phosphorylation de la FAK et de la paxilline par FAK et Src kinases. La phosphorylation de la paxilline au niveau des adhésions focales est responsable du recrutement de la vinculine, elle-même activée par le PIP_2 (Case *et al.,* 2015). La formation des adhésions focales par les intégrines et l'organisation des filaments d'actine requièrent la liaison d'ILK sur le domaine cytoplasmique des intégrines, assurant l'efficacité de l'adhésion focale à la matrice extracellulaire (Elad *et al.,* 2013). La stabilité des adhésions focales dépend des forces contractiles générées par l'activité du cytosquelette, régulées par la voie ROCK/myosine II. L'inhibition de l'activité Rho Kinase (ROCK) par un inhibiteur pharmacologique favorise la dissociation des adhésions focales mais n'inhibe pas leur formation *de novo* (Lavelin *et al.,* 2013). Les cinétiques d'assemblage et de désassemblage des adhésions focales sont régulées de l'activité de la myosine II. En effet, le « relâchement » cellulaire induit par le blocage de la contractilité due à la myosine II induit le désassemblage

des adhésions focales centrales et l'accumulation de petites adhésions focales à la périphérie cellulaire (Wolfenson *et al.*, 2011), ce qui pourrait engendrer la réorganisation du cytosquelete et modifier la migration cellulaire. La phosphorylation du résidu S1916 de la chaine lourde de la myosine IIA par Rac1 permet son assemblage dans les adhésions focales (Pasapera *et al.*, 2015).

Les points d'adhésion régulent la polymérisation de l'actine et de la myosine II via les Rho GTPases (Parsons *et al.*, 2010). Parallèlement, la contraction du complexe acto-myosine peut être inhibée par le complexe FAK/Src, permettant de limiter l'activation de RhoA au front de migration. En effet, le complexe FAK/Src peut réguler l'activation de p190RhoGAP. Cette protéine régulatrice des Rho GTPases module le relâchement temporaire de la tension du cytosquelette via FAK/Src (Arthur *et al.*, 2000, Ren *et al.*, 2000), ce qui facilite « l'étalement » des cellules notamment lorsqu'elles sont adhérentes à la fibronectine. La formation de fibres de stress est induite par l'activation de RhoA et Rac1 (Nobes and Hall, 1995), et ce processus est concomitant à l'activation des intégrines. Suite au relâchement du cytosquelette, les intégrines stimulent l'activité de RhoGEFs telles que p115RhoGEF et p190RhoGEF en faveur de RhoA, augmentant la contraction du complexe acto-myosine à l'arrière de la cellule. L'assemblage et le désassemblage des complexes d'adhérence sont donc coordonnés à l'avant et à l'arrière de la cellule pour optimiser le mouvement migratoire.

I.2.2.3. Polarité cellulaire et directionnalité des cellules en migration

La perte de la polarité épithéliale (apico-basale), à la suite de la TEM, est à l'origine de la désorganisation du tissu et représente donc un marqueur d'évolution des cancers épithéliaux. Dans les cellules épithéliales normales, la polarité cellulaire est dépendante de trois complexes : PAR, Crumbs et Scrib. Le gène PAR code deux protéines Par3 et Par6 associées à la protéine kinase C atypique (aPKC) pour former le complexe PAR (Iden and Collard, 2008). Le complexe PAR, lié à la Rho GTPase Cdc42 (Joberty *et al.*, 2000, Lin *et al.*, 2000) régule la polarité et la directionnalité des astrocytes et des fibroblastes (Etienne-Manneville and Hall, 2001, Gomes *et al.*, 2005). Dans un modèle d'étude de la migration des astrocytes par cicatrisation tissulaire, Cdc42 est activée et recrutée au front de migration. Une fois liée à Par6, Cdc42 favorise l'activation de aPKC permettant la réorientation du MTOC (MicroTubules Organizing Center) qui est le centre organisateur des microtubules à l'avant du noyau. Par6 peut également agir en tant que régulateur de RhoA. Au front de migration, Par6 recrute Smurf1 (Smad ubiquitination regulatory factor 1) qui favorise la dégradation de RhoA par le protéasome. Quant à Par3, elle

contrôle la formation des jonctions serrées par l'intermédiaire de Tiam1, une RhoGEF spécifique de Rac1 (Chen and Macara, 2005). D'autres molécules impliquées dans la réorientation du MTOC, telle la kinésine KIF11, sont impliquées dans la réponse au chimiotactisme induit par l'EGF, influençant la migration et l'invasion des cellules MDA-MB-231 (Wang and Lin, 2014).

La polarité est un acteur essentiel de la migration cellulaire. Il existe deux types de migration cellulaire : la migration aléatoire et la migration orientée en réponse à des stimuli extérieurs (chimiotactisme). Dans les deux cas, les cellules doivent être polarisées pour établir un axe « avant-arrière » (Ridley *et al.*, 2003). L'une des évidences de l'existence de cet axe est la répartition des Rho GTPases selon des gradients opposés. Rac et Cdc42 sont activées au front de migration tandis que Rho est active à l'arrière de la cellule où elle est responsable de la contraction du complexe acto-myosine.

Dans les cellules cancéreuses, la direction du mouvement migratoire est déterminée par des stimuli extérieurs responsables de l'activation de certains récepteurs (intégrines, cadhérines et récepteurs aux chimiokines) et par la polarité cellulaire, elle-même régulée par la polymérisation asymétrique de l'actine et la formation des complexes focaux d'adhésion. En effet, les intégrines et les RhoGAP, contrôlent la régulation des Rho GTPases en fonction du temps et influencent ainsi la directionnalité de la migration cellulaire. Par exemple, la RhoGAP p190A est nécéssaire à une migration orientée *in vitro* aussi bien qu'*in vivo* (Jiang *et al.*, 2008). La polarisation de l'actine au front de migration conduit à la formation d'une structure appelée lamellipode (voir I.2.3.1 Lamellipodes page 46), régulée par la PI3K (phosphoinositide 3 kinase) et Rac, toutes deux recrutées pour activer le complexe Arp2/3. Néanmoins, Cdc42 apparait comme la protéine régulatrice majeure de la polarité cellulaire (Etienne-Manneville, 2004, Stern, 2006). La fonction de Cdc42 la mieux caractérisée consiste en l'orientation du centre organisateur des microtubules MTOC à l'avant du noyau en direction du front de migration (Nobes and Hall, 1999, Etienne-Manneville and Hall, 2001). Cependant, Cdc42 est active au front de migration (Itoh *et al.*, 2002, Nalbant *et al.*, 2004) et la perturbation de son activité altère la directionnalité de la migration cellulaire (Allen *et al.*, 1998, Nobes and Hall, 1999).

L'implication de Cdc42 dans la migration cellulaire induit la régulation de plusieurs voies de signalisation. D'une part, Cdc42 est capable d'activer sont effecteur Pak1/2 pour favoriser le recrutement au front de migration de la RhoGEF βPIX et l'activation localisée de Rac. Ceci induit la formation de protrusions riches en actines F polarisées. D'autre part, Cdc42 active le complexe Par6/aPKC, conduisant à la polarisation du cytosquelette de microtubules

(Cau and Hall, 2005). Le rôle central des Rho GTPases dans la polarité et la directionnalité cellulaire est régi par les RhoGAP et les RhoGEF. Plus particulièrement, p190RhoGAP inhibe l'activité de RhoA au front de migration. Cette RhoGAP peut être phosphorylé par les Src kinases, favorisent le recrutement de p190RhoGAP à la membrane et atténue la contractilité du complexe acto-myosine.

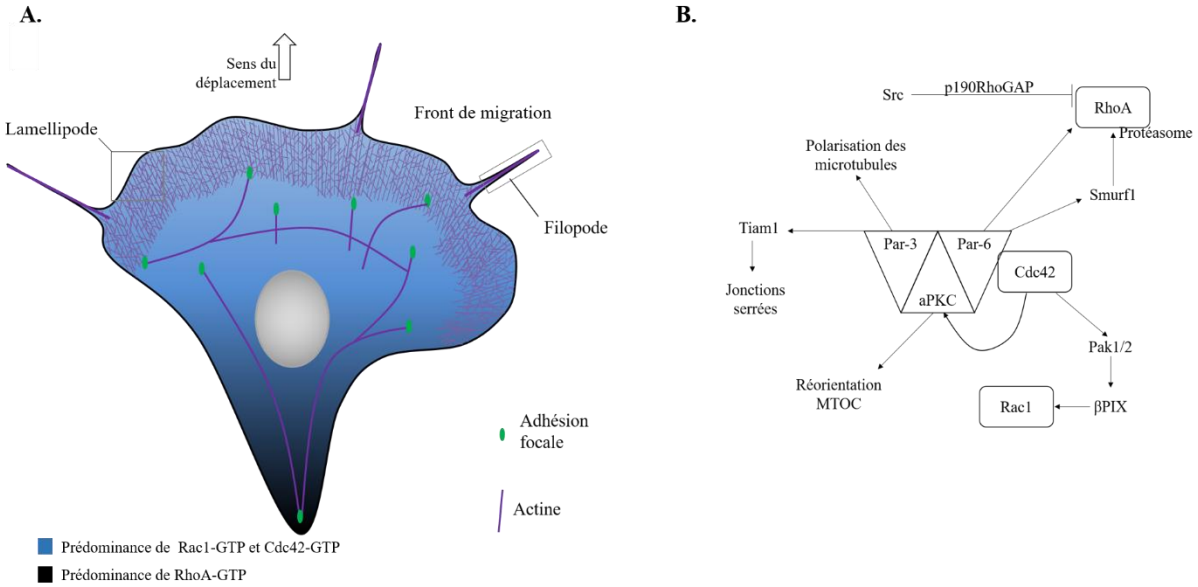

Figure 8 : RhoGTPases dans la directionnalité et la polarité cellulaire.

A. Répartition des Rho GTPases activées dans une cellule en migration et localisation des filopodes et lamellipodes. B. Régulation et fonction du complexe Par dans la polarité cellulaire. En se liant à Par-6, Cdc42 active aPKC responsable de la réorientation de MTOC. Cdc42 via Pak1/2 et βPIX active Rac1. Par-6 active également Smurf1 qui favorise la dégradation de RhoA par le protéasome. Src phosphoryle p190RhoGAP qui inhibe l'activation de RhoA. Par-3 polarise les microtubules et active Tiam1 responsable de la formation des jonctions serrées.

I.2.3. Structures cellulaires impliquées dans la migration des cellules cancéreuses

I.2.3.1. Lamellipodes

Le terme « lamellipode » décrit de plates extensions cytoplasmiques au front de migration de fibroblastes en mouvement (Abercrombie *et al.*, 1970). La migration cellulaire est initiée par l'élongation des lamellipodes à l'avant de la cellule, qui sont de larges structures membranaires et cytosoliques générées par la polymérisation de l'actine F barbée (Campellone and Welch, 2010). La structure des lamellipodes est schématisée dans la Figure 9.

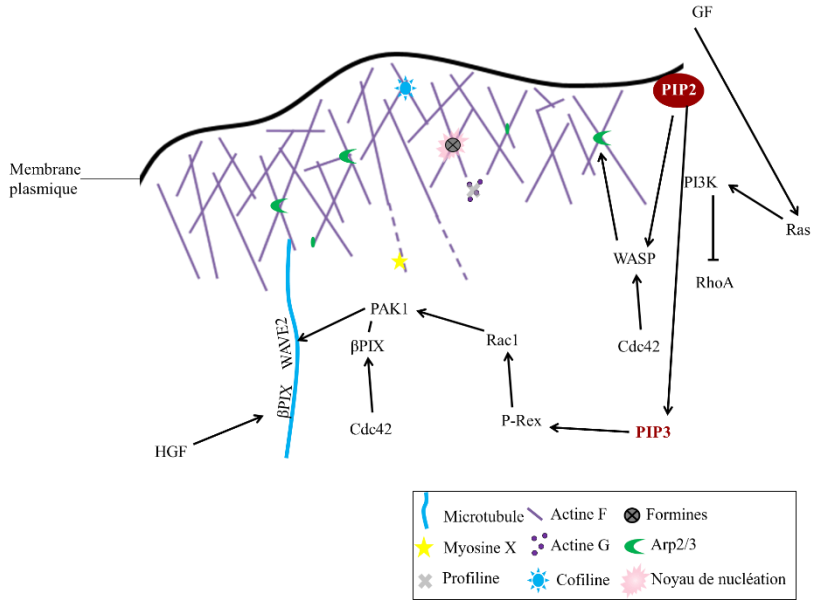

Figure 9 : Structure d'un lamellipode et facteurs associés à sa formation.

Les facteurs de croissance activent la voie Ras/PI3K, qui bloque l'activité de RhoA. PI3K phosphoryle PIP_2 générant le messager secondaire PIP_3, capable d'activer la RhoGEF P-Rex de Rac1. Rac1 active PAK qui, liée à β-PIX, favorise le transport de WAVE2 le long des microtubules. PIP_2 (Rivera *et al.*, 2009) et Cdc42 sont capables d'activer WASP, qui active ensuite Arp2/3.

Les acteurs impliqués dans le remodelage du cytosquelette d'actine sont nécessaires à la formation des lamellipodes. Succinctement, le complexe Arp2/3 qui stimule la polymérisation et la formation d'un dense maillage d'actine stabilisé par la cortactine, permet la formation des lamellipodes (Pollard *et al.*, 2000). Le complexe Arp2/3 est activé par WASP, lui- même activé par la Rho GTPase Rac1. La cofiline, protéine membre de la famille des ABP (actin binding protein), favorise la nucléation et la polymérisation de nouveaux filaments d'actine par Arp2/3 en formant des extrémités barbées d'actine F par désassemblage des microfilaments. Les formines (mDia1 et mDia2) sont responsables de la formation d'un noyau de nucléation qui initie la polymérisation de l'actine G en microfilaments, indépendamment ou non du complexe Arp2/3 (Ridley, 2011). L'activité des formines peut être augmentée par la profiline (Romero *et al.*, 2004, Gurel *et al.*, 2015). La myosine II semble également être impliquée dans la formation et la stabilisation des lamellipodes. En effet, des contractions acto-myosine II sont retrouvées à la base de la structure (Giannone *et al.*, 2007), et une étude suggère que la myosine II pourrait être responsable du désassemblage des microfilaments d'actine à l'arrière du lamellipode (Wilson *et al.*, 2010). La présence de RhoA, Rac1 et Cdc42 activés a été montrée dans ces structures (Machacek *et al.*, 2009) et certains de leur effecteurs et régulateurs sont impliqués dans leur formation. Parmi ces effecteurs, les sérine/thréonine

kinases PAK, engagées dans la régulation du cytosquelette d'actine et du réseau de microtubules (Bokoch, 2003) peuvent être activées par Rac et Cdc42 (Manser *et al.*, 1994). La RhoGEF βPIX de Cdc42 et Rac est capable d'interagir avec PAK (Manser *et al.*, 1998), pour favoriser la formation des lamellipodes.

La formation des lamellipodes dépend également du phospholipide phosphatidylinositol (3,4,5)-triphosphate (PIP_3) qui facilite l'activation de WAVE, régulateur de Arp2/3 (Lebensohn and Kirschner, 2009). Ce second messager lipidique produit par la PI3K (phosphoinositide 3 kinase), dont l'activation résulte de sa phosphorylation par la petite GTPase Ras dépendante des facteurs de croissance (Kolsch *et al.*, 2008), a été retrouvé augmenté dans les lamellipodes (Weiger *et al.*, 2009). PIP_3 est capable d'activer la RhoGEF P-Rex1 (Phosphatidylinositol 3,4,5-trisphosphate-dependent Rac exchanger 1 protein), reponsable de l'activation de Rac1 (Lucato *et al.*, 2015). La surexpression de cette RhoGEF dans le cancer du sein est asoccié à un mauvais pronostic (Sosa *et al.*, 2010).

La formation des lamellipodes est stimulée par de nombreux facteurs extracellulaires tels que les facteurs de croissance, présents dans le microenvironnement tumoral dont EGF et HGF. Dans la lignée de cellules cancéreuses mammaires de rat MTLn3, l'activation de la voie de signalisation de l'EGF est directement corrélée à une augmentation de l'invasion et de l'apparition des métastases (Xue *et al.*, 2006). Dans les cellules cancéreuses mammaires MDA-MB-231, l'HGF est capable d'induire la formation de lamellipodes via l'activation de Rac1 et PAK1, qui permettent le transport de WAVE2 (effecteur de Rac) le long des microtubules (Takahashi and Suzuki, 2008, 2009). Dans ce contexte, la stimulation des cellules avec l'HGF induit la colocalisation de βPIX et WAVE2 (Morimura *et al.*, 2009). Dans les cellules cancéreuses prostatiques, l'activation de WAVE3 par la voie de l'HGF augmente la migration et l'invasivité cellulaire (Moazzam *et al.*, 2015).

Au niveau du lamellipode, les points d'adhésion focale s'assemblent pour promouvoir les forces de traction et la myosine II favorise la maturation de ces points d'adhésion (Choi *et al.*, 2008).

I.2.3.2. Filopodes

Les filopodes sont l'un des facteurs clefs de la migration cellulaire puisqu'ils sont capables d'augmenter la motilité des cellules et sont considérés comme l'une des caractéristiques des cellules cancéreuses invasives (Vignjevic *et al.*, 2007). Par ailleurs, il a été

montré que de nombreux gènes associés à la formation des filopodes sont surexprimés dans les carcinomes mammaires de mauvais pronostique (Arjonen *et al.*, 2011).

Les filopodes sont des protrusions membranaires cylindriques de quelques dixièmes de microns de diamètre (0,1-0,3 µm) et de 1 à 40 µm de longueur (Mogilner and Rubinstein, 2005) composées de filaments d'actine organisés en faisceaux parallèles, hautement dynamiques (Small *et al.*, 2002). Les faisceaux d'actine composant les filopodes prennent naissance au niveau du réseau d'actine présent dans le lamellipode (Svitkina *et al.*, 2003, Small, 2010) (voir Figure 9) et s'étendent en direction du front de migration cellulaire. L'extrémité barbée des filaments d'actine contient de nombreuses ABP. L'addition de monomères d'actine G aux microfilaments se déroule à la pointe du filopodes. La croissance et la rétractation des filopodes résultent de la balance entre la polymérisation de l'actine à la pointe et le flux rétrograde vers la base de la structure dépendant de la myosine (Mellor, 2010). Il existe de petits filopodes appelés micropointes (microspike), dont la structure est similaire à celle des filopodes (Svitkina *et al.*, 2003). Les filopodes sont constitués de nombreuses protéines ; d'une part impliquées dans la dynamique du cytosquelette et d'autre part, d'intégrines et de cadhérines leur conférant un rôle de « senseur » du microenvironnement (Ridley *et al.*, 2003) et de structure importante dans l'adhésion cellule-cellule et cellule-matrice (Gardel *et al.*, 2010).

Les petites GTPases (Nobes and Hall, 1995, Pellegrin and Mellor, 2005), le complexe Arp2/3 (Pollard and Borisy, 2003), WAVE (Stradal and Scita, 2006), la myosine X (Bohil *et al.*, 2006, Tokuo *et al.*, 2007), la fascine (Vignjevic *et al.*, 2006, Jaiswal *et al.*, 2013) et les formines (Schirenbeck *et al.*, 2005, Yang *et al.*, 2007) sont des protéines clefs dans la formation des filopodes. La structure schématique des filopodes est présentée en Figure 10.

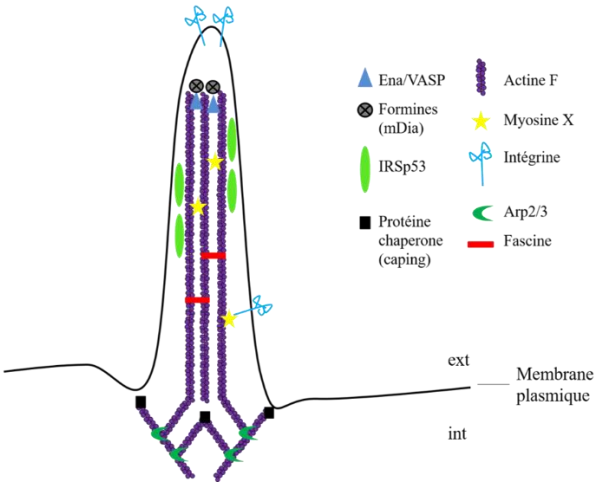

Figure 10 : Organisation des protéines constituant les filopodes.

Les faisceaux d'actine parallèles sont stabilisés par la fascine. Ena/VASP agit en synergie avec Arp/3 qui polymérise de nouveaux filaments. La Myosine X permet l'adressage des intégrines dans les invadopodes. Cdc42 active la formation du complexe IRSp53/Mena pour favoriser la formation des filopodes. La myosine permet l'adressage des intégrines dans les filopodes.

La Rho GTPase Cdc42 est la composante majeure de la formation des filopodes et interagit avec de nombreuses protéines constitutives des filopodes. Cdc42 intervient dans l'initiation de formation des filopodes via WASP. Elle est également capable de favoriser la formation du complexe IRSp53/Mena (Insulin-Receptor Substrate p53 et Mena, protéine de la famille Ena/VASP, voir ci-après) et d'induire la formation de filopodes dans des fibroblastes (Krugmann *et al.*, 2001). Cdc42 peut être activée par des protéines de la famille E2F1A, qui augmentent la quantité de PI(4,5)P_2 à la membrane plasmique, stimulant ainsi la formation des filopodes (Jeganathan *et al.*, 2008). D'autres Rho GTPases sont impliquées dans la formation des filopodes, ce sont les RIF (Rho In Filopodia). Elles agissent notamment par l'intermédiaire de la formine mDia2 qui induit la nucléation des microfilaments d'actine indépendamment de Cdc42 (Pellegrin and Mellor, 2005). Des effecteurs des Rho GTPases influent la formation des lamellipodes et des filopodes tels que PAK1 (Sells *et al.*, 1997) et PAK4. L'activation de PAK1 conduit à une augmentation de la migration des cellules HeLa et favorise la formation des filopodes dans ces cellules (Kameritsch *et al.*, 2015). PAK4 permet un enrichissement en actine corticale (Abo *et al.*, 1998) et la formation d'extrémités barbées d'actine (Spratley *et al.*, 2011).

Le complexe Arp2/3 intervient dans la nucléation de nouveaux filaments d'actine et peut être activé par les membres de la famille WASP (plus particulièrement WAVE2) (Lebrand *et al.*, 2004). La polymérisation des filaments d'actine peut être augmentée de façon synergique grâce à l'interaction de VASP (protéine de la famille Ena/VASP, Vasodilatator-Stimulated

Phosphoprotein) et Arp2/3 avec WAVE. En effet, le complexe Arp2/3 activé par WAVE crée un branchement d'actine directement transféré à VASP (Havrylenko *et al.*, 2015). Les protéines Ena/VASP sont localisées dans les points d'adhésion focale et dans les filopodes, et favorisent l'élongation des filaments d'actine de par leur activité « anticapping », c'est-à-dire qu'elles libèrent l'extrémité positive des filaments d'actine, la rendant accessible aux protéines responsables de la polymérisation ou dépolymérisation de l'actine (Tokuo and Ikebe, 2004). Les protéines qui possèdent une activité dite de « capping » stabilisent les filaments d'actine et sont capables de se lier aux extrémités positives et négatives des filaments d'actine pour prévenir la dissociation ou l'assemblage de nouveaux monomères d'actine G. Bien que non nécéssaire à la formation des filpodes induite par la mysoine X (Bohil *et al.*, 2006), l'adressage de la protéine VASP à l'extrémité des filopodes fait intervenir la myosine X (Tokuo and Ikebe, 2004), elle-même responsable de l'adressage des intégrines dans ces structures (Zhang *et al.*, 2004). L'ARNm de la myosine X est surexprimé dans le cancer du sein (Arjonen *et al.*, 2014). Par ailleurs, le transport des intégrines aux extrémités des filopodes favorise leur élongation et l'adhésion cellulaire (Zhang *et al.*, 2004).

La fascine est une ABP surexprimée dans divers carcinomes humains (Hashimoto *et al.*, 2005, Hashimoto *et al.*, 2006, Qualtrough *et al.*, 2009, Teng *et al.*, 2013) dont le cancer du sein (Esnakula *et al.*, 2014). Cette protéine permet de stabiliser les faisceaux d'actine dans les invadopodes (voir I.2.4.2 Invadosomes page 55) et augmente le potentiel métastatique des cellules cancéreuses de pancréas, ainsi que l'invasivité cellulaire via l'augmentation de la formation des filopodes (Li *et al.*, 2014). La fascine, dont l'expression peut être inhibiée par la p53, est fortement exprimée dans les cellules cancéreuses de colon, et favorise la formation des filopodes. Son expression est corrélée à l'invasivité cellulaire et à l'agressivité des tumeurs (Sui *et al.*, 2015).

Récemment, une étude immunohistochimique a permis de mettre en évidence la corrélation positive entre l'expression de la fascine et l'apparition de métastases chez des patientes atteintes d'un carcinome mammaire (Omran and Al Sheeha, 2015).

Les formines sont responsables de l'induction de la formation des filaments d'actine (Goode and Eck, 2007). Elles sont exprimées dans les lignées cancéreuses mammaires MDA-MB-231 (Kitzing *et al.*, 2010) et sont surexprimées dans plusieurs cancers dont les tumeurs mammaires (Nurnberg *et al.*, 2011). La structure des formines contient un domaine N-terminal GBD (G-protein Binding Domain) leur permettant d'être activées par les Rho GTPases. Plus particulièrement, mDia2 contient un motif CRIB (Cdc42 and Rac Interacting Domain) directement impliqué dans son interaction avec la Rho GTPase activatrice Cdc42

(Mellor, 2010). De plus, mDia2 est nécessaire à la formation des filopodes dépendante de Rif (Pellegrin and Mellor, 2005).

Au cours de la migration et de l'invasion cellulaire, les interactions cellule-cellule et cellule matrice sont primordiales, notamment pour initier les forces de contraction. Des structures d'adhésion ont été identifiées tout au long des filopodes, et sont importantes pour la stabilité de la structure (Jacquemet *et al.*, 2015), leur exacte composition reste cependant à déterminer.

I.2.3.3. Blebs

Les blebs sont des protrusions membranaires sphériques (de 2 à 15 µm de diamètre) qui s'étendent à partir du cytoplasme et se rétractent au niveau de leur site d'initiation. L'apparition d'un bleb résulte du décollement de la membrane plasmique et du cortex d'actine, conséquence de la contraction du complexe acto-myosine qui augmente la pression hydrostatique à l'intérieur de la cellule (Bovellan *et al.*, 2010). Alors que l'initiation de la formation de ces structures ne nécessitent pas de polymérisation d'actine (Charras and Paluch, 2008), l'expansion du bleb est stoppée et stabilisée par la formation d'actine F au niveau du cortex de la structure (Fackler and Grosse, 2008). La formation des blebs est plus couramment décrite dans des cellules en apoptose (Robertson *et al.*, 1978). Néanmoins, ils sont également observables pendant la cytodiérèse (Fishkind *et al.*, 1991), l'adhésion d'une cellule sur un substrat (Bereiter-Hahn *et al.*, 1990), l'activation des récepteurs P2X7 (Roger and Pelegrin, 2011), la migration et l'invasion d'une matrice 3D (Charras and Paluch, 2008). En effet, au cours de la migration cellulaire, les blebs forment une importante protrusion au front de migration (Charras and Paluch, 2008). Les blebs sont des structures caractéristiques de l'invasion de la MEC dite « amoeboide » (voir I.2.4.3 Invasion mésenchymateuse, amoeboïde et transitions page 58).

La formation des blebs se déroule en 3 étapes : initiation, expansion et rétraction. L'initiation de la formation des blebs peut résulter de deux mécanismes : de la dissociation de la membrane et du cortex d'actine, ou de la rupture du cortex d'actine. Ces deux mécanismes sont la conséquence de la contraction du complexe acto-myosine, qui dépend de l'activation de la myosine II par RhoA et ses effecteurs ROCK et MLCK (Charras and Paluch, 2008). Le cortex contractile est une fine couche de cytosquelette située sous la membrane plasmique riche en filaments d'actine, myosine II et ABP (Bray and White, 1988).

L'étape d'initiation est suivie de l'expansion du bleb, générée par l'augmentation de la pression à l'intérieur de la cellule. Cette phase ne dure que 5 à 30 secondes. La dernière étape

de la « vie » d'un bleb consiste en sa rétraction. Elle est corrélée à la repolymérisation du cortex d'actine (Laser-Azogui *et al.*, 2014). Dans les cellules en migration, de nouveaux blebs peuvent se former après la repolymérisation du cortex (Kardash *et al.*, 2010).

La formation de blebs dépend des types cellulaires. Certaines cellules sont capables de former spontanément des blebs résultant de la contraction du complexe acto-myosine, alors que d'autres sont capables de passer de l'élongation de protrusions riches en actine à la formation des blebs, en fonction du substrat. RhoA est l'actrice majeure dans la formation des blebs du fait de sa capacité à activer ROCK, induisant la phosphorylation de MLC2 (pMLC2) via l'inhibition de la MLC phosphatase. ROCK est un médiateur de la fonctionnalité de RhoA dans les cellules cancéreuses et son activation se traduit par l'augmentation de la contraction du complexe acto-myosine (O'Connor and Chen, 2014). Il a été montré dans les macrophages que RhoA est présente au niveau des blebs et que son inhibition ainsi que celle de ROCK, par l'utilisation d'inhibiteurs pharmacologiques ou de RhoGDI spécifiques de RhoA, diminue l'apparition des blebs (Charras *et al.*, 2006). Dans des cellules de mélanome, l'utilisation d'un inhibiteur de ROCK diminue également la formation des blebs, et l'activité de cette kinase est dépendante de l'activation de RhoA et RhoC (Sahai and Marshall, 2003). L'induction des blebs par la voie RhoA/ROCK a également été montrée dans une lignée cellulaire d'adénocarcinome (Cartier-Michaud *et al.*, 2012, de Toledo *et al.*, 2012). Dans un modèle d'étude de l'invasivité dans une matrice en trois dimensions, il a été montré que les cellules cancéreuses mammaires MDA-MB-231 sont capables de former des blebs principalement à l'arrière de la cellule, où la contraction de l'actine corticale est la plus forte. Ceci dépend de l'activation de la voie de signalisation RhoA/ROCK/Myosine II (Poincloux *et al.*, 2011).

I.2.4. Invasion de la matrice extracellulaire

I.2.4.1. Remodelage de la matrice extracellulaire

La composition des matrices extracellulaires varie en fonction des tissus (développement normal) mais également en fonction du contexte physiopathologique (fibroses et cancers). De par les protéines, les glycoprotéines et glycosaminoglycanes qui la composent, la rigidité et la densité de la matrice extracellulaire diffèrent (Friedl and Wolf, 2010). *In vivo*, les cellules cancéreuses sont limitées par une matrice généralement riche en collagène (collagène de type IV majoritaire dans la lame basale et de type I dans les tissus conjonctifs), qu'elles envahissent avant de coloniser les tissus environnants. Les capacités d'adaptation des

cellules cancéreuses aux différents microenvironnements rencontrés défini leur niveau d'agressivité et leur propension à former des métastases dans un site distant de la tumeur primaire. Dans un modèle murin, il a été montré que l'élévation de la proportion de collagène I dans le stroma augmente la rigidité de la matrice et est lié à l'invasion des tissus et le développement de métastases dans le cancer du sein (Provenzano *et al.,* 2008). Au cours du développement tumoral, l'augmentation de la rigidité de la matrice due à une augmentation de la quantité de collagène I favorise également le développement d'adhésions focales (Levental *et al.,* 2009) et stimule les signaux d'adhésion cellulaires relatifs à la voie FAK/Rho/ERK (Provenzano *et al.,* 2009). Les protéines composant la matrice extracellulaire peuvent stimuler l'activation des intégrines et promouvoir la migration cellulaire (Levental *et al.,* 2009). Dans des fibroblastes murins, la rigidité de la matrice extracellulaire influence l'activation du dimère α5β1, qui induit la voie de signalisation ROCK/myosine II et la réorganisation du cytosquelette (Balcioglu *et al.,* 2015). Les glycoprotéines de surface peuvent elles aussi jouer un rôle dans la migration et l'invasion cellulaire. C'est le cas de CD44, une glycoprotéine de surface impliquée dans les interactions cellule-cellule et cellule-matrice. La liaison de CD44 à l'acide hyaluronique, composant de la matrice extracellulaire, augmente l'activité Src kinase, qui phosphoryle Twist et permet sa translocation nucléaire (Bourguignon *et al.,* 2010). Twist participe à la transition épithélio-mésenchymateuse et active la transcription du gène codant Akt2, impliquée dans la survie et l'invasion des cellules cancéreuses mammaires (Cheng *et al.,* 2007).

La composition du milieu extracellulaire peut inhiber le phénotype malin des cellules cancéreuses. *In vitro,* il a été récemment montré que des cellules cancéreuses mammaires cultivées dans du milieu contenant 10 % d'albumen (blanc d'œuf) rétablissent leur polarité apico-basale, expriment des marqueurs épithéliaux (tels que E-cadhérine et β-caténine membranaire) et produisent la β-caséïne, marqueur de différenciation des cellules épithéliales mammaires. De plus, la présence d'albumen dans le milieu de culture permet d'induire la formation de structures 3D caractéristiques de glande mammaire différenciée (canaux et acini) même lorsque les cellules sont cultivées en 2D (D'Anselmi *et al.,* 2013).

Le remodelage de la matrice extracellulaire est fonction des protéases sécrétées par les cellules cancéreuses, mais également des cellules non cancéreuses de la tumeur telles que les macrophages et les fibroblastes associés à la tumeur (Afsharimani *et al.,* 2014, Ota *et al.,* 2014). Dans le cas du cancer du sein, il a été montré qu'une forte expression protéique d'inhibiteurs de protéases est corrélée à un bon pronostic (Bergamaschi *et al.,* 2008). Au cours de la TEM, le collagène IV majoritaire dans la lame basale est clivé et remplacé par du collagène I et de la

fibronectine, favorisant la migration cellulaire via l'activation des intégrines. Pendant la progression tumorale et plus particulièrement au cours du développement des métastases, les protéines de la MEC sont clivées par différentes enzymes dont les métalloprotéases (MMP), les adamalysines, les meprines et des cathepsines. Les MMP sont les plus connues et elles sont capables de cliver les composants de la MEC (dont collagènes, fibronectine, laminine, élastine, gélatine) (Bonnans *et al.*, 2014). La sécrétion d'enzymes protéolytiques est associée aux cellules cancéreuses de type mésenchymateuses, via la formation des invadopodes.

I.2.4.2. Invadosomes

Le terme « invadosome » regroupe deux structures cellulaires ayant des propriétés et fonctions équivalentes d'invasion de la matrice extracellulaire mais trouvées dans des modèles cellulaires différents : les podosomes dans les cellules saines et les invadopodes, dans les cellules cancéreuses. Les invadopodes sont des protrusions de cellules cancéreuses de 8 µm de diamètre et 5 µm de longueur (Linder, 2009, Brisson *et al.*, 2012), dans les matrices extracellulaires et capables de les dégrader (Chen, 1989, Buccione *et al.*, 2009), et en particulier dans la membrane basale (Schoumacher *et al.*, 2011) sous-jacente aux cellules épithéliales. Schématiquement, la formation des invadopodes semble se dérouler en trois étapes. Dans un premier temps, les cellules établissent des adhésions focales avec la matrice extracellulaire via les Src kinases, des intégrines, notamment α5β3 et β1, et la FAK (focal adhesion kinase). L'activation des intégrines induit l'autophoshorylation de FAK sur la tyrosine 397 qui le lie à Src, lui-même phosphorylé au niveau des adhésions focales (Chan *et al.*, 2009, Oser *et al.*, 2009). Dans un second temps, l'assemblage d'actine, cortactine, N-WASP, cofiline et Tks5 (tyrosine kinase substrate 5, protéine d'échaffaudage des invadopodes impliquée dans la croissance tumorale *in vitro* et *in vivo* (Blouw *et al.*, 2008, Blouw *et al.*, 2015)) forme des structures appelées « invadopodes immatures » (Artym *et al.*, 2006, Chan *et al.*, 2009, Desmarais *et al.*, 2009, Oser *et al.*, 2009). Ces invadopodes immatures sont ensuite détruits, ou stabilisés en invadopodes fonctionnels, capables de dégrader la matrice. Dans les invadopodes matures, la cofiline est séquestrée par la cortactine, ce qui la rend inactive. Une fois phosphorylée par des kinases de la famille Src ou Abl sur des résidus tyrosine Y421, Y466 et Y482 (Head *et al.*, 2003, Boyle *et al.*, 2007), la cortactine relargue la cofiline qui favorise la polymérisation de l'actine par Arp2/3 via la formation d'extrémités barbées. La fascine, impliquée dans la stabilisation des filopodes, intervient également dans la stabilisation du réseau d'actine présent dans les invadopodes, notamment lorsqu'elle est phosphorylée au

niveau du résidu sérine 39 (Li *et al.*, 2010). Enfin, la maturation des invadopodes se termine par l'adressage d'enzymes responsables de la dégradation de la MEC telles les MMP (Artym *et al.*, 2006, Oser *et al.*, 2009). La structure d'un invadopode mature est présentée en Figure 11.

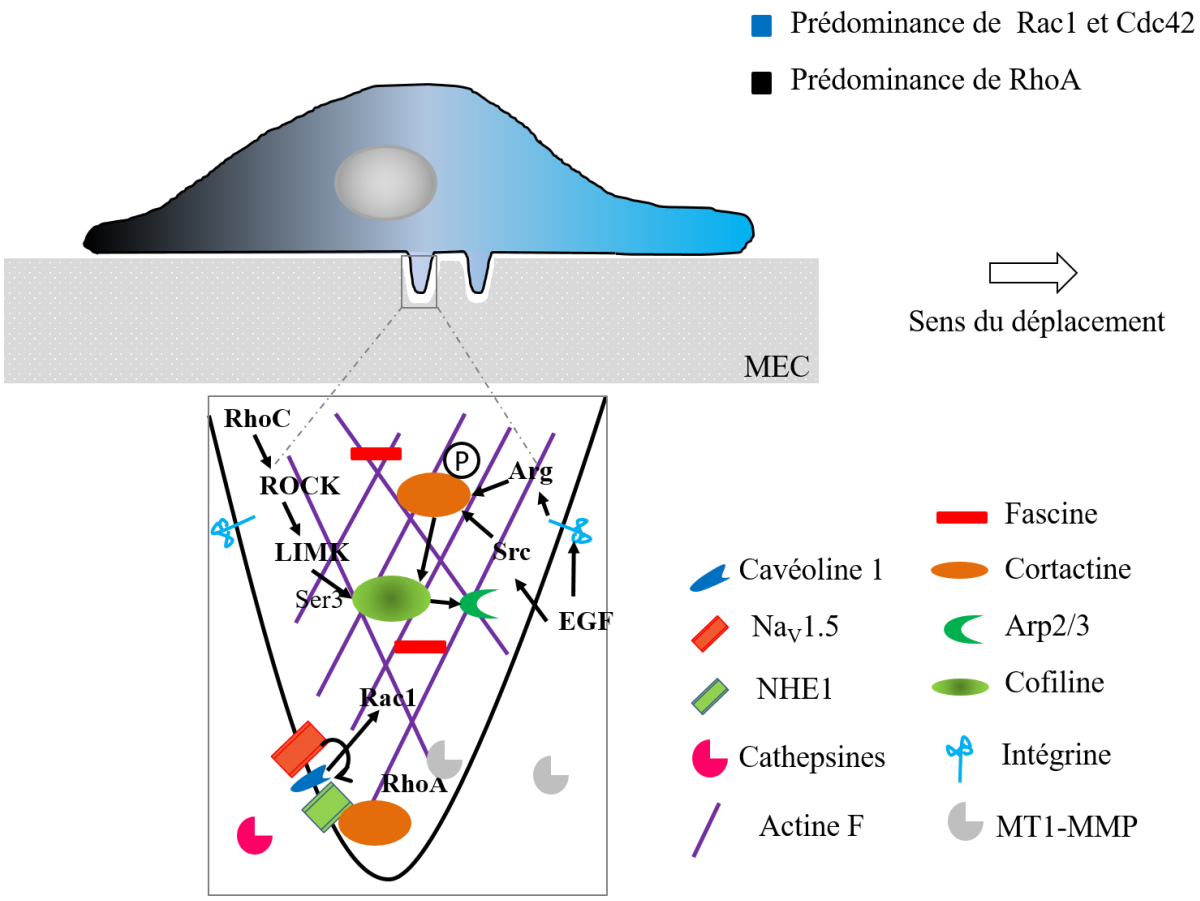

Figure 11 : Schéma d'un invadopode mature.

La phosphorylation de la cortactine permet le relargage de la cofiline qui active le complexe Arp2/3 responsable de la polymérisation de l'actine. RhoC active la LIMK via ROCK et phosphoryle la cofiline sur la sérine 3, libérant les filaments d'actine. RhoA favorise l'adressage de MT1-MMP à la membrane, responsable du clivage de la MEC. Le canal $Na_V1.5$ augmente l'activité NHE1, induisant une diminution du pH extracellulaire et l'activation des cathepsines.

La formation des invadopodes dans cellules cancéreuses est associée à leurs capacités invasives *in vitro* et métastatiques *in vivo*. C'est le cas dans le cancer du sein (Coopman *et al.*, 1998, Brisson *et al.*, 2013), de la vessie (Yamamoto *et al.*, 2011), du colon (Schoumacher *et al.*, 2010) et de la tête et du cou (Alblazi and Siar, 2015). Elle peut être stimulée par des facteurs de croissance tel l'EGF (Oser *et al.*, 2009) et la composition de la MEC (Gould and Courtneidge, 2014). Dans les cellules cancéreuses mammaires, il a été montré que la maturation de ces structures, responsables de la dégradation de la matrice, pouvait être médiée par la

phosphorylation de la cortactine via les tyrosines kinases Src et Arg en réponse à l'EGF (Mader *et al.*, 2011). La maturation des invadopodes dépendante de l'EGF requière l'activation de Arg par l'intégrine β1 (Beaty *et al.*, 2013). Cette voie régule l'interaction de l'échangeur sodium-proton NHE1 avec la cortactine qui serait modulée par les protéines ERM (Ezrin-Radixin-Moesin) (Bravo-Cordero *et al.*, 2013). La Rho GTPase RhoA est impliquée dans la maturation des invadopodes en favorisant le recrutement des metalloprotéases matricielles MT1-MMP au niveau des zones de dégradation de la MEC (Sakurai-Yageta *et al.*, 2008).

L'expression et l'activité de NHE1 dans les invadopodes (Brisson *et al.*, 2011, Brisson *et al.*, 2013, Beaty *et al.*, 2014) sont impliquées dans l'invasivité des cellules cancéreuses de par sa contribution dans l'élongation de ces structures (Busco *et al.*, 2010) et ses propriétés régulatrices du pH intra et extracellulaire. L'augmentation du pH intracellulaire due à l'activité de l'échangeur permet le relargage de la cofiline par la cortactine et favorise donc la polymérisation de l'actine (Magalhaes *et al.*, 2011). Dans une lignée cellulaire fortement invasive, l'activité de NHE1 favorise l'acidification du pH extracellulaire au niveau des invadopodes, permettant l'activation de cathepsines B et S capables de dégrader la matrice extracellulaire (Gillet *et al.*, 2009). Ces cathepsines jouent un rôle clef dans l'invasion de la MEC dépendante du canal sodique $Na_V1.5$. Ce dernier régule allostériquement l'activité de NHE1 le rendant plus actif pour une gamme de pH intracellulaires compris entre pH6,4 et pH7. Par ailleurs, $Na_V1.5$ en régulant l'activité Src kinase, stimule la phosphorylation de la cortactine et la dynamique du cytosquelette. Globalement, l'activité $Na_V1.5$ favorise l'activité protéolytique des invadopodes dans les cellules cancéreuses mammaires MDA-MB-231 (Brisson *et al.*, 2013). Le canal sodique $Na_V1.5$ et l'échangeur NHE1 sont colocalisés avec la cavéoline 1, dans des radeaux lipidiques. Les radeaux lipidiques sont des structures membranaires riches en cholestérol et sphingolipides, qui constituent de véritables plateformes de signalisation cellulaire (Gasparski and Beningo, 2015). Les cavéoles interagissent fortement avec le cytosquelette, et leur endocytose peut être modulée via une RhoGEF spécifique de Cdc42 (Head *et al.*, 2014). La cavéoline 1 favorise la migration de cellules cancéreuses et non cancéreuses. Dans les fibroblastes, la migration dépendante de la cavéoline 1 est associée à une accumulation de celle-ci à l'arrière des cellules et à l'activation de RhoA (Grande-Garcia *et al.*, 2007, Sun *et al.*, 2007). Dans les cellules microgliales, la phosphorylation de la cavéoline 1 dans les podosomes permet l'invasion (Vincent *et al.*, 2012). Dans des cellules cancéreuses à fort potentiel métastatique, la cavéoline 1 favorise la migration en activant Rac1 via la Rab GTPase Rab5 et la RhoGEF Tiam1 spécifique de Rac1 (Diaz *et al.*, 2014). Dans les cellules cancéreuses mammaires, l'activation de la Rho GTPase RhoC permet d'activer la kinase ROCK.

Cette kinase active ensuite par phosphorylation la LIM kinase, qui phosphoryle elle-même la cofiline sur la sérine 3. La cofiline ainsi inactivée n'est plus capable de se lier aux filaments d'actine pour favoriser leur dépolymérisation. De ce fait, la stabilisation de l'actine F contribue à la formation d'invadopodes (Bravo-Cordero *et al.*, 2011).

I.2.4.3. Invasion mésenchymateuse, amoeboïde et transitions MAT-AMT

Deux phénotypes invasifs ont été décrits. Le premier, dit « mésenchymateux », se caractérise par des cellules polarisée selon un axe « avant-arrière » du fait de la polymérisation asymétrique du cytosquelette, entrainant la formation de lamellipodes et filopodes au front de migration, et ont une morphologie allongée. Ces cellules migrent lentement (0,1-1 µm.min^{-1}) et sont capables de dégrader la matrice extracellulaire grâce aux structures invasives, les invadopodes. Ces cellules sont dites « path-generating », c'est-à-dire qu'elles sont capables de générer un « chemin » au travers de la matrice extracellulaire grâce à la sécretion d'enzymes protéolytiques. De plus, la dégradation de la MEC par des protéases est associée à l'invasivité cellulaire et au développement de métastases (Fearon and Vogelstein, 1990). Le second, dit « amoeboïde » est décrit ci-dessous. Les caractéristiques des phénotypes invasifs mésenchymateux et amoeboïde sont décrits dans la Table 3.

Table 3 : Mécanismes cellulaires et moléculaires impliqués dans les phénotypes mésenchymateux et amoeboïde.

D'après Friedl and Wolf, 2003.

Caractéristiques	Mésenchymateux	Amoeboïde
Forme des cellules	Allongée, « fibroblaste-like » (longueur 50-200 µm)	Arrondie/ellipsoïde, « amoeboid-like » (longueur 10-30 µm)
Vitesse de migration	Faible (0.1-1 µm.min^{-1})	Faible à élevée (1-10 µm.min^{-1})
Interactions cellule-matrice	Intégrines en clusters et points focaux	Intégrines non focalisées
Structure du cytosquelette d'actine	Corticale	Corticale, contraction du complexe acto-myosine
Forces d'adhésion générée	Fortes, fibres de traction	Faible, petites fibres
Remodelage protéolytique de la matrice	Présente à très étendue	Absente

Caractéristiques	Mésenchymateux	Amoeboïde
Mécanisme de migration cellulaire	Dépendant de la traction	Propulsif, diffusion du cytoplasme
Adaptation à la matrice	Génération de trajectoire, dégradation protéolytique de la matrice	Senseur de trajectoire, propulsion du cytoplasme vers l'avant, anneau de constriction
Cellules non néoplasiques, prototypiques	Fibroblastes, cellules de muscle lisse	Lymphocytes, neutrophile
Cellules néoplasique, carcinomes	Fibrosarcomes, glioblastomes, cancers épithéliaux dédifférenciés	Lymphomes, carcinome pulmonaire à petites cellules, carcinome prostatique à petites cellules
Structures cellulaires associées	Invadopodes, filopodes, lamellipode	Blebs

L'invasion amoeboïde a très souvent été décrite pour les cellules immunitaires (macrophages, lymphocytes et leucocytes) et elle est également observée pour les cellules cancéreuses. Il existe deux types de migration amoeboïde : le premier est caractérisé par des cellules non adhérentes au substrat et de morphologie arrondies, avançant dans la matrice de manière propulsive. Le second type de migration amoeboïde a été montré dans des cellules plus allongées que dans le premier type, capable de générer des protrusions au front de migration (comme les lamellipodes et les filopodes) et de faibles interactions avec la matrice (Friedl and Wolf, 2010). D'une manière générale, les cellules dites « amoeboïdes » présentent une vitesse de migration élevée (1-10 $\mu m.min^{-1}$), une morphologie arrondie et des blebs sont observés à la surface cellulaire. Ces cellules exercent de faibles adhésions avec la matrice et ne présentent pas ou peu de fibres de stress d'actine (Lammermann and Sixt, 2009). Les cellules qui migrent de manière amoeboïde sont capables d'envahir la matrice indépendamment de la protéolyse et présentent une forte force de contraction acto-myosine (régulée par RhoA/ROCK) pour déformer la matrice extracellulaire et se mouvoir au travers de celle-ci. (Sahai and Marshall, 2003, Wyckoff *et al.*, 2006). Le déplacement est de type dit propulsif.

La migration amoeboïde a été beaucoup étudiée dans les cellules de mélanomes, et ceci a permis de mettre en évidence différentes voies de signalisation impliquées dans le maintien de ce phénotype invasif. Par exemple, dans la lignée A375 qui présente un phénotype mésenchymateux, l'activation de Cdc42 augmente la contraction du complexe acto-myosine DOCK10 et Pak2. Ceci favorise la morphologie arrondie des cellules ainsi que leur invasivité.

Néanmoins dans ces cellules, l'inhibition de Cdc42 inhibe à la fois l'invasion mésenchymateux et amoeboïde. (Gadea *et al.*, 2008). Le maintien du phénotype amoeboïde est assuré par l'α-actinine 4 (ABP) dans ces mêmes cellules (Shao *et al.*, 2014). Dans d'autres lignées cellulaires, l'importance de la voie RhoA/ROCK/MLC dans l'invasion amoeboïde a été démontrée. En effet, la suractivation de RhoA et ROCK augmente l'invasion amoeboïde au travers une matrice de Matrigel™ de cellules de sarcome de rat et favorise le recrutement de pMLC au front de migration. Dans des cellules non invasives, l'activation de RhoA restaure le phénotype invasif (Kosla *et al.*, 2013). La surexpression de RhoA et RhoC augmente l'invasivité et la morphologie arrondie de fibroblastes embryonaires de souris via l'activation de la formine FMNL2, alors que l'extinction de l'expression de la formine Dia2 favorise le phénotype amoeboïde (Kitzing *et al.*, 2010).

Dans un environnement 3D, il a été montré que des mêmes cellules sont capables de migrer différemment suivant la rigidité de la matrice, la protéolyse extracellulaire et les facteurs de signalisation solubles (Wolf *et al.*, 2003, Petrie and Yamada, 2012). L'invasion amoeboïde fût initialement décrite comme indépendante de la protéolyse matricielle, mais l'étude du passage de cellules cancéreuses amoeboïdes au travers d'une matrice de collagène fait également intervenir sa dégradation (Hooper *et al.*, 2006). L'utilisation d'inhibiteurs de protéases induit une morphologie de type amoeboïde des cellules cancéreuses mammaires MDA-MB-231 (Wolf *et al.*, 2003). Récemment, il a été montré que la sécrétion de la métalloprotéase MMP9 favorise le phénotype amoeboïde et augmente la contraction acto-myosine dans des cellules de mélanome invasif. La MMP9 est surexprimée par la voie ROCK/Jak/Stat3, mais elle favorise la motilité cellulaire indépendamment de son domaine catalytique (Orgaz *et al.*, 2014).

Ces observations ont permis de montrer que les cellules pouvaient passer d'un phénotype mésenchymateux à amoeboïde et vice-versa, en fonction de la composition de la matrice extracellulaire (voir Figure 12). On parle alors de transition mésenchymato-amoeboïde (« mesenchymal-to-amoeboid transition », ou MAT en anglais) ou de transition amoeboïde mésenchymateuse (« amoeboid-to-mesenchymal », ou AMT en anglais). Elles confèrent par conséquent un caractère agressif aux cellules cancéreuses qui peut être associé au développement des métastases (Giannoni *et al.*, 2013). En effet, ces transitions permettent aux cellules de s'adapter aux différents microenvironnements lors de l'invasion des tissus, notamment au cours de l'intravasation et l'extravasation.

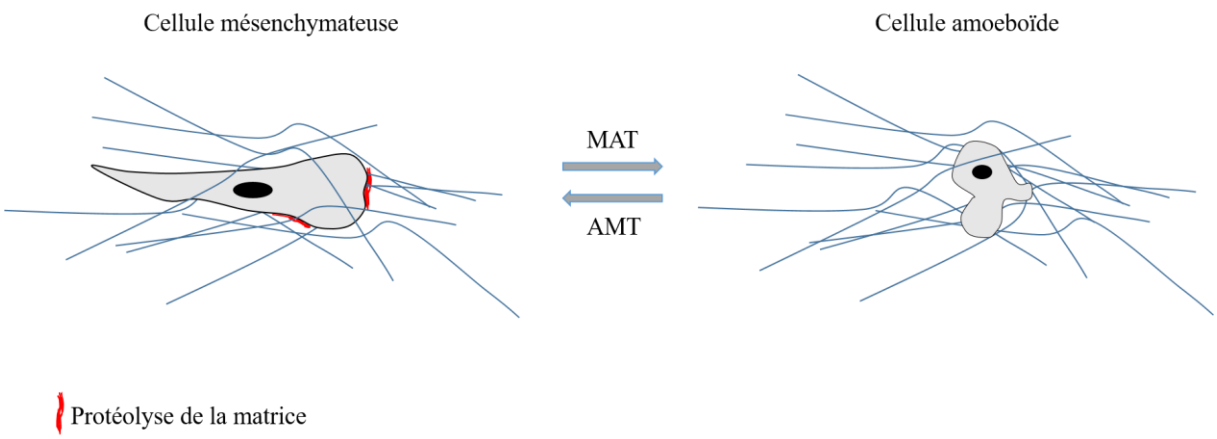

Figure 12 : Transition mésenchymato-amoeboïde (MAT) et transition amoeboïde mésenchymateuse (AMT). Les cellules cancéreuses mésenchymateuses sont capables d'envahir la matrice extracellulaire après protéolyse matricielle. En fonction des conditions environnementales, les cellules cancéreuses sont capables de subir la transition mésenchymato-amoeboïde réversible et sont ainsi capables d'envahir les tissus sans dégradation protéolytique de la matrice.

La MAT et l'AMT sont des phénomènes spontanés ou qui se produisent en réponse aux signaux du microenvironnement. Par exemple, l'invasion amoeboïde est souvent induite dans un environnement hypoxique ou expérimentalement, par l'utilisation d'inhibiteurs de protéases (Huang *et al.*, 2014, Hecht *et al.*, 2015). Les transitions MAT et AMT sont régulées par l'activité des Rho GTPases. Les protéines régulatrices de ces Rho GTPases (RhoGEFs, RhoGAPs et RhoGDIs) jouent donc un rôle important dans ces transitions. Il a notamment été montré que les RhoGDIs peuvent être phosphorylées par la protéine kinase C α (PKCα) sur les résidus sérine 34 et sérine 6, entrainant la dissociation de RhoA et RhoGDI (Garcia-Mata *et al.*, 2011). Récemment, l'implication de PKCα a été montrée dans les transitions MAT et AMT. Dans les cellules cancéreuses mammaires MDA-MB-231, l'activation pharmacologique de PKCα induit la MAT. En revanche, l'inhibition de PKCα (siARN ou dominant négatif) diminue l'invasion de ces cellules (Vaskovicova *et al.*, 2015). L'utilisation d'enzastaurine (inhibiteur de PKC) diminue l'expressoin génique d'uPAR (urokinase type plasminogen activator recpetor) et l'invasion cellulaire (Korner *et al.*, 2010). Sous l'activation de son ligand uPA, le récepteur uPAR induit la sécretion de MMP et la dégradation de la matrice. L'extinction de l'expression de ce récepteur permet de réduire à la fois le phénotype mésenchymateux et d'abolir le phénotype amoeboïde via la dérégulation de l'activité de RhoA et Rac1 (Margheri *et al.*, 2014).

Il a été montré que la composition de la MEC avait une influence sur le phénotype migratoire. Par exemple, les cellules de carcinosarcome mammaire sont capables de former des

lamellipodes lorsqu'elles sont ensemencées sur un substrat dont la rigidité est élevée (« elastic modulus » évalué en pascal, Pa), alors qu'elles forment préférentiellement des blebs sur un substrat moins dense (Bergert *et al.*, 2012). La composition du milieu extracellulaire peut activer les intégrines. Lorsque les cellules de fibrosarcomes HT1080 ont subi la MAT, l'expression de l'intégrine α2β1 est diminuée à la surface cellulaire. Par ailleurs, l'utilisation d'un anticorps bloquant dirigé contre cette intégrine diminue l'invasion mésenchymateuse sans affecter l'invasion amoeboïde. Le renouvellement des intégrines à la surface cellulaire est dépendant de la calpaïne, qui coopère avec les Src kinases pour moduler le renouvellement des adhésions focales dans les cellules mésenchymateuses. Dans des cellules amoeboïdes, la restauration du phénotype mésenchymateux par utilisation d'un inhibiteur de ROCK induit une augmentation de l'autophosphorylation de FAK sur le résidu Tyr397, et la dépendance à la calpaïne (Carragher *et al.*, 2006).

Les modifications morphologiques associées au changement de phénotype migratoire sont naturellement fonction du cytosquelette. En effet, la diminution expérimentale de l'activité du complexe Arp2/3 induit la transition entre les lamellipodes et les blebs, tandis que l'activation de Rac1 réduit la formation des blebs et induit la formation des lamellipodes (Bergert *et al.*, 2012). Par ailleurs, l'adressage de Rac1 à la membrane plasmique, ainsi que son activation, permettant l'induction de structures riches en actines tels que les lamellipodes sont sous le contrôle de Rab5, une petite GTPase importante dans le trafic vésiculaire (Palamidessi *et al.*, 2008). La RacGEF DOCK3 régule la transition entre la migration amoeboïde et mésenchymateuse et l'inhibition de Rac1 conduit à l'augmentation du mouvement amoeboïde au détriment du mouvement mésenchymateux (Sanz-Moreno *et al.*, 2008).

L'activation de la voie du TGFβ induit la TEM de la lignée de cellules épithéliale non cancéreuse mammaire MCF10A, qui déploie un large lamellipode riche en cortactine lorsqu'elles sont ensemencées sur une matrice de fibronectine. L'inhibition (pharmacologique ou par un siARN) du complexe Arp2/3 diminue le nombre d'adhésions focales et l'apparition de blebs, conférant aux cellules un phénotype amoeboïde (Beckham *et al.*, 2014).

L'existence de plusieurs phénotypes amoeboïdes est de plus en plus reportée dans la littérature. En effet, l'équipe de Piel (Liu *et al.*, 2015) a mis en évidence l'importance de la composition de la MEC sur l'induction d'un phénotype amoeboïde de type « A1 » ou « A2 ». Le phénotype A1 est caractérisé par la polymérisation locale de l'actine et une faible

contractilité acto-myosine. A l'inverse, le phénotype A2 se caractérise par un flux rétrograde d'actine cortical et une forte contraction du complexe acto-myosine. Les cellules de type A2 migrent plus rapidement que celles de phéntoype A1. Cette équipe a montré que l'augmentation de l'adhésion de fibroblastes humains au substrat via les intégrines diminue la vitesse de migration. En revanche, lorsque les cellules sont confinées dans un environnement spécifique, les lamellipodes sont moins larges et les cellules changent de morphologie. L'inhibition de l'expression de la taline inhibe la formation d'adhésion focale et induit la MAT (Liu *et al.*, 2015). Dans un modèle de cellules progénitrices de poisson zèbre, la formation de blebs stables (pouvant être assimilés au phénotype A2) induite par du LPA (lisophosphatidic acid, activateur de RhoA) résulte du flux rétrograde d'actine corticale (Ruprecht *et al.*, 2015).

II. Les sous-unités β des canaux sodiques dépendants du voltage (Na_V)

II.1. Régulation de la migration et de l'invasivité cellulaire des cellules cancéreuses par les canaux Na_V (Besson P.*et al,* How do voltage-gated sodium channels enhance migration and invasiveness in cancer cells ? BBA, 2015 Oct;1848(10 Pt B):2493-501).

Les sous-unités β ont été initialement décrites dans les cellules excitables comme régulatrices des propriétés électrophysiologiques des sous-unités α des canaux sodiques dépendants du voltage (Na_V). Les canaux sodiques dépendants du voltage Na_V sont des complexes protéiques membranaires dont l'activité, sous la forme de courant sodique (I_{Na}) est responsable de l'initiation et de la propagation de potentiels d'action dans les cellules excitables, dans lesquels ils ont été initialement décrits (Hodgkin and Huxley, 1952). Ils sont composés d'une sous-unité α dite sous-unité principale formant le domaine pore du canal, qui permet sélectivement le passage des ions Na^+ dans le sens du gradient électrochimique au travers de la membrane plasmique. Neuf ont été décrites : $Na_V1.1$ à $Na_V1.9$, codées par 9 gènes (*SCN1A* à *SCN5A* et *SCN8A* à *SCN11A*). Ces canaux sodiques sont classés en fonction de leurs propriétés pharmacologiques et en particulier de leur sensibilité à la tétrodotoxine (TTX), inhibiteur sélectif qui bloque le pore du canal (Noda *et al.*, 1989, Terlau *et al.*, 1991, Heinemann *et al.*, 1992). Les canaux sensibles à la TTX ($Na_V1.1$-1.4, $Na_V1.6$ et $Na_V1.7$) sont bloqués par des concentrations de TTX de l'ordre du nanomolaire, alors que les canaux résistants à la TTX ($Na_V1.5$, $Na_V1.8$ et $Na_V1.9$) sont bloqués par des concentrations de l'ordre du micromolaire ou centaine de micromolaire (Catterall *et al.*, 2003). Un courant sodique impliqué dans la régulation du potentiel invasif de cellules cancéreuses a été identifié dans les cancers mammaires (Roger *et al.*, 2003), prostatiques (Laniado *et al.*, 1997, Diss *et al.*, 2001), du col de l'utérus (Diaz *et al.*, 2007) et pulmonaires (Roger *et al.*, 2007). Dans les cellules cancéreuses mammaires, ce courant sodique a été attribué à l'expression fonctionnelle du canal $Na_V1.5$ résistant à la TTX (Fraser *et al.*, 2005, Gillet *et al.*, 2009). Absent dans les lignées faiblement invasives (MDA-MB-468, MCF-7), ce courant sodique a été enregistré dans la lignée

hautement invasive MDA-MB-231 (Roger *et al.*, 2003, Fraser *et al.*, 2005, Brackenbury *et al.*, 2007, Gillet *et al.*, 2009, Brisson *et al.*, 2011).

Plusieurs études ont montré l'implication de la fonctionnalité du canal dans la régulation de l'invasivité de ces cellules. En effet, l'utilisation de la TTX (Roger *et al.*, 2003, Gillet *et al.*, 2009, Brisson *et al.*, 2011), ou d'inhibiteurs pharmacologiques de $Na_V1.5$ tels que la Ranolazine (Driffort *et al.*, 2014), et la phénytoine (Yang *et al.*, 2012) permettent de réduire l'invasivité des cellules cancéreuses mammaires *in vitro* et *in vivo*. Au potentiel membranaire, les auteurs ont mis en évidence l'activation basale constitutive du canal grâce à un courant de fenêtre, augmentant l'activité d'efflux de protons de l'échangeur sodium-proton NHE1. $Na_V1.5$ et NHE1 ont été identifiés associés à la cavéoline dans les invadopodes, et stimulent l'invasion de la matrice extracellulaire via la promotion de l'activité des cathepsines B et S (Gillet *et al.*, 2009, Brisson *et al.*, 2011, Brisson *et al.*, 2013). Par ailleurs, l'activité $Na_V1.5$-NHE1 augmente l'activité des Src kinases (dont l'isoforme impliquée n'a pas encore été identifiée), la phosphorylation de la cortactine (Y421), induit des modifications du cytosquelette d'actine F et l'adoption par les cellules d'un phénotype allongé de type mésenchymateux (Brisson *et al.*, 2013). Ainsi, l'expression et l'activité des canaux Na_V dans les cellules cancéreuses semblent promouvoir l'invasion mésenchymateuse et l'activité protéolytique via la formation d'invadopodes. L'augmentation intracellulaire de la concentration en ions Na^+ induite par l'activité Na_V pourrait être responsable de l'activation de voies de signalisation, favorisant l'activité NHE1 et l'invasivité cellulaire. Dans la mesure où l'entrée de sodium module le potentiel membranaire (dépolarisation), l'étude des modifications de voies de signalisation sensibles au potentiel de membrane pourrait être intéressante dans la compréhension des mécanismes de régulation de l'invasion mésenchymateuse par $Na_V1.5$ (Yang and Brackenbury, 2013).

Les mécanismes d'implication des canaux Na_V dans l'invasivité cancéreuse ont été récemment discutés dans la revue ci-après (Besson *et al.*, 2015).

Biochimica et Biophysica Acta 1848 (2015) 2493–2501

Contents lists available at ScienceDirect

Biochimica et Biophysica Acta

journal homepage: www.elsevier.com/locate/bbamem

Review

How do voltage-gated sodium channels enhance migration and invasiveness in cancer cells?☆

Pierre Besson [a,b,*], Virginie Driffort [a], Émeline Bon [a], Frédéric Gradek [a], Stéphan Chevalier [a,b], Sébastien Roger [a,c]

[a] Inserm UMR1069 "Nutrition, Croissance et Cancer", Faculté de Médecine, Université François Rabelais de Tours, France
[b] Faculté de Sciences Pharmaceutiques, Université François Rabelais de Tours, France
[c] Faculté des Sciences et Techniques, Université François Rabelais de Tours, France

ARTICLE INFO

Article history:
Received 4 August 2014
Received in revised form 13 April 2015
Accepted 20 April 2015
Available online 25 April 2015

Keywords:
voltage-gated sodium channel
metastasis
migration
invasion
cancer
lipid raft

ABSTRACT

Voltage-gated sodium channels are abnormally expressed in tumors, often as neonatal isoforms, while they are not expressed, or only at a low level, in the matching normal tissue. The level of their expression and their activity is related to the aggressiveness of the disease and to the formation of metastases. A vast knowledge on the regulation of their expression and functioning has been accumulated in normal excitable cells. This helped understand their regulation in cancer cells. However, how voltage-gated sodium channels impose a pro-metastatic behavior to cancer cells is much less documented. This aspect will be addressed in the review. This article is part of a Special Issue entitled: Membrane channels and transporters in cancers.

Contents

1. Introduction

Voltage-gated sodium channel alpha subunits (VGSC, term that will be used throughout this article when not referring to a particular isoform) were discovered more than 60 years ago. They have been extensively characterized for the electrogenic role they play in neurons (NaV1.1, 1.2, 1.3, 1.6, 1.7, 1.8, and 1.9, respectively coded by genes *SCN1A*, *SCN2A*, *SCN3A*, *SCN8A*, *SCN9A*, *SCN10A*, *SCN11A*), skeletal muscle cells (NaV1.4, gene *SCN4A*) and cardiac muscle cells (NaV1.5, gene *SCN5A*). This role in the generation of the action potential and its propagation is now well described [1,2].

Abbreviations: AKAP, A kinase anchoring protein; GPCR, G protein-coupled receptors; NCX, sodium-calcium exchanger; NHE-1, type 1 Na+/H+ exchanger; PKA, protein kinase A; PKC, protein kinase C; TTX, tetrodotoxin; VGSC, voltage-gated sodium channel, pore forming α subunit

☆ This article is part of a Special Issue entitled: Membrane channels and transporters in cancers.

* Corresponding author at: INSERM UMR1069, "Nutrition, Croissance et Cancer", Faculté de Médecine, 10 Bvd Tonnellé, F-37032 TOURS cedex, France. Tel.: +33 247 36 60 63; fax: +33 247 36 62 26.
E-mail address: pierre.besson@univ-tours.fr (P. Besson).

http://dx.doi.org/10.1016/j.bbamem.2015.04.013
0005-2736/

Over the last two decades, an increasing number of studies have documented the expression of one or more types of these channels in non-excitable cells, where they regulate physiological functions such as phagocytosis, endocytosis, secretion, or motility [3], referred to as noncanonical roles for VGSC as reviewed recently by J.A. Black and S.G. Waxman, and more generally, cell proliferation [4], differentiation [5], as well as the organization of the cells during embryo development [4,6].

Many other studies during the same last two decades have described the anomalous expression of VGSC in cancer cells, where they were associated with increased cell motility or invasiveness, therefore increasing the risk of metastases development. Generally, comparative studies showed that they are not expressed, or only at a low level in the corresponding non-cancer cells [7].

Many studies have investigated how partner proteins regulate VGSC activity (for examples, see reviews [8–10]). However, how VGSC activity can increase the motility or invasiveness of cancer cells, therefore increasing the risk of metastases development, remains largely unknown. Some of the proteins that interact, directly or indirectly, with the channels and modulate their activity, also might be the vector through which VGSC exert their pro-invasive effect.

In this article, we will review the roles of VGSC in the motile and invasive properties of cancer cells, and the mechanisms or partner proteins proposed for these functions. We will also try to show which aspects are lacking for the understanding of their implication in the formation of metastases.

2. VGSC in cancer cells and normal corresponding tissues

VGSC have been discovered in a wide variety of metastatic cancers (see Table 1). They were reported in carcinoma cell lines derived from small-cell lung cancer [11], prostate cancer [12], melanoma [13], breast cancer [14], neuroblastoma [15], mesothelioma [16], non-small cell lung cancer [17], cervical cancer [18], ovarian cancer [19], and colon cancer [20]. VGSC are also present in other cancer types (gliomas [21,22] or lymphoma [23] or leukemia cells [23]). In some cancers, this is an abnormal expression of functional channels in cancer cells while their normal cognate cells are not known to have VGSC currents. This is suggested by two kinds of data: 1) electrophysiological investigations in corresponding normal cells could not detect inward sodium currents although the protein was present [17] or 2) the comparison of immunohistochemical stainings in tumor and non-tumor corresponding tissues have shown that VGSC were expressed in tumors, not in the normal epithelial biopsies [7,24]. In contrast, in the case of colon cancer, ovarian cancer, cervical cancer, glioma and leukemia, the expression of VGSC is not abnormal, but rather, the level of overexpression of VGSC in these tissues seems to be related to tumor aggressiveness. Indeed, the cognate stem cells, progenitor cells, or related normal cells (normal colon [20], normal ovary [25,26], normal cervix cells [27], glial cells [3] or leukocytes [28,29]) also express VGSC.

It is important to note that in some instances, the expressed isoform is a fully functional neonatal splice variant [24], which is active during embryonic life but is no longer expressed in the young and the adult. This is interesting regarding the possibilities to develop drugs that could be used to specifically inhibit the neonatal VGSC, leaving the adult isoform fully functional in the excitable cells. Therefore, there is a double abnormality: 1) the expression of a gene normally silenced in a tissue where it is not supposed to be expressed and 2) a neonatal isoform is produced by alternative splicing. This feature is often found in cancer cells where silenced genes become expressed again, resulting in dedifferentiation [30,31]. In the case of those VGSC that are expressed as neonatal isoform, not only the gene is transcribed in the wrong cells, but along with it, the genes of proteins that regulate developmental differential splicing [32].

3. Proteins that modulate the activity of voltage-gated sodium channels by direct or indirect interaction

A vast amount of knowledge is available concerning the proteins that directly or indirectly interact with, and modulate the expression and/or activity of VGSC (for reviews see [8–10]). Most of this knowledge was obtained in excitable cardiac and neuronal cells and was used as a guide for the investigations in cancer cells. Here are a few examples of the proteins with direct or indirect actions on VGSC, discovered in studies performed on excitable cells (Fig. 1).

VGSC, which consist of a main α subunit forming the channel, is associated with one or two β subunits among the four isoforms β1, β2, β3, and β4 (respectively encoded by genes *SCN1B*, *SCN2B*, *SCN3B* and *SCN4B*). These β subunits modulate the activation–inactivation properties of the channel, thus modulating the sodium current (for a review see [2]). They also exert other properties, not directly related to the regulation of the sodium flux, such as VGSC addressing to specific domains of the membrane; adhesion properties through interaction of their extracellular extremity with the extracellular matrix or *via trans* homophilic adhesion [33,34]; anchoring to the cytoskeleton through interaction with their intracellular C-terminal; and scaffolding for various other proteins (for a review see [35]). Another way β subunits could regulate sodium current density is by modulating the transcription of VGSC genes. It was reported that the intracytoplasmic domain of β2, after cleavage by protease BACE1, increased the transcription of *SCN1A* and increased the expression of NaV1.1 in mouse brain, but reduced its addressing to the membrane [36]. Subunit β4 was also reported to be a substrate of proteases BACE1 and γ-secretase in the brain of mice, and β1, β2 and β3 were substrates as well in transfected cell models [37].

VGSC have been shown to interact with many scaffolding (or adapter) proteins such as syntrophins and dystrophin [38], caveolin-3 in striated muscle [39], and ankyrin-G [40,41]. These scaffolding proteins recruit various other proteins to make multiprotein complexes in multifunctional lipid microdomains. The proteins recruited in the domains interact directly or indirectly with VGSC. Here are a few examples of the multiple partners that modulate VGSC expression, localization and activity.

Calmodulin and FHF (fibroblast growth factor homologous factor) associate with NaV1.5 C-terminal domain to form a ternary complex [42]. FHF also binds a scaffold protein (IB2) that recruits MAP kinases [43]. All these gathered proteins participate in the modulation of VGSC localization and activity by phosphorylation.

Ubiquitin ligases nedd4 and nedd4-2 bind VGSC, attach one, two, or more ubiquitin units and regulate the channel density at the membrane through internalization followed by degradation [44–47].

PKA and PKC can be recruited by another family of anchoring protein: AKAP (A kinase anchoring protein). It was shown in rat brain that NaV1.2 binds AKAP15, which recruits PKA and PKC. PKA activity on NaV1.2 reduces the sodium current and PKC activity further enhances this reduction. The platform constituted by the recruitment of PKA and PKC by AKAP near NaV1.2 allows the integration of several signaling pathways [48]. No other study reports such an association with other VGSC but the contrasting effects of phosphorylation by PKA and PKC on VGSC that are reported in different models (animal species, VGSC isoforms) could be in part due to the various members of AKAP expressed.

PKA is not always associated with AKAP but is also found associated with caveolin in caveolae (caveolin-containing lipid rafts) [49]. Since VGSC are also present in caveolae [50], the association between PKA and caveolin facilitates the regulation of VGSC presence/activity in the lipid rafts.

Fyn (a member of the src family kinases) which is present in lipid rafts [51] also interacts and phosphorylates VGSC [52,53].

Also present in lipid rafts [54], Sigma-1 receptor binds VGSC with a 4-fold symmetry (1 sigma-1 receptor per set of six transmembrane regions) [55] and regulate its activity [55,56]

Table 1
Occurrence of gene transcripts, protein, sodium currents, and role of VGSC in cancer cells and the corresponding non-cancer cells.

First reported on year:	Cancer tissue — mRNA, protein	Cancer tissue — Na+ current, function	Corresponding non-cancer tissue — mRNA, protein	Corresponding non-cancer tissue — Na+ current, function
1989 Small-cell lung cancer		VGSC current (type not identified) in small-cell lung cancer cells [11]	Expression of protein (immunolabeling) in normal lung biopsies [92].Expression (mRNA detection by RT-PCR) of NaV1.1 to NaV1.3 and NaV1.5 to NaV1.8 with different profiles in two immortalized normal lung epithelial cell lines; NaV1.7 protein detected in intracellular membranes, not at plasma membrane [17]. NaV1.7 protein immuno-detected faintly in epithelium of normal lung biopsies [7]	No VGSC currents detected [17].
2007 Non-small cell lung cancer	Expression (mRNA detection by RT-PCR) of NaV1.1 to NaV1.9 with different profiles [17]	VGSC currents in different non-small cell lung cancer cell lines; VGSC current involved in increased invasive capacity [17]		
1995 Prostate cancer		VGSC current (type not identified) in rat prostate cancer cells [12]; VGSC current involved in secretory activity [72]; major isoform identified as NaV1.7 [93]	Expression of mRNA (assessed by RT-qPCR) of all NaV1 isoforms except for NaV1.4 and NaV1.8 in normal prostate tissue and benign prostate hyperplasia [94]. Expression of VGSC protein (type not identified, immunolabeling) in normal prostate biopsies [95]	
1997 Melanoma		VGSC current (type not identified) in melanoma cells [13]		VGSC current (type not identified) in normal human melanocytes [96]
2002 Glioma	Expression (mRNA detection by RT-PCR) of NaV1.1, NaV1.2, NaV1.3, NaV1.4, and NaV1.6 in gliomas [21]		Expression (immunolabeling of protein) of NaV1.1, NaV1.5, and NaV1.6 [3]	NaV1.1 and NaV1.6 play role in cytokines release in glial cells [3]
2003 Breast cancer		NaV1.5 current in human highly invasive breast cancer cell line, role in invasive properties, no current or role in invasiveness in less invasive cancer cell lines [14]	No or very low expression (immunolabeling of protein) in biopsies of breast tissue [24]	No current in non-cancer human breast cell line [24]
2004 Lymphoma	Expression (mRNA detection by RT-PCR) of NaV1.5, NaV1.6, NaV1.7, and NaV1.9 in lymphoma cell line [23]	NaV1.5 plays a role in invasiveness [23]		VGSC current (type not identified) in normal human lymphocytes (3 cells out of 90)[97] Phagocytosis by macrophages regulated by NaV1.5; protein localized in late endosome [28]
2006 Mesothelioma	Expression (mRNA detection by RT-PCR) of NaV1.2, NaV1.6, and NaV1.7, and less for NaV1.3, NaV1.4, and NaV1.5 in mesothelioma cells along with the disappearance of the 3 potassium currents found in normal mesothelial cells [16]	Sodium current recorded in mesothelioma cells and involved in cell migration [16]		Normal mesothelial cells do not have any VGSC current while they express 3 main potassium currents [16]
2007 Cervix cancer	Expression (mRNA detection by RT-PCR) of NaV1.1, NaV1.4, NaV1.6, and NaV1.7 in cervical cancer cells [18]	Measurement of tetrodotoxin-sensitive VGSC currents in cervical cancer cells [18]	Expression (mRNA detection by RT-PCR) of NaV1.4 in normal cervix cells; [18]; proteins NaV1.6 and NaV1.7 were immuno-detected in normal cervix cells [27]	Current was not detectable in normal cervix cells [18,27]
2010 Colon cancer	Expression of NaV1.5 protein (immuno-detection) in colon cancer biopsies [20]	NaV1.5 current measured in colon cancer cell lines NaV1.5 expression involved in cancer cell invasiveness [20]	NaV1.5 protein immuno-detected faintly in biopsies of normal colon [20]	
2010 Ovarian cancer	Expression (mRNA detection by RT-PCR) of NaV1.1 to 1.9 in ovarian cancer cells; NaV1.5 immuno-detected in ovarian cancer cell lines and tumor biopsies [19]	Tetrodotoxin-resistant VGSC involved in cell invasive capacity [19]	VGSC protein (type not identified) expressed (western blot, immuno-staining of biopsies with pan NaV antibody) in normal corpus luteum cells of the ovary; VGSC identified as NaV member by RT-PCR [25,26]. Expression (mRNA detection by RT-PCR) of NaV1.1 to 1.9 in biopsies of normal ovary and benign ovarian tumors; NaV1.5 immuno-detected in biopsies of normal ovary and benign ovarian tumors [19]	VGSC current recorded, inhibited by tetrodotoxin; involved in physiological luteolysis of normal corpus luteum cells of the ovary [25,26]

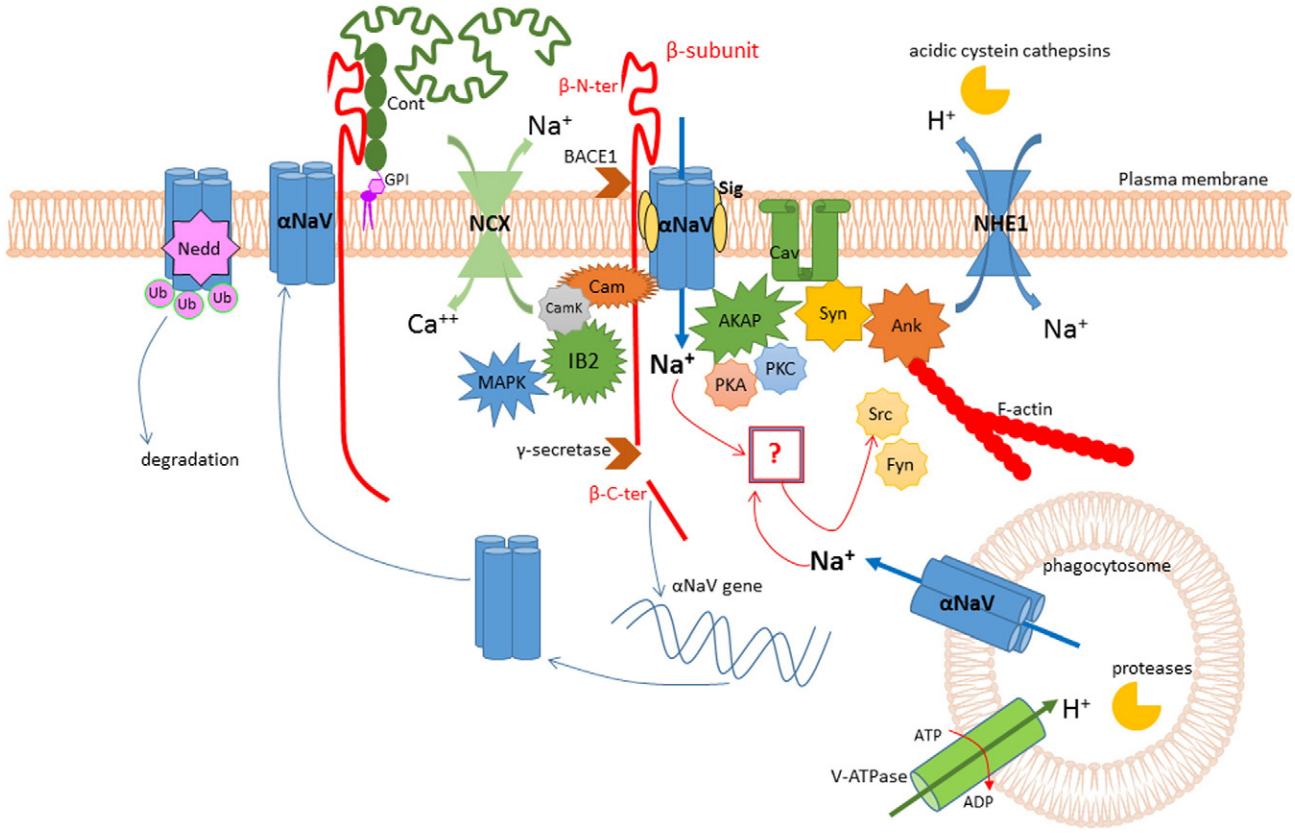

Fig. 1. Schematic interactions of scaffolding and regulatory proteins with VGSC at the plasma membrane and in endosomes. VGSC alpha-subunits (αNaV) interact with scaffolding proteins such as IB2 [43], AKAP [48], syntrophin (Syn) [38], ankyrin (Ank) [40,41], GPI-anchored contactin (Cont) [51,69], caveolin 3 (Cav) [39] and other proteins (sigma1 receptor: Sig [54–56]; VGSC beta subunits: β-subunit [2,33–35]) to make large multiprotein complexes. Kinases such as PKA [48,49,71], PKC [48], MAPK [43], and CamKII [68] are recruited in these complexes and modulate the activity of αNaV and also channel density at the membrane. The sodium-calcium exchanger (NCX) functioning in reverse mode was shown to be a part of this regulation through CamKII [68]. Proteases BACE1 and γ-secretase can cleave β-subunits [37]. The C-terminus of β1 subunit was shown to be a transcription factor for αNaV [36]. Ubiquitin ligase Nedd4 interacts with αNaV and transfers several ubiquitins (Ub), leading to the degradation of αNaV [44–47]. VGSC activity stimulates the invasiveness of cancer cells. It was shown that sodium entry through VGSC leads to the formation and activity of invadopodia [50,74–77], with the polymerization of actin and increase in sodium-proton exchanger type 1 (NHE1) activity [50,74], acidification of the extracellular surface of the plasma membrane making a favorable milieu for the activity of acidic cysteine cathepsins [73]. Similarly, the presence of αNaV in late endosomes of macrophages was shown to regulate endosomal acidification and phagocytosis [28]. How sodium ions are involved in the VGSC-dependent motility and invasiveness of cancer cells is not known (box with "?"). Candidate kinases are Fyn or members of the Src family kinases [51–53,69,74]. GPI: glycosylphosphatidylinositol.

Two VGSC α subunits can also interact with one another, as was recently shown; this interaction modulates the trafficking and activity of NaV1.5; the direct interaction is located at their N-terminal region [57,58].

The sodium-calcium exchanger NCX was also found to be associated with annexin-3 in lipid rafts of cardiac cells [59,60] and associated with various VGSC isoforms in intraepidermal nerve terminals [61].

Depending on the VGSC isoform and the excitable cells, many different proteins have been found to interact with VGSC (for more details, see reviews [8–10]).

It is therefore understandable that the large protein complexes comprising VGSC, in bringing multiple partners in close proximity to their multiple targets, permit the modulation of the channel activity.

It is important to stress that the association of partner proteins in membrane lipid rafts is dynamic and can be altered by post-translation modifications such as palmitoylation [62] or association with special phospholipids such as phosphatidylinositol-bis-phosphate PIP2 [63]. It is also dependent on the lipid composition of rafts as was shown in breast cancer cell line MDA-MB-435S: a protein complex comprising Orai1 and SK3 channels, which was functional within caveolin-rich lipid rafts, dissociated and became inactive upon the introduction of a synthetic analogue of ether-phosphatidylcholine [64]. It is then conceivable that modifications of dietary lipids or pharmacological intervention with synthetic lipid analogues might disrupt the pro-invasive property of VGSC. Reports on breast cancer cell line MDA-MB-231 indicate that NaV1.5 is sensitive to n-3 long chain polyunsaturated docosahexaenoic acid (DHA, 22:6n-3), which was supplemented in the culture medium. The sodium current and migration MDA-MB-231 cells, along with NaV1.5 mRNA and protein levels were reduced by DHA [65], as were invasiveness and the relation (explained below in Section 4) between the activities of NaV1.5 and NHE-1 [66].

4. Proteins that are, directly or indirectly, modulated by VGSC activity

In these large multiprotein complexes, the activity of the channel could in turn influence the behavior of one or several of the proteins in the scaffold (whether it is through Na + ions or through the modulation of membrane potential, or both, is not clear yet). This could be how a signal triggered by VGSC activity is transduced or propagated to produce its effects on motility or invasiveness of cancer cells.

For example (although the mechanism of regulation is not known), the activity of the channel was shown to regulate the splicing of VGSC mRNA: in a drosophila model of epilepsy, two splice variants differing in the region of the voltage sensor S4 of domain III were produced alternatively when the activity of the channel was left uncontrolled or when it was inhibited by phenytoin [67].

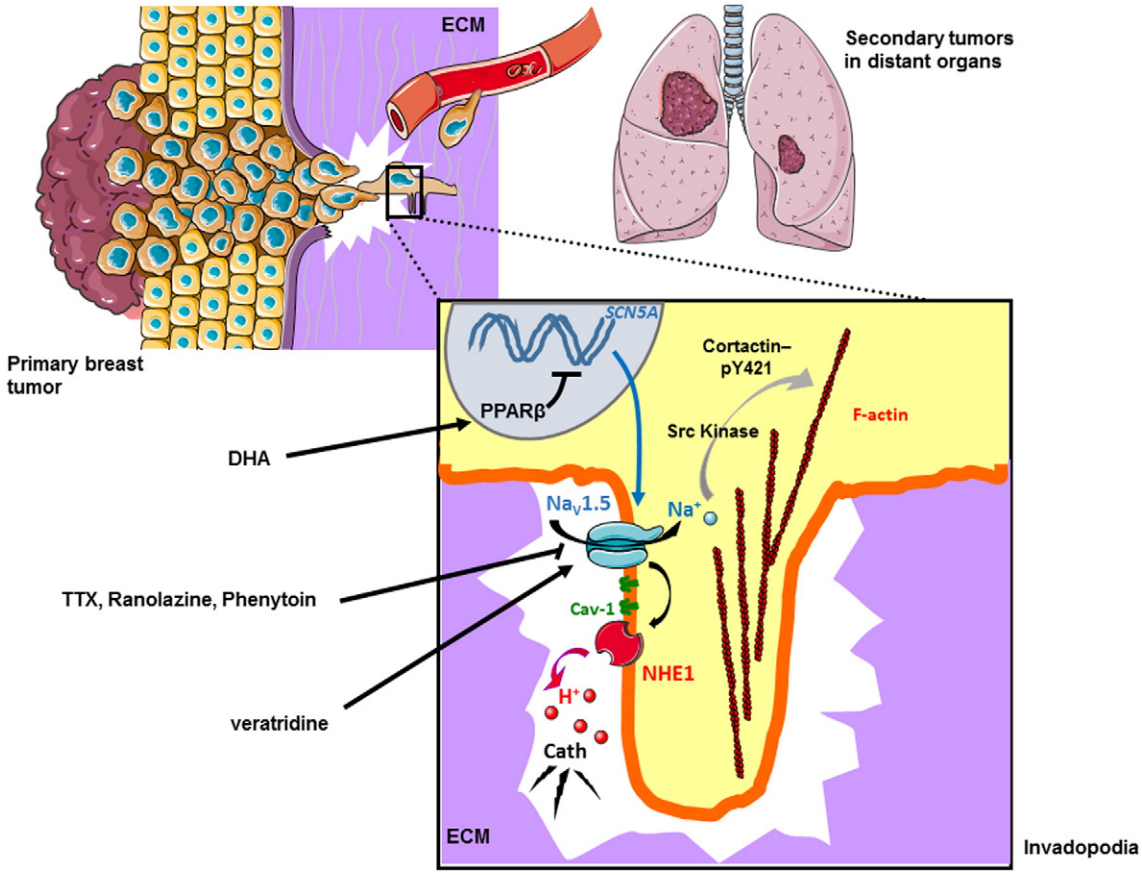

Fig. 2. $Na_V1.5$ promotes breast cancer cell invasiveness and metastatic progression. Invasive breast cancer cells escape from the primary tumor by degrading and migrating through the extracellular matrix (ECM), allowing them to reach the blood circulation and eventually to colonize and form secondary tumors (metastases) in distant organs, such as lungs. The proteolysis of the ECM by cancer cells is dependent on the formation and activity of protrusive structures, enriched in F-actin, called invadopodia (magnification). $Na_V1.5$ channels are abnormally expressed in highly invasive breast cancer cells [14,24], and are localized in caveolin-1 (Cav-1)-containing lipid rafts in invadopodia [50]. They are co-localized with Na+-H+ exchanger type 1 (NHE-1) and promote their activity of proton extrusion. This leads to a peri-invadopodial acidification favorable to the activity of acidic cysteine cathepsins (Cath), released by cancer cells, and to the ECM degradation [50,73]. Furthermore, $Na_V1.5$ activity sustains Src kinase activity, the phosphorylation (Y421) of the actin nucleation-promoting factor cortactin, and the polymerization of actin filaments [74]. These results suggest that $Na_V1.5$ activity in cancer cells enhances both the formation and ECM degradative activity of invadopodia. $Na_V1.5$ activity can be inhibited by sodium channels blockers such as tetrodotoxin (TTX), ranolazine and phenytoin thus reducing cancer cell invasiveness *in vitro* and metastatic colonization of organs *in vivo* [98,99]. The n-3 polyunsaturated fatty acid docosahexaenoic acid (DHA, 22:6n-3) reduces the expression of *SCN5A* gene through the participation of the lipid-sensitive transcription factor peroxisome proliferator activated receptor (PPAR)-β, therefore leading to a decreased activity of NHE-1 and a reduced invasion [65,66].

Another example is the report of a positive feedback loop in rat and mouse cardiac ventricular myocytes, where the sodium influx through NaV1.5 leads to the activation of the kinase CaMKII (resulting from the reverse-mode sodium-calcium-driven increase in intracellular calcium concentration that allows CaMKII and NaV1.5 interaction) and the reciprocal increase in NaV1.5 activity (from its phosphorylation by CaMKII), further increasing the intracellular sodium concentration [68].

Another example showing a reciprocity between VGSC and partner proteins was given by a study in cerebellar granule neurons. NaV1.6 localization at the axonal initial segment required its association with NaV β1 subunit. Reciprocally, the role played by β1 required NaV1.6 activity and sodium ions since the highly specific inhibitor of VGSC tetrodotoxin (TTX) or the reduction of extracellular sodium concentration reduced neurite outgrowth [69]. Neurite outgrowth also required the association of β1 with ankyrin-G, fyn kinase and contactin [51,69]. How sodium ions regulate the activity of the complex is however not known.

The VGSC protein could modulate the behavior of cells through non-electrogenic mechanisms. For example, it has been shown that zebrafish embryo cardiac cell proliferation is impaired if Scn5Lab (NaV1.5 ortholog in zebrafish) is not expressed and that this observation is apparently independent of the channel function since a sodium current cannot yet be recorded at this stage of the embryo development [4,6].

Sodium-calcium exchangers (NCX) were shown to be the link between VGSC activity and cell migration. In oligodendrocyte progenitor cells NG2, GABA(A) receptors induced a depolarization that was able to activate a voltage-gated sodium channel and a non-inactivating Na+ current, which in turn allowed the reverse mode functioning of NCX-1. This led to an increased calcium concentration and NG2 cell migration [70].

Available studies providing such examples of feedback are scarce, even more in cancer cell models. How the activity of VGSC can increase the motility or invasiveness of cancer cells, therefore increasing the risk of metastases development, remains largely unknown, merely because proteins that transduce the activity of VGSC into a signaling pathway have been less extensively studied than in neurons or cardiac cells.

As already indicated above, reactivation of silenced genes in cancer proteins is a frequent phenomenon [30,31]. Since carcinoma cells abnormally express adult or neonatal VGSC, it would not be surprising to find that they also express neuronal or muscular proteins that are capable of interaction with VGSC.

A few studies exist that try to elucidate how VGSC increase migration and invasiveness of cancer cells.

An interesting study performed in breast cancer cell lines MDA-MB-231 and MCF-7 identified a positive feedback loop between PKA and VGSC (neonatal nNaV1.5) in MDA-MB-231 cells, where PKA stimulation

increased mRNA and plasma membrane protein level of nNaV1.5 and increased cell migration and invasion. Further proof of the positive feedback loop was permitted with the use of TTX, which inhibited nNaV1.5, reduced migration and invasion, and also reduced the fraction of phosphorylated, active PKA [71]. This activity-dependent positive feedback was absent in MCF-7, which do not have VGSC activity.

Processing of the extracellular matrix by proteases is a potentiating phenomenon for migration and invasion of cancer cells. Endocytic or exocytic vesicle trafficking was studied in prostate cell lines expressing (Mat-Lylu) or not (AT-2) functional VGSC. Trafficking was shown to be twice as high in the highly metastatic Mat-Lylu cells as in the other less metastatic cell line. TTX treatment or Na+-free medium reduced vesicle trafficking by half in Mat-Lylu cells, but had no reducing effect in AT-2 cells which are devoid of VGSC, clearly indicating that VGSC activity and sodium ions were involved in the enhanced endocytic and exocytic vesicle trafficking [72]. A very interesting study in a monocytic cell line, THP-1, and in primary human monocyte-derived macrophages showed that VGSC were expressed intracellularly and were functional: NaV1.6 was associated with cytoskeletal filaments and the endoplasmic reticulum; NaV1.5 was localized in late endosomes. NaV1.5 was shown to be functional, resulting in the efflux of sodium from the endosomes and in intraendosomal acidification. Inhibition of NaV1.5 by TTX prevented phagocytosis, sodium efflux and endosomal acidification [28]. In a model of breast cancer using MDA-MB-231 cell line, in contrast to what was found in prostate cell line Mat-Lylu, secretion of acidic cathepsins was not a NaV1.5-dependent phenomenon. Rather, NaV1.5 enhanced the acidification of the extracellular perimembrane environment, creating a locally favorable milieu for the activity of extracellular matrix-degrading acidic cathepsins (Fig. 2). Invasion of the extracellular matrix, perimembrane acidification and cathepsins activity were reduced in the presence of TTX or when NaV1.5 expression was reduced by small-interfering RNA. In contrast, invasion was increased when the sustained sodium current present as a window current at the membrane potential of MDA-MB-231 cells was increased by a treatment with channel opener veratridine [73]. It was then shown in the same cells that the acidification of the perimembrane extracellular environment was due to a functional link between the activity of the Na+/H+ exchanger NHE-1 and that of NaV1.5. Decreasing the expression of NaV1.5 with small interfering RNA or reducing its activity by TTX treatment reduced the activity of NHE-1. The two proteins were detected at the same location in caveolin-rich membrane lipid rafts [50]. NHE-1, NaV1.5 and caveolin-1 co-immunoprecipitated, indicating a close association, and they were found at focal sites of matrix remodeling in invadopodia of MDA-MB-231 cells. It was also found that NaV1.5 enhanced the activity of NHE-1 through an allosteric regulation mechanism (the nature of which was not elucidated), rendering it more active at less acidic intracellular pH. In parallel of its action on NHE-1, NaV1.5 activity altered cell morphology, invadopodia formation, and actin cytoskeleton and promoted the phosphorylation of actin-nucleation-promoting factor cortactin on Y421 by a member of the Src family kinase [74]. VGSC are not only involved in the activity of invadopodia in cancer cells [50,74–76] or podosomes in normal cells [77] but they participate in their formation [74,77].

To summarize, VGSC activity can increase vesicle trafficking [72], enhance the activity of acidic cathepsins that digest the extracellular matrix [73], increase the activity of NHE-1 through an allosteric mechanism which arouses its activity for less acidic intracellular pH [50], facilitate the dynamics of invadopodia formation and activity, in part through the stimulation of Src kinase and actin cytoskeleton remodeling [74]. It is also important to note that, although they are not found at their generally known plasma membrane location, intracellular VGSC can be functional in some organelles as was shown in late endosomes of macrophages, where they participate in phagocytosis [28].

The rare studies investigating the events, downstream of VGSC, that enhance migration and invasion were performed in a limited array of breast or prostate cancer cell lines. Extending these studies to other cellular models (other breast and prostate cell lines, as well as other cancer types) would be helpful to elucidate the role of sodium ions or the protein itself as a scaffolding element.

5. Sodium appears to be an important factor, but so is membrane potential

VGSC could exert their effects on the enhancement of migration and invasion through the increase in Na+ concentration in the cytosol, through the change in membrane potential or through non-electrogenic mechanisms.

Several studies demonstrated that sodium was an important factor in the effects generated by VGSC current on migration and invasiveness: using a sodium-free extracellular medium [14,78] or, on the contrary, using channel opener veratridine alone [73,77] and veratridine plus channel blocker TTX [73] indicated that sodium was involved in VGSC-dependent migration and invasiveness.

Sodium influx is important as it depolarizes the membrane and can therefore allow the reverse mode functioning of sodium-calcium exchangers NCX [68,70], which will increase cytosolic calcium concentration and enhance migration/invasion [79].

In an experiment aiming to show if a regulatory feedback existed between the electrical activity of a neuron and VGSC density at the membrane of rat brain neurons, the importance of sodium was demonstrated. When VGSC were active, a reduction of their density could be observed within 15–30 min. This down-regulation was lost when TTX was used to inhibit the channel or when Li+ were used to replace Na+; the down-regulating effect was independent of the protein since, under condition of inhibition by TTX, the increase in intracellular sodium (triggered by the membrane ionophore monensin, capable of transporting Na^+) restored the down-regulation of VGSC [80].

Sensors of intracellular sodium concentration exist such as the sodium-dependent potassium channels Slack and Slick (for a review see [81]). If one postulates that cytosolic calcium concentration is increased by the reverse functioning of NCX, which occurs when the membrane potential is more depolarized than −40 mV, Slack and Slick would be irrelevant with the issue of regulation of migration and invasion. However, intracellular calcium concentration can increase through TRP channels or Orai channels, provided that they are activated by the proper condition [82]. Since the efflux of potassium through Slack and Slick will hyperpolarize the membrane, it will increase the driving force that will allow calcium to enter the cell through TRP or Orai.

It has been reported that Na+ could activate NMDA receptors, and that Src family kinases were involved in this effect but the authors were still looking for the sensor [83].

Although G protein-coupled receptors (GPCR) do not directly interact with VGSC, they could share common downstream signaling pathways and cooperate or compete for the final effect they are expected to generate. A recent study showed that GPCR possess a binding site for one sodium ion and that this ion is important for the stabilization and activity of the receptor. This could be considered a sensor of intracellular sodium concentration [84].

Therefore, it appears that Na+ is important in the downstream effects of VGSC but how it is sensed and whether all the proteins cited above are the direct Na+ sensors remains unexplained. Furthermore, similar regulatory effects of Na+ could occur in cancer cells which do not express VGSC. For example, cells expressing other Na+-permeable channels types such as purinergic receptor P2X7 [85] could have a similar Na+-dependent regulatory mechanism of invasive properties.

Membrane potential is modified by the influx of sodium through VGSC, but also by the other permeabilities that are active in the studied cells [79,86]. In cancer cells, membrane potential is generally depolarized as compared to excitable cells [86] and at this potential, VGSC present a window current that results in a permanent influx of sodium. Whether membrane potential is important or sodium is important, they are both intertwined and displacing the membrane potential to a more positive

or more negative potential could place the VGSC at a potential where they become fully inactive and no longer let sodium enter the cell.

Membrane potential is indeed very important for the conformation of plasma membrane proteins but also for the conformation of cytosolic proteins [79] as was shown for example for the phosphoinositide phosphatase Ci-VSP in *Xenopus* oocytes, or actin cytoskeleton in endothelial cells (for a review see [79]). The membrane potential of cells located at a distant site from the tumorigenic site is influential as well, as was shown in a recent study by Chernet and Levin [87]: hyperpolarizing cells in *Xenopus* embryos at a distant site from the tumorigenic oncogene-expressing cells resulted in a reduction of tumor-like structures formation. Hyperpolarization itself was sufficient, whether it was achieved through the activity of K+ or Cl− channels. The long distance signaling between the hyperpolarized cells and oncogene-expressing cells was apparently not an electrical signaling but was in part mediated through the production of butyrate by the host microbiota, the influx of butyrate into the oncogene-expressing cells and inhibition of histone deacetylase by butyrate, resulting in tumor cell proliferation arrest.

6. Non electrogenic role of VGSC

VGSC being part of the multiprotein scaffold in lipid rafts, in caveolae, they are likely to influence their partners through direct interaction. The example given above in Section 4, to show that VGSC can exert their effect through a non-electrogenic mechanism, was not a study on the migration or invasion of cancer cells but on the proliferation of zebrafish embryo cardiomyocytes [4,6]. To the best of our knowledge, no such study exists for cancer cells. This should be done, and could be done to the best using loss-of-function (non-pore) mutants of VGSC, although all of which, unfortunately for the sake of research, are not fully non-permeant [88–90].

7. Conclusion

The discovery of VGSC in cancer cells is quite recent when compared to excitable cells. However, understanding their functioning in cancer cells progressed at a fast rate thanks to all the knowledge that was accumulated studying neurons and muscle cells. Knowing how the expression and functioning of VGSC are regulated in cancer cells is certainly very valuable because it gives multiple different approaches as how to potentially decrease their activity and therefore reduce the formation of metastases. However, since VGSC are also expressed in normal macrophages and lymphocytes, inhibiting sodium channels altogether in immune cells and cancer cells might reduce the benefit that could be expected in the inhibition of metastases formation. For this reason, identifying the downstream proteins that are regulated by VGSC activity is also very important and would help find cancer cell specific treatments, by enlarging the array of therapeutic targets. The study by House *et al.* [20], presents a novel and very efficient bioinformatics approach combining the analysis of transcriptomics and invasion experiments, which allowed identifying a large array of genes/proteins involved in colon cancer cell behavior under the functional expression of NaV1.5. This method, called "factor graph nested effects model" [91] seeks interactions (transcriptional or functional) among silenced genes/proteins and downstream effect genes/proteins. This is a very powerful approach that could valuably be reproduced in many cancer types to predict the downstream effectors of VGSC in specific tissues. The abnormal expression of VGSC in cancer cells, particularly in the form of neonatal isoforms, suggests that some of the other partners of VGSC in the multiprotein platforms are likely to be neonatal isoforms as well. This should be investigated because what was discovered in normal excitable cells might not be identical in cancer cells. Finding the effectors that are sensitive to the intracellular sodium concentration will also be important and could help broaden the therapeutic arsenal against metastases. Moreover, if sodium concentration is the key, the discovery of the sodium sensors would enlarge this particular fight against metastases to tumors that do not express VGSC but express non-voltage-gated sodium transporters or sodium channels. Last, the study of the association of partner proteins in lipid rafts could help find pharmacological or nutritional lipids that would disrupt the association and reduce the pro-metastatic property of VGSC.

Transparency document

The Transparency document associated with this article can be found, in the online version.

Acknowledgment

We thank the "Ministère de la Recherche et des Technologies", "Inserm", "Université François Rabelais de Tours", "Ligue Nationale Contre le Cancer", "Région Centre" (grant "NaVMetarget" and LIPIDS project of ARD2020-Biomedicaments) and "Association CANCEN" for their financial support for our research.

References

[1] W.A. Catterall, From ionic currents to molecular mechanisms: the structure and function of voltage-gated sodium channels, Neuron 26 (2000) 13–25.
[2] W.A. Catterall, Voltage-gated sodium channels at 60: structure, function and pathophysiology, J. Physiol. 590 (2012) 2577–2589.
[3] J.A. Black, S. Liu, S.G. Waxman, Sodium channel activity modulates multiple functions in microglia, Glia 57 (2009) 1072–1081.
[4] S.S. Chopra, D.M. Stroud, H. Watanabe, J.S. Bennett, C.G. Burns, K.S. Wells, T. Yang, T.P. Zhong, D.M. Roden, Voltage-gated sodium channels are required for heart development in zebrafish, Circ. Res. 106 (2010) 1342–1350.
[5] K. Kis-Toth, P. Hajdu, I. Bacskai, O. Szilagyi, F. Papp, A. Szanto, E. Posta, P. Gogolak, G. Panyi, E. Rajnavolgyi, Voltage-gated sodium channel Nav1.7 maintains the membrane potential and regulates the activation and chemokine-induced migration of a monocyte-derived dendritic cell subset, J. Immunol. 187 (2011) 1273–1280.
[6] J.S. Bennett, D.M. Stroud, J.R. Becker, D.M. Roden, Proliferation of embryonic cardiomyocytes in zebrafish requires the sodium channel scn5Lab, Genesis 51 (2013) 562–574.
[7] T.M. Campbell, M.J. Main, E.M. Fitzgerald, Functional expression of the voltage-gated Na(+)-channel Nav1.7 is necessary for EGF-mediated invasion in human non-small cell lung cancer cells, J. Cell Sci. 126 (2013) 4939–4949.
[8] G.S. Adsit, R. Vaidyanathan, C.M. Galler, J.W. Kyle, J.C. Makielski, Channelopathies from mutations in the cardiac sodium channel protein complex, J. Mol. Cell. Cardiol. 61 (2013) 34–43.
[9] D. Shao, K. Okuse, M.B. Djamgoz, Protein–protein interactions involving voltage-gated sodium channels: post-translational regulation, intracellular trafficking and functional expression, Int. J. Biochem. Cell Biol. 41 (2009) 1471–1481.
[10] D. Shy, L. Gillet, H. Abriel, Cardiac sodium channel NaV1.5 distribution in myocytes via interacting proteins: the multiple pool model, Biochim. Biophys. Acta 1833 (2013) 886–894.
[11] J.J. Pancrazio, M.P. Viglione, I.A. Tabbara, Y.I. Kim, Voltage-dependent ion channels in small-cell lung cancer cells, Cancer Res. 49 (1989) 5901–5906.
[12] J.A. Grimes, S.P. Fraser, G.J. Stephens, J.E. Downing, M.E. Laniado, C.S. Foster, P.D. Abel, M.B. Djamgoz, Differential expression of voltage-activated Na+ currents in two prostatic tumour cell lines: contribution to invasiveness in vitro, FEBS Lett. 369 (1995) 290–294.
[13] D.H. Allen, A. Lepple-Wienhues, M.D. Cahalan, Ion channel phenotype of melanoma cell lines, J. Membr. Biol. 155 (1997) 27–34.
[14] S. Roger, P. Besson, J.Y. Le Guennec, Involvement of a novel fast inward sodium current in the invasion capacity of a breast cancer cell line, Biochim. Biophys. Acta 1616 (2003) 107–111.
[15] S.W. Ou, A. Kameyama, L.Y. Hao, M. Horiuchi, E. Minobe, W.Y. Wang, N. Makita, M. Kameyama, Tetrodotoxin-resistant Na+ channels in human neuroblastoma cells are encoded by new variants of Nav1.5/SCN5A, Eur. J. Neurosci. 22 (2005) 793–801.
[16] G. Fulgenzi, L. Graciotti, M. Faronato, M.V. Soldovieri, F. Miceli, S. Amoroso, L. Annunziato, A. Procopio, M. Taglialatela, Human neoplastic mesothelial cells express voltage-gated sodium channels involved in cell motility, Int. J. Biochem. Cell Biol. 38 (2006) 1146–1159.
[17] S. Roger, J. Rollin, A. Barascu, P. Besson, P.I. Raynal, S. Iochmann, M. Lei, P. Bougnoux, Y. Gruel, J.Y. Le Guennec, Voltage-gated sodium channels potentiate the invasive capacities of human non-small-cell lung cancer cell lines, Int. J. Biochem. Cell Biol. 39 (2007) 774–786.
[18] D. Diaz, D.M. Delgadillo, E. Hernandez-Gallegos, M.E. Ramirez-Dominguez, L.M. Hinojosa, C.S. Ortiz, J. Berumen, J. Camacho, J.C. Gomora, Functional expression of voltage-gated sodium channels in primary cultures of human cervical cancer, J. Cell. Physiol. 210 (2007) 469–478.
[19] R. Gao, Y. Shen, J. Cai, M. Lei, Z. Wang, Expression of voltage-gated sodium channel alpha subunit in human ovarian cancer, Oncol. Rep. 23 (2010) 1293–1299.
[20] C.D. House, C.J. Vaske, A.M. Schwartz, V. Obias, B. Frank, T. Luu, N. Sarvazyan, R. Irby, R.L. Strausberg, T.G. Hales, J.M. Stuart, N.H. Lee, Voltage-gated Na+ channel SCN5A

is a key regulator of a gene transcriptional network that controls colon cancer invasion, Cancer Res. 70 (2010) 6957–6967.
[21] M. Schrey, C. Codina, R. Kraft, C. Beetz, R. Kalff, S. Wolfl, S. Patt, Molecular characterization of voltage-gated sodium channels in human gliomas, Neuroreport 13 (2002) 2493–2498.
[22] A.D. Joshi, D.W. Parsons, V.E. Velculescu, G.J. Riggins, Sodium ion channel mutations in glioblastoma patients correlate with shorter survival, Mol. Cancer 10 (2011) 17.
[23] S.P. Fraser, J.K. Diss, L.J. Lloyd, F. Pani, A.M. Chioni, A.J. George, M.B. Djamgoz, T-lymphocyte invasiveness: control by voltage-gated Na+ channel activity, FEBS Lett. 569 (2004) 191–194.
[24] S.P. Fraser, J.K. Diss, A.M. Chioni, M.E. Mycielska, H. Pan, R.F. Yamaci, F. Pani, Z. Siwy, M. Krasowska, Z. Grzywna, W.J. Brackenbury, D. Theodorou, M. Koyuturk, H. Kaya, E. Battaloglu, M.T. De Bella, M.J. Slade, R. Tolhurst, C. Palmieri, J. Jiang, D.S. Latchman, R.C. Coombes, M.B. Djamgoz, Voltage-gated sodium channel expression and potentiation of human breast cancer metastasis, Clin. Cancer Res. 11 (2005) 5381–5389.
[25] A. Bulling, F.D. Berg, U. Berg, D.M. Duffy, R.L. Stouffer, S.R. Ojeda, M. Gratzl, A. Mayerhofer, Identification of an ovarian voltage-activated Na+ -channel type: hints to involvement in luteolysis, Mol. Endocrinol. 14 (2000) 1064–1074.
[26] A. Bulling, C. Brucker, U. Berg, M. Gratzl, A. Mayerhofer, Identification of voltage-activated Na+ and K+ channels in human steroid-secreting ovarian cells, Ann. N. Y. Acad. Sci. 868 (1999) 77–79.
[27] E. Hernandez-Plata, C.S. Ortiz, B. Marquina-Castillo, I. Medina-Martinez, A. Alfaro, J. Berumen, M. Rivera, J.C. Gomora, Overexpression of NaV 1.6 channels is associated with the invasion capacity of human cervical cancer, Int. J. Cancer 130 (2012) 2013–2023.
[28] M.D. Carrithers, S. Dib-Hajj, L.M. Carrithers, G. Tokmoulina, M. Pypaert, E.A. Jonas, S.G. Waxman, Expression of the voltage-gated sodium channel NaV1.5 in the macrophage late endosome regulates endosomal acidification, J. Immunol. 178 (2007) 7822–7832.
[29] W.L. Lo, P.M. Allen, Self-awareness: how self-peptide/MHC complexes are essential in the development of T cells, Mol. Immunol. 55 (2013) 186–189.
[30] J.F. Lechner, Y. Wang, F. Siddiq, J.M. Fugaro, A. Wali, F. Lonardo, J.C. Willey, C.C. Harris, H.I. Pass, Human lung cancer cells and tissues partially recapitulate the homeobox gene expression profile of embryonic lung, Lung Cancer 37 (2002) 41–47.
[31] M. Monk, C. Holding, Human embryonic genes re-expressed in cancer cells, Oncogene 20 (2001) 8085–8091.
[32] A. Kalsotra, T.A. Cooper, Functional consequences of developmentally regulated alternative splicing, Nat. Rev. Genet. 12 (2011) 715–729.
[33] A.M. Chioni, W.J. Brackenbury, J.D. Calhoun, L.L. Isom, M.B. Djamgoz, A novel adhesion molecule in human breast cancer cells: voltage-gated Na+ channel beta1 subunit, Int. J. Biochem. Cell Biol. 41 (2009) 1216–1227.
[34] M. Nelson, R. Millican-Slater, L.C. Forrest, W.J. Brackenbury, The sodium channel beta1 subunit mediates outgrowth of neurite-like processes on breast cancer cells and promotes tumour growth and metastasis, Int. J. Cancer 135 (2014) 2338–2351.
[35] G.A. Patino, L.L. Isom, Electrophysiology and beyond: multiple roles of Na+ channel beta subunits in development and disease, Neurosci. Lett. 486 (2010) 53–59.
[36] D.Y. Kim, B.W. Carey, H. Wang, L.A. Ingano, A.M. Binshtok, M.H. Wertz, W.H. Pettingell, P. He, V.M. Lee, C.J. Woolf, D.M. Kovacs, BACE1 regulates voltage-gated sodium channels and neuronal activity, Nat. Cell Biol. 9 (2007) 755–764.
[37] H.K. Wong, T. Sakurai, F. Oyama, K. Kaneko, K. Wada, H. Miyazaki, M. Kurosawa, B. De Strooper, P. Saftig, N. Nukina, Beta subunits of voltage-gated sodium channels are novel substrates of beta-site amyloid precursor protein-cleaving enzyme (BACE1) and gamma-secretase, J. Biol. Chem. 280 (2005) 23009–23017.
[38] B. Gavillet, J.S. Rougier, A.A. Domenighetti, R. Behar, C. Boixel, P. Ruchat, H.A. Lehr, T. Pedrazzini, H. Abriel, Cardiac sodium channel Nav1.5 is regulated by a multiprotein complex composed of syntrophins and dystrophin, Circ. Res. 99 (2006) 407–414.
[39] E.F. Shibata, T.L. Brown, Z.W. Washburn, J. Bai, T.J. Revak, C.A. Butters, Autonomic regulation of voltage-gated cardiac ion channels, J. Cardiovasc. Electrophysiol. 17 (Suppl. 1) (2006) S34–S42.
[40] P.J. Mohler, I. Rivolta, C. Napolitano, G. LeMaillet, S. Lambert, S.G. Priori, V. Bennett, Nav1.5 E1053K mutation causing Brugada syndrome blocks binding to ankyrin-G and expression of Nav1.5 on the surface of cardiomyocytes, Proc. Natl. Acad. Sci. U. S. A. 101 (2004) 17533–17538.
[41] G. Lemaillet, B. Walker, S. Lambert, Identification of a conserved ankyrin-binding motif in the family of sodium channel alpha subunits, J. Biol. Chem. 278 (2003) 27333–27339.
[42] C. Wang, B.C. Chung, H. Yan, S.Y. Lee, G.S. Pitt, Crystal structure of the ternary complex of a NaV C-terminal domain, a fibroblast growth factor homologous factor, and calmodulin, Structure 20 (2012) 1167–1176.
[43] M. Goldfarb, Fibroblast growth factor homologous factors: evolution, structure, and function, Cytokine Growth Factor Rev. 16 (2005) 215–220.
[44] J.A. Ekberg, N.A. Boase, G. Rychkov, J. Manning, P. Poronnik, S. Kumar, Nedd4-2 (NEDD4L) controls intracellular Na(+)-mediated activity of voltage-gated sodium channels in primary cortical neurons, Biochem. J. 457 (2014) 27–31.
[45] A.B. Fotia, J. Ekberg, D.J. Adams, D.I. Cook, P. Poronnik, S. Kumar, Regulation of neuronal voltage-gated sodium channels by the ubiquitin-protein ligases Nedd4 and Nedd4-2, J. Biol. Chem. 279 (2004) 28930–28935.
[46] J.S. Rougier, M.X. van Bemmelen, M.C. Bruce, T. Jespersen, B. Gavillet, F. Apotheloz, S. Cordonier, O. Staub, D. Rotin, H. Abriel, Molecular determinants of voltage-gated sodium channel regulation by the Nedd4/Nedd4-like proteins, Am. J. Physiol. Cell Physiol. 288 (2005) C692–C701.
[47] M.X. van Bemmelen, J.S. Rougier, B. Gavillet, F. Apotheloz, D. Daidie, M. Tateyama, I. Rivolta, M.A. Thomas, R.S. Kass, O. Staub, H. Abriel, Cardiac voltage-gated sodium channel Nav1.5 is regulated by Nedd4-2 mediated ubiquitination, Circ. Res. 95 (2004) 284–291.
[48] A.R. Cantrell, V.C. Tibbs, F.H. Yu, B.J. Murphy, E.M. Sharp, Y. Qu, W.A. Catterall, T. Scheuer, Molecular mechanism of convergent regulation of brain Na(+) channels by protein kinase C and protein kinase A anchored to AKAP-15, Mol. Cell. Neurosci. 21 (2002) 63–80.
[49] C.W. Dessauer, Adenylyl cyclase-A-kinase anchoring protein complexes: the next dimension in cAMP signaling, Mol. Pharmacol. 76 (2009) 935–941.
[50] L. Brisson, L. Gillet, S. Calaghan, P. Besson, J.Y. Le Guennec, S. Roger, J. Gore, Na(V)1.5 enhances breast cancer cell invasiveness by increasing NHE1-dependent H(+) efflux in caveolae, Oncogene 30 (2011) 2070–2076.
[51] W.J. Brackenbury, T.H. Davis, C. Chen, E.A. Slat, M.J. Detrow, T.L. Dickendesher, B. Ranscht, L.L. Isom, Voltage-gated Na+ channel beta1 subunit-mediated neurite outgrowth requires Fyn kinase and contributes to postnatal CNS development in vivo, J. Neurosci. 28 (2008) 3246–3256.
[52] C.A. Ahern, J.F. Zhang, M.J. Wookalis, R. Horn, Modulation of the cardiac sodium channel NaV1.5 by Fyn, a Src family tyrosine kinase, Circ. Res. 96 (2005) 991–998.
[53] M. Ahn, D. Beacham, R.E. Westenbroek, T. Scheuer, W.A. Catterall, Regulation of Na(v)1.2 channels by brain-derived neurotrophic factor, TrkB, and associated Fyn kinase, J. Neurosci. 27 (2007) 11533–11542.
[54] C.P. Palmer, R. Mahen, E. Schnell, M.B. Djamgoz, E. Aydar, Sigma-1 receptors bind cholesterol and remodel lipid rafts in breast cancer cell lines, Cancer Res. 67 (2007) 11166–11175.
[55] D. Balasuriya, A.P. Stewart, D. Crottes, F. Borgese, O. Soriani, J.M. Edwardson, The sigma-1 receptor binds to the Nav1.5 voltage-gated Na+ channel with 4-fold symmetry, J. Biol. Chem. 287 (2012) 37021–37029.
[56] M. Johannessen, S. Ramachandran, L. Riemer, A. Ramos-Serrano, A.E. Ruoho, M.B. Jackson, Voltage-gated sodium channel modulation by sigma-receptors in cardiac myocytes and heterologous systems, Am. J. Physiol. Cell Physiol. 296 (2009) C1049–C1057.
[57] J. Clatot, A. Ziyadeh-Isleem, S. Maugenre, I. Denjoy, H. Liu, G. Dilanian, S.N. Hatem, I. Deschenes, A. Coulombe, P. Guicheney, N. Neyroud, Dominant-negative effect of SCN5A N-terminal mutations through the interaction of Na(v)1.5 alpha-subunits, Cardiovasc. Res. 96 (2012) 53–63.
[58] N. Neyroud, A. Ziyadeh-Isleem, J. Clatot, I. Deschenes, A. Coulombe, P. Guicheney, P371 Role of the N- and distal C-terminal domains in Nav1.5 alpha-subunit interaction, Cardiovasc. Res. 103 (Suppl. 1) (2014) S68.
[59] J. Bossuyt, B.E. Taylor, M. James-Kracke, C.C. Hale, Evidence for cardiac sodium-calcium exchanger association with caveolin-3, FEBS Lett. 511 (2002) 113–117.
[60] I. Kuszczak, S.E. Samson, J. Pande, D.Q. Shen, A.K. Grover, Sodium-calcium exchanger and lipid rafts in pig coronary artery smooth muscle, Biochim. Biophys. Acta 1808 (2011) 589–596.
[61] A.K. Persson, J.A. Black, A. Gasser, X. Cheng, T.Z. Fischer, S.G. Waxman, Sodium-calcium exchanger and multiple sodium channel isoforms in intra-epidermal nerve terminals, Mol. Pain 6 (2010) 84.
[62] I. Levental, M. Grzybek, K. Simons, Greasing their way: lipid modifications determine protein association with membrane rafts, Biochemistry 49 (2010) 6305–6316.
[63] R.M. Epand, Proteins and cholesterol-rich domains, Biochim. Biophys. Acta 1778 (2008) 1576–1582.
[64] A. Chantome, M. Potier-Cartereau, L. Clarysse, G. Fromont, S. Marionneau-Lambot, M. Gueguinou, J.C. Pages, C. Collin, T. Oullier, A. Girault, F. Arbion, J.P. Haelters, P.A. Jaffres, M. Pinault, P. Besson, V. Joulin, P. Bougnoux, C. Vandier, Pivotal role of the lipid Raft SK3-Orai1 complex in human cancer cell migration and bone metastases, Cancer Res. 73 (2013) 4852–4861.
[65] B. Isbilen, S.P. Fraser, M.B. Djamgoz, Docosahexaenoic acid (omega-3) blocks voltage-gated sodium channel activity and migration of MDA-MB-231 human breast cancer cells, Int. J. Biochem. Cell Biol. 38 (2006) 2173–2182.
[66] R. Wannous, E. Bon, L. Gillet, J. Chamouton, G. Weber, L. Brisson, J. Gore, P. Bougnoux, P. Besson, S. Roger, S. Chevalier, Suppression of PPARbeta, and DHA treatment, inhibit Na1.5 and NHE-1 pro-invasive activities, Pflugers Arch. (2014)http://dx.doi.org/10.1007/s00424-014-1573-4 (15 July 2014, ahead of print).
[67] W.H. Lin, C. Gunay, R. Marley, A.A. Prinz, R.A. Baines, Activity-dependent alternative splicing increases persistent sodium current and promotes seizure, J. Neurosci. 32 (2012) 7267–7277.
[68] L. Yao, P. Fan, Z. Jiang, S. Viatchenko-Karpinski, Y. Wu, D. Kornyeyev, R. Hirakawa, G.R. Budas, S. Rajamani, J.C. Shryock, L. Belardinelli, Nav1.5-dependent persistent Na+ influx activates CaMKII in rat ventricular myocytes and N1325S mice, Am. J. Physiol. Cell Physiol. 301 (2011) C577–C586.
[69] W.J. Brackenbury, J.D. Calhoun, C. Chen, H. Miyazaki, N. Nukina, F. Oyama, B. Ranscht, L.L. Isom, Functional reciprocity between Na+ channel Nav1.6 and beta1 subunits in the coordinated regulation of excitability and neurite outgrowth, Proc. Natl. Acad. Sci. U. S. A. 107 (2010) 2283–2288.
[70] X.P. Tong, X.Y. Li, B. Zhou, W. Shen, Z.J. Zhang, T.L. Xu, S. Duan, Ca(2+) signaling evoked by activation of Na(+) channels and Na(+)/Ca(2+) exchangers is required for GABA-induced NG2 cell migration, J. Cell Biol. 186 (2009) 113–128.
[71] A.M. Chioni, D. Shao, R. Grose, M.B. Djamgoz, Protein kinase A and regulation of neonatal Nav1.5 expression in human breast cancer cells: activity-dependent positive feedback and cellular migration, Int. J. Biochem. Cell Biol. 42 (2010) 346–358.
[72] M.E. Mycielska, S.P. Fraser, M. Szatkowski, M.B. Djamgoz, Contribution of functional voltage-gated Na+ channel expression to cell behaviors involved in the metastatic cascade in rat prostate cancer: II. Secretory membrane activity, J. Cell. Physiol. 195 (2003) 461–469.
[73] L. Gillet, S. Roger, P. Besson, F. Lecaille, J. Gore, P. Bougnoux, G. Lalmanach, J.Y. Le Guennec, Voltage-gated sodium channel activity promotes cysteine cathepsin-dependent invasiveness and colony growth of human cancer cells, J. Biol. Chem. 284 (2009) 8680–8691.
[74] L. Brisson, V. Driffort, L. Benoist, M. Poet, L. Counillon, E. Antelmi, R. Rubino, P. Besson, F. Labbal, S. Chevalier, S.J. Reshkin, J. Gore, S. Roger, NaV1.5 Na(+) channels

allosterically regulate the NHE-1 exchanger and promote the activity of breast cancer cell invadopodia, J. Cell Sci. 126 (2013) 4835–4842.
[75] M. Egeblad, Z. Werb, New functions for the matrix metalloproteinases in cancer progression, Nat. Rev. Cancer 2 (2002) 161–174.
[76] M.M. Mohamed, B.F. Sloane, Cysteine cathepsins: multifunctional enzymes in cancer, Nat. Rev. Cancer 6 (2006) 764–775.
[77] M.D. Carrithers, G. Chatterjee, L.M. Carrithers, R. Offoha, U. Iheagwara, C. Rahner, M. Graham, S.G. Waxman, Regulation of podosome formation in macrophages by a splice variant of the sodium channel SCN8A, J. Biol. Chem. 284 (2009) 8114–8126.
[78] R. Onkal, J.H. Mattis, S.P. Fraser, J.K. Diss, D. Shao, K. Okuse, M.B. Djamgoz, Alternative splicing of Nav1.5: an electrophysiological comparison of 'neonatal' and 'adult' isoforms and critical involvement of a lysine residue, J. Cell. Physiol. 216 (2008) 716–726.
[79] A. Schwab, A. Fabian, P.J. Hanley, C. Stock, Role of ion channels and transporters in cell migration, Physiol. Rev. 92 (2012) 1865–1913.
[80] B. Dargent, F. Couraud, Down-regulation of voltage-dependent sodium channels initiated by sodium influx in developing neurons, Proc. Natl. Acad. Sci. U. S. A. 87 (1990) 5907–5911.
[81] L.K. Kaczmarek, Slack, Slick and sodium-activated potassium channels, ISRN Neurosci. 2013 (2013) 354262, http://dx.doi.org/10.1155/2013/354262.
[82] M. Gueguinou, A. Chantome, G. Fromont, P. Bougnoux, C. Vandier, M. Potier-Cartereau, KCa and Ca channels: the complex thought, Biochim. Biophys. Acta 1843 (2014) 2322–2333.
[83] X.M. Yu, The role of intracellular sodium in the regulation of NMDA-receptor-mediated channel activity and toxicity, Mol. Neurobiol. 33 (2006) 63–80.
[84] W. Liu, E. Chun, A.A. Thompson, P. Chubukov, F. Xu, V. Katritch, G.W. Han, C.B. Roth, L.H. Heitman, A.P. IJzerman, V. Cherezov, R.C. Stevens, Structural basis for allosteric regulation of GPCRs by sodium ions, Science 337 (2012) 232–236.
[85] B. Jelassi, A. Chantome, F. Alcaraz-Perez, A. Baroja-Mazo, M.L. Cayuela, P. Pelegrin, A. Surprenant, S. Roger, P2X(7) receptor activation enhances SK3 channels- and cystein cathepsin-dependent cancer cells invasiveness, Oncogene 30 (2011) 2108–2122.
[86] M. Yang, W.J. Brackenbury, Membrane potential and cancer progression, Front. Physiol. 4 (2013) 185.
[87] B.T. Chernet, M. Levin, Transmembrane voltage potential of somatic cells controls oncogene-mediated tumorigenesis at long-range, Oncotarget 5 (2014) 3287–3306.
[88] P.G. Meregalli, H.L. Tan, V. Probst, T.T. Koopmann, M.W. Tanck, Z.A. Bhuiyan, F. Sacher, F. Kyndt, J.J. Schott, J. Albuisson, P. Mabo, C.R. Bezzina, H. Le Marec, A.A. Wilde, Type of SCN5A mutation determines clinical severity and degree of conduction slowing in loss-of-function sodium channelopathies, Heart Rhythm. 6 (2009) 341–348.
[89] A. Schroeter, S. Walzik, S. Blechschmidt, V. Haufe, K. Benndorf, T. Zimmer, Structure and function of splice variants of the cardiac voltage-gated sodium channel Na(v)1.5, J. Mol. Cell. Cardiol. 49 (2010) 16–24.
[90] S. Zumhagen, M.W. Veldkamp, B. Stallmeyer, A. Baartscheer, L. Eckardt, M. Paul, C.A. Remme, Z.A. Bhuiyan, C.R. Bezzina, E. Schulze-Bahr, A heterozygous deletion mutation in the cardiac sodium channel gene SCN5A with loss- and gain-of-function characteristics manifests as isolated conduction disease, without signs of Brugada or long QT syndrome, PLoS One 8 (2013) e67963.
[91] C.J. Vaske, C. House, T. Luu, B. Frank, C.H. Yeang, N.H. Lee, J.M. Stuart, A factor graph nested effects model to identify networks from genetic perturbations, PLoS Comput. Biol. 5 (2009) e1000274.
[92] P.U. Onganer, M.B. Djamgoz, Small-cell lung cancer (human): potentiation of endocytic membrane activity by voltage-gated Na(+) channel expression in vitro, J. Membr. Biol. 204 (2005) 67–75.
[93] J.K. Diss, S.N. Archer, J. Hirano, S.P. Fraser, M.B. Djamgoz, Expression profiles of voltage-gated Na(+) channel alpha-subunit genes in rat and human prostate cancer cell lines, Prostate 48 (2001) 165–178.
[94] B. Shan, M. Dong, H. Tang, N. Wang, J. Zhang, C. Yan, X. Jiao, H. Zhang, C. Wang, Voltage-gated sodium channels were differentially expressed in human normal prostate, benign prostatic hyperplasia and prostate cancer cells, Oncol. Lett. 8 (2014) 345–350.
[95] M. Abdul, N. Hoosein, Voltage-gated sodium ion channels in prostate cancer: expression and activity, Anticancer Res. 22 (2002) 1727–1730.
[96] B. Ekmehag, B. Persson, P. Rorsman, H. Rorsman, Demonstration of voltage-dependent and TTX-sensitive Na(+)-channels in human melanocytes, Pigment Cell Res. 7 (1994) 333–338.
[97] M.D. Cahalan, K.G. Chandy, T.E. DeCoursey, S. Gupta, A voltage-gated potassium channel in human T lymphocytes, 1985.
[98] V. Driffort, L. Gillet, E. Bon, S. Marionneau-Lambot, T. Oullier, V. Joulin, C. Collin, J.C. Pages, M.L. Jourdan, S. Chevalier, P. Bougnoux, J.Y. Le Guennec, P. Besson, S. Roger, Ranolazine inhibits NaV1.5-mediated breast cancer cell invasiveness and lung colonization, Mol. Cancer 13 (2014) 264.
[99] M. Nelson, M. Yang, A.A. Dowle, J.R. Thomas, W.J. Brackenbury, The sodium channel-blocking antiepileptic drug phenytoin inhibits breast tumour growth and metastasis, Mol. Cancer 14 (2014) 13.

II.2. Généralités sur les sous-unités β : fonctions et propriétés physiopathologiques

La sous-unité principale α, bien que suffisante expérimentalement pour générer un courant sodique (Qiao *et al.*, 2014), est physiologiquement associée à une ou plusieurs sous-unités β (β1 à β4 transmembranaires et β1B soluble extracellulaire) initialement décrites comme étant auxiliaires de la sous-unité α. Ces sous-unités β sont en effet capables de moduler l'adressage membranaire (Ishikawa *et al.*, 2013, Laedermann *et al.*, 2013), les cinétiques d'activation et d'inactivation (Isom *et al.*, 1994, Grieco *et al.*, 2005, Hakim *et al.*, 2010) et la transcription du gène de la sous-unité α (Kim *et al.*, 2014). Initialement décrites dans les cellules excitables, les sous-unités β ont été plus récemment montrées comme étant exprimées dans les tissus non excitables. Elles pourraient posséder par ailleurs des rôles indépendants de la sous-unité α en agissant notamment en tant que protéines d'adhésions cellulaires (Malhotra *et al.*, 2000, Malhotra *et al.*, 2002, Malhotra *et al.*, 2004, Kim *et al.*, 2005).

Les sous-unités β des canaux sodiques dépendants du voltage (β1, β1B, β2, β3 et β4) sont des protéines de 25 à 40 kDa codées par 4 gènes situés chez l'Homme sur le chromosome 11 : *SCN1B, SCN2B, SCN3B* et *SCN4B* respectivement. La sous-unité β1B est issue d'un épissage alternatif du gène *SCN1B*. À l'exception de β1B, elles sont composées d'un domaine extracellulaire N-terminal de type « Immunoglobulin-like » (Ig-like), d'un segment transmembranaire et d'un court domaine cytosolique C-terminal. Contrairement aux sous-unités β1 et β3 qui interagissent avec les sous-unités α par des liaisons faibles, les sous-unités β2 et β4 sont associées au domaine pore de façon covalente via un pont disulfure qui s'établit su les domaines extracellulaires de ces deux protéines. Ces protéines peuvent être clivées par des sécretases (Wong *et al.*, 2005) et subir d'autres modifications post-traductionnelles de type glycosylation et phosphorylation (Isom *et al.*, 1992, Johnson *et al.*, 2004). Les structures protéiques des sous-unités β ainsi que certaines mutations associées à des pathologies sont présentées dans la Figure 13.

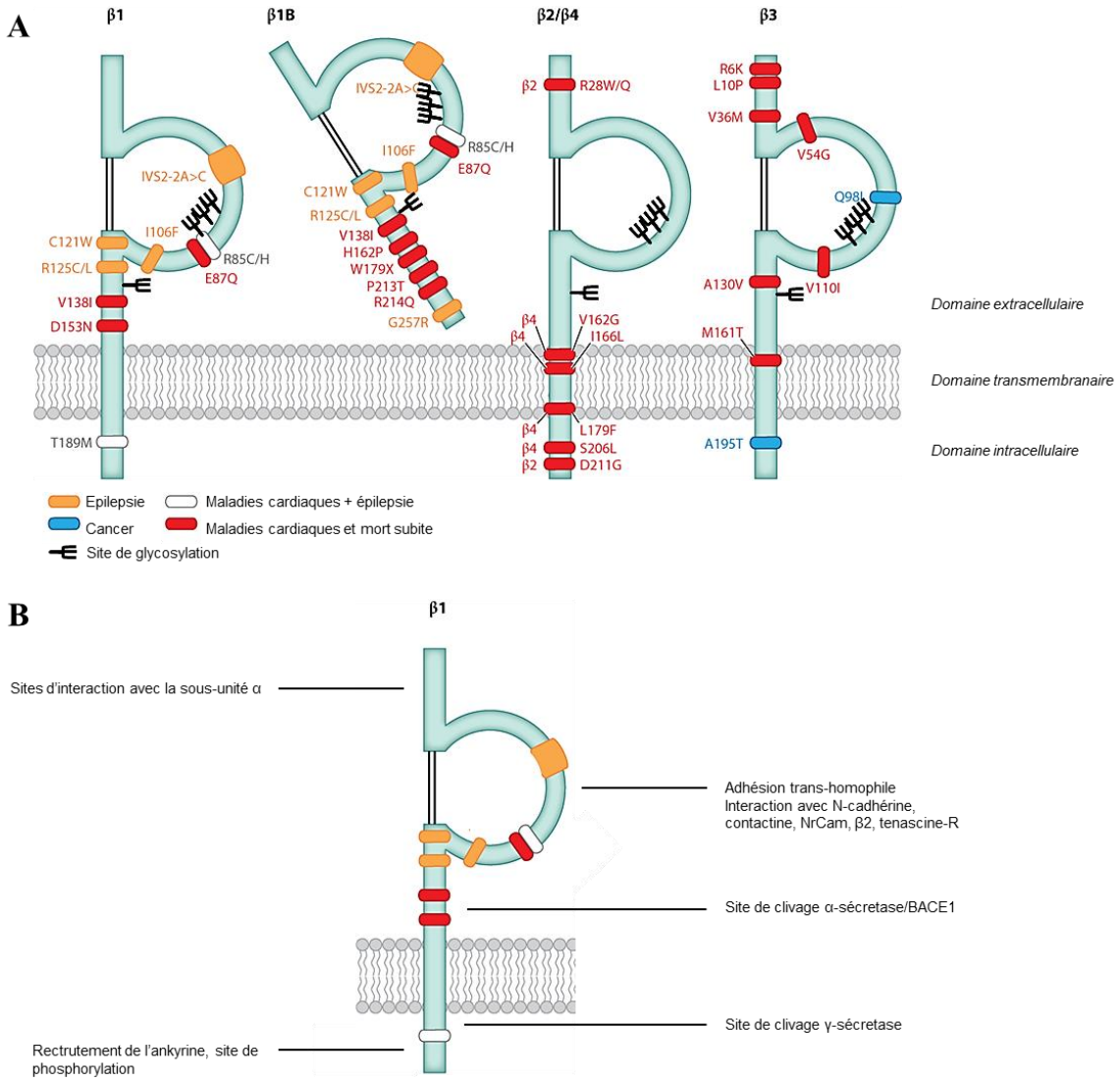

Figure 13 : Structure des sous-unités β des canaux sodiques dépendants du voltage et mutations impliquées dans diverses pathologies.

A. Les pathologies les plus courantes associées à des mutations des sous-unités β sont l'épilepsie (en jaune et blanc), le cancer (en bleu), et les maladies cardiaques (en rouge et blanc). B. Carte fonctionnelle de β1. Les sites de clivage par les sécretases sont indiqués par la légende : en extracellulaire, site de clivage de BACE1, en intracellulaire, site de slivage de la γ-secrétase. D'après O'Malley and Isom, 2015, Patel and Brackenbury, 2015.

II.3. Rôles des sous-unités β dans les pathologies et le cancer

II.3.1. β1

La sous-unité β1, codée par le gène *SCN1B* est la plus étudiée à ce jour. Elle a été pour la première fois purifiée dans le cerveau de rat, et elle est aussi exprimée dans le cœur, le muscle squelettique et la moelle épinière (Hartshorne and Catterall, 1984). La coexpression de cette

protéine avec la sous-unité α $Na_V1.2$ accélère l'inactivation du canal et augmente le courant de pic dans un système de surexpression dans des oocytes de Xénope (Isom *et al.*, 1992). Elle est également exprimée chez la souris (Tong *et al.*, 1993) où elle est rapidement associée au phénotype "frémissant" de souris atteinte d'une anomalie génétique (mutation *quivering, qv*) (Grosson *et al.*, 1996). La première implication pathologique de la sous-unité β1 chez l'Homme a été décrite en 1998, caractérisée par une mutation de type perte de fonction. La mutation d'une cystéine extracellulaire en tryptophane (C121W) perturbe le pont disulfure intracaténaire qui stabilise le domaine « Ig-like ». Cette mutation est associée à i) une modification des cinétiques d'activation du canal $Na_V1.4$ du muscle squelettique (Moran and Conti, 2001, Tammaro *et al.*, 2002), ii) une suppression des interactions homophiles (interaction entre deux mêmes protéines) d'adhésion cellulaire (Meadows *et al.*, 2002), iii) des convulsions et des crises d'épilepsie chez l'Homme dues à une hyperexcitabilité neuronale via une modification des cinétiques d'activation et d'inactivation de $Na_V1.4$ *in vitro* (Wallace *et al.*, 1998). Dans une modèle de surexpression hétérologue (cellules HEK293T), la sous-unité β1 augmente la transcription du gène *SCN9A* (codant pour $Na_V1.7$) d'une part, et l'adressage membranaire du canal d'autre part, et favoriserait sa glycosylation (Laedermann *et al.*, 2013). La régulation des propriétés de la sous-unité α par la sous-unité β1 semble également résulter d'un encombrement stérique. En effet, le domaine Ig-like des sous-unités β est très volumineux et perturberait le pore du canal (Zhang *et al.*, 2013).

β1 a aussi été décrite comme impliquée dans le syndrome de Brugada. Il s'agit d'une canalopathie cardiaque héréditaire autosomique dominante caractérisée par des troubles de la conductivité pouvant être dus à des mutations de type perte de fonction du canal sodique $Na_V1.5$. Dans cette maladie, l'expression de β1 favoriserait l'association d'une sous-unité α Nav1.5 mutée (non fonctionnelle) avec une sous-unité α Nav1.5 sauvage conduisant à un phénotype dominant négatif responsable de la réduction du courant sodique (Mercier *et al.*, 2012).

Cependant, l'expression de β1 a également été associée au syndrome de QT long. Dans un modèle de souris déficientes pour cette protéine, sur un électrocardiogramme les intervalles RR (entre deux dépolarisation des ventricules cardiaques) et QT (entre la dépolarisation des ventricules et leur repolarisation complète) sont plus longs, et l'intensité du courant de pic $Na_V1.5$ est plus grande (gain de fonction). Dans ce modèle, l'extinction d'expression de β1 n'entraine pas de phénomène compensatoire avec les autres sous-unités β (Lopez-Santiago *et al.*, 2007), contrairement au modèle de surexpression dans des cellules HEK293T. En plus de son action régulatrice sur la sous-unité α, la sous-unité β1 possède des rôles indépendants de

l'activité du canal. En effet, elle a été identifiée comme molécule d'adhésion cellulaire (CAM, cell adhesion molecule) puisqu'elle interagit avec de nombreuses autres molécules de la même famille telles que la N-cadhérine, et la tenascine R. Ces adhésions sont regroupées sous le terme interaction hétérophiles (O'Malley and Isom, 2015). L'interaction de la sous-unité β1 avec la contactine, une molécule d'adhésion extracellulaire liée au glycophosphatidylinositol (Kazarinova-Noyes *et al.*, 2001, Chen *et al.*, 2004), favorise l'extension des neurites de neurones granulaires du cervelet de rat (Davis *et al.*, 2004). La formation du complexe β1/contactine active la kinase Fyn associée aux radeaux lipidiques (Wolven *et al.*, 1997), elle-même impliquée dans l'extension des neurites dépendants des molécules d'adhésions neurales NCAM (Beggs *et al.*, 1994). Dans les cardiomyocytes, les interactions cellule-cellule sont favorisées par la formation d'un complexe complexe N-cadhérine/connexine 43/ankyrine B/β1 phosphorylée (Malhotra *et al.*, 2004). D'après les auteurs, β1 s'associe avec le récepteur phosphotyrosine phosphatase RPTPβ (Ratcliffe *et al.*, 2000) qui module directement la phosphorylation du complexe cadhérine-caténine impliqué dans la transition épithélio-mésenchymateuse.

Depuis plusieurs années, il est démontré que la sous-unité β1 est exprimée dans des cellules cancéreuses de sein (Chioni *et al.*, 2009, Gillet *et al.*, 2009, Nelson *et al.*, 2014), du col de l'utérus (Hernandez-Plata *et al.*, 2012), du poumon non à petites cellules (Roger *et al.*, 2007), et de la prostate (Diss *et al.*, 2008). La diminution d'expression de β1 par un siARN diminue l'adhésion cellulaire de lignées cancéreuse mammaire MCF-7 (Chioni *et al.*, 2009) et pulmonaires A549 et H460, et augmente l'invasivité de ces cellules *in vitro* (Campbell *et al.*, 2013). Une surexpression expérimentale de la protéine dans la lignée cancéreuse mammaire fortement invasive MDA-MB-231 réduit la motilité de ces cellules via au augmentation des capacité d'adhésion à la matrice. En revanche dans cette lignée, β1 favorise la prolifération et/ou la survie des cellules (Chioni *et al.*, 2009).

Il a récemment été montré que la sous-unité β1 est plus exprimée dans les tissus mammaires cancéreux en comparaison aux tissus mammaires sains. Dans un modèle de xénogreffe orthotopique, l'injection de cellules MDA-MB-231 surexprimant β1 produit des tumeurs mammaires dont la taille et la croissance était plus rapide que celles issues de l'injection de MDA-MB-231WT. De plus, la surexpression de β1 dans les cellules cancéreuses potentialiserait le développement des métastases pulmonaires et hépatiques (Nelson *et al.*, 2014), suggérant que le mico-environnement joue un rôle promordial dans l'augmentation de l'invasivité *in vivo* par β1.

II.3.2. β2

La sous-unité β2 a été décrite pour la première fois en même temps que la sous-unité β1 dans le cerveau de rat (Hartshorne and Catterall, 1984). Physiologiquement, cette sous-unité permet l'adressage membranaire des sous-unités $Na_V\alpha$. Dans des neurones hippocampiques de souris déficientes pour β2, la diminution de l'adressage des sous-unités α à la membrane plasmique induit une réduction du courant I_{Na} (Chen *et al.*, 2002). Elle est impliquée dans de nombreuses pathologies en tant que modulateur des propriétés électrophysiologiques des canaux sodiques dépendants du voltage.

L'extinction de l'expression de β2 dans des cardiomyocytes ventriculaires de chien augmente l'intensité du courant sodique de fin de créneau, modifiant les cinétiques de déclenchement des potentiels d'action (Mishra *et al.*, 2011). En revanche, dans un modèle murin, la délétion de cette sous-unité exerce une action neuroprotectrice vis-à-vis d'une encéphalomyélite allergique expérimentale en atténuant le niveau de courant persistant au niveau des axones lésés (démyélinisés) (O'Malley *et al.*, 2009). Des mutations de type « perte de fonction » de β2 ont été reportées chez des patients atteints de fibrillations auriculaire, induisant une diminution de l'intensité du courant Na_V (Watanabe *et al.*, 2009). L'expression de β2 mutée jouerait également un rôle dans le syndrome de Brugada puisqu'il a été montré dans des cellules ovariennes de hamster chinois CHO, qu'une mutation non-sens de la protéine entraine une diminution de l'adressage membranaire de $Na_V1.5$ (Riuro *et al.*, 2013).

La sous-unité β2, au même titre que les autres sous-unités, possède des propriétés de molécule d'adhésion cellulaire. Elle interagit avec des molécules de la matrice extracellulaire comme la tenascine-C, ce qui favorise notamment l'expression des métalloprotéases matricielles au cours de la réparation tissulaire (Tremble *et al.*, 1994). Elle interagit également avec la tenascine-R via sa boucle N-terminale Ig-like (Srinivasan *et al.*, 1998), ce qui permettrait de réguler les interactions cellule-cellule nécessaires à la croissance et la myélinisation des axones. A l'inverse de β1, β2 diminuerait l'extension des neurites de neurones granulaires cérébelleux (Davis *et al.*, 2004). Dans des cellules humaines de neuroblastome, le domaine intracellulaire de β2, produit du clivage de la protéine par la γ-sécretase, jouerait le rôle de facteur de transcription pour augmenter l'expression du gène *SCN1A* codant la sous-unité $Na_V1.1$ (Kim *et al.*, 2007a). L'accumulation du domaine C-terminal de β2 généré par le clivage par la sécretase BACE1 (beta-site amyloid precursor protein cleaving enzyme 1) dans les neurones de souris est associée à une modification de l'activité neuronale et des déficits cognitifs (Corbett *et al.*, 2013).

La sous-unité β2 est exprimée dans les cancers du sein (Chioni *et al.*, 2009, Nelson *et al.*, 2014), du col de l'utérus (Hernandez-Plata *et al.*, 2012), du poumon non à petites cellules (Roger *et al.*, 2007), et de la prostate (Diss *et al.*, 2008, Jansson *et al.*, 2012). *In vitro,* dans la lignée cellulaire cancéreuse prostatique LNCaP, la surexpression de β2 induit une élongation des cellules et une augmentation de la migration cellulaire en 2 dimensions (technique de la cicatrice) et une augmentation de l'adhésion à un substrat, qui semble être dépendante des facteurs de croissance. Dans le même temps, la surexpression de β2 mène à une augmentation de l'invasivité des cellules au travers d'un insert recouvert de Matrigel™ (Jansson *et al.*, 2012). Ce même groupe a démontré que la boucle extracellulaire de β2 a une forte affinité pour la laminine. Sur ce substrat, la surexpression de β2 dans les cellules LNCaP augmente leur prolifération, migration, et invasion suggérant un rôle de β2 dans l'invasion métastatique périneurale (Jansson *et al.*, 2014). De plus, la sous-unité β2 jouerait un rôle dans la formation des filopodes au cours du développement des neurones hippocampiques de rat (Maschietto *et al.*, 2013).

II.3.3. β3

La sous-unité β3 a été décrite au début des années 2000 par l'équipe de AP Jackson au niveau du système nerveux central (Morgan *et al.*, 2000) et du cœur (Fahmi *et al.*, 2001). Elle module la réactivation de la sous-unité $Na_V1.5$ dans des cellules cardiaques de mouton (Fahmi *et al.*, 2001) ainsi que sur un modèle de surexpression des sous-unités β dans des cellules CHO (Ko *et al.*, 2005). De nombreuses mutations de la protéine ont été identifiées et associées à plusieurs canalopathies. Chez des victimes de syndrome de mort subite du nourrisson, des mutations non-sens dans le domaine extracellulaire de β3 ont été identifiées. Elles sont responsables d'une augmentation de la densité du courant sodique dans le syndrome de la mort subite du nourrisson (Tan *et al.*, 2010). Dans le syndrome de Brugada, la mutation de β3 par substitution d'un résidu valine en position 110 par un résidu isoleucine induit une diminution du courant $Na_V1.5$ par inhibition de l'adressage membranaire de la sous-unité α (Ishikawa *et al.*, 2013). Dans un modèle de coexpression de $Na_V1.2$ et β3 dans les cellules HEK, l'intensité du courant sodique est augmentée (Merrick *et al.*, 2010). Il a été suggéré que β3 pouvait moduler l'adressage membranaire de $Na_V1.8$ en masquant par interaction physique le signal de rétention de $Na_V\alpha$ dans le réticulum endoplasmique dans des cellules COS-7 (Zhang *et al.*, 2008). A partir d'une étude d'homologie structurale de β3 par rapport à β1, il a été proposé que ces deux sous-unités puissent former un hétérodimère via des liaisons hydrophobes entre leurs

domaines extracellulaires (Liu *et al.*, 2014). Par ailleurs, les domaines C-terminaux de ces deux sous-unités interagissent avec les résidus cytoplasmiques lysine 1846 à arginine 1886 du domaine pore (Spampanato *et al.*, 2004).

L'implication de β3 dans le cancer est encore peu connue, mais des mutations non-sens ont été identifiées dans des biopsies de cancer colorectal de grade élevé (Sjoblom *et al.*, 2006). Elle est exprimée dans le cancer du poumon non à petites cellules (Roger *et al.*, 2007, Campbell *et al.*, 2013), le cancer de la prostate (Diss *et al.*, 2008), le cancer du col de l'utérus (Hernandez-Plata *et al.*, 2012) mais n'est pas exprimée dans les cellules cancéreuses mammaires hautement invasives MDA-MB-231 (Gillet *et al.*, 2009). Il a été reporté que le gène *SCN3B* pourrait être sous la dépendance de p53, et l'induction de ce gène augmente la chimiosensibilité et l'apoptose des cellules cancéreuses de colon et du poumon (Adachi *et al.*, 2004).

II.3.4. β4

La quatrième sous-unité β est la moins bien caractérisée. Elle a été identifiée dans les neurones sensoriels ainsi que dans le système nerveux central au niveau du cortex, de l'hippocampe, du cervelet et de la moelle épinière de rats (Yu *et al.*, 2003). Elle module les propriétés électrophysiologiques des sous-unités principales $Na_V1.2$, $Na_V1.4$ et $Na_V1.5$ (Yu *et al.*, 2003) et $Na_V1.6$ (Barbosa *et al.*, 2015). Des mutations de la protéine ont été retrouvées dans les canalopathies (Remme *et al.*, 2009) et est connue pour jouer un rôle dans le syndrome du QT Long, caractérisé par un allongement de l'espace QT sur un électrocardiogramme. Dans ce syndrome, une mutation non-sens est retrouvée sur le gène *SCN4B* conduisant à la substitution d'un résidu leucine par un résidu phénylalanine en position 179 sur la protéine (L179F-β4).
La coexpression de L179F-β4 et $Na_V1.5$ induit un gain de fonction de $Na_V1.5$ et un décalage de l'inactivation du canal en fonction du voltage, ce qui augmente le courant de fenêtre, le courant persistant et génère des arythmies cardiaques. Dans ce cas le courant persistant, mesuré en fin de créneau est également augmenté (Medeiros-Domingo *et al.*, 2007). Une autre mutation non-sens (S206L) a également été reportée dans le syndrome de la mort subite du nourrisson (Tan *et al.*, 2010).
L'expression du gène *SCN4B* est dérégulée dans un modèle murin de la maladie de Huntington (Oyama *et al.*, 2006). La sous-unité β4 est composée à son extrémité cytoplasmique de groupements lysine et de résidus hydrophobes. De ce fait, elle représente une cible potentielle de protéases permettant la levée du blocage des courants sodiques dans les neurones de Purkinje (Grieco *et al.*, 2005).

La sous-unité β4 est ciblée par différentes enzymes protéolytiques. BACE1 cliverait β4 en extracellulaire entre les résidus 149 et 150, permettant la libération de la boucle Ig-like. La γ-sécretase clive quant à elle β4 en intracellulaire, libérant un fragment C-terminal (Wong *et al.*, 2005). Dans les neurones pyramidaux, la surexpression expérimentale de l'extrémité C-terminale de β4 génère un courant résurgent (Grieco *et al.*, 2005). La surexpression de la protéine totale favorise l'extension des neurites d'une part (Oyama *et al.*, 2006, Miyazaki *et al.*, 2007) et la formation de filopodes dans des cellules de neuroblastome Neuro2a (Miyazaki *et al.*, 2007) d'autre part.

A ce jour, l'éventuelle implication de β4 dans les cancers n'a pas été confirmée mais certaines études montrent une diminution de l'expression de la protéine dans des biopsies de cancer du col de l'utérus, et dans des cellules cancéreuses invasives (pour revue, Roger *et al.*, 2015).

Objectifs de la thèse

Au laboratoire, des études précédentes ont pour la première fois mis en évidence l'expression fonctionnelle du canal sodique dépendant du voltage $Na_V1.5$ dans les cellules cancéreuses mammaires MDA-MB-231 et son rôle dans l'invasivité cellulaire (Roger *et al.*, 2003). Dans ces cellules, le courant sodique favorise l'activité de l'échangeur sodium proton NHE1 (Brisson *et al.*, 2011), conduisant à une acidification du pH périmembranaire des cellules cancéreuses. Cette acidification favorise l'activité des protéases à cystéine (cathepsines B et S), en partie responsables de la dégradation protéolytique de la MEC (Gillet *et al.*, 2009). La dégradation de la MEC est diminuée par un apport en DHA (22:6n-3), via la diminution de l'expression et de l'activité de $Na_V1.5$ et de l'activité de NHE1 (Wannous *et al.*, 2015). Les canaux sodiques dépendants du voltage sont composés d'une sous-unité principale α qui forme le domaine pore et d'une ou plusieurs sous-unités β (β1 à β4) dans les cellules excitables. Dans les cellules cancéreuses mammaires MDA-MB-231, seules les sous-unités β1, β2 et β4 sont exprimées. Une étude préliminaire menée au laboratoire a mis en évidence que la sous-expression expérimentale de β1 et β2 réduit l'invasivité cellulaire alors que la sous-expression de la sous-unité β4 l'augmente. Contrairement aux sous-unités β1 et β2, l'implication de la sous-unité β4 dans le cancer n'est pas étudiée. Les trois premiers objectifs de cette thèse ont été i) d'étudier l'expression de la sous-unité β4 dans des tissus mammaires cancéreux et des cellules cancéreuses ii) d'étudier la signification clinique de l'expression de la sous-unité β4 dans des biopsies de tissus mammaires sains et de différents grades cancéreux, iii) de déterminer l'importance de la sous-unité β4 dans la biologie de la cellule cancéreuse.

Dans les cellules excitables, l'expression de β4 module l'activité $Na_V1.5$, nous avons donc dans un second temps déterminé si la régulation de l'invasivité cancéreuse par la sous-unité β4 est dépendante de la régulation de la sous-unité principale $Na_V1.5$. Après avoir répondu à ces objectifs (Bon *et al*, article 1), nous nous sommes intéressés à la régulation de l'expression de la protéine β4. Il a été montré que la supplémentation en AGPI n-3, et plus particulièrement en DHA, favorisent la chimiosensibilisation de la tumeur et augmentent la survie des patientes traitées pour un cancer du sein métastasé (Bougnoux *et al.*, 2009, Bougnoux *et al.*, 2010). Une étude préliminaire réalisée au laboratoire a montré qu'un traitement des cellules cancéreuses mammaires MDA-MB-231 par le DHA (10 µM) augmente l'expression de la sous-unité β4. *In vitro*, le traitement au DHA réduit l'invasivité des cellules cancéreuse mammaires (Wannous *et al.*, 2015). Les quatrième et cinquième objectifs de cette thèse ont donc été iv) de déterminer si l'inhibition de l'invasivité cancéreuse par le DHA implique la surexpression de β4 et v) d'étudier le mécanisme de régulation de l'expression de la sous-unité β4 par le DHA (Bon *et al*, article 2).

Matériels et Méthodes spécifiques de la thèse

Dans cette partie, seules les techniques mises au point au laboratoire au cours de ce stage doctoral seront détaillées. Les techniques classiquement utilisées au laboratoire sont décrites dans le matériel et méthode des articles.

I. Time lapse et analyse des fichiers

La technique de microscopie time-lapse permet de capturer des images d'évènements dynamiques à des intervalles de temps réguliers et déterminés par l'utilisateur. Cette technique nous a permis de mesurer et de quantifier la vitesse de migration des lignées cancéreuses mammaires MDA-MB-231luc shCTL, MDA-MB-231luc shβ4 MDA-MB-231luc surexβ4 et MDA-MB-231luc transfectées de façon transitoire avec les différents plasmides d'expression des fragments de la protéine β4. Les cellules ont été ensemencées à raison de 4000 cellules par centimètre carré, 24 heures avant le lancement de l'acquisition. Les cellules sont placées dans une chambre à atmosphère contrôlée (37° C, 5% CO_2, saturation en humidité, Okolab, Boldline). Les vidéos de time-lapse ont été obtenues grâce à la caméra Nikon DS-QI2, reliée au microscope Nikon éclipse Ti. Le logiciel NIS Element nous a permis de définir les paramètres d'acquisition des images. Les positions x/y/z définies à l'aide de la platine motorisée, permettent d'obtenir des images en différents champs en parallèle. Les paramètres d'acquisition des images ont alors été définis pour quantifier la vitesse de migration des lignées cellulaires : 1 image par minute durant 3 heures d'acquisition soit 181 images récoltées par champ.

L'analyse des fichiers obtenus a été effectuée à l'aide du plugin « manual tracking » du logiciel Fiji (Fiji Is Just ImageJ). Ce module permet de suivre les cellules manuellement au cours du temps. Les données récoltées pour chaque cellule suivie recensent les coordonnées des points associés à la position de la cellule à chaque temps t et la vélocité, cette dernière étant calculée en fonction des paramètres définis avant l'analyse (intervalle de temps et calibration des positions x/y). La vitesse, le déplacement et la distance parcourue seront calculés à partir des coordonnées xy.

- Calcul de la distance

La distance parcourue par les cellules au cours de l'acquisition est calculée en additionnant la totalité des déplacements effectués par la cellule au cours de la vidéo. La formule de calcul utilisée est la suivante, dont x/y correspondent aux coordonnées (en µm) et t au temps (en min) :

$$\text{Distance (µm)} = \sum_{t0}^{t181} \sqrt{((x_{t+1}-x_t)^2+(y_{t+1}-y_t)^2)}$$

- Calcul du déplacement

Le déplacement de la cellule correspond à la différence entre les coordonnées des points t_{181} et t_1, schématisé dans la Figure 14.

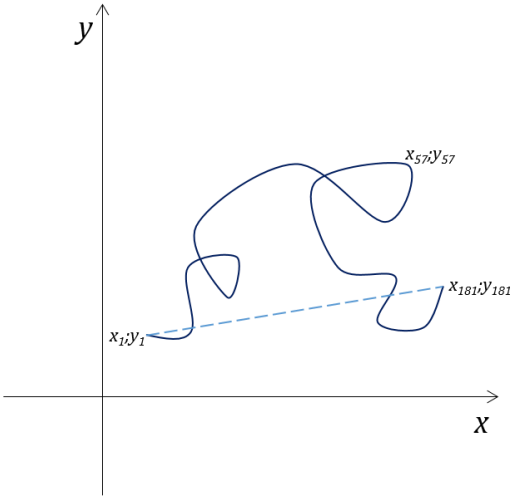

Figure 14 : Schématisation du déplacement et de la distance parcourus par les cellules.

La distance parcourue par la cellule est représentée en trait plein. Elle est déterminée par la somme des déplacements de la cellule (déterminés par les coordonnées x/y) sur toute la durée de l'acquisition (soit 181 points). Le déplacement de la cellule est représenté en pointillés. Il est calculé en soustrayant aux coordonnées du temps t_{181} les coordonnées du temps t_1.

Le calcul du déplacement est donc effectué de la manière suivante :

$$\text{Déplacement } (\mu m) = \sqrt{((x_{181}-x_1)^2+(y_{181}-y_1)^2)}$$

- Calcul de la vitesse

La vitesse moyenne des cellules est calculée en divisant la distance totale parcourue sur la durée d'acquisition, dans notre cas :

$$\text{Vitesse } (\mu m.min^{-1}) = \frac{\sum_{t1}^{t181}\sqrt{((x_{t+1}-x_t)^2+(y_{t+1}-y_t)^2)}}{181}$$

Les variations obtenues entre le déplacement d'une cellule et la distance parcourue par cette même cellule donnent une indication de la trajectoire. Bien que les expériences aient été conduites sans chimioattractant, une cellule ayant une distance et un déplacement élevés aura une migration plus orientée qu'une cellule ayant parcourue une grande distance avec un petit

déplacement. L'accélération des cellules est mesurée en valeur absolue de la vitesse au temps *t* soustraite à la vitesse au temps t_{+1}.

II. Clonage et mesure d'activité du promoteur du gène *SCN4B*

La séquence promotrice putative du gène *SCN4B* a été analysée par bioinformatique à l'aide du logiciel MatInspector (Genomatix). Ce logiciel a permis d'identifier des éléments de réponse putatifs aux PPARs (PPRE, PPAR Response Element). Différentes séquences du promoteur putatif ont été clonées en fonction des PPRE, grâce à l'utilisation de couples d'amorces spécifiques. Les couples d'amorces utilisés pour le clonage sont présentées dans la Table 4 page 95.

II.1. Clonage du promoteur du gène *SCN4B*

II.1.1. Plasmides utilisés

Plasmides d'expression des récepteurs nucléaires PPAR

Les plasmides d'expression pSG5-mPPARα, pSG5—mPPARβ et pSG5-mPPARγ (Lazennec *et al.*, 2000) sont des plasmides d'expression contenant respectivement les séquences codantes pour PPARα, PPARβ ou PPARγ de souris, clonées en aval du promoteur du virus SV40 du plasmide pSG5 (ref 216201 Stratagene).

Plasmides rapporteurs

Le plasmide $(PPRE)_3$-TK-Luc contient trois copies d'une séquence PPRE consensus insérées au niveau du site de restriction unique *Sal*I du plasmide TK-Luc. Ces séquences consensus sont situées en amont du promoteur tyrosine kinase (TK) et du gène rapporteur luciférase (Luc) (Mangelsdorf *et al.*, 1991).

Le plasmide rACOX_PPRE-pGLuc (Fourcade *et al.*, 2001) contient le PPRE du gène de l'acyl-coezyme A oxidase (ACOX) de rat inséré entre les sites de restriction *Hind*III et *Bam*HI dans le plasmide pGLuc (Bardot *et al.*, 1993) en amont du promoteur β-globine de lapin et du gène rapporteur luciférase.

Le plasmide pCMV-β-gal (ref 631719, Clonetech), utilisé comme rapporteur de standardisation de la transfection, contient le gène de la β-galactosidase cloné en aval du promoteur du cytomégalovirus (CMV).

Le plasmide pUC18 (SD0051, Fermentas), a été utilisé pour ajuster la quantité d'ADN à transfecter.

Plasmides rapporteurs luciférase contenant des séquences promotrices du gène SCN4B

Le plasmide rapporteur pGL4.10 (E6651, Promega) contient en amont du gène luciférase un site multiple de clonage pour l'insertion du promoteur étudié d'une part, et le gène β-lactamase de résistance à l'ampicilline permettant la sélection des colonies d'autre part.

II.1.2. Obtention des séquences promotrices par PCR

Le clone BAC (Bacterial Artificial Chromosome) CTD 3185N4 (Invitrogen) contient la séquence du promoteur du gène *SCN4B*, situé sur le chromosome 11 chez l'Homme. Ce clone a été utilisé comme matrice pour la PCR. Sept amorces sens contenant le site de restriction *Kpn*I à l'extrémité 5' et une amorce anti-sens contenant le site de restriction *Xho*I à l'extrémité 5' ont été conçues et synthétisées (Sigma-Aldrich) afin d'amplifier sept séquences nucléotidiques en amont du gène *SCN4B* supposées contenir une activité promotrice. Les amorces utilisées sont présentées dans la Table 4. Les fragments amplifiés par ces amorces sont délimités par les sites e restriction *Kpn*I et *Xho*I, permettant leur insertion orientée dans le plasmide rapporteur.

Table 4 : Amorces permettant l'amplification du promoteur putatif du gène *SCN4B*.

Les sites de restriction des enzymes *Kpn*I (en 5' des amorces sens) et *Xho*I (en 5' des amorces anti-sens) sont indiqués en minuscules. Chaque amorce sens a été utilisée avec l'amorce anti-sens (pSCN4B+80bp) pour amplifier les fragments du promoteur du gène *SCN4B*, dont les tailles attendues sont indiquées en paires de bases. Les nombres permettant de dénommer les amorces correspondent à la position de l'amorce sur le promoteur par rapport au codon d'initiation de la transcription.

Dénomination	Séquence (5' - 3')	Taille attendue (pb)
p*SCN4B*-3409bp (sens)	gaatggtaccAACCCTACACGAATCCCCAAGGAA	3489
p*SCN4B*-2549bp (sens)	gaatggtaccAGATATCCCTGCAGCTCTGTCCCTC	2629
p*SCN4B*-2534bp (sens)	gaatggtaccAAGCCTGCGGACCTGGAGACAGATG	2434
p*SCN4B*-2002bp (sens)	gaatggtaccTGTAGTGAGAGGGGCTCTTGTGCATGC	2082

Dénomination	Séquence (5' - 3')	Taille attendue (pb)
p*SCN4B*-1899bp (sens)	gaatggtaccGTGCACACCTGATATGGCCAGC	1979
p*SCN4B*-1402bp (sens)	gaatggtaccAAGAAGGCGGTGCGTTGGTGTGC	1432
p*SCN4B*+80bp (anti-sens)	gaatctcgagCAAGCTGGGGCTGCCTTACCC	

La PCR a été réalisée dans le tampon Long PCR Buffer (1,5 mM $MgCl_2$, 2,5 unités de Long PCR Enzyme mix, 0,2 mM de dNTP), 100 ng d'ADN matrice et 0,5 µM d'amorces sens et anti-sens. Les paramètres utilisés pour la PCR sont décrits dans la Table 5.

Table 5 : Description des cycles de PCR permettant l'amplification des fragments du promoteur *SCN4B*.

Etape	Température (°C)	Durée	Nombre de cycles
1-dénaturation	94	5 minutes	1
2-dénaturation	94	30 secondes	25
3-hybridation des amorces	65	30 secondes	
4-élongation	68	5 minutes	
5-fin	68	5 minutes	1

Les produits de PCR ainsi obtenus ont été purifiés par électrophorèse sur gel d'agarose 1% (tampon Tris-Acetate 40 mM, EDTA 1 mM) et extraits à partir de ce dernier grâce au kit Nucleospin Extract II, PCR clean-up Gel Extraction (740609.250, Macherey-Nagel) selon les recommandations du fabricant.

II.1.3. Insertion des fragments p*SCN4B* dans le plasmide pGL4.10

Les 7 fragments, obtenus par PCR et délimités par les sites de restrictions *Kpn*I en 5' et *Xho*I en 3', et le plasmide pGL4.10 ont été digérés par 10 unités de chaque enzyme *Kpn*I (ER0521, Fermentas) et *Xho*I (ER0691, Fermentas) dans du tampon Tango (33 mM Tris-acetate pH 7,9, 10 mM Mg-acetate, 66 mM K-acetate, 0,1 $mg.mL^{-1}$ Serum Albumine Bovine, Invitrogen) pour libérer les extrémités cohésives.

Le plasmide pGL4.10 digéré par *Kpn*I et *Xho*I a été traité par la phosphatase alcaline (M1821, Promega), pendant 1 heure à 37°C dans du tampon de déphosphorylation (50 mM Tris-HCl pH 9,3, 1 mM $MgCl_2$, 0,1 mM $ZnCl_2$, 1 mM spermidine) afin d'éviter une ligature du plasmide sur lui-même. Les fragments du promoteur et le plasmide ainsi traités ont été purifiés sur gel d'agarose 1%. Chaque fragments a été lié au plasmide pGL4.10 par une unité d'enzyme T4 DNA ligase (M1801, Promega) dans du tampon ligase (300 mM Tris HCl pH 7,8, 100 mM $MgCl_2$, 100 mM DTT, 10 mM ATP) pendant 15 heures à 4°C.

II.1.4. Transformation bactérienne

Les produits de ligature obtenus ont été mis en présence de 100 µL de bactéries supercompétentes (XL1 Blue MR SuperComp Cells, 200229, Agilent Technologies). Après une incubation de 30 minutes à 4°C, les bactéries ont été soumises à un choc thermique (42°C, 45 secondes) pour permettre l'entrée des plasmides. Elles ont ensuite été replacées à 4°C pendant 3 minutes pour faciliter la reformation de leurs membranes, puis elles ont été mises en culture dans du milieu LB Broth Base (12780-052, Invitrogen, France) à 37°C sous agitation pendant une heure. Enfin les bactéries transformées ont été isolées sur du milieu LB lennox agar (Invitrogen, 22700-025, France) contenant 100 $ng.\mu L^{-1}$ d'ampicilline (37°C pendant 15 heures).

II.1.5. Extraction et vérification des constructions plasmidiques

Les colonies bactériennes isolées après la transformation ont été mises en culture dans du milieu LB Broth Base contenant 100 $ng.\mu L^{-1}$ d'ampicilline pendant 15 heures à 37°C sous agitation. L'ADN plasmidique contenu dans les bactéries a été extrait à l'aide du kit Plasmid DNA NucleoBond® Xtra Midi EF (740420, Macherey Nagel) selon les recommandations du fabricant. L'insertion des fragments du promoteur du gène *SCN4B* dans le plasmide pGL4.10 a été vérifiée par digestion enzymatique et séquençage. Les produits de digestion enzymatique ont été séparés par électrophorèse sur gel d'agarose 1% et leurs tailles comparées au marqueur de taille déposé en parallèle. Les plasmides ont ensuite été validés par séquençage et amplifiés. Les ADN plasmidiques ont été purifiés sur colonne échangeuse d'ions (740420, Macherey Nagel ®), précipités puis solubilisés dans de l'eau ultrapure stérile.

II.2. Activité du promoteur du gène *SCN4B*

II.2.1. Transfection transitoire des cellules MDA-MB-231

Afin de mesurer l'activité du promoteur putatif du gène *SCN4B*, les cellules MDA-MB-231 ont été transfectées de façon transitoire avec les plasmides rapporteurs à l'aide de la Lipofectamine 2000 (11668-019, Invitrogen) selon les recommandations du fabricant, avec un rapport de 1 µL pour 500 ng d'ADN plasmidique.

Pour les expériences de gène rapporteur, les cellules ont été ensemencées 24 heures avant transfection transitoire à raison de 75000 cellules par cm² dans des plaques 24 puits. Le jour de la transfection, les cellules ont été lavées avec du PBS puis mises en présence d'un mélange ADN-Lipofectamine 2000 dans 300 µL de milieu optiMEM® contenant, par puits : 250 ng de plasmide rapporteur luciférase, 30 ng de pCMV-βgal, 50 ng de plasmide d'expression codant les récepteurs nucléaires PPAR. Pour ajuster la quantité d'ADN à 500 ng, 170 ng de plasmide pUC18 ont été ajoutés. Quatre heures post-transfection, le milieu de transfection a été remplacé par 1 mL de DMEM+5% SVF contenant ou non un agoniste pharmacologique de PPARα 'WY14643, 10µM). Chaque condition a été réalisée en triplicat

II.2.2. Lyse cellulaire et mesure des activités enzymatiques luciférase et β-galactosidase

La mesure de l'activité luciférase est le reflet de l'activité du promoteur putatif et l'activité β-galactosidase permet de normaliser les résultats (contrôle de transfection).

Quarante-huit heures après transfection, les cellules ont été lavées avec du PBS puis lysées avec 100 µL de tampon de lyse Reporter Lysis Buffer (E397A, Promega). Les lysats récoltés ont été centrifugés pendant 5 minutes à 12000 x g à +4°C pour éliminer les débris cellulaires. Seuls les surnageants ont été utilisés pour mesurer les activités enzymatiques.

L'activité luciférase a été déterminée en mesurant l'émission de lumière résultant de l'oxydation de la luciférine (E1483, Promega) en oxiluciférine en présence d'ATP, par la luciférase exprimée par le plasmide rapporteur. Vingt microlitres de lysat cellulaire ont été mis en présence de 20 µL de luciférine+ATP et la lumière émise a été mesurée par le luminomètre GloMax® 20/20 pendant 10 secondes.

L'activité β-galactosidase est déterminée en mesurant l'absorbance associée à l'apparition du rouge de phénol issu de la dégradation du CPRG (Chlorophenol-red β-galactopyranoside) par

la β-galactosidase. Dans une plaque 96 puits, 10 µL de lysat cellulaire ont été incubés 15 minutes à 37°C avec 190 µL d'une solution tampon (sodium phosphate 0.1 M pH 7.4, $MgCl_2$ 1 mM,
β-mercaptoéthanol 45 mM et CPRG 1 mM). L'absorbance a été mesurée par le lecteur Spectra Max 190 (Molecular Devices) à la longueur d'onde de 574 nm.

II.2.3. Méthode d'analyse des résultats

Pour chaque transfection des plasmides rapporteurs, la valeur d'activité luciférase a été rapportée à la valeur d'activité β-galactosidase obtenue dans la même condition. Les triplicats ont permis de calculer la moyenne et l'erreur standard à la moyenne (sem) pour chaque condition.

Results

I. Manuscript 1: *SCN4B* is a tumour suppressor gene that prevents mesenchymal amoeboid transitions in breast cancer cells

Title page Research Article

SCN4B IS A TUMOUR SUPPRESSOR GENE THAT PREVENTS MESENCHYMAL-AMAEBOID TRANSITIONS IN BREAST CANCER CELLS

Emeline BON[1], Virginie DRIFFORT[1], Frédéric GRADEK[1], Carlos MARTINEZ-CACERES[2], Monique ANCHELIN[3], Pablo PELEGRIN[2], Maria-Luisa CAYUELA[3], Séverine MARIONNEAU-LAMBOT[4], Thibauld OUILLER[4], Roseline GUIBON[1,5] , Gaëlle FROMONT-HANKARD[1,5], Jorge GUTIERREZ-PAJARES[1], Isabelle DOMINGO[1], Eric PIVER[5,6], Alain MOREAU[6], Julien BURLAUD-GAILLARD[7], Stéphan CHEVALIER[1,8§], Pierre BESSON[1,8§] & Sébastien ROGER[1,9,10§]

[1] Inserm UMR1069, Nutrition, Croissance et Cancer; Université François-Rabelais de Tours, France

[2] Murcia's BioHealth Research Institute, Murcia, Spain

[3] Telomerase, Cancer and Aging Group, Murcia, Spain

[4] Cancéropôle du Grand Ouest, Nantes, France

[5] CHRU de Tours, France

[6] Inserm, U966; Université François-Rabelais de Tours, France

[7] Laboratoire de Biologie Cellulaire - Microscopie Electronique, Faculté de Médecine ; Université François-Rabelais de Tours, France

[8]UFR Sciences Pharmaceutiques, Université François-Rabelais de Tours, France

[9] UFR Sciences et Techniques, Département de Physiologie Animale, Université François-Rabelais de Tours, France

[10] Institut Universitaire de France, Paris, France

§, these authors contributed equally as last authors

Correspondence should be addressed to:

Dr. Sébastien Roger, Inserm UMR1069, 10 Boulevard Tonnellé, 37032 Tours, France, Tel : (+33) 2 47 36 61 30, Fax: (+33) 2 47 36 62 26, Email: sebastien.roger@univ-tours.fr

Running head: *SCN4B* is a tumour suppressor gene

Key words: β subunit, voltage-gated sodium channels, cancer cell invasiveness, mesenchymal-amoeboid transition, metastases

Summary

The development of metastases largely relies on the capacity of individual cancer cells to invade extracellular matrices using two forms of movements called “mesenchymal invasion” and “amoeboid invasion”. Most aggressive cells show phenotypical switches between these two modes conferring them the ability to adapt to different extracellular matrices. These transitions are orchestrated by Rho family GTPases but the signalling pathway upstream RhoGTPase activation is not well characterized.

Here we show that *SCN4B* gene, encoding for the β4 protein, initially characterized as being an auxiliary subunit of voltage-gated sodium channels in excitable tissues, is expressed in normal epithelial cells, and that the reduction of its expression is reduced in breast cancer biopsies, correlates with high grade primary and metastatic tumours. In breast cancer cells, we found that the loss of its expression dramatically potentiates cell invasiveness by increasing the activity of RhoA GTPases and regulating the conversion between mesenchymal and amoeboid phenotypes. This phenotypical switch promotes primary tumour growth and metastatic colonization of organs. Conversely, *SCN4B* overexpression reduces cancer cell invasiveness and tumour progression. These results demonstrate a role of *SCN4B*/β4 in tumour progression and entitles the *SCN4B* gene as a tumour-suppressor gene.

Introduction

Despite the important advances in primary cancer detection and therapy, breast cancer still remains the primary cause of women death by cancer worldwide. As in the vast majority of epithelial cancers, breast cancer patients mostly die because of metastases appearance and growth in distant organs, rather than from complications of the primary tumour [1]. At the cellular level, the acquisition of both high migration and high invasion potencies through extracellular matrices (ECM) by cancer cells are key components in the metastatic cascade [2]. These capacities rely on signalling pathways that control cytoskeletal dynamics in cancer cells, regulate cell-cell and cell-matrix interactions and ECM remodelling through the participation of diverse proteases. However, during the last decade a lot of information regarding the different processes of cancer cell migration and invasiveness have been reported [3] such as the "mesenchymal mode", undertaken by cells harbouring an elongated fibroblast-like morphology, with a rear-front cell polarity, self-generating a path in the ECM by proteolytic remodelling. In two-dimensional models, this is proposed to be performed by invadosomal structures which are F actin-rich organelles, protrusive into the ECM and responsible for its proteolysis through the recruitment of both membrane-associated -such as the membrane type 1- matrix metalloproteinase (MT1-MMP)- and extracellularly-released soluble proteases such as MMP2, MMP9, cysteine cathepsins or serine proteases [4,5]. The other invasive phenotype is so-called "amoeboid mode", in which cancer cells, by analogy to amoeba protozoa cells, show no obvious polarity. Indeed these cancer cells appear to have a rounded morphology, and display a high migration motility and invasiveness characterized by strong actomyosin contractions used to propel the cell movement which deforms and squeezes inside the small gaps of the ECM with no need to degrade it. While cancer cell types may be preferentially engaged into one mode or another, the most aggressive cancer cells show high plasticity and are able to switch from one phenotype to another, depending on the constraints of the environment, the composition and stiffness of the ECM [6]. These are called the mesenchymal-amoeboid (MAT) or amoeboid-mesenchymal (AMT) transitions, which are known to be orchestrated by Rho GTPases members [7-9]. Obviously, these transitions offer selective advantages and compensation mechanisms to migratory cancer cells, which presumably abrogate the efficacy of anticancer treatments [10]. Indeed, attempts to reduce cancer cell invasiveness and metastatic dissemination by interfering with proteolytic activity and ECM remodelling have largely failed because of the adaptive compensatory mechanism sustaining protease-independent processes [11].

Voltage-gated sodium channels (Na_V) are multimeric transmembrane complexes composed of one large pore-forming principal subunit (9 genes cloned, giving 9 proteins belonging to a single family $Na_V1.1$-1.9 owing to their high level of homology) [12,13] and one or two smaller transmembrane subunits (4 genes cloned *SCN1B* to *SCN4B*, giving five subunits, β1, β1B, β2, β3 and β4, which all possess a single membrane spanning domain with the exception of β1B) often characterized as being auxiliary [14]. The activity of Na_V channels, following an initial membrane depolarization, gives rise to Na^+ currents generating and propagating the action potential in excitable cells such as neurons, skeletal and cardiac muscle cells. As a result of their initial discovery and study in cells generating action potentials, the expression and activity of these proteins are considered as being hallmarks of excitable cells. Besides these relatively well-characterized functions of Na_V channels in excitable cells, multiple studies have recently demonstrated their functional expression in multiple normal non-excitable cells, in which they were proposed to regulate cellular functions such as survival or proliferation, cell migration, cell differentiation, endosome acidification, phagocytosis and podosome formation. These were recently referred to as the "non-canonical roles" of Na_V [15]. As recently reviewed, Na_V channels appeared to be abnormally expressed in human and rodent carcinoma cell lines and biopsies and their activity was associated with the acquisition of aggressive features and cancer progression. [16-18]. The expression of the $Na_V1.5$ isoform in breast tumours is associated with metastases development and patients' death [19,20]. In highly aggressive human breast cancer cells, the activity of $Na_V1.5$ is not associated with cell excitability but enhances ECM degradation and cancer cell invasiveness [21], thus favouring metastases development [22,23]. $Na_V1.5$-dependent invasiveness has been shown to be mediated through the allosteric modulation of the Na^+-H^+ exchanger NHE1 and the subsequent acidification of the pericellular microenvironment and activation of extracellular acidic cysteine cathepsins [24-26]. Furthermore, $Na_V1.5$ activity sustained Src kinase activity, the polymerisation of the F-actin cytoskeleton and the adoption by cells of a spindle-shaped elongated morphology [26]. Altogether, these results indicated a critical role of $Na_V1.5$ in the "mesenchymal invasion"mode. In comparison, the participation of non-pore-forming *SCNxB*/β subunits in oncogenic processes was not that much studied, except for a recent study on the *SCN1B*/β1 protein [27], and whether they could play important roles during carcinogenesis and cancer progression towards high metastatic grades remains largely unknown.

SCN4B/β4 low expression in human breast cancer tissues associates with poor prognosis and increased cancer cell invasiveness.

The expression of β4 protein, encoded by the most recently cloned gene of the *SCNxB* family, *SCN4B* [28], is mostly studied in excitable cells such as neuron or cardiac cells in which mutations have been linked to sodium channelopathies [29,30]. However, our initial immunohistochemical analyses performed on normal mammary tissues indicated a high expression of β4 proteins in non-excitable mammary epithelial cells. The level of expression of β4 was also very high in mammary hyperplasia and dysplasia but was remarkably reduced in biopsies of both lobular and ductal mammary carcinoma biopsies (Fig. 1A and B). The most important reduction in *SCN4B*/β4 expression was observed when progressing from *in situ* grade I to invasive grade II breast tumours. The expression of *SCN4B*/β4 protein was very low or totally absent in most of grade II, grade III primary tumours studied as well as in lymph node metastases (LNM) (Fig.1 C and D). The down-regulation of the *SCN4B* gene expression in breast cancer tissues, compared to non-cancer tissues, was also found to be highly significant in *in silico* RNA expression analyses performed from published microarrays studies (Fig. 1E) and to be associated with a higher risk of metastatic relapse or death in breast cancer patients (Fig. 1F and G). By comparison we assessed the level of expression of the other *SCNxB* genes and studied the correlation with the expression level with metastatic relapses in breast cancer patients. It appeared from in silico studies that *SCN1B*, *SCN2B* and *SCN3B* genes were down-regulated in cancer compared to non-cancer tissues (Suppl. Fig. 1A, C and E). However, there was no correlation between the level of expression of these genes and the risk of metastatic relapse (Suppl. Fig. 1B, D and F). Importantly, *SCN1B* and *SCN4B* genes seemed to be the two most highly expressed genes in non-cancer tissues (Suppl. Fig. 1G), and *SCN4B* the most strongly down-regulated in breast cancer (Suppl. Fig. 1H). *SCN4B* expression levels were also analysed in other epithelial cancers, such as lung, prostate, colon and rectal cancers. Similarly, in data coming from two published studies [31,32], *SCN4B* expression was found to be down-regulated in lung cancer compared to normal lung tissues (Suppl. Fig. 2A and B) and our immunohistochemical analyses performed in lung cancer tissue microarrays also identified a tendency for a decreased protein expression in high grade primary lung tumours and metastases (Suppl. Fig. 2C and D). *SCN4B* expression was also found to be down-regulated in prostate, colon and rectal cancers compared to normal tissues (Suppl. Fig. 2E, F and G). These initial results suggested that *SCN4B*/β4 is normally expressed in normal epithelial cells (as confirmed by immunohistochemical analyses of normal oesophagus, Suppl. Fig. 3) and that a loss of expression was associated with the gain in invasive properties by cancer cells and the aggressive

progression of epithelial tumours. Correlatively, we found that *SCN4B* expression was higher in non-cancer epithelial mammary MCF-10A cell line compared to several breast cancer cell lines such as MCF-7, MDA-MB-468, MDA-MB-435s and MDA-MB-231 (Fig. 2A). Particularly, the expression level of *SCN4B* gene appeared very low in the highly invasive and metastatic MDA-MB-231 breast cancer cell line, known to express functional $Na_V1.5$ channels [22]. Using non-quantitative PCR and western blotting experiments we showed that *SCN4B* gene was expressed at the mRNA level (Fig. 2B) and at the protein level (Fig. 2C) in MDA-MB-231 cells genetically modified to express the luciferase gene (MDA-MB-231-Luc cells), as it was the case for *SCN1B*/β1 and *SCN2B*/β2, but not for *SCN3B*/β3, thus confirming previously published results performed with wild-type MDA-MB-231 cells [24]. In order to investigate the potential involvement of *SCNxB*/β subunit expression in the invasive phenotype, we performed transient silencing of these genes using commercial small interfering RNA specific for each of these three genes (si*SCN1B*, si*SCN2B* or si*SCN4B*), and compared the β protein expression to that in cells transfected with a control null-target siRNA (siCTL). This was responsible for a significant (65% to 80%) decrease in protein level, as compared to β protein expression in cells transfected with a control null-target siRNA (siCTL), 48 hr after cell transfection with siRNA (Fig. 2D). While the reduced expression of *SCN1B*/β1 or *SCN2B*/β2 decreased cancer cell invasiveness through Matrigel™-coated invasion chambers, by 42.8 ± 6.6% and 51.7 ± 0.3%, respectively, the inhibition of *SCN4B* expression enhanced cancer cell invasiveness by 62.4 ± 12.2% (Fig. 2E and F). We also analysed the effect of knocking-down the expression of *SCN4B* on MDA-MB-231-Luc *in vivo* cancer cell invasiveness using the zebrafish model of micrometastasis [33,34]. Approximately 61% of the zebrafish embryos injected with MDA-MB-231-Luc siCTL cells presented more than 5 cells outside of the yolk sac 48 hr after injection. In comparison, approximately 87% of the embryos presented micrometastases when the MDA-MB-231-Luc cells were transfected with si*SCN4B*, resulting in an increase of the zebrafish colonization index by 1.41 ± 0.08 fold (Fig. 2H).

The loss of *SCN4B*/β4 expression promotes human cancer cell invasiveness independently of the pore-forming Na_V subunit of voltage-gated sodium channels

In the human MDA-MB-231 line, cancer cell invasiveness was demonstrated to be importantly regulated by the activity of the pore-forming $Na_V1.5$ sodium channel [19,20,24]. Therefore, we initially hypothesized that the loss of *SCN4B* expression would increase $Na_V1.5$ activity in highly aggressive cancer cells. To trial this hypothesis we constructed MDA-MB-231-Luc-derived cell lines stably expressing a null-target small hairpin RNA (shCTL cells), or expressing

a shRNA targeting the expression of *SCN5A* gene encoding for $Na_V1.5$ proteins (sh*SCN5A* cells) as already described in our previous study [22] or expressing a shRNA targeting *SCN4B* transcripts (sh*SCN4B* cells). As indicated in Suppl. Fig. 4A, the sh*SCN4B* resulted in a 81.1 ± 0.2% decrease of mRNA expression. The three cell lines displayed identical viability and growth properties, when compared together as well as compared to the parental MDA-MB-231-Luc cell line (Suppl. Fig. 4B). In shCTL cells, sodium currents are known to be generated by the sole $Na_V1.5$ channel isoform which, while commonly referred to (because of the high concentration which is required) as tetrodotoxin (TTX)-resistant, can be almost fully inhibited by 30 µM TTX [22]. Similarly to already reported results, the inhibition of $Na_V1.5$ sodium currents in shCTL cells using 30 µM TTX reduced invasiveness by 45.3 ± 4.3% [24]. In comparison, sh*SCN5A* cells, which do not express the $Na_V1.5$ channel, showed an invasiveness 43.4 ± 5.1% smaller than shCTL cells, which was not further reduced by the addition of TTX. Knocking-down the expression of *SCN4B* gene, with an interfering RNA sequence (sh*SCN4B*) different from those used in siRNA experiments (si*SCN4B*, as in Fig. 2E and F) resulted in a similar potentiation of aggressiveness. Sh*SCN4B* cells invasiveness was 276.8 ± 26.2% as compared to shCTL cells. Surprisingly, the treatment of cells with 30 µM TTX, a concentration that inhibits all Na_V channels with the exception of the very resistant $Na_V1.8$, did not reduce cancer cell invasiveness (Fig. 3A). To assess this possible independence of $Na_V1.5$ in the increased invasiveness mediated by the loss of *SCN4B* expression, we silenced *SCN5A* expression in sh*SCN4B* cells. This was responsible for a tendency, yet not significant, to reduce cancer cell invasiveness, which was still 186.6 ± 25.0% as compared to shCTL cells (Fig. 3B). Then, we transiently inhibited the expression of *SCN4B* using si*SCN4B* siRNA in sh*SCN5A* cells, which no longer express $Na_V1.5$ channels. To definitively understand whether or not this increase of cancer cell invasiveness was dependent on Na_V channels, cells were also treated or not with 3 or 30 µM TTX, respectively inhibiting all TTX-sensitive channels ($Na_V1.1$-1.4 and $Na_V1.6$-1.7) and all TTX-sensitive plus $Na_V1.5$ and $Na_V1.9$ TTX-resistant channels, or with 30 nM of the specific $Na_V1.8$ inhibitor A803467 35. As shown on Fig. 3C, silencing *SCN4B* expression with si*SCN4B* in sh*SCN5A* cells was responsible for a similar increase of cell invasiveness (+251.7 ± 20.8%) similar the one observed in sh*SCN4B* cells which express Na_V (Fig. 3A). Furthermore, neither TTX nor A803467 reduced invasiveness of sh*SCN5A* cells transfected with siCTL or si*SCN4B* (Fig. 3C). This clearly demonstrated that the increase of invasiveness in cancer cells which do not express *SCN4B* gene was not a consequence of the up-regulation of $Na_V1.5$ or any other Na_V channel. Because $Na_V1.5$ channel has been reported as being an important regulator of the mesenchymal invasion in breast cancer cells through the potentiation of NHE1-

dependent H^+ efflux and extracellular matrix degradation [22,25,26], we further investigated its regulation in sh*SCN4B* cells. Patch-clamp recordings revealed, contrarily to our initial assumptions, that the loss of *SCN4B* expression significantly decreased the maximal peak sodium current (I_{Na}) amplitude as observed in the I_{Na}-voltage relationship (Fig. 3D), suggesting a reduction of channel density at the plasma membrane. This could be due to the reduction of *SCN5A* expression level as assayed by quantitative PCR (Suppl. Fig. 4C and D). In sh*SCN4B* cells, the I_{Na} activation-voltage relationship was slightly depolarized as compared to the one of shCTL cells ($V_{1/2}$-activation were -37.2 ± 0.9 mV and -40.1 ± 1.0 mV, respectively, p=0.037). More importantly, the I_{Na} availability-voltage relationship was also significantly shifted to a more depolarized potential in sh*SCN4B* as compared to the one of shCTL cells ($V_{1/2}$-availability were -80.6 ± 1.6 mV and -86.3 ± 1.6 mV, respectively, p=0.016) (Fig. 3E) suggesting that even though there are less $Na_V1.5$ channels, they might be more active at the membrane potential of cancer cells (comprised between -30 and -40 mV) through an increased persistent window current. Indeed, while the I_{Na} peak current was reduced in sh*SCN4B* cells, the persistent I_{Na} current recorded for membrane depolarisation from -100 to -30 mV was strictly identical (Fig. 3F and G). Therefore, the ratio I_{Na} persistent/ I_{Na} peak was significantly bigger in shSCN4B cells (Fig. 3H). The sensitivity of I_{Na} to TTX was unchanged in sh*SCN4B* cells and could be almost fully inhibited by 30 µM TTX (inhibited by 85.6±2.9%) (Fig. 3I). Because, the persistent I_{Na} window current was similar in shCTL and sh*SCN4B* cells, there was no difference in the efflux of H^+ in the two cell lines as measured as previously published [25] at the addition of 130 mM NaCl in NH_4Cl-pulse-wash-acidified cells in a sodium-free solution (Fig. 3J and K). As a consequence, sh*SCN4B* cells demonstrated identical, but not increased, ECM degradative activities as compared to shCTL cells (Fig. 3M). Eventually, we assessed the effect of knocking-down the expression of *SCN4B*, using siRNA, on the invasive properties of cancer cell lines know to express functional Na_V channels (Na_V+) contributing to the mesenchymal invasion such as the non-small cell human lung cancer H460 or the human prostate cancer PC3 cell lines, and of cancer cell lines known to not express Na_V channels (Na_V-) such as the human breast MDA-MB-468 and the non-small cell lung A549 cancer cell lines [21,36,37]. In all cancer cell lines tested, the si*SCN4B* significantly increased the invasiveness, which range from 123.7±8.3% for PC3 cells and up to 160.9±9.5% in A549 cells, as compared to siCTL (Fig. 3N).

The loss of *SCN4B*/β4expression promotes cancer cell invasiveness independently of ECM degradation by promoting the non-proteolytic RhoA-dependent amoeboid cell migration.

As previously shown, cells which do not not express *SCN4B* do have the ability to degrade the ECM (Fig. 3M). However, the pharmacological inhibition of proteases with GM6001 (MMP inhibitor), leupeptin (cysteine, serine and threonine peptidases inhibitor), or E64 (cysteine cathepsin inhibitor) did not prevent the increase in invasiveness observed in sh*SCN4B* as compared to shCTL cells (Fig. 4A). The more potent effect was observed with GM6001 which reduced sh*SCN4B* cell invasiveness by about 32%. These observations suggested that the enhancement of invasivity was not due to an increase in ECM proteolysis and prompted us to analyse the migratory abilities of cell lines using time-lapse cell tracking experiments (Fig. 4B). As expected, the loss of *SCN4B* expression significantly increased the migration speed (medians are 0.889 µm.min^{-1} for shCTL and 1.265 µm.min^{-1} for sh*SCN4B* cells, $p<0.001$), as well as the track length after 3 hr-long measurements (medians are 177.76 µm for shCTL and 246.73 µm for sh*SCN4B* cells, $p<0.001$) with no apparent changes in cell adhesion properties (Suppl. Fig. 4E) or net displacement (Suppl. Fig. 4F). This increase in migration velocity is evocative of the amoeboid phenotype, characterized by a rounded morphology, the presence of blebs at the cell surface and a relative independence of the interaction with the substratum revealed by a decreased number of filopodial structures. As a matter of fact, sh*SCN4B* cells demonstrated striking changes in morphology with a higher circularity index (0.48±0.02 vs. 0.34±0.02 in sh*SCN4B* and shCTL, respectively, $p<0.001$, Fig. 4E), a decreased number of filopodia per cell (medians were 19.0 vs. 44.5 in sh*SCN4B* and shCTL, respectively, $p<0.001$, Fig. 4F and G), and an increase in the number of blebs per cell (medians were 100.5 vs. 27.5 in sh*SCN4B* and shCTL, respectively, $p<0.001$, Fig. 4F and H). These blebs were relatively small with a diameter comprised between 0.5 and 0.7 µm (Fig. 4F). The morphological changes observed in sh*SCN4B* cells might result from a Mesenchymal-Amoeboid transition (MAT) that could confer to cancer cells the ability to squeeze and migrate through small gaps of the ECM. This particularity was observed using scanning electron microscopy, and sh*SCN4B* cells demonstrated the ability to migrate through a matrix composed of Matrigel™, probably after they open a narrow interstice by focalized degradation (Fig. 4I and Suppl. Fig. 5). The interconversions between mesenchymal and amoeboid modes of invasion are known to be orchestrated by Rho GTPases and the amoeboid movement mainly relies on the RhoA-ROCK-pMLCII signalling pathway. We therefore assessed and compared the proportion of active (GTP-bound) Rho GTPases in shCTL and sh*SCN4B* cells by pull-down assays (Fig. 4J) and found a significant increase in RhoA activity concomitant with decreases in Rac1 and Cdc-42

activity (Fig. 4K). Furthermore, the inhibition of myosin II with blebbistatin [38] significantly reduced sh*SCN4B* cancer cell invasiveness by approximately 27%, while it had no effect on shCTL cell invasiveness (Fig. 4L). Interestingly, proximity ligation assays indicated a close association of the *SCN4B*/β4 protein and RhoA in shCTL cells (Fig. 4M) while no signal was observed in sh*SCN4B* cells (Suppl. Fig. 6). Because the reduced expression of *SCN4B* increases cancer cell aggressiveness, we investigated whether its stable experimental overexpression (oe*SCN4B*) in MDA-MB-231-Luc cells could have opposite effects. Fig. 5A shows that the overexpression of *SCN4B* gene, confirmed by qPCR (Suppl. Fig. 7A) and western blotting (Suppl. Fig. 7B) experiments, significantly reduced cancer cell invasiveness by 51.6±6.8% in oe*SCN4B* as compared to control cells and by about 82% as compared to sh*SCN4B* cells. To further investigate the regulation of $Na_V1.5$ channel activity and $Na_V1.5$-dependent invasiveness, we performed invasion experiments in presence, or not, of 30 µM TTX. While TTX reduced the invasion of control (oeCTL) cells to an extent similar to that found in wild-type or shCTL cells (i.e. a reduction of cancer cell invasiveness by 30.7±4.0%) it had no further effect on reducing the invasive properties of oe*SCN4B* cells (Fig. 5B). Overexpressing *SCN4B* did not affect cancer cell growth and viability (Suppl. Fig. 7C). These results suggested that the overexpression of *SCN4B* not only reduced the invasiveness related to the *SCN4B*/β4 protein-dependent signalling pathway but also inhibited the participation of the Na_V-dependent mesenchymal invasion. To test this hypothesis we analysed I_{Na} in oe*SCN4B* cells. As shown on Fig. 5C, the maximal peak I_{Na} current was not different in oe*SCN4B* cells as compared to oeCTL or shCTL cells. In oe*SCN4B* cells, the I_{Na} activation-voltage relationship was not different from the one of oeCTL cells ($V_{1/2}$-activation were -42.5 ± 0.4 mV and -43.9 ± 1.7 mV, respectively) and the I_{Na} availability-voltage relationship was slightly but not significantly shifted towards hyperpolarized values in oe*SCN4B* as compared to the one of oeCTL cells ($V_{1/2}$-availability were -87.8 ± 1.3 mV and -86.0 ± 1.6 mV, respectively, p=0.016). This was not statistically significant either when compared to the I_{Na} $V_{1/2}$-availability in shCTL cells (-86.3 ± 1.6 mV, p=0.437), but significant when compared to the $V_{1/2}$-availability in sh*SCN4B* cells (-80.6 ± 1.6 mV, p<0.002). Nevertheless, we measured a decrease in the I_{Na} persistent/I_{Na} peak ratio in oe*SCN4B* cells as compared with oeCTL (Fig. 5E), and a significant reduction of the focalized matrigel™ degradation (Fig. 5F) suggesting that the overexpression of *SCN4B*/β4 protein slightly reduced the persistent window current and associated ECM proteolytic (mesenchymal) activity in cancer cells. The overexpression of *SCN4B*/β4 protein was also accompanied with a reduction in the cell circularity index (from 0.49± 0.02 to 0.38±0.02 in oeCTL and oe*SCN4B*, respectively, p<0.001, Fig. 5G), a reduction in the migration speed (medians are

0.983 µm.min^{-1} for oeCTL and 0.520 µm.min^{-1} for oe*SCN4B* cells, p<0.001, Fig. 5H) and a significant reduction of RhoA activity (Fig. 5I and J). Overall, these results indicate that *SCN4B*/β4 protein expression could reduce the Na_V-dependent mesenchymal invasion and prevent the mesenchymal-amoeboid transition (MAT).

SCNxB/β proteins have initially been characterized as being auxiliary subunits of Na_V channels because both proteins could be immunoprecipitated in excitable cells and also because they have been shown to regulate the plasma membrane addressing, the biophysical properties and even the pharmacology of pore-forming Na_V. They are also known to be not only auxiliary to Na_V channels but also to possess their own functions, especially through the participation of the immunoglobulin (Ig)-like extracellular domain enabling them to act as cell adhesion molecules (CAM) [14]. In order to investigate the participation of *SCN4B*/β4 protein domains that are involved in the inhibition of the MAT, we constructed different variants of the protein intended to be overexpressed in sh*SCN4B* cells. For this purpose, the nucleotide sequence was mutated so that the transcripts would not be targeted by the shRNA. Eight nucleotides were substituted which conserved the amino acids. The full-length sequence was called "full-length rescue" sequence as it allowed the expression of a normal β4 protein in sh*SCN4B* cells. We also constructed two truncated variants of the *SCN4B*/β4 protein: a N-terminal truncated protein (from residue 1 to residue T161), called "ΔN-ter", containing the transmembrane and C-terminal intracellular domain of the *SCN4B*/β4 protein but completely devoid of the Ig-like extracellular domain, and a *SCN4B*/β4 protein truncated in the C-terminus region, from residue K185, and identified as being "ΔC-ter" (Fig. 5K). The ΔC-ter construct contained the same 8 substituted nucleotides with conservation of the amino acids sequence so that it could be expressed in sh*SCN4B* cells. Sh*SCN4B* cells were transfected with the empty vector (pSec) or with the three different *SCN4B*/β4 variants and cell invasiveness was analysed. The reintroduction of the full-length *SCN4B*/β4 protein significantly reduced cancer cell invasiveness as compared with the empty vector, and as such operated as an effective rescue. Interestingly, the ΔC-ter variant, which possessed the extracellular domain, was ineffective, whereas the ΔN-ter variant, inhibited cell invasiveness to the same extent as the full-length rescue (Fig. 5L). Correlatively, only the full-length rescue and the ΔN-ter proteins reduced the speed of migration (Fig. 5M) and RhoA activity (Fig. 5N) in sh*SCN4B* cells. These data therefore demonstrate that the intracellular C-terminus of the *SCN4B*/β4 protein, and not the extracellular Ig-like domain, is needed to inhibit MAT in breast cancer cells.

The loss of *SCN4B*/β4 expression promotes primary breast tumour growth and metastasis development in vivo.

Because the loss of *SCN4B* expression promoted cancer cell invasiveness *in vitro,* we supposed that it would also promote metastases development from breast tumours. We therefore developed two *in vivo* models to further study these aspects. In the first one, we assessed the importance of *SCN4B* down-regulation or overexpression in human breast cancer cells for the colonisation of organs. Sh*SCN4B* or oe*SCN4B* cells, both presenting identical growth and viability properties *in vitro* (Suppl. Fig. 7C) and similarly expressing the luciferase gene (Suppl. Fig. 7D), were injected in the tail vein of NMRI nude mice. At completion of the study, after 9 weekd of experiments, there was no statistical difference in the animal body weights between the two experimental groups (Suppl. Fig. 7E). Mice were sacrificed and the isolated organs (lungs, brain, liver, bones from rachis/ribs and legs) were analysed ex vivo for bioluminescent imaging after luciferin injection (Fig. 6A). In the sh*SCN4B* group, all mice showed lung colonisation (7/7) and no other organs were colonised. In the oe*SCN4B* group, only one mouse out of eight had lung colonisation and there was no bioluminescent signal in other organs. Altogether, there was a strong reduction of lung colonisation by cancer cells overexpressing *SCN4B*/β4 as compared to those which do not express β4 protein (Fig. 6B). We then used an orthotopic xenograft model of mammary cancer in which sh*SCN4B* or oe*SCN4B* cells were injected into the mammary fat pad of NOD SCID mice, and the primary tumour growth was analysed as a function of time for [22] weeks. There was no statistical difference in the evolution of animal body weights between the two experimental groups (8 mice/group, Fig. 6C). The growth of primary mammary tumours, measured with a calliper (Fig. 6D) or by bioluminescent imaging (Fig. 6E and F) was reduced in mice implanted with oe*SCN4B* cells compared to those implanted with sh*SCN4B*. Overall, these results indicate that the loss of *SCN4B* expression in cancer cells potentiates their aggressiveness and stimulates primary tumour growth as well as metastatic organ colonization.

Conclusions

Aggressive cancer cells show an important plasticity enabling them to switch from one invasion mode to another, and conferring them the ability to adapt to their microenvironment, matrix composition, meshwork and stiffness. Here, we have identified the expression of *SCN4B* gene as an important modulator of cancer cell invasiveness, tumour growth and metastases development. The *SCN4B*/β4 protein was initially characterized as being expressed in some excitable cells in which it acts as an auxiliary subunit of voltage-gated sodium (Na_V) channels. This study shows for the first time that this protein is expressed in non-cancerous epithelial cells, which do not express Na_V channels. Furthermore, the expression of *SCN4B*/β4 is reduced in cancer tissues, and more particularly when tumours gain invasive properties (transition from grade I to grade II) to be almost not expressed in high grade tumours and metastases. At the cellular level, the loss of *SCN4B*/β4 in cancer cells promotes their invasiveness by allowing an increase in the mesenchymal-amoeboid transition, yet leaving the ECM-degradative activity intact. This change in cell phenotype is supported by the overactivation of the RhoA GTPase. Inversely, the overexpression of *SCN4B*/β4 reduces cancer cell invasiveness, primary tumour growth and metastatic progression, supporting the concept that the *SCN4B* gene might represent a tumour-suppressor gene.

This study also demonstrates that the *SCN4B*/β4 protein possesses both conducting, regulating Na_V channels, and specific non-conducting roles in cancer cells. Indeed, the loss of *SCN4B* gene expression in cancer cells left Na_V-dependent invasiveness unaffected, through the maintenance of a persistent sodium current that regulates ECM proteolysis, but also increased Na_V-independent amoeboid-related cell migration, through the dynamic regulation of RhoGTPases. This latter property is under the control of the intracellular C-terminus domain and independent of the extracellular CAM domain. We showed that in less invasive cells RhoA co-localized with *SCN4B*/β4 protein. This interaction might occur in the C-terminal domain of the *SCN4B*/β4 protein and one could hypothesize that its loss in highly invasive cells releases RhoA from a submembrane localization authorizing its activation and the acquisition of an amoeboid phenotype.

Acknowledgements

This work was supported by "Ministère de la Recherche et des Technologies", Inserm, "Ligue Nationale Contre le Cancer", Région Centre (grant “NaVMetarget”), project “ARD2020 Biodrugs” and “Association CANCEN”.

Author information

The authors declare no competing financial interests. Correspondence and requests for materials should be addressed to S.R. (sebastien.roger@univ-tours.fr)

References

1 Parkin, D. M., Bray, F., Ferlay, J. & Pisani, P. Global cancer statistics, 2002. CA Cancer J Clin 55, 74-108 (2005).

2 Fidler, I. J. Understanding bone metastases: the key to the effective treatment of prostate cancer. Clinical advances in hematology & oncology : H&O 1, 278-279 (2003).

3 Friedl, P. & Alexander, S. Cancer invasion and the microenvironment: plasticity and reciprocity. Cell 147, 992-1009 (2011).

4 Linder, S., Wiesner, C. & Himmel, M. Degrading devices: invadosomes in proteolytic cell invasion. Annu Rev Cell Dev Biol 27, 185-211 (2011).

5 Brisson, L., Reshkin, S. J., Gore, J. & Roger, S. pH regulators in invadosomal functioning: Proton delivery for matrix tasting. Eur J Cell Biol 91, 847-860 (2012).

6 Wolf, K. & Friedl, P. Extracellular matrix determinants of proteolytic and non-proteolytic cell migration. Trends Cell Biol 21, 736-744, doi:10.1016/j.tcb.2011.09.006 (2011).

7 Sanz-Moreno, V. et al. Rac activation and inactivation control plasticity of tumor cell movement. Cell 135, 510-523, doi:10.1016/j.cell.2008.09.043 (2008).

8 Sahai, E. & Marshall, C. J. Differing modes of tumour cell invasion have distinct requirements for Rho/ROCK signalling and extracellular proteolysis. Nat Cell Biol 5, 711-719, doi:10.1038/ncb1019 (2003).

9 Wyckoff, J. B., Pinner, S. E., Gschmeissner, S., Condeelis, J. S. & Sahai, E. ROCK- and myosin-dependent matrix deformation enables protease-independent tumor-cell invasion in vivo. Curr Biol 16, 1515-1523, doi:10.1016/j.cub.2006.05.065 (2006).

10 Friedl, P. & Wolf, K. Tumour-cell invasion and migration: diversity and escape mechanisms. Nat Rev Cancer 3, 362-374 (2003).

11 Wolf, K. et al. Compensation mechanism in tumor cell migration: mesenchymal-amoeboid transition after blocking of pericellular proteolysis. J Cell Biol 160, 267-277 (2003).

12 Goldin, A. L. et al. Nomenclature of voltage-gated sodium channels. Neuron 28, 365-368 (2000).

13 Catterall, W. A. Voltage-Gated Sodium Channels at 60:Structure, Function, and Pathophysiology. J Physiol (2012).

14 O'Malley, H. A. & Isom, L. L. Sodium channel beta subunits: emerging targets in channelopathies. Annu Rev Physiol 77, 481-504, doi:10.1146/annurev-physiol-021014-071846 (2015).

15 Black, J. A. & Waxman, S. G. Noncanonical roles of voltage-gated sodium channels. Neuron 80, 280-291, doi:10.1016/j.neuron.2013.09.012 (2013).

16 Besson, P. et al. How do voltage-gated sodium channels enhance migration and invasiveness in cancer cells? Biochim Biophys Acta 1848, 2493-2501, doi:10.1016/j.bbamem.2015.04.013 (2015).

17 Roger, S., Gillet, L., Le Guennec, J. Y. & Besson, P. Voltage-gated sodium channels and cancer: is excitability their primary role? Front Pharmacol 6, 152, doi:10.3389/fphar.2015.00152 (2015).

18 Brackenbury, W. J. Voltage-gated sodium channels and metastatic disease. Channels (Austin) 6 (2012).

19 Yang, M. et al. Therapeutic potential for phenytoin: targeting Na(v)1.5 sodium channels to reduce migration and invasion in metastatic breast cancer. Breast Cancer Res Treat (2012).

20 Fraser, S. P. et al. Voltage-gated sodium channel expression and potentiation of human breast cancer metastasis. Clin Cancer Res 11, 5381-5389 (2005).

21 Roger, S., Besson, P. & Le Guennec, J. Y. Involvement of a novel fast inward sodium current in the invasion capacity of a breast cancer cell line. Biochim Biophys Acta 1616, 107-111 (2003).

22 Driffort, V. et al. Ranolazine inhibits NaV1.5-mediated breast cancer cell invasiveness and lung colonization. Mol Cancer 13, 264, doi:10.1186/1476-4598-13-264 (2014).

23 Nelson, M., Yang, M., Dowle, A. A., Thomas, J. R. & Brackenbury, W. J. The sodium channel-blocking antiepileptic drug phenytoin inhibits breast tumour growth and metastasis. Mol Cancer 14, 13, doi:10.1186/s12943-014-0277-x (2015).

24 Gillet, L. et al. Voltage-gated Sodium Channel Activity Promotes Cysteine Cathepsin-dependent Invasiveness and Colony Growth of Human Cancer Cells. J Biol Chem 284, 8680-8691 (2009).

25 Brisson, L. et al. Na(V)1.5 enhances breast cancer cell invasiveness by increasing NHE1-dependent H(+) efflux in caveolae. Oncogene 30, 2070-2076 (2011).

26 Brisson, L. et al. NaV1.5 Na+ channels allosterically regulate the NHE-1 exchanger and promote the activity of breast cancer cell invadopodia. J Cell Sci 126, 4835-4842 (2013).

27 Nelson, M., Millican-Slater, R., Forrest, L. C. & Brackenbury, W. J. The sodium channel beta1 subunit mediates outgrowth of neurite-like processes on breast cancer cells and promotes tumour growth and metastasis. Int J Cancer 135, 2338-2351 (2014).

28 Yu, F. H. et al. Sodium channel beta4, a new disulfide-linked auxiliary subunit with similarity to beta2. J Neurosci 23, 7577-7585 (2003).

29 Medeiros-Domingo, A. et al. SCN4B-encoded sodium channel beta4 subunit in congenital long-QT syndrome. Circulation 116, 134-142, doi:10.1161/CIRCULATIONAHA.106.659086 (2007).

30 Tan, B. H. et al. Sudden infant death syndrome-associated mutations in the sodium channel beta subunits. Heart rhythm : the official journal of the Heart Rhythm Society 7, 771-778, doi:10.1016/j.hrthm.2010.01.032 (2010).

31 Okayama, H. et al. Identification of genes upregulated in ALK-positive and EGFR/KRAS/ALK-negative lung adenocarcinomas. Cancer Res 72, 100-111, doi:10.1158/0008-5472.CAN-11-1403 (2012).

32 Hou, J. et al. Gene expression-based classification of non-small cell lung carcinomas and survival prediction. PLoS One 5, e10312, doi:10.1371/journal.pone.0010312 (2010).

33 Marques, I. J. et al. Metastatic behaviour of primary human tumours in a zebrafish xenotransplantation model. BMC Cancer 9, 128 (2009).

34 Jelassi, B. et al. P2X(7) receptor activation enhances SK3 channels- and cystein cathepsin-dependent cancer cells invasiveness. Oncogene 30, 2108-2122 (2011).

35 Jarvis, M. F. et al. A-803467, a potent and selective Nav1.8 sodium channel blocker, attenuates neuropathic and inflammatory pain in the rat. Proc Natl Acad Sci U S A 104, 8520-8525, doi:10.1073/pnas.0611364104 (2007).

36 Roger, S. et al. Voltage-gated sodium channels potentiate the invasive capacities of human non-small-cell lung cancer cell lines. Int J Biochem Cell Biol 39, 774-786 (2007).

37 Diss, J. K., Archer, S. N., Hirano, J., Fraser, S. P. & Djamgoz, M. B. Expression profiles of voltage-gated Na(+) channel alpha-subunit genes in rat and human prostate cancer cell lines. Prostate 48, 165-178 (2001).

38 Kovacs, M., Toth, J., Hetenyi, C., Malnasi-Csizmadia, A. & Sellers, J. R. Mechanism of blebbistatin inhibition of myosin II. J Biol Chem 279, 35557-35563, doi:10.1074/jbc.M405319200 (2004).

39 Jezequel, P. et al. bc-GenExMiner: an easy-to-use online platform for gene prognostic analyses in breast cancer. Breast Cancer Res Treat 131, 765-775 (2012).

40 Gore, J., Besson, P., Hoinard, C. & Bougnoux, P. Na(+)-H+ antiporter activity in relation to membrane fatty acid composition and cell proliferation. Am J Physiol 266, C110-120 (1994).

41 Soderberg, O. et al. Direct observation of individual endogenous protein complexes in situ by proximity ligation. Nat Methods 3, 995-1000 (2006).

42 Arredouani, M. S. et al. Identification of the transcription factor single-minded homologue 2 as a potential biomarker and immunotherapy target in prostate cancer. Clin Cancer Res 15, 5794-5802, doi:10.1158/1078-0432.CCR-09-0911 (2009).

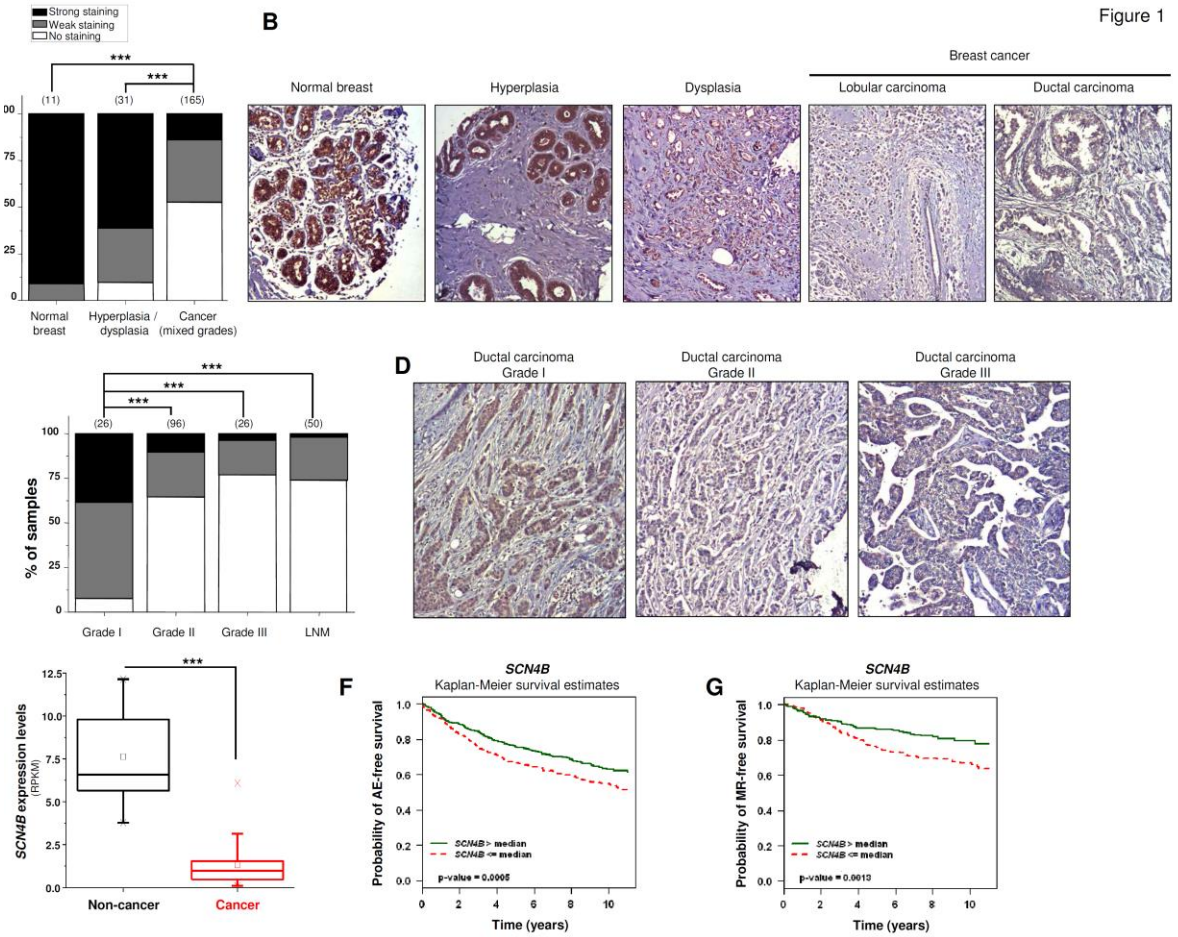

Figure 1: *SCN4B* down-regulation in human breast cancer tissues associates with poor prognosis. A-D, the protein (β4) expression of the *SCN4B* gene was analysed by immunohistochemistry on tissues arrays containing normal breast, hyperplasic, dysplasia, breast cancer (from grade I to grade III) and lymph node metastases (LNM) samples. *SCN4B*/β4 protein staining was analysed and samples were stratified in "no staining", "weak staining" or "strong staining" groups. **A**, Proportion of samples showing no (white), weak (gray) or strong (black) β4 staining in normal breast, compared to mammary hyperplasia/dysplasia and cancer (mixed grades) samples. The number of samples per condition is indicated between brackets. *SCN4B*/β4 protein staining was significantly stronger in normal compared to cancer samples ($p<0.001$), and in hyperplasia/dysplasia compared to cancer samples ($p<0.001$). **B**, Representative β4 staining pictures from normal breast, hyperplasia, dysplasia, lobular and ductal breast carcinoma samples. **C**, Proportion of samples showing no, weak or strong β4 staining in cancer samples, from grade I to grade III, and in LNM samples. The number of samples per condition is indicated between brackets. β4 staining was significantly stronger in grade I cancer samples compared to more advanced cancer samples (grades II, III and LNM) ($p<0.001$). **D**, Representative pictures of β4 staining pictures from grade I, II and III ductal carcinoma samples. **E**, Expression of the *SCN4B* gene in non-cancer (n= 29) and in breast cancer tissues (n= 145) was analysed in The Cancer Genome Atlas (TCGA) and RNA expression is expressed as reads per kilobase per million (RPKM). Box plots indicate the first quartile, the median, and the third quartile, squares indicate the mean. *SCN4B* gene was significantly down-regulated in cancer tissues ($p<0.001$). **F and G,** Prognostic analyses of gene expression in breast cancers were performed using the software ***Breast Cancer Gene-Expression Miner*** (bc-GenExMiner v3.0; http://bcgenex.centregauducheau.fr) developed by the Integrated Center of Oncology René Gauducheau (Nantes-Saint Herblain, France), based on DNA microarrays results collected from

published cohorts. Statistical tests were conducted on each of the individual cohorts and on pooled cohorts as described [39]. **F**, Kaplan-Meier Any Event (AE)-free survival analyses were performed on data pooled from cohorts (see Methods) for the expression of *SCN4B* gene (n= 1,024 patients). Any event are defined as being metastatic relapse or patient death. A weak expression of *SCN4B* gene (≤median of the pooled cohorts) was associated with a decrease in the AE-free survival (p= 0.0005). **G**, Kaplan-Meier metastatic-relapse (MR)-free survival analyses were performed on data pooled from cohorts for the expression of *SCN4B* gene (n= 661 patients). A weak expression of *SCN4B* gene (≤median of the pooled cohorts) was associated with a decrease in the MR-free survival (p= 0.0013). Cox results are displayed on the graph.

Figure 2

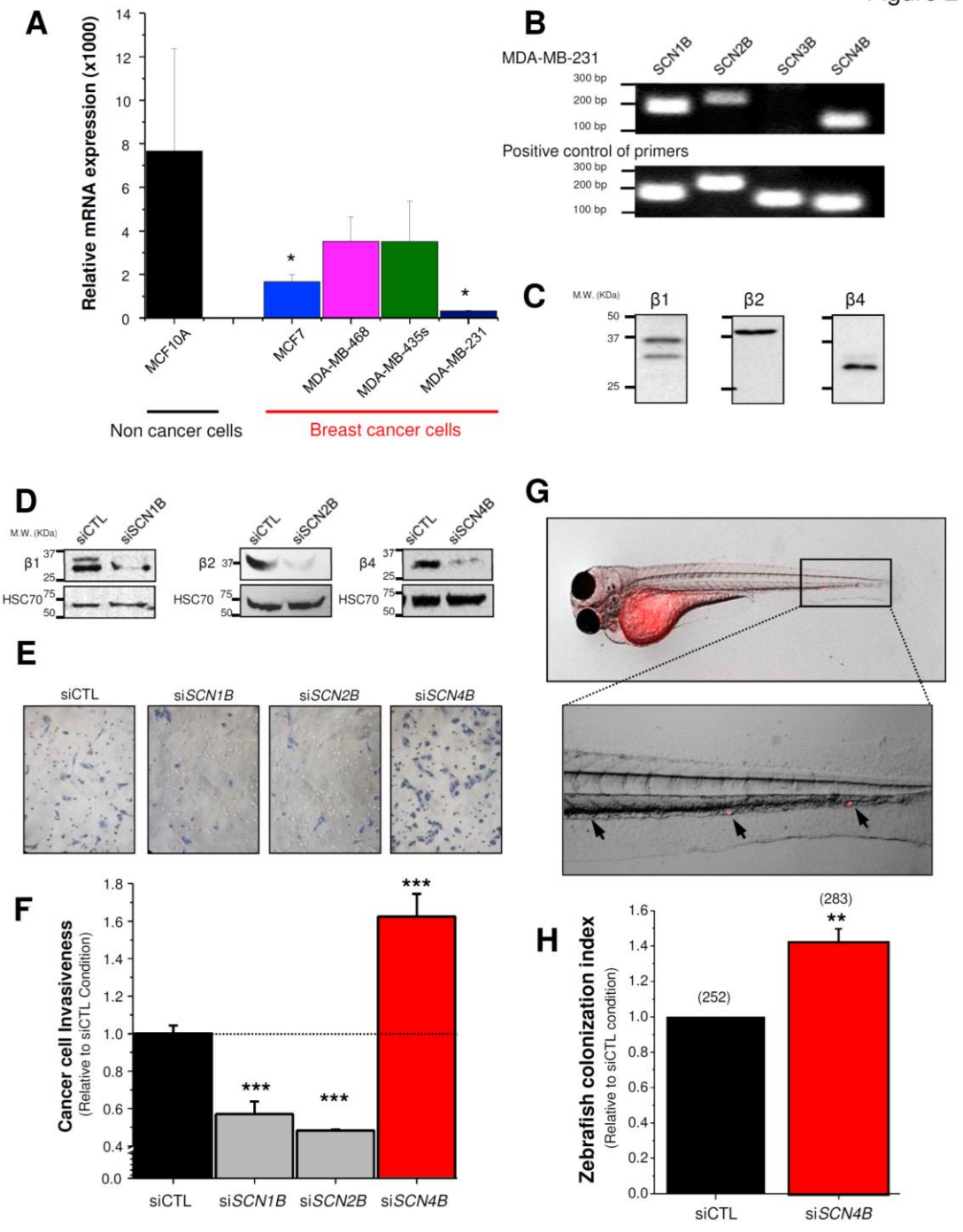

Figure 2: Expression of the *SCN4B* gene encoding for β4 subunit of voltage-gated sodium channels in human breast cancer cell lines and contribution to cancer cell invasiveness.

A, The expression of *SCN4B* gene (mRNA) was studied by RT- quantitative PCR in human mammary epithelial non-cancer MCF-10A and cancer MCF7, MDA-MB-468, MDA-MB-435s and MDA-MB-231 cell lines. Results are given as expression relative to *HPRT-1* gene expression (n= 6-12 separate experiments). * denotes that *SCN4B* expression level is significantly different from the *SCN4B* expression level from the non-cancer mammary epithelial cell line MCF-10A at $p<0.05$. **B**, The expression of *SCNxB* genes was analysed in MDA-MB-231-Luc breast cancer cells by RT-PCR using primers specific for *SCN1B*, *SCN2B*, *SCN3B* or *SCN4B*. PCR products were then analysed by electrophoresis in 1.8%-agarose gels containing ethidium bromide, and visualized by UV trans-illumination. Plasmids encoding human *SCN1B*, *SCN2B*, *SCN3B* or *SCN4B* genes were used as positive controls of PCR primers. **C**, Representative western blotting experiments showing protein expression for β1 (*SCN1B*), β2 (*SCN2B*) and β4 (*SCN4B*), but no β3 (*SCN3B*) expression, in MDA-MB-231-Luc breast cancer cells. **D**, MDA-MB-231-Luc cells were transfected with scrambled siRNA (siCTL) or with siRNA directed against the expression of the *SCN1B* gene (si*SCN1B*), the *SCN2B* gene (si*SCN2B*), or the *SCN4B* gene (si*SCN4B*) and the efficacy of siRNA transfection was assessed by western blotting experiments 48hr after transfection using specific antibodies for β1, β2 or β4 proteins, respectively. HSC70 was used as a control for sample loading. **E**, Representative images of fixed and haematyoxylin-stained MDA-MB-231 cell invasion on the Matrigel®-coated inserts. Cancer cells were transfected with scrambled siCTL or with siRNA directed against the expression of the *SCNxB* gene (si*SCNxB*) as explained previously. **F,** Summary of cancer cell invasiveness results from 8 independent experiments, for MDA-MB-231 cells were transfected with siCTL or si*SCNxB*. The results were expressed relative to the control cells transfected with siCTL. *** denotes a significant difference from the siCTL at $p<0.001$. **G,** Representative image of a zebrafish embryo injected in the yolk sac with MDA-MB-231 cells stained with the vital fluorescent tracker CM-Dil in the yolk sac and showing sites of colonization. A magnification of the highlighted region containing human cancer cells (see arrows) colonizing organs of the embryo is shown below. **H**, Zebrafish colonization index of MDA-MB-231 cancer cells expressing (siCTL) or not (si*SCN4B*) the *SCN4B* gene. The numbers between brackets indicates the number of embryos examined for each condition from three different experiments. ** indicates a significant differences from the siCTL condition at $p<0.01$.

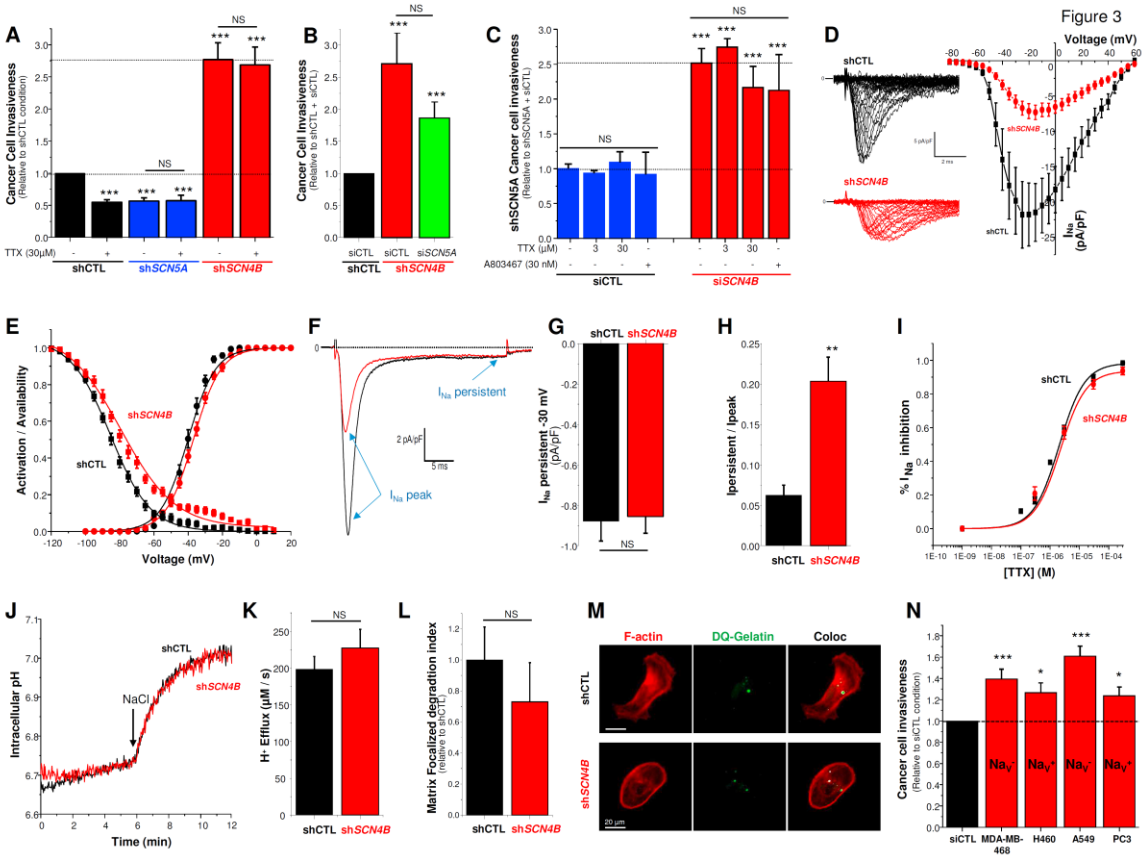

Figure 3: The loss of *SCN4B* expression (β4 subunit) promotes human cancer cell invasiveness independently of pore-forming Na$_V$ subunit of voltage-gated sodium channels.

A, Cancer cell invasiveness was assessed using Matrigel™-invasion chambers from MDA-MB-231-Luc cells stably transfected with null-target shRNA (shCTL), *SCN5A*-targeting shRNA (sh*SCN5A*) or *SCN4B*-targeting shRNA (sh*SCN4B*), in absence (-) or presence (+) of 30 µM tetrodotoxin (TTX). The results from 8-10 independent experiments and were expressed relative to the control cells transfected with shCTL in absence of TTX. NS stands for no statistical difference and *** denotes a significant difference from the shCTL at $p < 0.001$. **B**, Cancer cell invasiveness was likewise assessed in shCTL or sh*SCN4B* cells, transiently transfected with null-target siRNA (siCTL) or *SCN5A*-targeting siRNA (si*SCN5A*). The results from 6 independent experiments and were expressed relative to shCTL cells transfected with siCTL. NS stands for no statistical difference and *** denotes a significant difference from the shCTL/siCTL condition at $p < 0.001$. **C**, Cancer cell invasiveness was assessed in MDA-MB-231-Luc cells stably expressing the *SCN5A*-targeting shRNA (sh*SCN5A*), thus which do not express the Na$_V$1.5 protein, transiently transfected with null-target siRNA (siCTL) or *SCN4B*-targeting siRNA (si*SCN4B*), in absence (-) or presence (+) of two different TTX concentrations (3 or 30 µM), or 30 nM of the Na$_V$1.8 inhibitor A803467. The results from 6 independent experiments were expressed relative to sh*SCN5A* cells transfected with siCTL, in absence of any Na$_V$ inhibitor. NS stands for no statistical difference and *** denotes a significant difference from the sh*SCN5A*/siCTL condition at $p < 0.001$. **D**, Sodium current (I_{Na})-voltage relationships in shCTL (black squares, n= 17) and in sh*SCN4B* (red circles, n= 22) cells obtained from a holding potential of -100 mV. There was a significant difference at $p<0.001$ between the two conditions in the voltage range between -50 and +45 mV. **E**, Activation-(●) and availability-(■) voltage relationships obtained in the same shCTL (black symbols) and sh*SCN4B* (red symbols) cells as in D. **F**, Representative sodium currents obtained from shCTL (black trace) and

sh*SCN4B* (red trace) cells for a membrane depolarisation from -100 to -30 mV showing I_{Na} peak and I_{Na} persistent currents. "0" indicates the 0 current level. **G**, Mean I_{Na} persistent currents obtained for a membrane depolarisation from -100 to -30 mV from 18 shCTL and 21 sh*SCN4B* cells. NS stands for not statistically different. **H**, Mean ratios of I_{Na} persistent / I_{Na} peak currents obtained for a membrane depolarisation from -100 to -30 mV from 18 shCTL and 21 sh*SCN4B* cells. ** indicates a statistical difference from shCTL at $p<0.01$. **I**, Dose-response effect of TTX on inhibiting I_{Na} peak elicited by a membrane depolarization from -100 to -5 mV in shCTL (black squares) and in sh*SCN4B* (red circles) cells. **J**, Representative intracellular pH evolution, measured using the pH-sensitive cell permeant BCECF-AM probe, in NH_4Cl-acidified shCTL (black trace) and sh*SCN4B* (red trace) cells in a Hank's solution in absence of NaCl. 130 mM NaCl (NaCl) was added at the time indicated by the arrow and was responsible for an intracellular alkalinisation. **K**, H^+ efflux measurements after the addition of 130 mM NaCl in the similar conditions as in J. N= 20 independent experiments. NS stands for no statistical difference. **L**, MDA-MB-231 shCTL or sh*SCN4B* cells were cultured on a Matrigel™-composed matrix containing DQ-Gelatin® as a fluorogenic substrate for gelatinolytic proteases. A "Matrix-Focalized-degradation index" was calculated as being F-actin foci (red labelling, phalloidin-Alexa594) co-localised with focused proteolytic activities (green). Merging areas are represented as white pixels and were counted for every cell assessed. The analysis represents results obtained with 442 and 448 cells for shCTL and sh*SCN4B*, respectively. NS stands for no statistical difference. **M**, Representative pictures showing matrix degradation areas (green spots) and F-actin foci (red spots) in shCTL and sh*SCN4B* cells. Merging points (coloc) appear as white pixels which were counted. Numbers of white pixels by cell were measured then normalized to the mean value obtained in shCTL cells. **N**, Cancer cell invasiveness was assessed using Matrigel™-invasion chambers for MDA-MB-468 breast, H460 and A549 non-small-cell lung, and PC3 prostate cancer cells transfected with null-target siRNA (siCTL, black bar) or *SCN4B*-targeting siRNA (si*SCN4B*, red bars). Cancer cell lines known to express or not to express functional Na_V channels are indicated as Na_V+ and Na_V-, respectively. The results from 3-12 independent experiments and were expressed relative to the results obtained with same cells transfected with siCTL. * denotes a significant difference from the siCTL at $p<0.05$ and *** at $p < 0.001$.

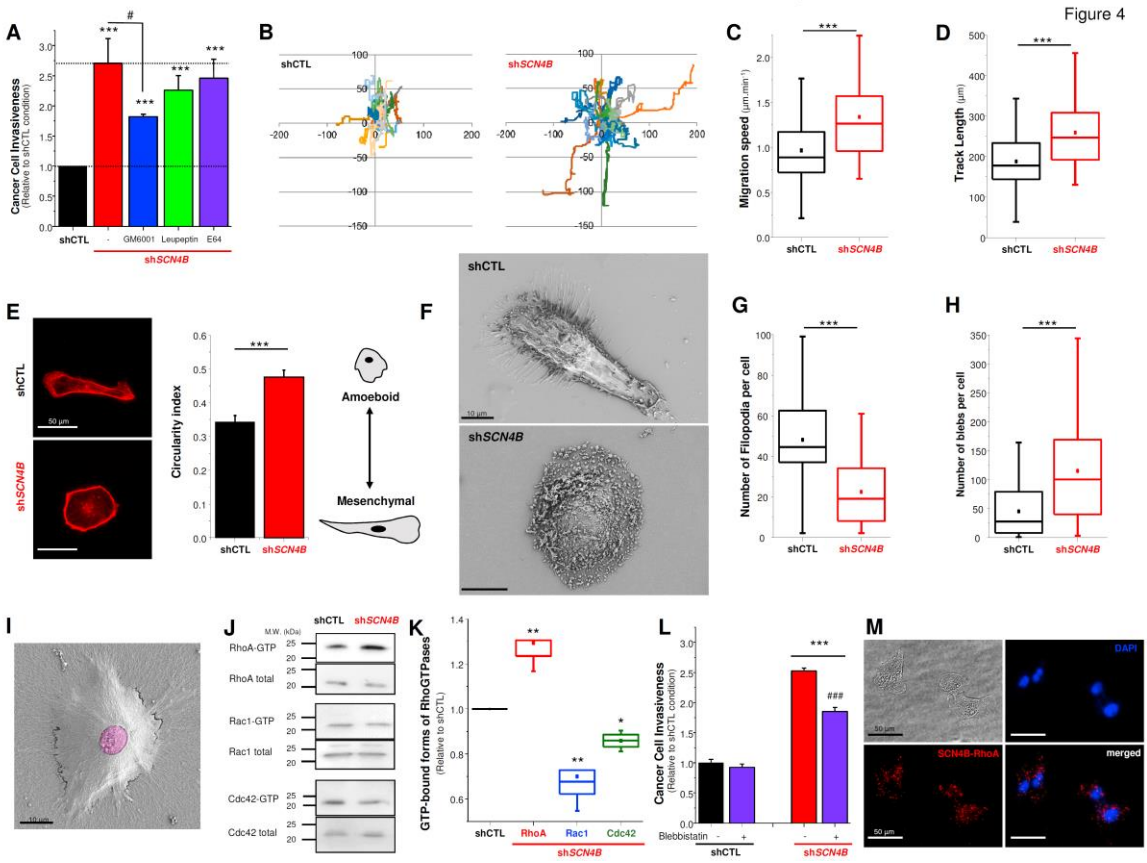

Figure 4: The loss of *SCN4B* expression (β4 subunit) promotes human cancer cell invasiveness by promoting non-proteolytic RhoA-dependent amoeboid cell migration.

A, Cancer cell invasiveness was assessed using Matrigel™-invasion chambers from shCTL or sh*SCN4B*, in absence (-) or presence of the proteases inhibitors GM6001 (10 µM), leupeptin (200 µM) or E64 (100 µM). The results from 3-7 independent experiments were expressed relative to shCTL cells in absence of inhibitors. *** denotes a statistical difference from the shCTL at $p<0.001$, and # indicates a statistical difference from sh*SCN4B* at $p<0.05$. **B,** Cancer cell migration of shCTL and sh*SCN4B* cells measured by time-lapse microscopy to track the movement of cells over 180 min, 1 frame / min (n= 20 representative cells in each condition). Distances are indicated in µm. **C,** The speed of migration (in $\mu m.min^{-1}$) was analysed in shCTL and sh*SCN4B* from time-lapse experiments and results shown were obtained from 106 and 96 cells, respectively. *** denotes a statistical difference from the shCTL at $p<0.001$. **D,** The track length of cell migration (in µm) was analysed over 180 min in shCTL and sh*SCN4B* from time-lapse experiments and results shown were obtained from 106 and 96 cells, respectively. *** denotes a statistical difference from the shCTL at $p<0.001$. **E**, F-actin cytoskeleton was stained with phalloidin-AlexaFluor594 in shCTL and sh*SCN4B* cells and a cell circularity index was calculated using ImageJ© software (n= 88 cells analysed in each cell type). A circularity index approaching "1" indicates a perfect circle, which is more characteristic of the amoeboid phenotype. In comparison, mesenchymal cells are more elongated and would have a circularity index approaching "0". **F**, Representative pictures of shCTL and sh*SCN4B* cells, grown on glass coverslips, analysed by scanning electron microscopy. Scale bars, 10 µm. **G**, The number of filopodia per cell was counted from electron microscopy pictures in shCTL and sh*SCN4B* cells (n= 60 and 66 cells, respectively). **H**, The number of blebs per cell was counted from scanning electron micrographs in shCTL and sh*SCN4B* cells (n= 82 cells in each cell type). **I**, Scanning electron microscopy observations of sh*SCN4B* cell

invasion 24 hr after cells were seeded on a layer of Matrigel™ (4 mg/mL) coated on the glass coverslip. The coloured part is the tip of the cell observable above the Matrigel™ layer, while the non-coloured part shows that the cell has invaded and penetrated inside the matrix. Scale bar, 10 µm. **J**, GST-RBD pull-down assay in shCTL and sh*SCN4B* cells. Western blots showing active RhoA-GTP, active Rac1-GTP or active Cdc42-GTP, pulled down by GST-RBD and detected by anti-RhoA, anti-Rac1, or anti-Cdc42 in western blot. By comparison total forms of RhoA, Rac1 and Cdc42 are shown. **K**, Quantification of GTP-bound RhoGTPases. The activity of GTP-bound (active) RhoGTPase was normalized to its total protein level, and was expressed relatively to that in shCTL cells. Data from 5 independent experiments. ** denotes a statistical difference from the shCTL at p<0.01, and * at p<0.05. **L**, Cancer cell invasiveness was assessed using Matrigel™-invasion chambers from shCTL or sh*SCN4B*, in absence (-) or presence of the myosin II inhibitor blebbistatin (50 µM). The results from 3 independent experiments and were expressed relative to shCTL cells in absence of blebbistatin. *** denotes a statistical difference from the shCTL at p<0.001, and ### indicates a statistical difference from sh*SCN4B* at p<0.001. **M**, *In situ* proximity ligation assays (Duolink "In cell co-IP") showing a strong proximity between *SCN4B* proteins (β4) and RhoA in shCTL cells (red dots). Nuclei were stained with DAPI (blue). Scale bars, 50 µm.

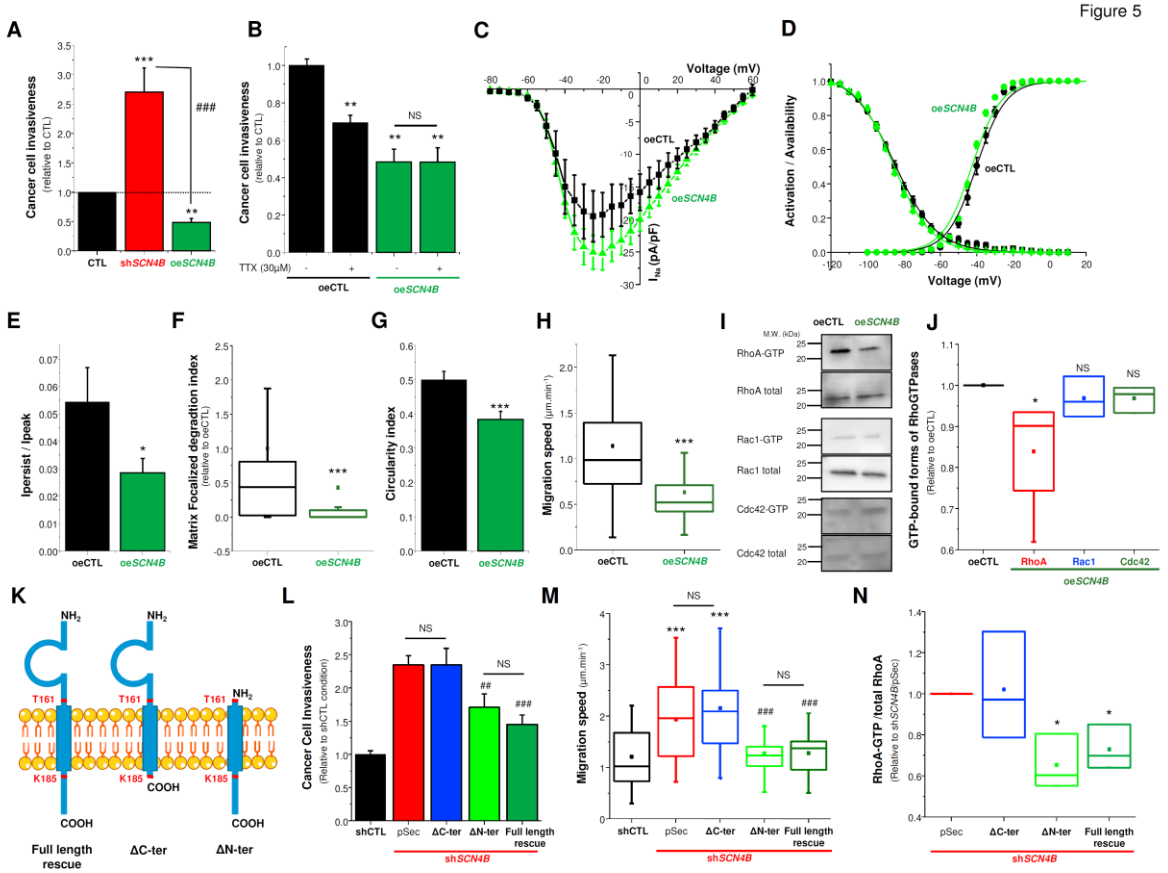

Figure 5: *SCN4B* protein (β4 subunit) inhibits cancer cell invasiveness through its intracellular C-terminus and not through its extracellular Ig-like domain.

A, Cancer cell invasiveness was assessed using Matrigel™-invasion chambers from CTL, sh*SCN4B* and oe*SCN4B* cells, in absence (-) or presence of TTX (30 µM). The results from 6 independent experiments were expressed relative to oeCTL cells in absence of TTX. *** denotes a statistical difference from CTL at p<0.001, ** at p<0.01. ### denotes a statistical difference from sh*SCN4B* at p<0.001. NS stands for not statistically different. **B,** Cancer cell invasiveness was assessed using Matrigel™-invasion chambers from oeCTL and oe*SCN4B* cells, in absence

(-) or presence of TTX (30 µM). The results from 6 independent experiments were expressed relative to oeCTL cells in absence of TTX. ** denotes a statistical difference from the oeCTL at p<0.01. NS stands for not statistically different. **C**, Sodium current (I_{Na})-voltage relationships in oeCTL (black squares, n= 17) and in oe*SCN4B* (green triangles, n= 31) cells obtained from a holding potential of -100 mV. **D**, Activation-(●) and availability-(■) voltage relationships obtained in the same oeCTL (black symbols) and oe*SCN4B* (green symbols) cells as in C. **E**, Mean ratios of I_{Na} persistent / I_{Na} peak currents obtained for a membrane depolarisation from -100 to -30 mV from 18 oeCTL and 29 oe*SCN4B* cells. * indicates a statistical difference from oeCTL at p<0.05. **F**, MDA-MB-231 oeCTL or oe*SCN4B* cells were cultured on a Matrigel™-composed matrix containing DQ-Gelatin®, and a "Matrix-Focalized-degradation index" was calculated as being F-actin foci (red labelling, phalloidin-Alexa594F) co-localised with focused proteolytic activities (green). The analysis represents results obtained with 77 and 69 cells for oeCTL and oe*SCN4B*, respectively. *** indicates a statistical difference from oeCTL at p<0.001. **G**, A cell circularity index was calculated from oeCTL and oe*SCN4B* cells (n= 73 cells analysed in each cell type). *** indicates a statistical difference from oeCTL at p<0.001. **H**, The speed of migration (in µm.min^{-1}) was analysed in oeCTL and oe*SCN4B* from time-lapse experiments and results shown were obtained from 47 cells in each condition. *** denotes a statistical difference from the oeCTL at p<0.001. **I,** GST-RBD pull-down assay in oeCTL and oe*SCN4B* cells. Western blots showing active RhoA-GTP, active Rac1-GTP or active Cdc42-GTP, pulled down by GST-RBD and detected by anti-RhoA, anti-Rac1, or anti-Cdc42 in western blot. By comparison total forms of RhoA, Rac1 and Cdc42 are shown. **J**, Quantification of GTP-bound RhoGTPases in oe*SCN4B* cells. The activity of GTP-bound (active) RhoGTPase was normalized to its total protein level, and was expressed relatively to that in oeCTL cells. Data from 4 independent experiments. * denotes a statistical difference from the oeCTL at p<0.05. NS stands for not statistically different. **K**, Cartoon showing the transmembrane structure of the β4 protein, encoded by the *SCN4B* gene. The extracellular domain contain an Ig-like structure. By site-directed nucleotide substitutions in the *SCN4B* sequence, which are conservative for the amino acid sequence we have generated a sequence that is not recognized by the small hairpin RNA targeting *SCN4B* expression. This sequence has been inserted into a pSec expression vector in order to overexpress the full-length β4 protein (called "Full-length rescue") in sh*SCN4B* cells. Alternatively, we have also created truncated versions of the β4 protein: one being deleted in its intracellular C-terminus, from residue K185, and called "ΔC-ter", and one being deleted from its extracellular N-terminus up to residue T161, and called "ΔN-ter". The nucleotide sequences were inserted into the pSec mammalian expression vector. **L**, Cancer cell invasiveness was assessed using Matrigel™-invasion chambers from shCTL and sh*SCN4B,* transfected with an empty expression vector (pSec), or transfected with "ΔN-ter", "ΔC-ter" or "Full-length rescue" encoding sequences. $^{###}$ denotes a statistical difference from sh*SCN4B*/pSec at p<0.001 and $^{##}$ at p<0.01. NS stands for not statistically different. **M**, The speed of migration (in µm.min^{-1}) was analysed in shCTL and sh*SCN4B*, transfected with an empty expression vector (pSec), or transfected with "ΔN-ter", "ΔC-ter" or "Full-length rescue" encoding sequences, from time-lapse experiments and results shown were obtained from 30 cells in each condition. *** denotes a statistical difference from the shCTL at p<0.001. $^{###}$ denotes a statistical difference from the sh*SCN4B*/pSec at p<0.001. NS stands for not statistically different. **N**, Quantification of GTP-bound RhoA in sh*SCN4B* cells, transfected with empty vector (pSec), with "ΔN-ter", "ΔC-ter" or "Full-length rescue" encoding sequences. The activity of GTP-bound (active) RhoAe was normalized to its total protein level, and was expressed relatively to that in sh*SCN4B*/pSec cells. Data from 3 independent experiments. * denotes a statistical difference from the sh*SCN4B*/pSec at p<0.05.

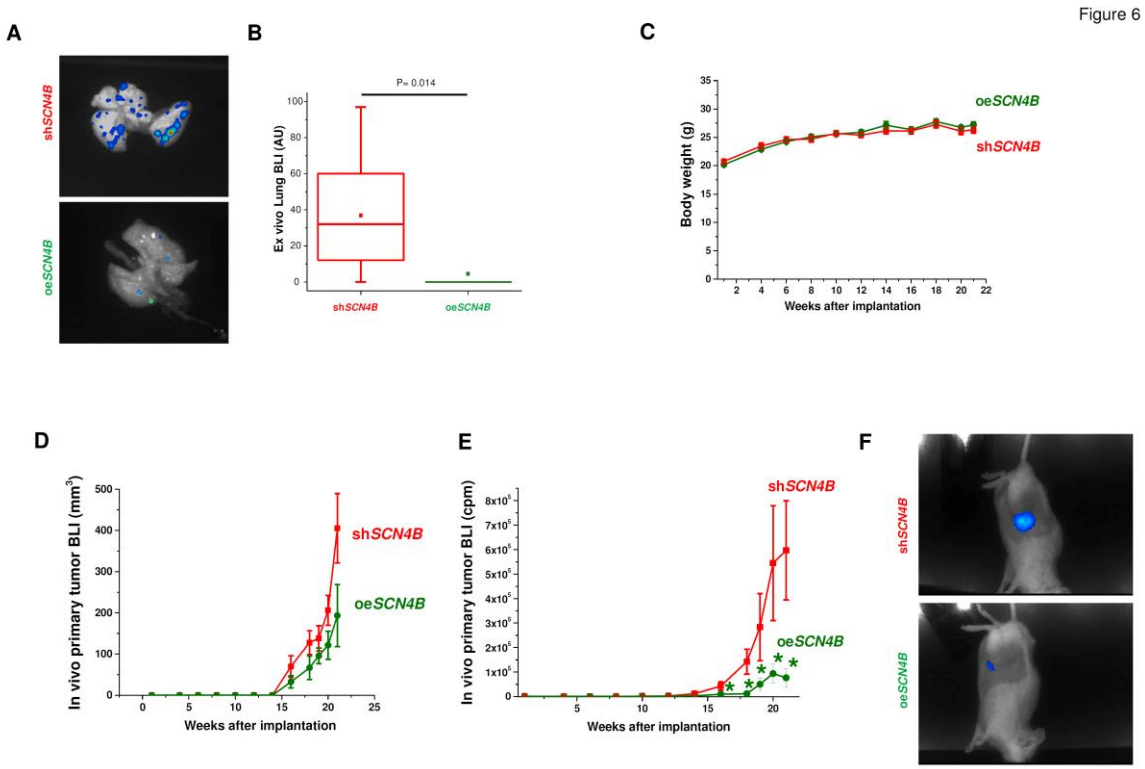

Figure 6: *SCN4B* expression inversely correlates with primary tumor growth and metastatic development *in vivo*. A, Bioluminescent imaging (BLI) performed in NMRI nude mice injected in the tail vein (experimental model for metastatic colonisation) with MDA-MB-231-Luc cells which do not express (sh*SCN4B)*, or which overexpress *SCN4B* gene (oe*SCN4B*). Representative *ex vivo* lung BLI, after organ isolation, at completion of the study (9th week after cell injection). **B**, BLI quantification of excised lungs from n= 7 mice injected with sh*SCN4B* cells and n= 8 mice injected with oe*SCN4B* cells. **C**, Evolution of NOD SCID mice bearing sh*SCN4B*- or oe*SCN4B*-induced mammary tumours (orthotopic mammary tumour model) as a function of weeks after implantation with sh*SCN4B* (n= 8 mice) and oe*SCN4B* (n= 8 mice) cells, respectively. **D**, Mean ± sem mammary tumour volume (mm^3), measured with a calliper, as a function of weeks after implantation of sh*SCN4B* or oe*SCN4B* cells. **E**, Mean ± sem *in vivo* BLI value of tumours (expressed in cpm) as a function of time recorded in the whole body of mice in the same experimental groups as indicated previously. * denotes a statistical difference from the sh*SCN4B* group at $p<0.05$. **F**, Representative bioluminescent images of mammary tumours in sh*SCN4B* and oe*SCN4B* experimental groups, taken at the 21st week after cell implantation.

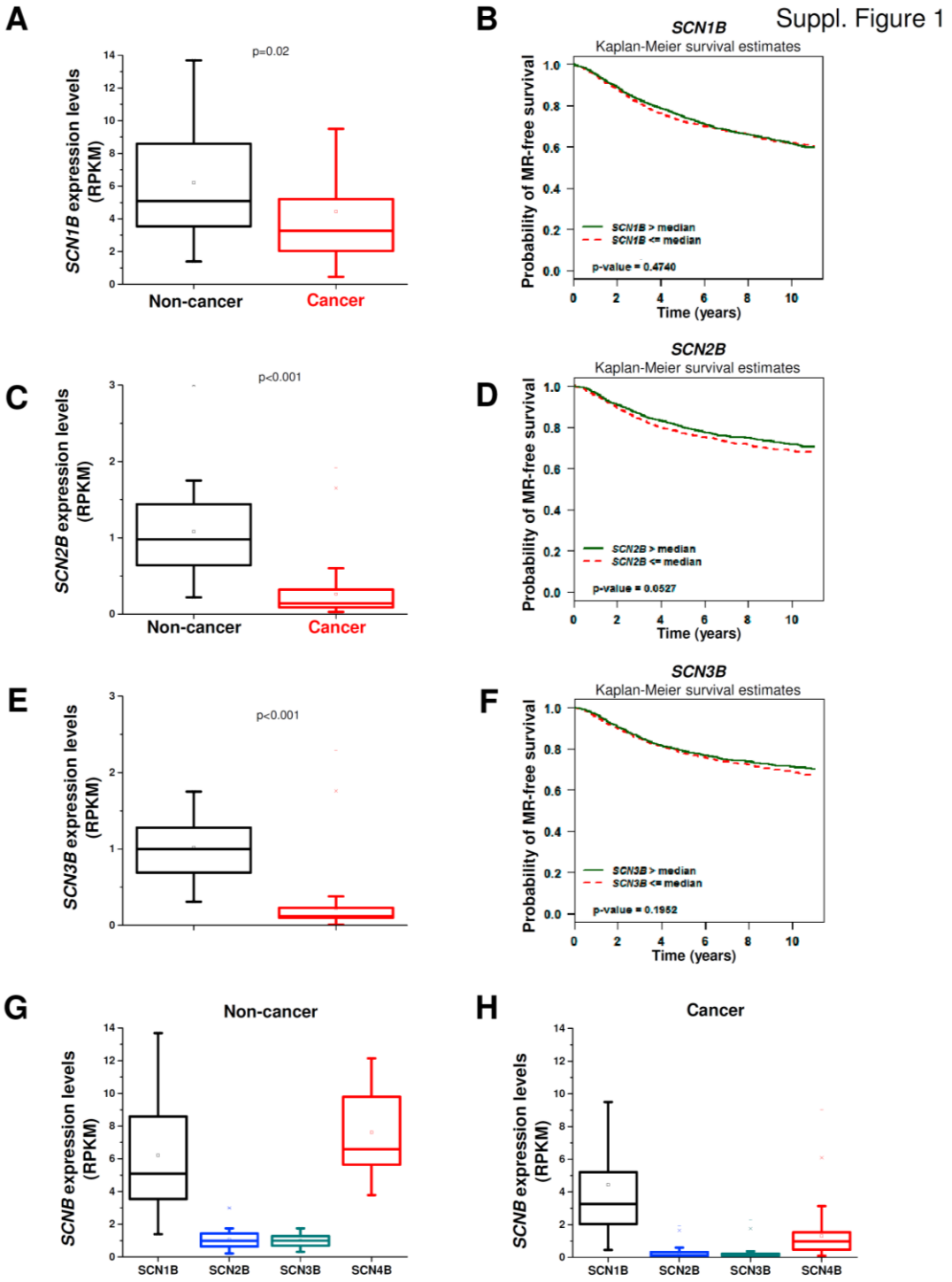

Supplementary Figure 1: *SCNxB* gene expression in human breast cancer tissues and associations with patient survival without metastatic relapse.

A, **C, E**, Expression of the *SCNxB* gene in non-cancer (n= 29) and in breast cancer tissues (n= 145) was analysed in The Cancer Genome Atlas (TCGA) and RNA expression is given as reads per kilobase per million (RPKM). Box plots indicate the first quartile, the median, and the third quartile, squares indicate the mean. **A**, *SCN1B* gene was significantly down-regulated in cancer compared to non-cancer tissues (p=0.02). **C**, *SCN2B* gene was significantly down-regulated in cancer compared to non-cancer tissues (p<0.01) and **E**, *SCN3B* gene was also significantly down-regulated in cancer compared to non-cancer tissues (p<0.01). **B, D, F,** Kaplan-Meier analyses

of Metastatic relapse (MR)-free survival performed on data pooled from cohorts (see Methods) for the expression of **B**, *SCN1B* gene (n= 5,436 patients), **D**, *SCN2B* gene (n=3,826 patients), **F**, *SCN3B* gene (3,751 patients). For these three genes, there was no statistical difference in MR-free survival between groups highly expressing (> median) and weakly expressing (<median) the considered *SCNxB* gene. **G-H**, Analyses of RNA expression levels (expressed in RPKM) of *SCNxB* genes in **G**, non-cancer (n= 29) and in **H**, breast cancer tissues (n= 145), from The Cancer Genome Atlas (TCGA).

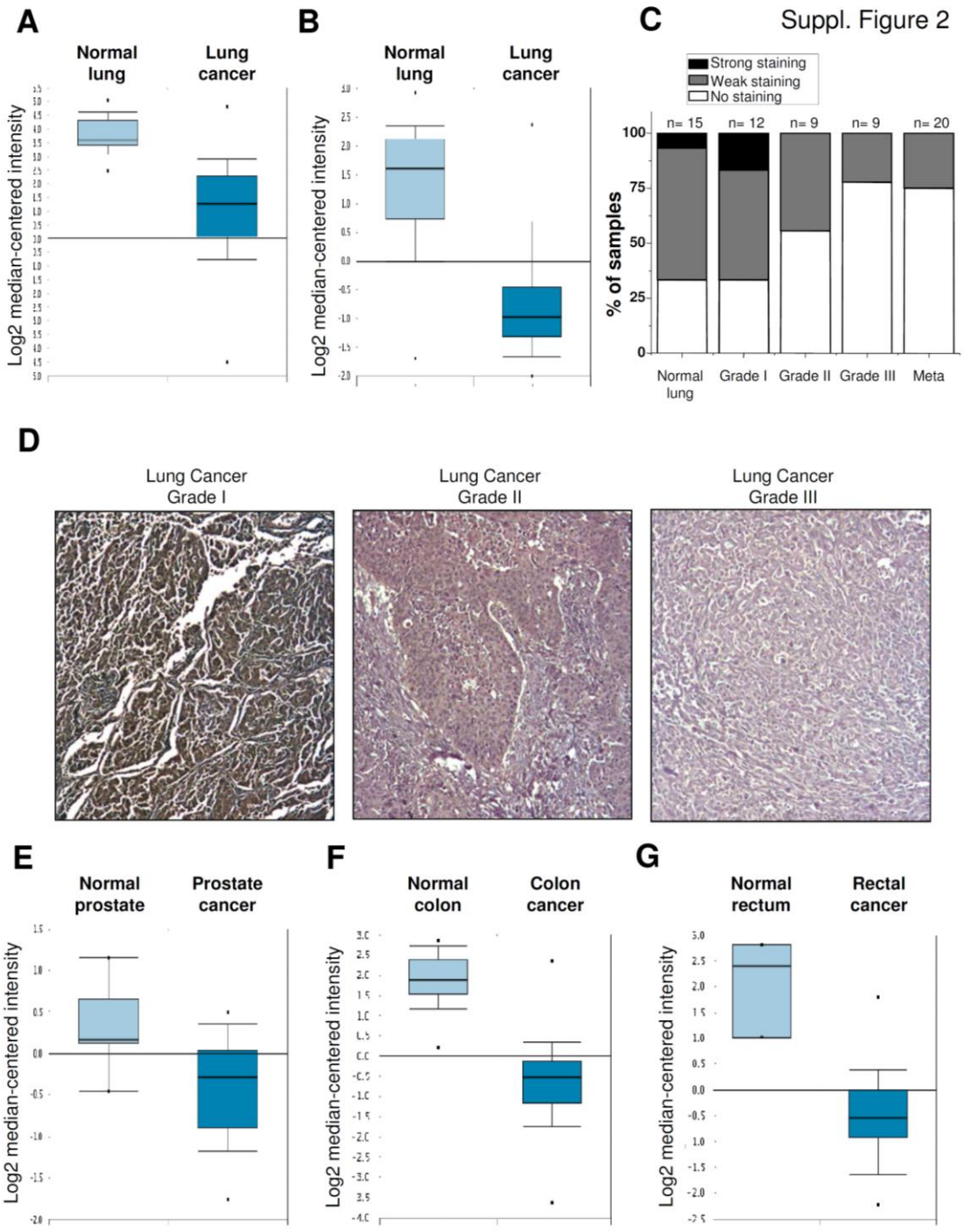

Supplementary Figure 2: *SCN4B* gene down-regulation in human cancer tissues.

See previous page. The expression level of the *SCN4B* gene was assessed from published data in normal lung and in lung adenocarcinomas, reporting information regarding 19,574 genes, using the Affymetrix Human Genome U133 Plus 2.0 Array**. A**, In the Okayama *et al.* lung cancer study group [31], there was a significant reduction ($p<0.001$) of *SCN4B* expression in lung adenocarcinoma tissues (n=226) compared to normal lung tissues (n=20). **B**, In the Hou *et al.* Non-small-cell Lung cancer study [32], there was a significant reduction ($p<0.001$) of *SCN4B* expression in lung adenocarcinoma tissues (n=45) compared to normal lung tissues (n=65). **C**, the protein (β4) expression of the *SCN4B* gene was analysed by immunohistochemistry on tissues arrays containing normal lung and lung cancer (from grade I to grade III) tissues, as well as metastases (Meta) samples. β4 staining was analysed and samples were stratified in "no staining", "weak staining" or "strong staining" groups. Diagrams indicate the proportion of samples showing no (white), weak (gray) or strong (black) β4 staining in normal and cancer lung samples. The number of samples per condition is indicated between brackets. There was a tendency, yet not statistically different, for a reduced expression of β4 in high grade lung adenocarcinomas. **D**, Representative β4 staining pictures from grade I, grade II and grade III lung adenocarcinoma. **E**, The expression level of the *SCN4B* gene was assessed in normal and prostate adenocarcinomas [42]. Gene expression was assessed using Affymetrix GeneChip U133 array (Plus 2.0 chip) consisting of >52,000 transcripts from whole human genome transcripts. There was a significant reduction ($p=0.004$) of *SCN4B* expression in prostate carcinomas (n=13) compared to normal prostate gland (n=8) and. **F**, Using the TCGA colorectal statistics for mRNA sequencing, the *SCN4B* expression was analysed and there was a significant reduction ($p<0.001$) of *SCN4B* expression in prostate carcinomas (n=101) compared to normal colon (n=19). **G**, Similarly, the *SCN4B* expression was significantly reduced ($p<0.001$) in rectal carcinomas (n=60) compared to normal rectum (n=3).

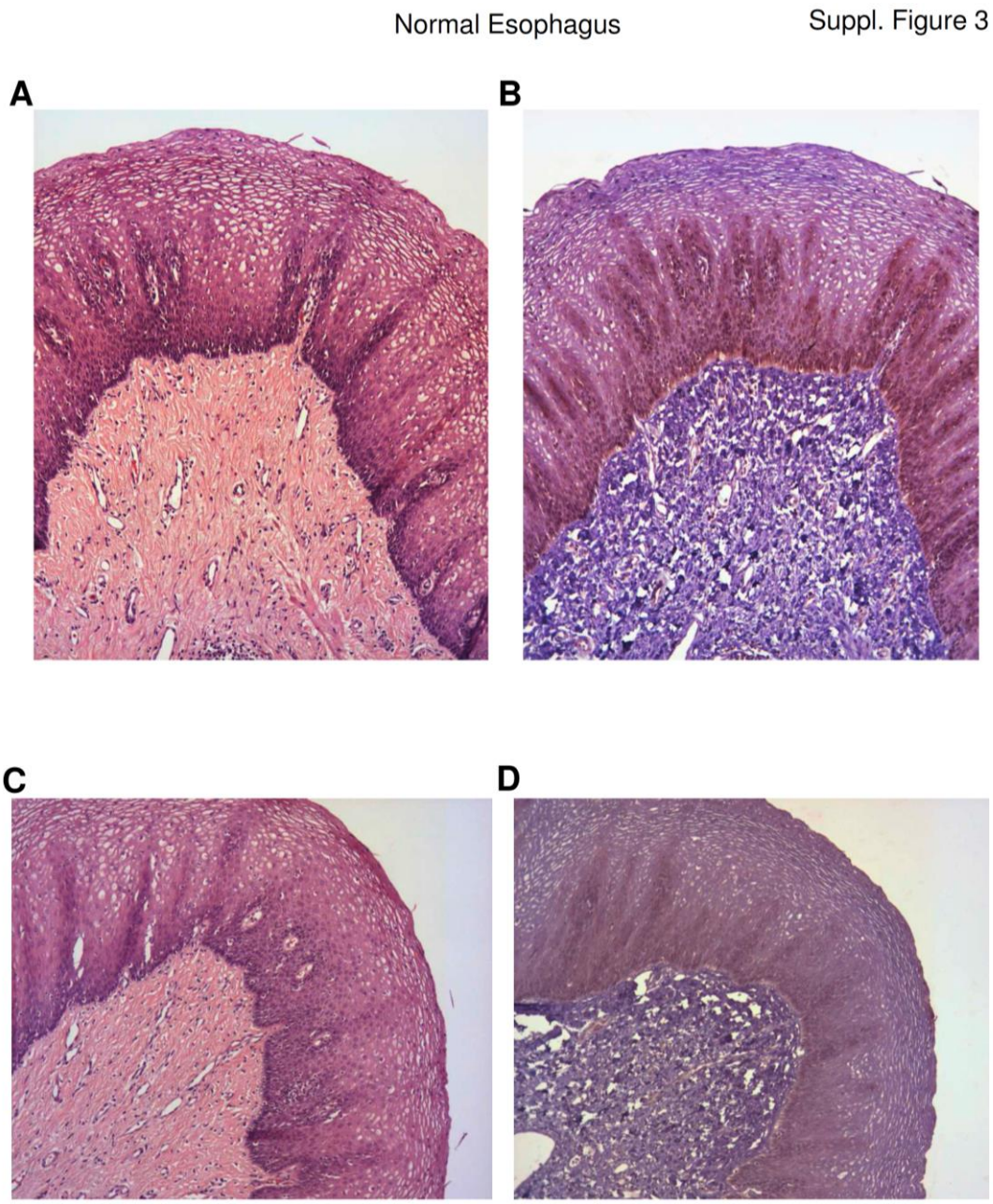

Supplementary Figure 3: *SCN4B* protein expression (β4) in normal oesophagus.

Two normal human oesophagus samples were stained with haematoxylin and eosin (**A, C**) and the protein expression of β4 was analysed by immunohistochemistry (**B, D**).

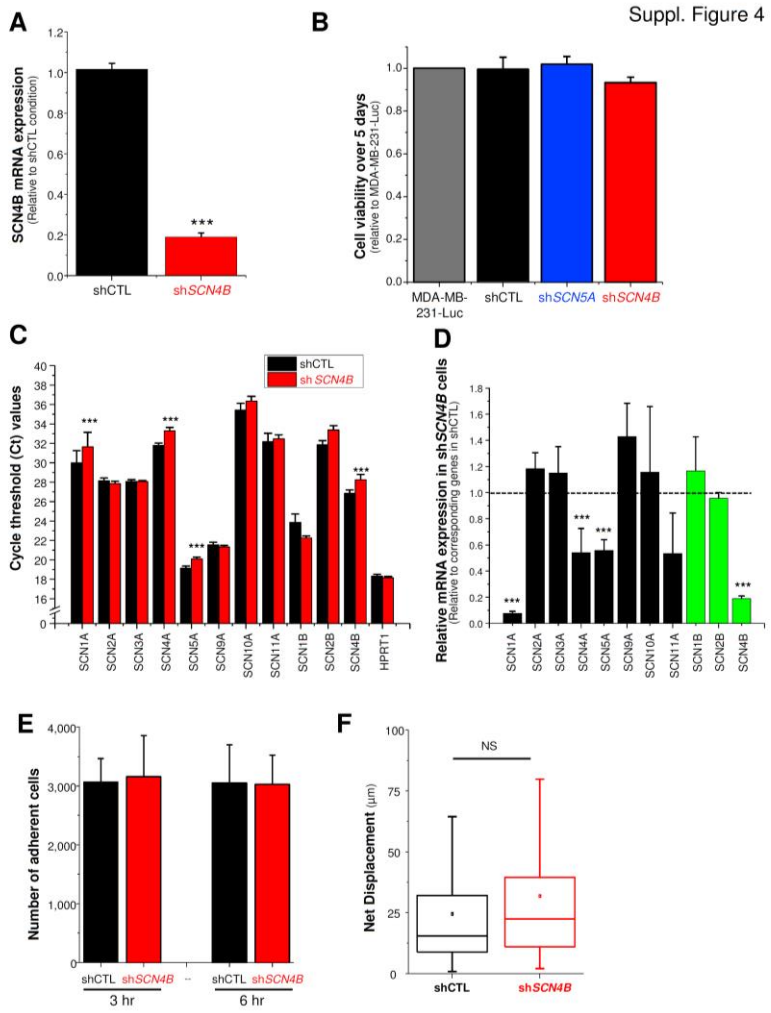

Supplementary Figure 4:

A, Expression of *SCN4B* gene mRNA in shCTL and sh*SCN4B* cells, expressed as a ratio of the shCTL condition, from 37 independent real-time PCR experiments. *** indicates a statistical difference from shCTL at p<0.001. **B**, Comparison of MDA-MB-231-Luc, shCTL, sh*SCN5A* and sh*SCN4B* cell growth and viability measured by the MTT assay after 5 days culture, expressed relative to the MDA-MB-231-Luc cell line (n= 3 independent experiments). **C**, The mRNA expression of pore-forming *SCNxA* and auxiliary *SCNxB* subunits gene was assessed by real-time PCR in shCTL and sh*SCN4B* cells, and expressed as Cycle Threshold values (Ct). *SCN8A* and *SCN3B* are not indicated in the graph because their gene expression was undetectable after 40 amplification cycles. These results come from 3-6 independent experiments. *** indicates a statistical difference from the corresponding gene expression in shCTL cells at p<0.001. **D**, Relative mRNA expression of pore-forming *SCNxA* and auxiliary *SCNxB* subunits gene, assessed by real-time PCR in sh*SCN4B* cells, expressed as a ratio of *HPRT1* gene expression and of the expression of corresponding genes in shCTL cells. Results from 3-6 independent experiments. *** indicates a statistical difference from the corresponding gene expression in shCTL cells at p<0.001. **E**, Cancer cell adhesion was assessed in the two cell types, shCTL and sh*SCN4B*, and the number of adherent cells was counted 3hr or 6hr after cell seeding. **F**, The net displacement (in µm) from migrating cancer cell was analysed after 180 min in shCTL and sh*SCN4B* cell lines from time-lapse experiments and results shown were obtained from 106 and 96 cells, respectively. NS stands for no statistical difference.

Suppl. Figure 5

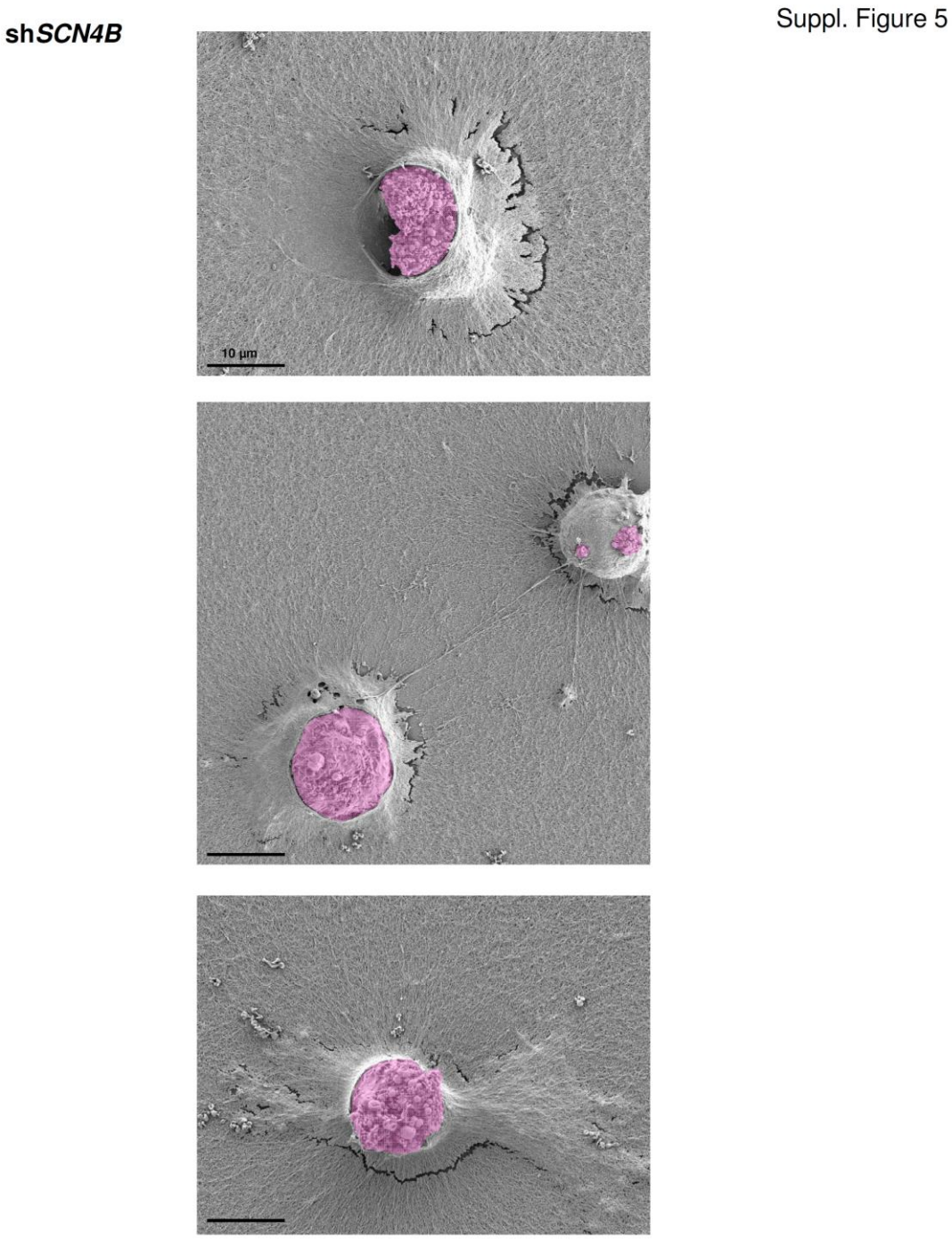

Supplementary Figure 5:

Scanning electron microscopy observations, 24 hr after cell seeding of sh*SCN4B* cell invasion through Matrigel™ (4 mg/mL) coated on the glass coverslip. Scale bars, 10 µm.

Suppl. Figure 6

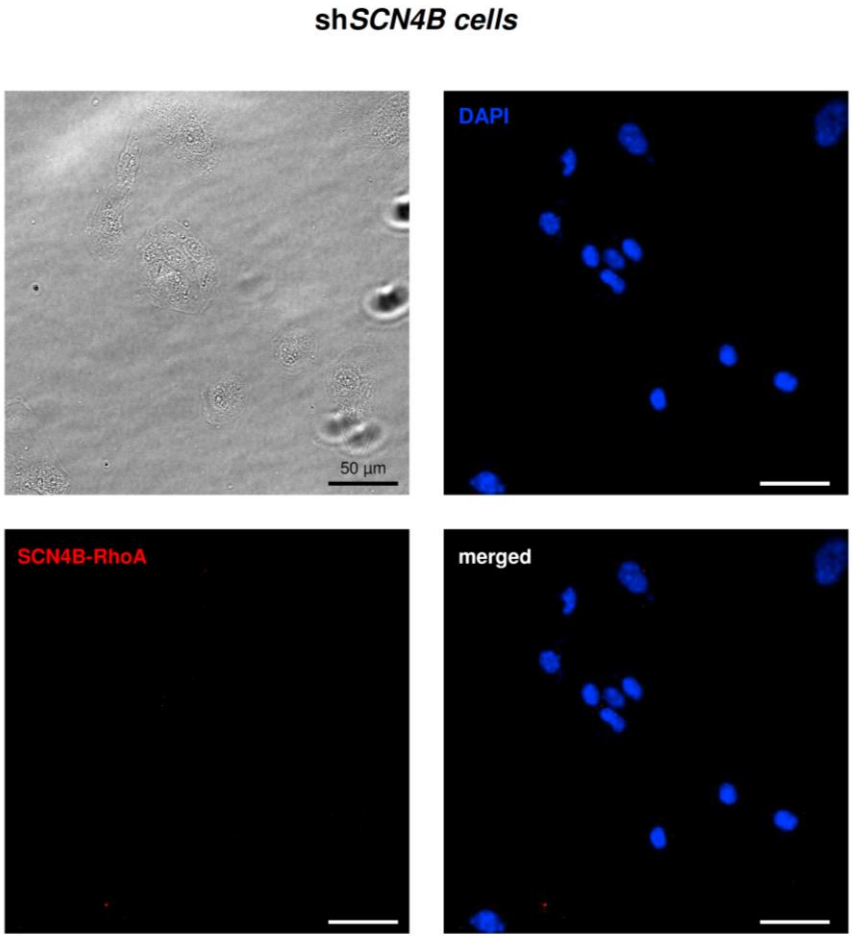

Supplementary Figure 6:

In situ proximity ligation assays (Duolink "In cell co-IP") showing the absence of any proximity signal between *SCN4B* proteins (β4) and RhoA in sh*SCN4B* cells (red dots). Nuclei were stained with DAPI (blue). Scale bars, 50 µm.

Suppl. Figure 7

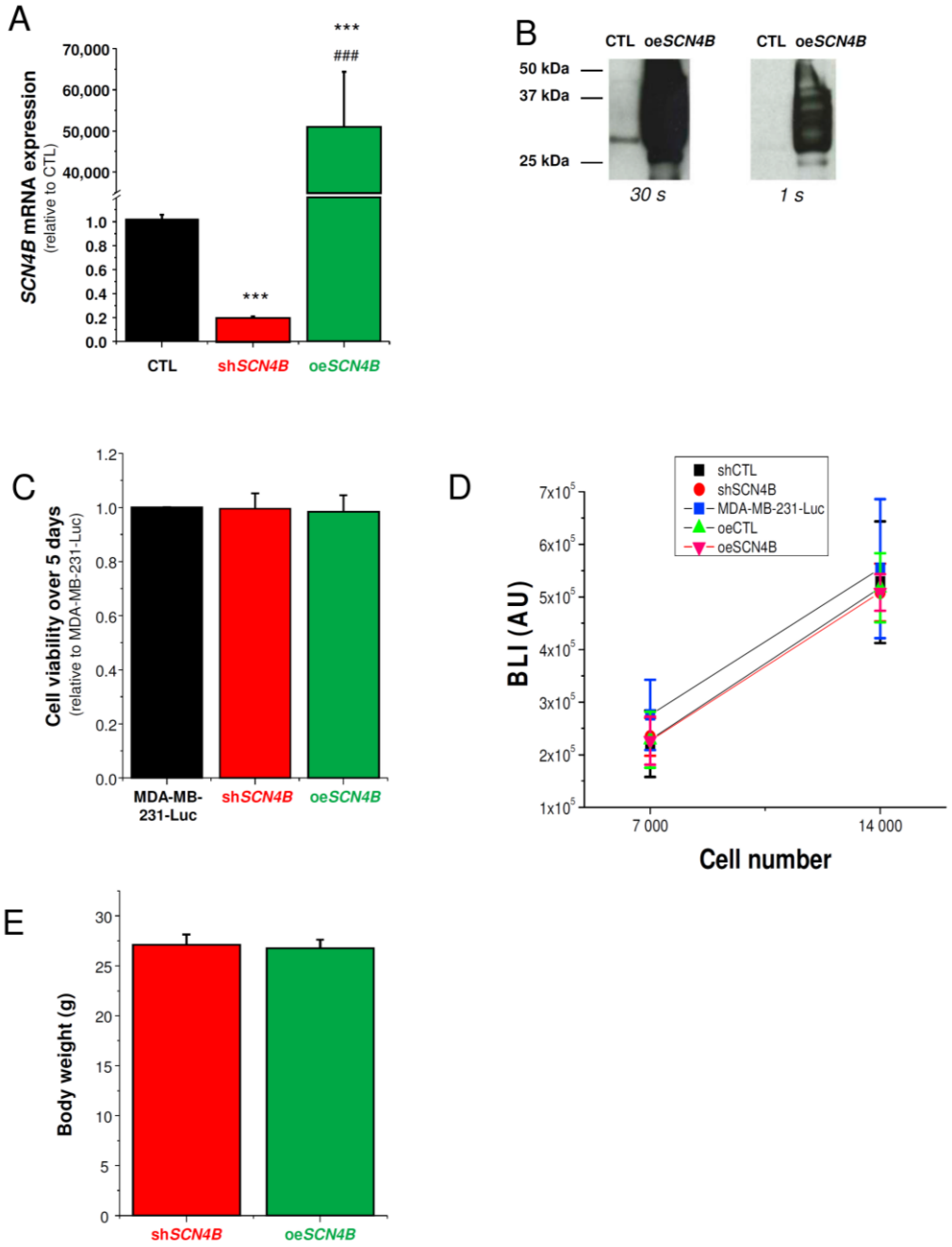

Supplementary Figure 7:

A, Relative mRNA expression of *SCN4B* gene, assessed by real-time PCR in CTL, sh*SCN4B* and oe*SCN4B* cells, expressed as a ratio of *HPRT1* gene expression and relative to the expression in CTL cells. The results from 18 independent experiments. *** indicates a statistical difference from CTL cells at $p<0.001$, and ### indicates a statistical difference from sh*SCN4B* cells at $p<0.001$. **B**, Western blot experiments showing the high expression of *SCN4B* proteins (β4) in oe*SCN4B* cells. These are representative blots at 30 and 1 s exposure time. **C**, Comparison of MDA-MB-231-Luc, sh*SCN4B* and oe*SCN4B* cell growth and viability measured by the MTT assay after 5 days culture, expressed relative to the MDA-MB-231-Luc cell line (n= 3 independent experiments). **D**, MDA-MB-231-Luc derived cell lines derived cell lines were seeded at different densities (7,000 and 14,000 cells/well of a 96-

well plate). After 24 hr growth, cells were lysed and the bioluminescent signal (BLI) was measured after the addition of luciferin (Luciferase Assay System kit, Promega) and expressed as arbitrary units (AU). Results are expressed as mean ± sem. There was no difference between the 5 conditions tested (MDA-MB-231Luc, shCTL, sh*SCN4B*, oeCTL, oe*SCN4B*). **E**, Mice injected with sh*SCN4B* (n=7) and oe*SCN4B* (n=8) cells in the tail vein showed identical body weight (g) at the completion of the study (9 weeks after cell injection).

Supplementary Table I: PCR primers sequences and expected amplicon size

Gene	protein	Forward primers (5' – 3')	Reverse primers (5' – 3')	Expected size (bp)
SCN1A	$Na_V1.1$	TTCATGGCTTCCAATCCTTC	TAGCCCCACCTTTGATTTTG	178
SCN2A	$Na_V1.2$	GCCAGCTTATCAATCCCAAA	TCTTCTGCAATGCGTTGTTC	192
SCN3A	$Na_V1.3$	CAAAGGGAAGATCTGGTGGA	AAAGGCCAATGCACCACTAC	115
SCN4A	$Na_V1.4$	TCAACAACCCCTACCTGACC	ACGGACGAGTTCCCATCATA	148
SCN5A	$Na_V1.5$	CACGCGTTCACTTTCCTTC	CATCAGCCAGCTTCTTCACA	208
SCN8A	$Na_V1.6$	CGCCTTATGACCCAGGACTA	GTGCCTCTTCCTGTTGCTTC	247
SCN9A	$Na_V1.7$	GGCTCCTTGTTTTCTGCAAG	TGGCTTGGCTGATGTTACTG	196
SCN10A	$Na_V1.8$	ACCTGGTGGTGCTTAACCTG	TGCTGAAGAAGCTGCAAAGA	168
SCN11A	$Na_V1.9$	CTGTGGTCCTGGTCATTGTG	TGCATTCGCTTCTTGCATAC	233
SCN1B	β1	TGCGCTATGAGAATGAGGTG	GAAGAAGAGCAGGCGGTAGA	176
SCN2B	β2	GTACGATGTGTCGGTGATGC	AGATGACCACAGCCAGGAAG	203
SCN3B	β3	GAGGGCGGTAAAGATTTCCT	AGAGGCCAGAGTCGTTCAGA	154
SCN4B	β4	GAAGTCTGACCCCAAGGTGA	CACATGGCAGGTGTATTTGC	139
HPRT1	Hprt1	TTGCTGACCTGCTGGATTAC	TATGTCCCCTGTTGACTGGT	119

Methods

Prognostic analyses of gene expression in breast cancers – Analyses were performed using the software ***Breast Cancer Gene-Expression Miner v3.0*** (bc-GenExMiner v3.0; http://bcgenex.centregauducheau.fr) developed by the Integrated Center of Oncology René Gauducheau (Nantes-Saint Herblain, France), based on DNA microarrays results collected from published cohorts [39]. Briefly, several statistical tests are conducted on each cohort and on all cohorts pooled together with data from all studies previously converted to a common scale with a suitable normalization. The prognostic impact of each gene is evaluated by means of univariate Cox proportional hazards model. Results are displayed by cohorts and pool and are illustrated in a forest plot. Kaplan-Meier curves are then obtained on the pool with the gene values dichotomised according to gene expression median (calculated from the pool). Cox results corresponding to dichotomised values are displayed on the graph.

In Silico RNA expression analyses – The expression of *SCNxB* genes in cancer tissues was studied using the web-based "The Cancer Genome Atlas" (http://cancergenome.nih.gov) from the US National Cancer Institute and the National Human Genome Research Institute that integrates database of molecular and clinical annotation.

Data are expressed as RPKM (reads per kilobase per million), a method of quantifying gene expression from RNA sequencing data by normalizing for total read length and the number of sequencing reads. More than 20,500 genes are sequenced per sample.

Immunohistochemistry **-** The degree of β4 protein expression (*SCN4B* gene) in normal and dysplastic mammary tissues, as well as mammary ductal and lobular carcinomas was analysed by standard ABC immunohistochemistry procedure. Thus, tissue microarrays (TMA) from formalin-fixed, paraffin-embedded mammary tissues were purchased from US Biomax Inc. (ref. BR1003, BC081120, BR10010a, Rockville, USA), comprising normal, hyperplastic and dysplastic mammary samples, lobular and ductal mammary carcinomas (separated in well (grade I), moderate (grade II) and poorly (grade III) differentiated carcinomas), and lymph node metastases samples. Similar analyses were also performed in a lung TMA (LC951, US Biomax Inc) containing normal lung, cancer lung (grades IA to IIIB) tissues and metastases (in lymph nodes, bones and intestine). Briefly, after deparaffination and rehydration, sections were treated with a high-pH (Tris buffer/EDTA, pH 9.0) target retrieval procedure (Dako PT-link, Dako, Carpinteria, USA). Endogenous peroxidase was then blocked by a commercial solution (Dako REAL^{Tm}), and incubated overnight with 1:100 dilution of the primary polyclonal rabbit antibody anti-*SCN4B*/β4 (HPA017293, Sigma-Aldrich, Saint-Quentin, France) at 4ºC. Sections were then incubated with a commercial anti-rabbit labelled polymer (Dako EnVision^{Tm} FLEX, Dako) for 30 min. at RT. Immunoreaction was finally revealed with 3-3´ Diaminobenzidine solution (Dako) for 5 minutes. Positive reaction was identified by a cytoplasmic dark-brown precipitated. To determine the degree of protein expression in tissues a qualitative scale was used, for negative (-), weak (+) and strong (++) cytoplasmic expression.

Inhibitors and chemicals and antibodies **-** Tetrodotoxin was purchased from Latoxan (France), and A803467 from R&D systems (Lille, France). Fluorescent probes and conjugated antibodies were purchased from Fischer Scientific (Illkirch, France). Drugs and chemicals were purchased from Sigma-Aldrich (France).

Cell culture and cell lines **–** All cell lines were originally from the American Type Culture Collection (LGC Promochem, France) and were grown at 37°C in a humidified 5% CO_2 incubator. The immortalized normal mammary epithelial cells MCF-10A were cultured in DMEM/Ham's F-12, 1:1 mix containing 5% horse serum (Invitrogen, France), 10 µg/mL insulin, 20 ng/mL epidermal growth factor, 0.5 µg/mL hydrocortisone, and 100 ng/mL cholera toxin. MCF-7, MDA-MB-468, MDA-MB-435s breast cancer cells were cultured in DMEM supplemented with 5% FCS. PC3 prostate, H460 and A549 non-small-cell lung cancer cells were cultured in DMEM supplemented with 10% FCS. MDA-MB-231-Luc human breast cancer cells, stably expressing the luciferase gene [22], were cultured in DMEM supplemented with 5% FCS. We constructed a lentiviral vector encoding a short hairpin RNA (shRNA) specifically targeting human *SCN5A* transcripts using the same protocol as previously described [34]. The sequence encoding sh*SCN5A*, inhibiting the expression of $Na_V1.5$ protein, was obtained by DNA polymerase fill-in of two partially complementary primers: 5'-GGATCCCCAAGGCACAAGTGCGTGCGCAATTCAAGAGA-3' and 5'-AAGCTTAAAAAAAGGCACAAGTGCGTGCGCAATCTCTTGAA-3'.

Similarly, we constructed a lentiviral vector encoding a short hairpin RNA (shRNA) specifically targeting human *SCN4B* transcripts, inhibiting the expression of β4 protein. The sequence encoding the sh*SCN4B* was obtained by

DNA fill-in of two partially complementary primers; this also allowed introducing two restriction enzyme sites to facilitate manipulations. Forward primer: shβ4-BamHI 5'-GGATCCCCCAGCAGTGACGCATTCAAGATTCTTCAAGAGA-3'and reverse primer: shβ4-HindIII 5'-AAGCTTAAAAA-CAGCAGTGACGCATTCAAGATTC-TCTCTTGAA-3'. We also constructed a lentiviral vector expressing an untargeted shRNA (pLenti-shCTL), using the following primers: 5′-GGATCCCCGCCGACCAATTCACGGCCGTTCAAGAGACG-3′ and 5'-AAGCTTAAAAAGCCGACCAATTCACGGCCGTCTCTTGAACG-3'. We constructed an expression plasmid encoding *SCN4B* sequence to overexpress β4. This sequence was synthetized by Proteogenix (Dijon, France) and inserted in pcDNA3.1, using the following primers: 5'-GGATCCGCCGCCACC-3' and 5'-GCGGCCGCCTCGAG-3'. We designed the mutated sequences coding for the "Full-length *SCN4B*/β4 rescue" and truncated proteins, which were then synthetized by Proteogenix (Dijon, France) and all sequences obtained were inserted into pSecTag2 hygro B vecor (ref V910-20, Invitrogen) with the In-fusion® HD cloning Plus kit (Clonetech). We constructed a plasmid containing the sequence of the N-terminally truncated (from residue 1 to residue T161, "ΔN-ter") protein containing the transmembrane and C-terminal intracellular domain of the *SCN4B*/β4 protein. The sequence was obtained by PCR elongation using two specific primers: forward primer 5'-GCGCCGTACGAAGCTGACCTGGAGTTCAGCGAC-3' and reverse primer 5'-ACACTGGAGTGGATCTCACACTTTTGAAGGTGGTT-3'. Similarly, a *SCN4B*/β4 protein truncated in the C-terminus, from residue K185 and identified as being "ΔC-ter" was designed. Importantly, for "ΔC-ter" and "full-length rescue" the nucleotide sequence mutated by substitution to avoid the shRNA targeting native *SCN4B* gene. The protein sequence remained unaffected. The sequence targeted by the shRNA was 5'-CAGCAGTGACGCATTCAAGATTC-3', while the substituted untargeted sequence was the following 5'-TAGTAGCGATGCCTTTAAAATAC-3'.

RNA extraction, Reverse transcription, and real-time PCR - Total RNA extraction from cancer and non-cancer cells was performed by using RNAgents® Total RNA Isolation System (Promega, France). RNA yield and purity were determined by spectrophotometry and only samples with an A260/A280 ratio above 1.6 were kept for further experiments. Total RNA were reverse-transcribed with the RT kits Ready-to-go® You-prime First-Strand Beads (Amersham Biosciences, UK). Random hexamers $pd(N)_6$ 5'-Phosphate (0.2 µg, Amersham Biosciences) were added and the reaction mixture was incubated at 37°C for 60 min. Real time PCR experiments were performed as previously described [24]. Primers sequences and expected amplicon sizes are given in supplementary table I.

Small interfering RNA transfection and efficacy assessment - MDA-MB-231-Luc human breast cancer cells were transfected with 20 nM small interfering RNA (siRNA) targeting the expression of *SCN1B* (si*SCN1B*, sc-97849), *SCN2B* (si*SCN2B*, sc-96252), *SCN4B* (si*SCN4B*, sc-62982), or scrambled siRNA (siCTL, siRNA-A sc-37007), which were produced by Santa Cruz Biotechnology and were purchased from Tebu-Bio (France), Transfection was performed with Lipofectamine RNAi max (Invitrogen, France) according to the manufacturer's instructions, and used 24 hr after transfection. The efficiency of siRNA transfection was verified by quantitative polymerase chain reaction (qPCR) using an iCycler® system (BioRad, USA) and western blotting.

***Western blotting experiments*-** Cells were washed with PBS and lysed in presence of a lysis buffer (50 mM Tris, pH7, 100 mM NaCl, 5 mM $MgCl_2$, 10% glycerol, 1 mM EDTA), containing 1% Triton-X-100 and protease inhibitors (Sigma-Aldrich, France). Cell lysates were cleared by centrifugation at 16,000 x *g* for 10 min. Western blotting experiments were performed according to standard protocols. Total protein concentrations were determined using the Pierce® BCA Protein Assay Kit Thermo scientific (Fisher Scientific, France). Protein sample buffer was added and the samples were boiled at 100°C for 3 min. Total protein samples were electrophoretically separated by sodium dodecyl sulphate-polyacrylamide gel electrophoresis in 10% gels, and then transferred to polyvinylidene difluoride membranes (Millipore, USA). The *SCNxB*/β proteins were detected using anti-*SCN1B*/β1 (1/1,000, AV35028, Sigma-Aldrich), anti-*SCN2B*/β2 (1/200, HPA012585, Sigma-Aldrich), and anti-*SCN4B*/β4 (1/1,000, HPA01293, Sigma-Aldrich) rabbit polyclonal primary antibodies, and horseradish peroxidase (HRP)-conjugated goat anti-rabbit IgG secondary antibody at 1:2,000 (TebuBio, France). HSC70 protein was detected as a sample loading control using anti-HSC70 mouse primary antibody at 1:30,000 (TebuBio) and HRP-conjugated anti-mouse-IgG secondary antibodies at 1:2,000 (TebuBio). Proteins were revealed using electrochemiluminescence-plus kit (Pierce® ECL Western Blotting Substrate, Fisher Scientific, France) and captured on Kodak Bio-Mark MS films (Sigma-Aldrich, France).

RhoGTPases Pull-down assays – Pull-down assays were performed according to the manufacturer's protocol (Cat#BK030, RhoA/Rac1/Cdc42 Activation Assay Combo Biochem Kit™, Cytoskeleton, Inc.). Briefly, cells were washed on ice with ice-cold PBS, then lysed and scraped with ice-cold cell lysis buffer containing protease inhibitors (Sigma-Aldrich, St Quentin, France). Cell lysates were clarified by centrifugation at 10000 x g, +4°C, 1 min, and the supernatant was snap-freezed in liquid nitrogen. 10 µL of clarified cell lysate were used to perform protein assay (Cat#23225, BCA protein assay, Thermofischer). 300 µg of total proteins were incubated with 10 µg of PAK-PDB beads or 30 µg Rhotekin-RBD beads for 1 hr on a rotator at +4°C. Samples and beads were washed with 500 µL washing buffer, resuspended in Laemmli buffer and boiled for 2 min prior performing western blotting experiments. Antibodies for RhoA, Rac1 and Cdc42 were provided with the kit and used according to the manufacturer's protocol.

***Cellular electrophysiology* -** Patch pipettes were pulled from borosilicate glass to a resistance of 3-5 MΩ. Currents were recorded, in whole-cell configuration, under voltage-clamp mode of the patch-clamp technique, at room temperature, using an Axopatch 200B patch clamp amplifier (Axon Instrument, USA). Analogue signals were filtered at 5 kHz, and sampled at 10 kHz using a 1440A Digidata converter. Cell capacitance and series resistance were electronically compensated by about 60%. The P/2 sub-pulse correction of cell leakage and capacitance was used to study Na^+ current (I_{Na}). Sodium currents were recorded by depolarizing the cells from a holding potential of –100 mV to a maximal test pulse of –30 mV for 30 ms every 500 ms. The protocol used to build sodium current-voltage (I_{Na}-V) relationships was as follows: from a holding potential of –100 mV, the membrane was stepped to potentials from –80 to +60 mV, with 5-mV increments, for 50 ms at a frequency of 2 Hz. Availability-voltage relationships were obtained by applying 50 ms prepulses using the I_{Na}-V curve procedure followed by a depolarizing pulse to –5 mV for 50 ms. In this case, currents were normalized to the amplitude of the test current without a prepulse. Conductance through Na^+ channels (g_{Na}) was calculated as already described [21]. Current amplitudes were normalized to cell capacitance and expressed as current density (pA/pF).

The Physiological Saline Solution (PSS) had the following composition (in mM): NaCl 140, KCl 4, $MgCl_2$ 1, $CaCl_2$ 2, D-Glucose 11.1, and HEPES 10, adjusted to pH 7.4 with NaOH (1 M). The intrapipette solution had the following composition (in mM) : KCl 130, NaCl 15, $CaCl_2$ 0.37, $MgCl_2$ 1, Mg-ATP 1, EGTA 1, HEPES 10, adjusted to pH 7.2 with KOH (1 M).

Measurement of intracellular pH - Cells were incubated for 30 min at 37°C in Hank's medium containing 2 µM BCECF-AM (2',7'-bis-(2-carboxyethyl)-5-(and-6)-carboxyfluorescein; excitation 503/440 nm; emission 530 nm). Excess dye was removed by rinsing the cells twice with PSS. H^+ efflux was measured as previously described [25,40].

Cell viability - Cells were seeded at $4x10^4$ cells per well in a 24-well plate and were grown for a total of 5 days. Culture media were changed every day. Viable cells number was assessed by the tetrazolium salt assay as previously described [24] and normalised to the appropriate control condition (MDA-MB-231-Luc or shCTL).

Cell Adhesion protocol – Cells were seeded at $2x10^5$ cells per well in 6-well plate. After 3hr or 6hr incubation, the culture medium containing non-adherent cells was remove and wells were then gently washed with D-PBS containing Ca^{2+} and Mg^{2+}. Cells were fixed in 100% ice-cold methanol, then stained with DAPI. Cells adhering to the well were counted manually.

In vitro Invasion Assays – Cell invasiveness was analysed as previously described [25] using culture inserts with 8-µm pore size filters covered with Matrigel™ (Matrigel™-invasion chambers, Becton Dickinson, France). Briefly, the upper compartment was seeded with $6x10^4$ cells in DMEM supplemented with 5% fetal calf serum (FCS). The lower compartment was filled with DMEM supplemented with 10% FCS (or 15% FCS for non-small cell lung and prostate cancer cells), as a chemoattractant. After 24 hr at 37°C, remaining cells were removed from the upper side of the membrane. Cells that had invaded and migrated through the insert and were attached to the lower side were stained with DAPI and counted on the whole area of the insert membrane. *In vitro* invasion assays were performed in triplicate in each separate experiments.

Epifluorescence imaging – For the assessment of extracellular matrix degradation, cells were cultured for 24h on glass coverslips coated with a matrix composed of Matrigel™ (4 mg/mL) and containing or not DQ-gelatin® (25 µg/mL, Thermofischer) as a fluorogenic substrate of gelatinases. They were then washed in PBS, fixed with 3.7% ice-cold paraformaldehyde in PBS. Cells were permeabilized with a solution containing 50 mM NH_4Cl, 1% BSA and 0.02% saponin, then saturated in a solution containing 3% BSA and 3% NGS. F-actin was stained with phalloidin-AlexaFluor594. Epifluorescence microscopy was performed with a Nikon TI-S microscope and analysed using both NIS-BR software (Nikon, France) and ImageJ© software 1.38I (http://rsbweb.nih.gov/ij). Pixels corresponding to the co-localization of F-actin condensation areas and focal spots of DQ-gelatin proteolysis (excitation wavelength: 495 nm, emission wavelength: 515 nm) were quantified per cell, giving a Matrix-focalized-degradation index.

For the assessment of cell morphology, cells were cultured for 24h on glass coverslips and F-actin was stained with phalloidin-AlexaFluor594. A circularity index was calculated from pictures as being

$4\pi \cdot Area/Perimeter^2$. A value approaching 0 indicates an increasingly elongated shape while a value of 1.0 indicates a perfect circle.

Proximity Ligation assays were performed as previously described [26] according to standard protocols using the Duolink-"In-cell Co-IP" kit (OLink Biosciences) [41] using anti-*SCN4B* and Anti-RhoA primary antibodies.

Scanning Electron Microscopy - Cells were fixed by incubation for 24 hr in 4% paraformaldehyde, 1% glutaraldehyde in 0.1 M phosphate buffer (pH 7.2). They were then washed in phosphate-buffered saline (PBS) and post-fixed by incubation with 2% osmium tetroxide for 1 hr. Samples were then fully dehydrated in a graded series of ethanol solutions and dried in hexamethyldisilazane (HMDS, Sigma, St-Louis, MO). Finally, Cells were coated with 40 Å platinum, using a GATAN PECS 682 apparatus (Pleasanton, CA), before observation under a Zeiss Ultra plus FEG-SEM scanning electron microscope (Oberkochen, Germany).

Zebrafish maintenance and in vivo zebrafish invasion assays - Zebrafish (*Danio rerio*), from the Zebrafish International Resource Centre (ZIRC), were maintained in re-circulating tanks according to standard procedures ("The zebrafish handbook: a laboratory use of zebrafish, *Brachydanio rerio*"). Adult fish were maintained at 26ºC, with a light/dark cycle of 14/10 hr, and were fed twice daily, once with dry flake food (PRODAC) and once with live *Aretmia Salina* (MC 450, IVE AQUACULTURE). Zebrafish embryos were maintained in egg water at 28.5ºC, fed during 5 days with NOVO TOM and with live arthemia at 11 days of life. The experiments were performed in compliance with the Guidelines of the European Union Council for animal experimentation (86/609/EU) and were approved by the Bioethical Committee of the University Hospital Virgen de la Arrixaca (Spain). The colonization of zebrafish embryos was previously described [34]. Briefly, MDA-MB-231 breast cancer cells transfected with small interfering RNA targeting the expression of *SCN4B* gene (Si*SCN4B*) or null-target siRNA (siCTL) were trypsinized 24hr after transfection, washed and stained with the vital cell tracker red fluorescent CM-Dil (Vibrant, Invitrogen). 50 labelled cells were injected into the yolk sac of dechorionated zebrafish embryos using a manual injector (Narishige). Fish with fluorescently-labelled cells appearing outside the implantation area at 2 hr post-injection were excluded from further analysis. All other fishes were incubated at 35ºC for 48 hr and analysed with a SteReo Lumar V12 stereomicroscope with an AxioCam MR5 camera (Carl Zeiss). The evaluation criteria for embryos being colonized by human cancer cells was the presence of more than 5 cells outside of the yolk sac. A zebrafish (ZF) colonization index was calculated as being the proportion of embryos being colonized (by at least 5 human cancer cells) in the si*SCN4B* condition divided the proportion of invaded embryos in the siCTL condition.

In Vivo tumour models – All animals were bred and housed at the In Vivo platform of the Cancéropôle Grand Ouest at Inserm U892 (Nantes, France) under the animal care license n° 44278. The project was approved by the national ethical committee (ref n°00085.01).

Experimental model for metastatic colonisation - Unanaesthetized 6-week-old female NMRI Nude Mice (Charles River laboratories) were placed into a plastic restraining device, and 2×10^6 MDA-MB-231-Luc cells (sh*SCN4B*/oe*SCN4B*) suspended in 100 µL PBS were injected into the lateral tail vein through a 25-gauge needle as previously described [22]. At necropsy, *ex vivo* BLI measurement for each collected organ was performed within

15 min after D-luciferin intraperitoneal injection (150 mg/kg). Photons emitted by cancer cells were counted by bioluminescent imaging (ΦimageurTM, BIOSPACE Lab) and expressed in counts per minute (cpm).

Orthotopic breast tumour model – Six week-old female Rag2-/- Il2rg-/- mice (NOD SCID, Charles River laboratories) were injected into the sixth right inguinal mammary fat pad with $2x10^6$ MDA-MB-231-Luc cells (sh*SCN4B* or oe*SCN4B*) suspended in 100 µL PBS whilst under isoflurane anesthesia. Tumour growth was monitored by bioluminescence imaging [22]. Animal weight was measured every week or every other week, and the primary tumour volume (mm^3) was measured with a calliper and calculated as length x height x width (in mm). Mice were euthanized 22 weeks following implantation of tumour cells and metastatic bioluminescence was measured [22].

Statistical analyses – Statistical analyses on immunohistochemistry staining were performed using the Yate's chi-squared test using the online interactive Chi-square test software Quantsy (http://quantpsy.org). Other data were displayed as mean ± standard error of the mean (n = sample size) and were analysed using parametric statistical tests (Student's t test, or ANOVA) when they were following a normal distribution and equal variances. Alternatively, when samples were not following a normal distribution, or when variances failed to be comparable, date were displayed as box Box plots indicating the first quartile, the median, and the third quartile, and squares for comparison of means are indicated as squares. In these cases, adequate non-parametric statistical tests were used (Mann-Whitney rank sum tests, Dunn's tests, ANOVA on ranks). Statistical analyses were performed using SigmaStat 3.0 software (Systat software Inc) and statistical significance is indicated as: *, $p < 0.05$; **, $p<0.01$ and ***, $p<0.001$. NS stands for not statistically different.

II. Manuscript 2: DHA and PPARα-regulated expression of $Na_V\beta4$ subunit inhibit cancer cell invasiveness

II.1. Introduction

Breast cancer is the first cause of women death by cancer worldwide. Most of breast cancer patient die because of metastasis appearance and growth. Metastasis development partly relies on the ability of breast cancer cells to degrade and invade the extracellular matrix. A diet enriched in n-3 long chain polyunsaturated fatty acids (PUFA), and specifically in docosahexaenoic acid (DHA, 22:6n-3) increases survival and chemotherapy efficacy in breast cancer patients with severe metastatic disease (Bougnoux *et al.*, 2009, Bougnoux *et al.*, 2010). N-3 PUFA enriched diet would represent a new strategy to improve breast cancer treatment and prevention of metastasis with no additional side effect to chemotherapy. DHA is a natural ligand of peroxisome proliferator–activated receptors (PPAR) (Xu *et al.*, 1999, Wahli and Michalik, 2012). PPAR are nuclear receptors that bind to their response elements (PPRE) on the promoter sequence of target genes regulating cell survival, metabolism or inflammatory response (Peters *et al.*, 2012), and breast cancer cell proliferation and invasiveness (Peters *et al.*, 2012, Wannous *et al.*, 2013, Yuan *et al.*, 2013, Wannous *et al.*, 2015). It has been shown that DHA reduces several cancer cell line invasiveness through different mechanisms. For example, DHA increases matrix metalloprotease inhibitor secretion in renal carcinoma cells (McCabe *et al.*, 2005), it decreases secretion of the granzyme B matrix protease in pancreatic and bladder cancer cell lines (D'Eliseo *et al.*, 2012), it inhibits prostate cancer cells invasiveness through inhibition of EMT (Bianchini *et al.*, 2012) and it inhibits breast cancer cells invasiveness through regulation of $Na_V1.5$ sodium current (Wannous *et al.*, 2015). However, the mechanisms involved, and their relative importance, are not well characterized. In MDA-MB-231 breast cancer cells, our previous work demonstrated that the inhibition of PPARβ expression with siRNA and/or DHA treatments, decreases voltage-dependent sodium channel $Na_V1.5$ expression and activity and, in turn, reduces the $Na_V1.5$-dependent ECM proteolytic degradation (Wannous *et al.*, 2015). $Na_V1.5$ sodium channels are composed by one α pore-forming subunit and one or two β subunits (β1, β2, β3 or β4). Emerging evidences suggest that β subunits might be involved in cancer cell invasiveness (Roger *et al.*, 2015). β1 subunit overexpression in breast cancer cells promotes cell invasiveness through *trans*-homophilic adhesion (Nelson *et al.*, 2014). We recently showed that expression of the β4 subunit is reduced in metastatic breast cancer biopsies. When its expression is reduced, it promotes cells invasiveness *in vitro* as well as metastatic colonization of organs in zebrafish embryos. Furthermore, such regulation of β4-dependent cell invasiveness appears to occur independently of $Na_V1.5$-dependent regulation of cell invasiveness (Bon *et al*, manuscript 1). The aim of this

study was to investigate whether the inhibition of cancer cell invasiveness by DHA involved the upregulation of β4 expression.

II.2. Materials and Methods

II.2.1. Reagents

Pharmacological agonist for PPARα WY14643 (10 µM) was purchased from Enzo Life Science. DHA and AA (arachidonic acid, 20:4n-6), were purchased from Sigma-Aldrich (Saint Quentin Fallavier, France) and a stock solution at 150 mM was prepared in 100% ethanol. SiRNA (sc-37007 for siCTL, sc-36307 for PPARα, sc-36305 for PPARβ, sc-29455 for PPARγ) were purchased from Tebu-Bio (France). Lipofectamine 2000 and Lipofectamine RNAiMax were purchased from Invitrogen (France).

II.2.2. Cell cultures and DHA treatments

Human breast carcinoma cell lines MDA-MB-231 and MDA-MB-435s, (American Type Culture Collection, LGC promochem) were cultured in Dulbecco's Modified Eagle's Medium (DMEM) supplemented with 5% fetal calf serum. The human colon cancer cell line HCT116 was cultured in optiMEM supplemented with 5% fetal calf serum. For RNA quantification, cells were plated 24 hours prior treatment in 6-well plates (300 000 cells/well) with DHA 10 µM or control vehicle (0.01% ethanol) for 3, 6, 9 or 24 hours. For protein quantification, MDA-MB-231 cells were plated 24 hours prior treatment in 6-well plates (300 000 cells/well) with DHA 10 µM or vehicle (0.01% ethanol) for 24, 48 or 72 hours. MDA-MB-231 shCTL and shβ4 cells were obtained as previously described (Bon *et al*, manuscript 1).

II.2.3. RNA extraction, reverse transcription, QPCR and western blotting

Total RNA were extracted using Nucleospin ®RNA II Columns (Macherey Nagel) and reverse transcribed with PrimeScript RT Reagent Kit (Takara Bio Ing). Quantitative (real time) PCR experiments were performed in duplicate with MyIQ thermocycler (Biorad) using SYBR® Primex Ex Taq™ kit (Takara Bio Ing). Beta4, PPARα, $Na_V1.5$ and NHE1 mRNA expression were expressed relatively to HPRT1 mRNA and control condition as relative quantity $Q=2^{-\Delta\Delta Ct}$.

Western Blot experiments were performed as previously described (Bon *et al*, manuscript 1) using anti-*SCN4B* antibody (1/1000, ref HPA017293, Sigma-Aldrich, France).

II.2.4. Plasmid constructs

SCN4B promoter sequences were amplified from the clone BAC CTD 318N4 (Invitrogen). Seven forward primers containing *KpnI* enzyme clivage site at the 5' extremity and one reverse primer containing *XhoI* enzyme cleavage site at the 5'extremity were designed and synthetized (Sigma-Aldrich). Amplified sequences were inserted into pGL4.10 (Promega) reporter luciferase vector and sequenced.

Fragments of 885, 631 and 278 bp were synthetized and designed to contain one HindIII enzyme cleavage site at the 5' extremity and BamHI cleavage site at the 3' extremity. Sequences were inserted in pGLuc (Bardot *et al.*, 1993) reporter vector containing the luciferase gene upstream of the minimal β-globin promoter.

II.2.5. Transfection and transactivation assay

SiRNA (4 nM), were transfected using Lipofectamine RNAi max (Invitrogen) 48 hr prior to perform invasion assay. RNA extraction were performed as previously described (Wannous *et al.*, 2013). MDA-MB-231 cells were transfected with Lipofectamine 2000 (Invitrogene) according to manufacturer's protocol. 24 hours prior treatment, cells were transfected with a mix of plasmid DNA containing 30 ng of the reporter vector pCMVβ-galactosidase (Clonetech), to standardize the transactivation assay, and 250 ng of the reporter luciferase vector. These two vectors were cotransfected with 50 ng of PPARα expression plasmid (pSG5-PPARα) or corresponding empty vector (pSG5). Six hours post –transfection, the transfection medium (optiMEM + plasmid DNA mix) was replaced by complete medium (DMEM+5% FBS) and cells were treated with PPARα agonist (WY14683, 10 µM). For DHA treatment, transfection medium was replaced 6 hours post-transfection with complete medium cells were treated with DHA 10 µM 48 hours post-transfection. Luciferase and β-galactosidase activities were measured 48 hours post-transfection using Luciferase Assay System (Promega) following the manufacturer's recommendations. Luc activity was set at 100% in the condition of no treatment and no overexpression of PPARα. Beta–galactosidase activity was determined measuring absorbance at 574 nm after chlorophenol-red β-galactopyranoside degradation in β–galactosidase buffer (sodium phosphate 0,1 M pH7.4, $MgCl_2$ 1mM, β-mercaptoethanol 45 mM

and chlorophenol-red β-galactopyranoside 1 mM). For each condition transactivation assays were repeated at least three times, in triplicate.

II.2.6. Zebrafish maintenance and *in* vivo zebrafish metastatic assays

Zebrafish (ZF; *Danio rerio*), from the International Resource Centre, were maintained as previously described (Jelassi *et al.*, 2013). Briefly, MDA-MB-231shβ4 breast cancer cells were pre-treated for 48 hours with DHA 10 µM, trypsinized, washed and stained with the vital cell tracker red fluorescent CM-Dil (Vibrant; Invitrogen). 50 labeled cells were injected into the yolk sac of dechorionated ZF embryos using a manual injector (Narishige, London, UK). Fishes with fluorescently labeled cells appearing outside the implantation area 2 hours after injection were excluded from further analysis. All other fishes were incubated at 35°C for 48 hours, then analysed with a SteReo Lumar V12 stereomicroscope with an AxioCam MR5 camera (Carl Zeiss, Barcelona, spain). The evaluation criteria for assessing invasion of ZF embryos was the presence of more than three cells outside of the yolk. A ZF invasion index was calculated as being the proportion of embryos being invaded in the condition of interest divided by the proportion of total invades in the control condition (shCTL or in DHA).

II.2.7. Data analysis and statistics

The average results are expressed as mean±standard error of the mean from the number of cells or assays indicated in the figure legends. Statistical analyses were performed using GraphPad Prism4. Statistical significance was determined using the analysis of *t*-test or Mann-Whitney rank sum tests, depending on the normality and equal variance of samples or not. Statistically differences are indicated as follows: *p<0.05, **p<0.01 and ***p<0.001.

II.3. Results

II.3.1. DHA stimulates β4 mRNA and protein expression

Since both DHA treatment (Blanckaert *et al.*, 2010, Wannous *et al.*, 2015) and β4 overexpression reduce MDA-MB-231 breast cancer cells invasiveness (Bon *et al*, manuscript 1), we tested whether DHA could stimulate β4 mRNA expression. MDA-MB-231 cells were treated with 10 µM of DHA, a non-cytotoxic concentration reducing MDA-MB-231 cell

invasiveness. At the mRNA level, DHA (Figure 15A), but not arachidonic acid (AA, 20:4n-6, Figure 15B), significantly increases β4 mRNA expression in MDA-MB-231 cells from 4.5 hours (1.5±0.27 fold, n=4) to 24 hours (1.53±0.24 fold, n=6) post treatment and a maximal upregulation of β4 mRNA expression is obtained after 6 hours of DHA treatment (1.77±0.25 fold). Similarly, DHA significantly increases β4 mRNA expression in MDA-MB-435s breast cancer cells and HCT116 colon cancer cells with a maximal effect at 24 hours (1.55±0.18) and 3 hours (1.94±0.2) respectively. Consistent with its effect on β4 mRNA level, DHA also increases β4 protein expression at 24 hours (1.6±0.38 fold), 48 hours (1.63±0.15) and 72 hours (2.14±0.23) after treating MDA-MB-231 cells (Figure 15C).

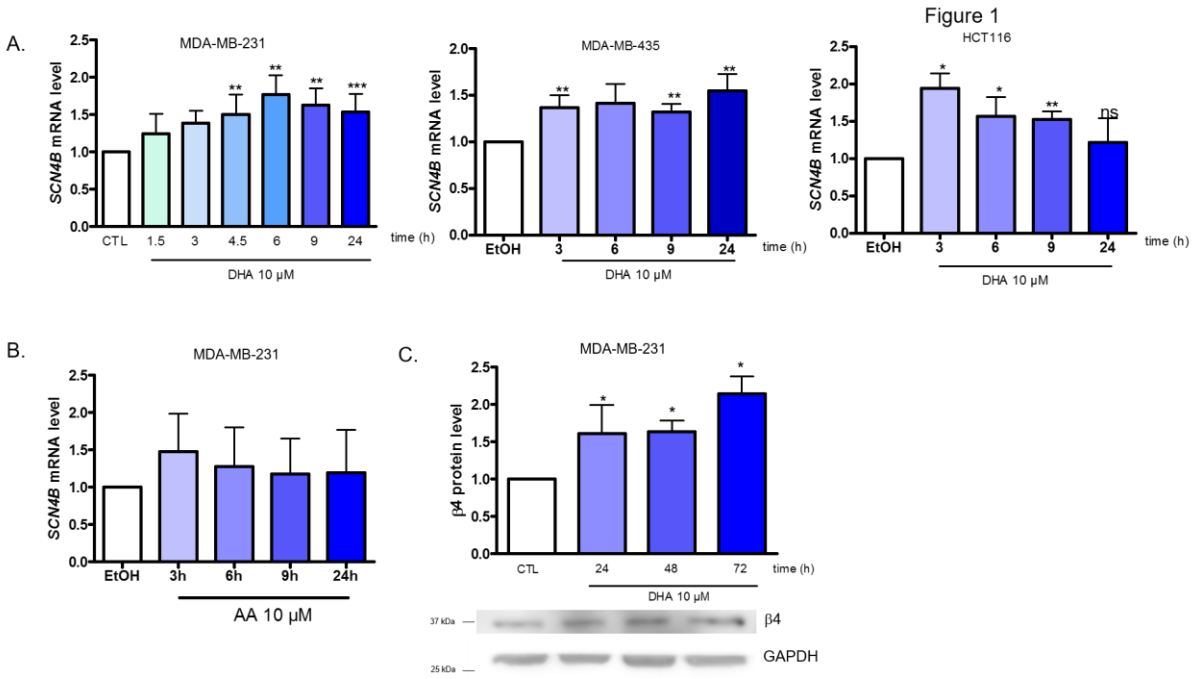

Figure 15 : DHA treatment increases β4 expression in cancer cell lines

MDA-MB-231, MDA-MB-435 and HCT116 cell lines were treated with 10 µM of DHA. MDA-MB-231 cells were treated with 10 µM of AA. A. Total RNA was extracted after 1.5, 3, 4.5, 6, 9 or 24 hours of DHA treatment and qPCR was performed after cDNA retro-transcription. Amount of β4 mRNA were compared to a control treatment (CTL, ethanol 0.01%) and normalized with *HPRT1* housekeeping gene expression (MDA-MB-231 n=4 to 10 per time point, MDA-MB-435 n=5, HCT116 n=4 to 5). B. MDA-MB-231 cell line were treated with 10 µM of arachidonic acid (AA; n=3). C. Total protein extracts were harvested after 24, 48 or 72 hours pf DHA treatment and β4 protein expression was quantified and compared to a control treatment (CTL, ethanol 0.01%) and normalized with Hsc70. n=4. *p<0.05, **p<0.01 and ***p<0.001

II.3.2. DHA stimulates *SCN4B* gene promoter activity through PPAR response element

The promoter region of *SCN4B*, coding for β4, has not been characterized so far. We performed a bioinformatic analysis of the 3.8 kb sequence located immediately 5' upstream of the start codon of *SCN4B*. Using MatInspector software (Genomatix), the sequence analysis highlighted 10 putative PPAR Response Elements (PPRE) showing a similarity superior to 70% as compared with consensus PPRE. Sequences and position of these putative PPRE are shown in Table 6.

Table 6 : Putative PPRE sequences alignment identified with MatInspector (Genomatix) analysis.
Sequence alignment of putative PPRE sequences located in the nucleotide sequence of the putative promoter -3800bp upstream of the start codon (+1). Positions on the plus (+) or minus (-) strand are indicated and position are relative to the start codon (+1).

PPRE	***Position***	***Sequence (5'-3') (brin)***	***Similarity to consensus PPRE (%)***
consensus		AACTAGGNCAAAGGTCA (+)	100
p*SCN4B*-PPRE$_1$	-3405 to -3383	AGATAGTTTTGAAAAGGTAAGAG (+)	85,1
p*SCN4B*-PPRE$_2$	-3381 to -3359	TGTCAAAAGGTCAGAGCTCCTTC (-)	88,9
p*SCN4B*-PPRE$_3$	-3374 to -3352	GAGAGGGTGTCAAAAGGTCAGAG (-)	91,2
p*SCN4B*-PPRE$_4$	-2993 to -2971	GGGAAGGTGGGGAGAGGACACTG (+)	88,3
p*SCN4B*-PPRE$_5$	-2901 to -2879	CCTGCTCTGGGCAGGGGTCACTT (+)	81,5
p*SCN4B*-PPRE$_6$	-2878 to -2856	AGGAGGTGAGCCAAAGGGAAGGA (-)	86,7
p*SCN4B*-PPRE$_7$	-2570 to -2548	AAGTCCTGGAGCAAAGGTACAAA (+)	83,4
p*SCN4B*-PPRE$_8$	-2314 to -2292	AGAGCAGTGGGCAAGGGACAGCT (-)	72,9
p*SCN4B*-PPRE$_9$	-2249 to -2227	CAGATCTGGGGAATAGGGAATTC (+)	77,3
p*SCN4B*-PPRE$_{10}$	-1540 to -1518	GACAACCAGGTCAGAGGGCTGAG (-)	90,7

Subsequent to this analysis, reporter plasmid (pGL4.10) constructs containing six different fragments of the *SCN4B* 3.4 kb putative promoter region were prepared. The 3,4 kb sequence was successively truncated in 5' in order to eliminate distant isolated PPREs or groups of PPRE (when impossible to individualize them), determining 6 sequences of different sizes (3489 bp,

2629 bp, 2434 bp, 2082 bp, 1979 bp, 1482bp shown in Figure 16A). Each fragment of the promoter was found to be active when inserted in a pGL4.10 vector in MDA-MB-231 cells (see Figure 16A). Luciferase activity were then assessed after DHA treatments (10 µM), and were expressed as a ratio of the control condition (ethanol 0.01%) with the corresponding sequence tested. Cells were treated with 10 µM fatty acids. Durations for each separate experiment: 1.5, 3, 4.5 or 6 hours. For all sequences, excepted for the 1482 bp, DHA stimulated the luciferase activity with a maximum increase comprised between 1.5 and 6 hours (data not shown). The maximal activity for each experiment in the time comprised between 1.5 to 6 hours was taken in account for the statistical analysis.

A treatment of 10 µM DHA significantly increased luciferase activity of the 5 fragments (3489 bp by 1.85±0.16, 2626 bp by 1.18±0.05, 2434 bp by 1.27±0.18, 2082 bp by 1.29±0.03, 1979 bp by 1.17±0.07), but not statistically significantly for the 1482 bp (1.32±0.20) as compared to the control condition (ethanol, EtOH, n=5). The statistical difference between DHA induced-activation of 3489 bp (1.85±0.16) and 2629 bp fragments (1.18±0.05) might be explained by the presence of 4 PPRE ($PPRE_1$, $PPRE_2$, $PPRE_3$ indivisibles and $PPRE_4$) in the 3489 but not in the 2629 bp fragments. To determine whether these $PPRE_{1-4}$ are involved in the DHA-induced activation of *SCN4B* promoter, a 3489 bp sequence in which each of the 4 PPRE cited above were invalidated by nucleotide substitution (3489mut) was synthetized (Figure 16C) and luciferase assay were performed. The sequences 3489WT and 3489mut are both equally active (at a same level) in MDA-MB-231 cells in the absence of DHA treatment (Figure 16C). However, DHA-induced activation of 3489WT sequence was significantly reduced by 64% when $PPRE_{1-4}$ are invalidated (from 1.60±0.09, n=12 to 1.26±0.07, n=7, Figure 16D) Indicating that these 4 response elements ($PPRE_{1-4}$) are involved in the upregulation of *SCN4B* by DHA. To further characterize this regulation, we synthetized 3 sequences of 885 bp, 631 bp and 278 bp from the sequence lacking in 5' promoter of 2629 bp as compared to the 3489 bp. These fragments were cloned in the pGLuc reporter plasmid, containing β-globin promoter ensuring a minimal activity. The 885 bp, 631 bp and 278 bp sequences are active in MDA-MB-231 cells in the absence of DHA treatment (see Figure 16E). DHA treatment also significantly induces activation of all these 3 sequences (885 bp 1.26±0.04, 631 bp 1.26±0.06 and 278 bp 1.29±0.10, n=5) but to a lesser extent to the 3489 bp fragment. Hence, DHA-increases of 3489WT activity involves at least one of the $PPRE_{1-4}$ located in its 5' 885 bp sequence.

Figure 16 : DHA increases SCN4B promoter activity in region containing PPRE 1, 2, 3 and 4.

See next page. A. Representation of 6 fragments containing respectively 10, 7, 5, 4, 3, 2 and 1 PPRE successively eliminated from the 5' end. Constructs were transfected in MDA-MB-231 cells and luciferase activity was assessed 48 after transfection (n=7). B. MDA-MB-231 were transfected with 6 plasmid constructs. 48 hours after transfection, cells were treated with DHA for 1.5, 3, 4.5 or 6 hours or vehicle (EtOH, ethanol, 0.01%) prior assessing luciferase activity (n=5). C. Representation of 3489 bp WT and mutated (mut) fragments. PPRE 1, 2, 3 and 4 were invalidated in 3489mut fragments. Luciferase activities of these 2 constructs were assessed and normalized with 3489WT luciferase activity 48 hours after transfection of MDA-MB-231 cells. D. MDA-MB-231 cells were transfected with 3489WT or 3489mut constructs. 48 hours after transfection cells were treated with DHA for 1.5, 3, 4.5 or 6 hours or vehicle (EtOH, ethanol, 0.01%) prior assessing luciferase activity (n=7). E. Schematic construction of 885 bp, 631 bp and 278 bp fragments containing $PPRE_{1,2,3}$ and $PPRE_4$, $PPRE_{1,2,3}$ or $PPRE_4$ respectively. F. MDA-MB-231 cells were transfected with 885 bp, 631 bp and 278 bp plasmid constructs. 48 hours after transfection cells were treated with DHA for 1.5, 3, 4.5 or 6 hours or vehicle (EtOH, ethanol, 0.01%) prior assessing luciferase activity (n=5). *p<0.05, **p<0.01, ***p<0.001.

Figure 14

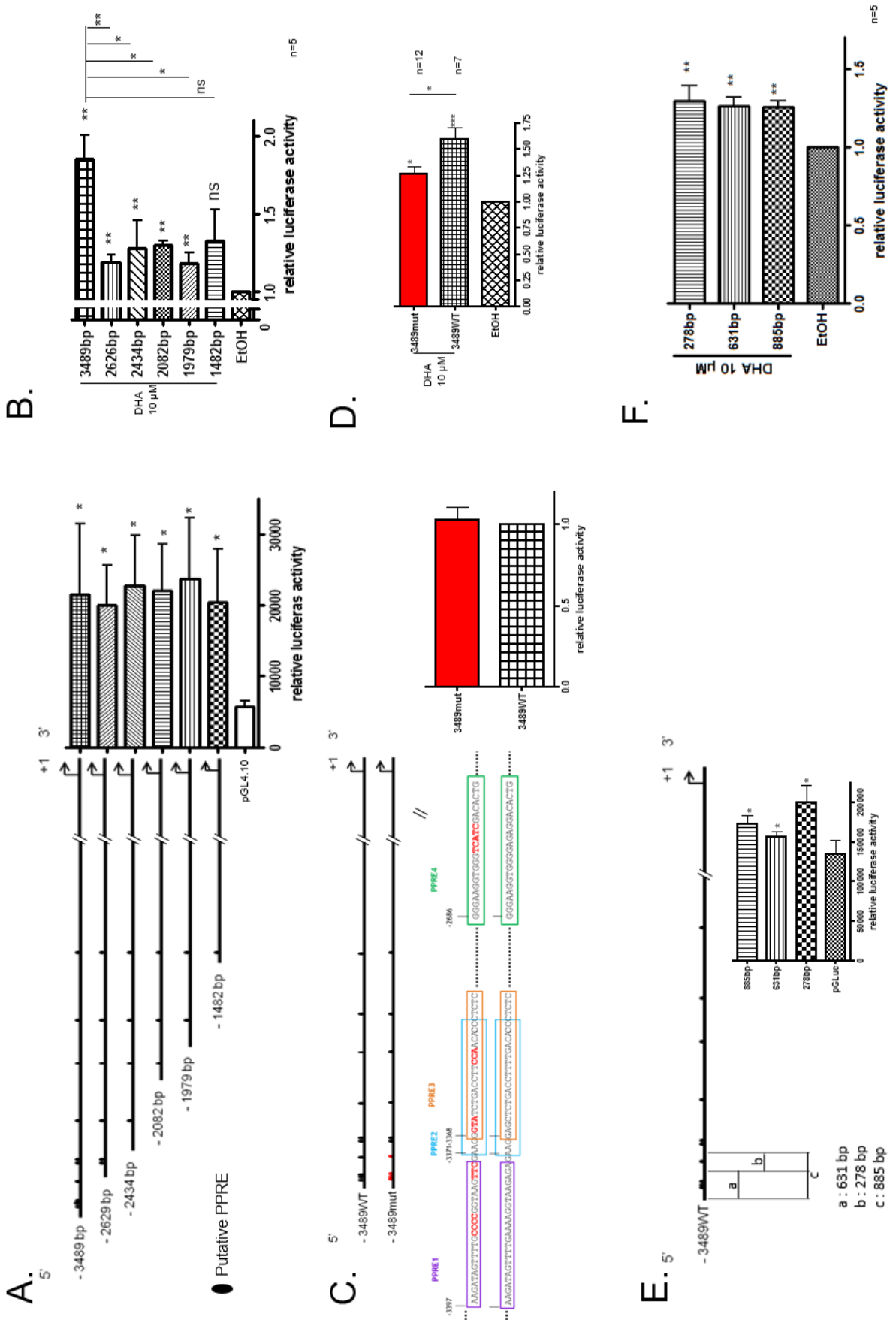
A.
5'
3'
+1
- 3489 bp
- 2629 bp
- 2434 bp
- 2082 bp
- 1979 bp
- 1482 bp
pGL4.10
Putative PPRE
relative luciferas activity
0
10000
20000
30000
B.
3489bp
2626bp
2434bp
2082bp
1979bp
1482bp
EtOH
DHA 10 µM
ns
relative luciferase activity
n=5
C.
5'
3'
+1
- 3489WT
- 3489mut
PPRE1
PPRE2
PPRE3
PPRE4
-3397
-3371-3368
-2686
relative luciferase activity
D.
3489mut
3489WT
EtOH
DHA 10 µM
n=12
n=7
relative luciferase activity
E.
5'
3'
+1
- 3489WT
a
b
c
a : 631 bp
b : 278 bp
c : 885 bp
885bp
631bp
278bp
pGLuc
relative luciferase activity
F.
278bp
631bp
885bp
EtOH
DHA 10 µM
n=5
relative luciferase activity

II.3.3. SiPPARα induces β4 mRNA expression and inhibits breast cancer cell invasiveness

Since PPRE are involved in DHA-stimulated activity of *SCN4B* promoter, we investigated which PPAR might be involved in up-regulating β4 mRNA expression by using siRNA directed against PPARα, PPARβ or PPARγ. SiRNA targeting PPARα and PPARγ both increase statistically significantly β4 mRNA level in MDA-MB-231 cells (see Figure 17A, 2.17±0.32, n=9 and 3.46±1.11, n=3 respectively) whereas siPPARβ had no effect on β4 mRNA expression (0.99±0.34, n=3). Experimental inhibition of PPARβ expression significantly reduces MDA-MB-231 invasiveness (-48%, $p<0.05$) as shown previously (Wannous *et al.*, 2015) and siPPARα also significantly reduces cell invasiveness (-38%, $p<0.05$), whereas siPPARγ did not modify cell invasiveness (see Figure 17B).

In identical conditions, siPPARβ reduced $Na_V1.5$ mRNA and protein expression, but not NHE1 mRNA and protein expression, and inhibited cell invasiveness, by reducing $Na_V1.5$ and NHE1 activities (Wannous *et al*., 2015 and Supplementary Figure 20 page 160). Similarly to siPPARβ, siPPARα also reduced cell invasiveness and $Na_V1.5$ mRNA expression (Supplementary Figure 20) suggesting that siPPARα-dependent invasiveness combines two molecular mechanisms: the down-regulation of $Na_V1.5$ mRNA expression and the up-regulation of β4 mRNA expression (Figure 17A). SiPPARγ increases both $Na_V1.5$ mRNA expression (Supplementary Figure 20A) and β4 mRNA expression (Figure 17A) and not NHE1 mRNA expression (Supplementary Figure 20B), without modifying cell invasiveness (Figure 17B), suggesting that $Na_V1.5$ pro-invasive and β4 anti-invasive activities might compensate each other in this particular siPPARγ treatment condition.

Then, we specifically investigated PPARα-dependent regulation of *SCN4B* promoter activity. Effects of PPARα overexpression, in presence or not of its specific agonist (W14643 10 µM), on 3489WT (see Figure 17C) and 3489mut (see Figure 17D) activation were investigated.

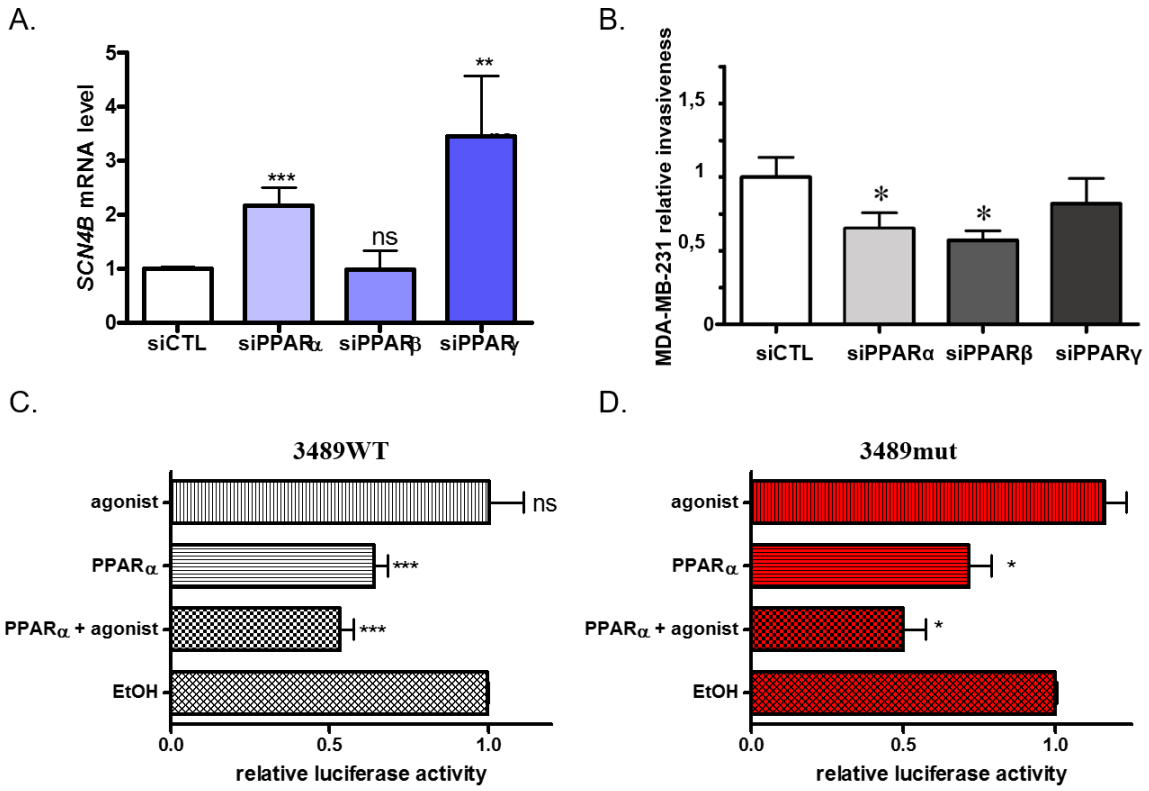

Figure 17 : PPARα modulates β4 mRNA expression and *SCN4B* promoter activity.

A. MDA-MB-231 cells were transfected with siRNA control or targeting PPARα, PPARβ or PPARγ and β4 mRNA expression was assessed 48 hours after transfection. B. MDA-MB-231 cells were transfected with siRNA control or targeting PPARα, PPARβ or PPARγ and transwell invasion assay was performed 24 hours post transfection as previously described (Wannous *et al.*, 2015) C. MDA-MB-231 cells were transfected with 3489WT plasmid and PPARα expression plasmid or corresponding empty vector. 6 hours after transfection, cells were treated with WY14643 10µM or vehicle (ethanol, EtOH, 0.01%). Luciferase activity was assessed after 48 hours of treatment. D. MDA-MB-231 cells were transfected with 3489mut plasmid and PPARα expression plasmid or corresponding empty vector. 6 hours after transfection, cells were treated with WY14643 10µM or vehicle (ethanol, EtOH, 0.01%). Luciferase activity was assessed after 48 hours of treatment. *p<0.05, **p<0.01, ***p<0.001

In both case, activation of endogenous PPARα with agonist has no effect on luciferase activities (3489WT 1.00±0.10, n=7 and 3489mut 1.16±0.06, n=4) but overexpression of exogenous PPARα significantly decreases both 3489WT and 3489mut activation (0.64±0.04, n=7 and 0.72±0.07, n=4 respectively). Exogenous PPARα overexpression together with agonist treatment decreases both 3489WT and 3489mut activities (0.53±0.04, n = 10 and 0.50±0.06, n= 4 respectively) without additional effect as compared to PPARα overexpression alone. Altogether, these results show that inhibition of PPARα expression increases β4 mRNA level while PPARα overexpression decreases *SCN4B* promoter activity. The latter occurs

independently of the 4 first PPRE of the promoter region while the increase in β4 mRNA upon DHA treatment is PPRE dependent.

II.3.4. Combined DHA and siPPARα treatments additionally increase β4 mRNA level

A potential additional effect between DHA and PPARα for up-regulating concomitantly β4 mRNA level was then tested. MDA-MB-231 cells were transfected with siRNA control (siCTL) or siPPARα and treated with 10 µM DHA. As shown previously (Wannous *et al.*, 2013), DHA treatment significantly reduces PPARα mRNA level (0.81±0.06, n=9, Figure 18A) and it increases β4 mRNA level (1.97±0.36, n=4, Figure 18B). SiPPARα significantly enhances β4 mRNA level (1.61±0.12, n=4, Figure 18B), consistent with DHA-treatment reducing PPARα expression and increasing β4 mRNA expression. In combination with siPPARα, DHA additionally increases β4 mRNA level (from 1.97±0.36 to 2.92±1.01, n=4) but there is no synergistic amplification of both treatment (see Figure 18B).

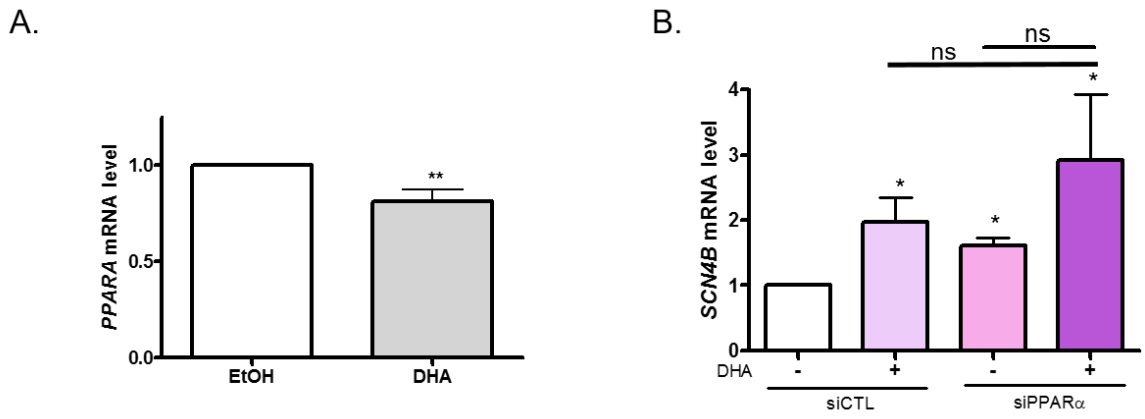

Figure 18 : Combined DHA and siPPARα treatments further increase β4 mRNA level.

A. MDA-MB-231 cells were treated with DHA for 3, 6 or 9 hours. mRNA expression was analysed by RealTime PCR, normalized with *HPRT1* gene expression and compared to the control condition (vehicle, ethanol). B. MDA-MB-231 cells were transfected with siCTL or siPPARα 48 hours prior DHA treatment. Cells were treated with DHA 10 µM during 3, 6 or 9 hours and maximal effect per experiment was selected for the analysis. *p<0.05, **p<0.01.

II.3.5. DHA-induced inhibition of cell invasiveness is β4-dependent in zebrafish colonization assay

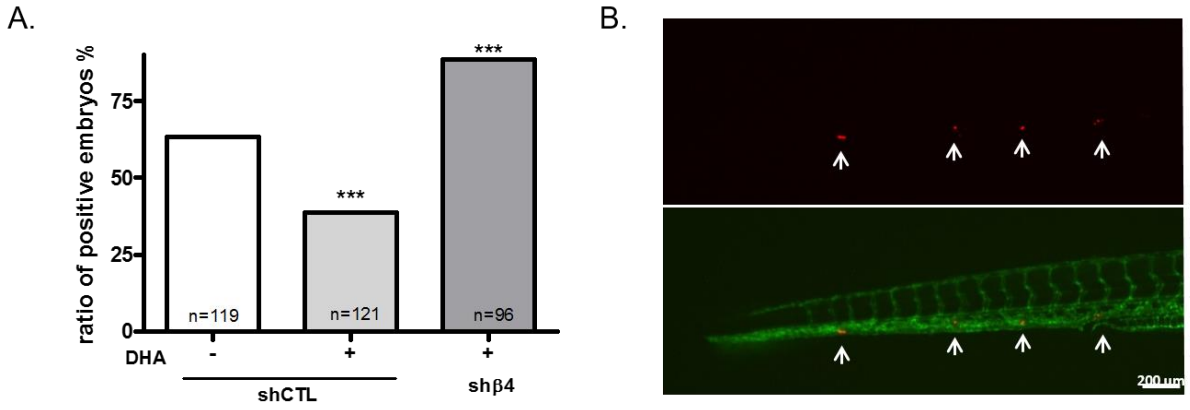

Figure 19 : Reduced organ colonization of zebrafish upon DHA treatment of MDA-MB-231 is abolished when β4 expression is suppressed.

A. MDA-MB-231shCTL and shβ4 cells were pre-treated with DHA (10 µM, 48 hours) or control vehicle prior injection to zebrafish embryos. Graph represents percentage of positive embryos in each condition (shCTL 63.3% n=119, shCTL DHA 38.84% n=121, shβ4 DHA 88.54% n=96. B. Image showing tail of zebrafish embryos *fli* (expressing GFP in endothelial cells) and MDA-MB-231shβ4 cells CM-Dil stained (red). ***p<0.001.

We have previously shown that β4 silenced-expression increases metastatic spread of MDA-MB-231 cells in zebrafish embryos (Bon *et al*, manuscript 1). It was important to test that DHA-reduced invasiveness depends on β4 expression. In shCTL cells, DHA pre-treatment significantly inhibits metastatic colonization (-24.2%, p<0.001) which is consistent with results obtained with cultured MDA-MB-231 cells. However, there is significantly more metastatic spreading in zebrafish embryos injected with DHA-pre-treated cells, indicating that DHA effect was lost in shβ4 injected embryos.

Supplementary data

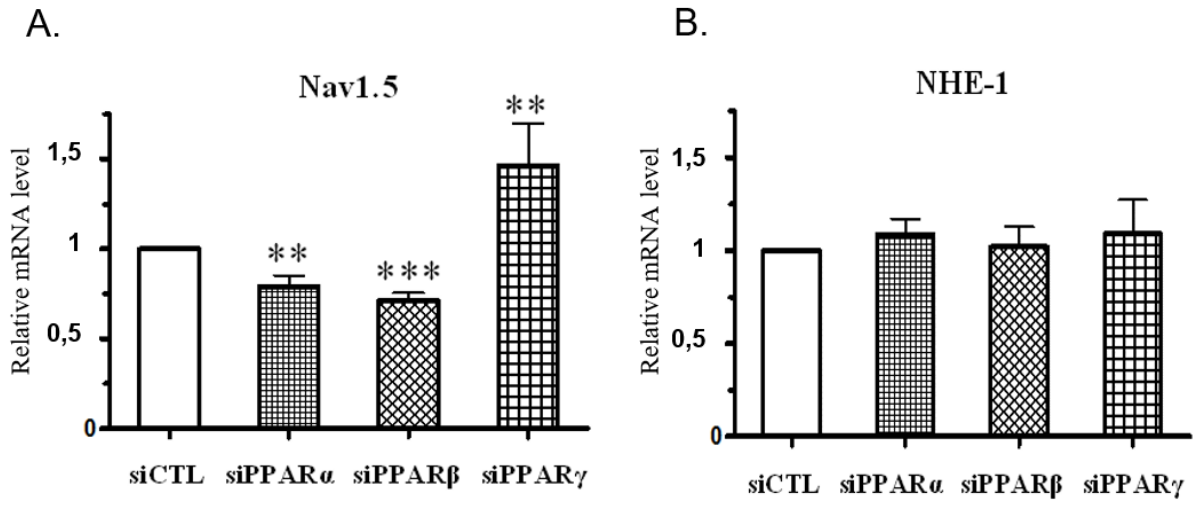

Supplementary Figure 20 : siPPAR regulate $Na_V1.5$ but not NHE1 mRNA expression.

MDA-MB-231 cells were transfected with siRNA control or targeting PPARα, PPARβ or PPARγ and β4 mRNA expression was assessed 48 hours after transfection. . Total RNA were harvested and analysed by RealTime PCR, normalized with *HPRT1* gene expression and compared to the control condition (siCTL). A. Expression of $Na_V1.5$ mRNA level. B. Expression of NHE1 mRNA level. **p<0.01, ***p<0.001.

II.4. Discussion

In this study, we show for the first time that DHA can reduce highly invasive MDA-MB-231 breast cancer cell invasiveness by stimulating tumor suppressor β4 mRNA expression. Several *in vitro* studies have previously shown that DHA treatment can decrease cancer cells invasiveness by various mechanisms (McCabe *et al.*, 2005, Bianchini *et al.*, 2012, D'Eliseo *et al.*, 2012), including by inhibiting the pro-invasive $Na_V1.5$ channel mRNA expression and sodium current in MDA-MB-231 breast cancer cells (Gillet *et al.*, 2009; Wannous *et al.*, 2015). Independently of such $Na_V1.5$ effect, the $Na_V\beta4$ subunit inhibits MDA-MB-231 cells invasiveness (Bon *et al.*, manuscript 1).

The present study shows that *i*) DHA stimulates β4 mRNA and protein expression in MDA-MB-231 cells, *ii*) $PPRE_{1-4}$ located in the 885 bp 5' region of β4 promoter sequence are necessary for such DHA effect, *iii*) PPARα overexpression decreases *SCN4B* promoter activity but independently of $PPRE_{1-4}$, *iv*) in parallel of reducing cell invasiveness, inhibition of PPARα expression with siRNA, used alone or in combination with DHA which also reduces PPARα, increases β4 mRNA level and finally *v*) suppression of β4 expression in MDA-MB-231 cells prevent DHA-induced reduction of organ colonization in zebrafish embryos.

Altogether, these data highlight a mechanism by which decreasing PPAR expression stimulates β4 expression and reduces $Na_V1.5$ expression, leading to a decreased cell invasiveness (see Figure 21). A supplementation with DHA mimics such effect of siPPAR and it also enhances β4 expression through a $PPRE_{1-4}$-dependent mechanism contributing to further reducing cell invasiveness.

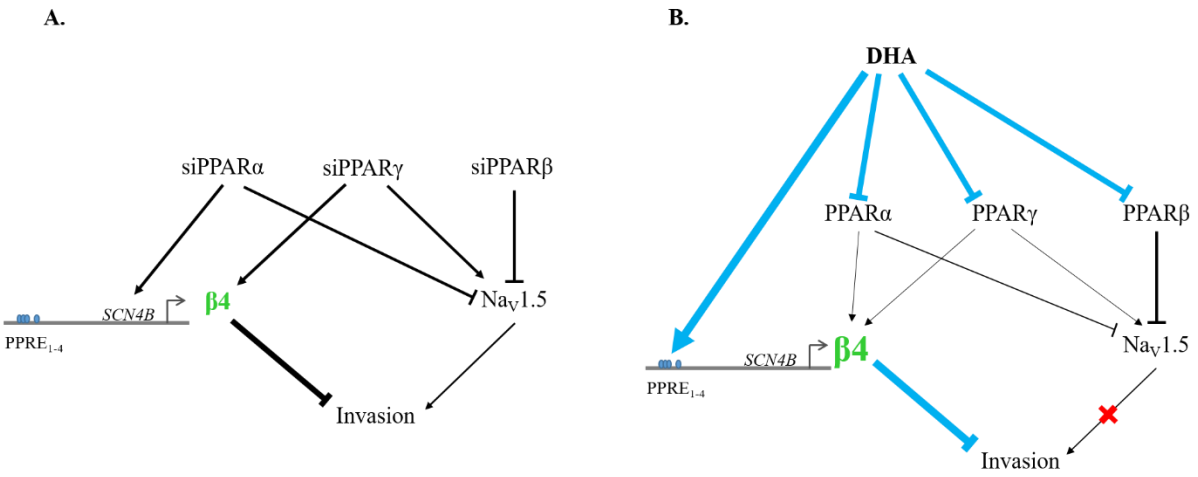

Figure 21 : Mechanism of PPAR- and DHA- dependent regulation of cell invasiveness.

A. SiPPARα enhances β4 expression and decreases $Na_V1.5$ expression thus decreasing cell invasiveness. SiPPARγ increases both β4 and $Na_V1.5$ expression, which does not impact cell invasiveness, possibly through a compensatory mechanism between these two targets. SiPPARβ decreases $Na_V1.5$ expression, which in turn, contributes to decreasing cell invasiveness. B. DHA decreases PPARα, PPARβ and PPARγ expression, leading to enhanced β4 expression and reduced $Na_V1.5$ expression. DHA also increases *SCN4B* promoter activity through $PPRE_{1-4}$ identified in its promoter region. Altogether, those multiple DHA effects on PPAR/PPRE signaling pathways reduces cell invasiveness by stimulating β4 expression.

DHA-induced stimulation of *SCN4B* promoter activity is maximal for the 3489 bp promoter fragment, the only one containing $PPRE_{1-4}$, as compared to smaller promoter fragments. DHA also reduces PPARα expression and PPARα-dependent reduction of *SCN4B* does not involve $PPRE_{1-4}$. Since MatInspector analysis revealed 6 others putative PPRE located from -2629 bp to -1 bp upstream of the *SCN4B* start codon, those might be the effectors of the PPARα-dependent inhibition of *SCN4B* promoter. Consistent with such a $PPRE_{1-4}$-dependent DHA effect and $PPRE_{1-4}$-independent PPARα effect upregulating β4 expression, there is an additional, but not synergistic effect of siPPARα combined with DHA treatment whereas in both separated conditions *SCN4B* mRNA level is increased. Fatty acids activation of PPARs mediate transcription of numerous target genes involved in glucose and lipid metabolism (Ferré, 2004) whereas several biological effects are independent of these nuclear receptors. We

identified several other putative response elements by MatInspector in *SCN4B* promoter, those included response elements targeted by IRFF (Interferon Regulatory Factors), or GATA (GATA binding factors). These two response elements, in addition to PPRE, have been shown to be effectors of DHA and could regulate *SCN4B* promoter (Kielar *et al.*, 2000, Attakpa *et al.*, 2009).

To conclude, we demonstrated that the novel tumor suppressor gene *SCN4B* is positively regulated by DHA treatment, shedding new light on the therapeutic interest of n-3 polyunsaturated fatty acids dietary supplementation for metastatic breast cancer patients.

Discussion

This PhD project was divided in two parts whose aims were to investigate *i*) the regulation of β4-dependent cell invasiveness and *ii*) whether the inhibition of cancer cell invasiveness by DHA involved the upregulation of β4 expression.

In the first part of the study, we show that β4 is strongly expressed in normal human breast tissues and weakly expressed in high grade human breast tumors tissues and even absent in metastatic lymph node. Those results are similar with lung tumor tissues. Moreover, expression of *SCN4B* mRNA is inversely correlated with metastatic breast cancer patient's survival. *In vitro*, β4 reduced expression in highly invasive breast cancer cell line MDA-MB-231 enhances cell invasiveness, whereas reducing β1 and β2 expression decrease cell invasiveness. These data indicate that inhibition of β4 expression might be involved in cancer progression and/or metastatic development. Maintaining or stimulating β4 expression with pharmacological and/or nutritional intervention might be an innovative strategy in cancer therapy.

Since β4 is a $Na_V1.5$ modulator-subunit in excitable cells, and since $Na_V1.5$ activity promotes invasiveness of MDA-MB-231 non-excitable cells (Roger *et al.*, 2007, Gillet *et al.*, 2009, Brisson *et al.*, 2011, Brisson *et al.*, 2013, Wannous *et al.*, 2015) , we first investigated whether β4-dependent regulation of cell invasiveness relies on a β4-dependent regulation of sodium channel activity. Inhibition of sodium current with TTX in shCTL cells, but not in shβ4 cells reduced cell invasiveness. Moreover, even if the I_{Na}-reduction in shβ4 cells might be explained by a decrease in addressing $Na_V1.5$ at the membrane, it did not impact the persistent sodium current. As a result, the loss of β4 expression did not impact NHE1-dependent H^+ efflux. Those data demonstrates that β4-dependent regulation of cell invasiveness is independent of $Na_V1.5$. Furthermore, when examining the ECM degradation, we found that proteolytic activity of shβ4 cells is not different to shCTL cells, which is consistent with the β4 not modifying $Na_V1.5$ and NHE1 activities. In a previous study we have shown that $Na_V1.5$ activity increases NHE1 efflux thus increasing extracellular acidification and enhances mesenchymal invasion (Brisson *et al.*, 2011, Brisson *et al.*, 2013). In the present study, we have show on the one hand that the loss of β4 did not modify NHE1 activity, i.e. did not acidify the extracellular pH and on the other hand that the loss of β4 expression enhances cell invasiveness through acquisition of an amoeboid phenotype, i.e. inter alia blebs formation. Those results are not contradictory to a recent study in which the authors have shown that blebs formation, characteristic of the amoeboid phenotype, is induced by an alkaline extracellular pH (Khajah *et al.*, 2015). MDA-MB-231 shβ4 cells are able to degrade the matrix but the use of protease inhibitors did

not prevent the increase of cell invasiveness in shβ4 cells, suggesting an increased shβ4 cell migration, later on confirmed by time-lapse video microscopy. Indeed, shβ4 cells migrated more rapidely than the control cells. Based on the literature (Friedl and Wolf, 2003), shCTL cells migration speed is characteristic of mesenchymal phenotype (0.1-1 $\mu m.min^{-1}$), and shβ4 cells migration speed is characteristic of the amoeboid phenotype (1-10 $\mu m.min^{-1}$). In order to study this possible phenotype switch, we further investigated cell morphology by microscopy. Circularity index was assessed and, on glass, shβ4 cells exhibited a more circular morphology than shCTL cells. Scanning electron microscopy analyses revealed that, shβ4 cells had less filopodia and more blebs than shCTL cells. However, on Matrigel™ substrate, the number of filopodia in shβ4 cells and shCTL cells was not affected, but it is two fold higher in shβ4 cells than in shCTL cells on glass (see Figure 24 page 175). This result suggests that the loss of β4 expression in MDA-MB-231 cells increases cell capacity to switch between amoeboid and mesenchymal phenotypes and to adapt their invasive phenotype according to the substrate. *In vivo,* the loss of β4 expression in highly breast cancer cells might confer higher abilities to migrate through extracellular matrices, with or without proteolysis, especially during extravasation and intravasation in blood or lymph vessels. Since shβ4 increased invasiveness was due to an increased migration speed, and to an acquired amoeboid phenotype, we assessed the activity of small RhoGTPases characteristics of mesenchymal or amoeboid phenotype. On the one hand, Rac1GTPase and Cdc42GTPase are known to be involved in lamellipodia and filopodia extension at the cell front associated with mesenchymal phenotype (see I.2.3.1 Lamellipodes page 46 and I.2.3.2 Filopodes page 48). On the other hand, RhoAGTPase is known to be responsible for the acto-myosin contractility at the rear edge associated with amoeboid phenotype (see I.2.2.1 Motilité cellulaire page 37 and I.2.3.3 Blebs page 52). Pull down assays highlighted that basal activity of RhoAGTPase was enhanced in shβ4 cells, and Cdc42GTPase and Rac1GTPase activity were decreased in those cells as compared to shCTL cells. This reinforced our hypothesis concerning loss of β4-induced amoeboid phenotype of breast cancer cells. Nevertheless, in prostate cancer cells, Cdc42 activity also promotes trans-endothelial migration (Reymond *et al.,* 2012). This difference might be explained by *i*) mechanisms involved in breast and prostate cell lines are differents and *ii*) the strong effect of β4 underexpression on cell invasiveness as compared to the soft reduction of Cdc42 activation in shβ4 cells. To confirm those results, pull down assays were performed on breast cancer cells overexpressing β4 subunit. In this case, RhoAGTPase activity was decreased by β4 overexpression. It has been recently shown that in MDA-MB-231 cells, inhibiting RhoA expression decreases $Na_V1.5$ channel expression and activity. Interestingly, the authors

highlighted a positive feed-back of $Na_V1.5$ on RhoA activity and show that enchanced RhoA activity increased $Na_V1.5$ sodium current, leading to an increased cell invasiveness (Dulong *et al.*, 2013). This result is consistent with our study in which we established that the loss of β4 expression enchances RhoA activity and cell invasiveness. Depending on these data, we suggested that β4 expression could provide RhoA activation through a possible interaction between both proteins, and a Duolink assay showed that β4 and RhoA are closed enough. It has been frequently reported that extracellular domain of β subunits might play a central role in adhesion since they may act as cell adhesion molecules. Since we have shown that β4 regulates cells invasiveness and might interact with RhoA, we cloned truncated β4 proteins and performed invasion assays. Surprisingly, it appears that β4 N-terminal fragment (Δ-Cter) did not reduce shβ4 invasiveness but β4 C-terminal fragment (Δ-Nter) strongly reduced shβ4 invasiveness, suggesting that β4-regulated invasivity depends on C-terminal fragment and might be due to a modification of RhoA activity. RhoA activity was measured in presence of the fragments of β4 proteins and confirmed the fact that β4 C-terminal (Δ-Nter) reduces RhoA activity. *In vivo* experiments confirmed the regulation of cancer cell invasion capacities by β4 expression. Our data suggest that β4 might act as a MAT inhibitor, but the mechanistic has to be further investigated. In a fibrosarcoma cell line, expression of the actin-associating protein Tm5NM1 blocks mesenchymal motility without transition to amoeboid motility, but this mechanism involves inhibition of Src kinase activity (Lees *et al.*, 2011) whereas the loss of β4 expression did not modify this parameter (data not shown).

Given the importance of over-expressing β4 in cancer cells to prevent both MAT and invasiveness, in the second part of this thesis, we decided to focus on potential β4 regulation by DHA which is well known to inhibit cancer cell invasiveness. One mode of action by which DHA itself reduces breast cancer cell proliferation and invasiveness is by reducing PPAR expression (Wannous *et al*., 2013). We have shown in the present study that on the one hand DHA can induce *SCN4B* transcription through $PPRE_1$ to $PPRE_4$, and on the other hand, that PPARα-induced inhibition of *SCN4B* promoter activity did not depend on those $PPRE_1$ to $PPRE_4$. Such data highlight a combined mechanism by which decreasing PPAR expression, with siPPAR and/or DHA treatments, stimulates β4 expression and reduces $Na_V1.5$ expression, leading to a decreased cell invasiveness. Those multiple DHA effect on PPAR/PPRE signaling oathway reducing cell invasiveness by stimulating β4 expression, advocate for the therapeutic interest in n-3 PUFA dietary supplementation, such as DHA, to complete current treatments of metastatic breast cancer patients. Indeed, in metastatic breast cancer patients, such DHA

treatment used in combination with current chemotherapies has been tested with positive outcomes (Bougnoux *et al.*, 2009, Bougnoux *et al.*, 2010).

It is also interesting to examine the mechanism(s) by which n-3 PUFA provided by the diet, might be "protectives" against cancer and/or metastasis appearance. Indeed, several studies performed in human cancerous cell lines (Barascu *et al.*, 2006, Blanckaert *et al.*, 2010, Kang *et al.*, 2010, Lu *et al.*, 2010, Mandal *et al.*, 2010, Cao *et al.*, 2012, Wannous *et al.*, 2013, Xue *et al.*, 2014) and in murine mammary tumour model (Colas *et al.*, 2006, Kang *et al.*, 2010, Kornfeld *et al.*, 2012, Xue *et al.*, 2014) have shown that n-3 PUFA, and most particularly DHA alone, slow down cell proliferation and tumor growth. Alpha-linolenic acid (ALA, 18:3n-3) and DHA have been inversely associated with the risk of breast cancer (Bougnoux *et al.*, 1999, Maillard *et al.*, 2002), but those observations relatives to beneficial effect of DHA have not been found in all studies of nutritional epidemiology (Larsson *et al.*, 2004). This suggests that other components of diet such as PUFA n-6/PUFA n-3 rate (Simopoulos, 2004), presence of antioxidants (Cognault *et al.*, 2000) or carotenoids (Maillard *et al.*, 2006) can modulate the effect of AGPI n-3 on breast cancer risk in women.

Similarly, in colon cancer, more and more evidences suggest that n-3 PUFA dietary supplementation, such as EPA (eicosapentaenoic acid, 20:5n-3), or fish oil mixture decrease colorectal cancer risk and have chemopreventive effect (Cockbain *et al.*, 2012). Recently, a phase II trial confirmed that EPA nutritional uptake (2 g daily for 30 days) is well incorporated in tumors and it decreases colon cancer liver metastasis and may have an antiangiogenic effect (Cockbain *et al.*, 2014). In a mouse model of colon cancer (Hawcroft *et al.*, 2012), EPA inhibited synthesis of prostaglandins E2, known as a tumor enhancer (Wang and Dubois, 2006). EPA supplementation decreases cell motility *in vitro* and might be responsible for a decrease in invasiveness *in vivo* (Hawcroft *et al.*, 2012). It has also been shown that expression of PPARβ is associated with poor prognosis in colon cancer patients (Yoshinaga *et al.*, 2011) and that PPARα and PPARγ ligands are able to inhibit the formation of precursor lesion for colon carcinoma in a rat model (Tanaka *et al.*, 2001) or reduce polyp formation in a mouse model (Niho *et al.*, 2003). The query of online database bc-GenExMiner (v3.0; http://bcgenex.centregauducheau.fr) suggests that mRNA of the three PPARs could potentially represent a good marker prognosis in breast cancer (Thesis of Ramez Wannous, 2014). The overexpression of PPARα and PPARγ mRNA seems to be a good prognosis marker ($p=0.047$ and $p=0.0006$ respectively). In contrast, PPARβ mRNA could be a good prognosis marker if it is underexpressed ($p=0.0059$).

To conclude, DHA is able to reduce breast cancer cell invasiveness through β4 upregulation, to inhibit PPAR expression, thus reducing Na_V-dependent and β4-dependent invasiveness. The combination of DHA supplementation along with PPAR ligands might represent novel strategies to improve cancer therapies and to reduce metastases appearance.

Conclusions - Perspectives

Breast cancer treatment, and most particularly metastasis therapy, remains major issue in preventing cancer-associated death. The understanding of cellular and molecular mechanisms of metastasis development is a prerequisite to prevent metastatic spread.

Voltage-gated sodium channels Na_V are expressed in multiple cancers and by its expression and activity, promotes cell invasiveness. Sodium channel Na_V are composed by one α pore-forming subunit associated with one or two β subunits. In the course of this thesis, we have shown that the β4 subunit is weakly expressed in high grade tumors and almost absent in metastatic lymph node. Furthermore, inhibiting the β4 subunit expression promoted breast cancer cell invasiveness *in vitro* and *in vivo*. We highlighted a mechanism by which expression of this protein decreases cancer cell invasiveness, independently of the Na_Vα pore-forming subunit and sodium current. Indeed, we have shown that the loss of β4 expression promoted amoeboid phenotype, that is to say acquisition of a rounded morphology, blebs at the cell surface, elevated migration, increased speed and enhanced RhoA GTPases activity. Consistent with this, overexpressing β4 reduced extracellular matrix proteolysis, migration speed, and RhoA GTPase activity. Thus, all those results lead us to conclude that β4 expression prevents mesenchymal to amoeboid transition in cancer cells, thus limiting aggressiveness of cancer cells and metastatic development (see Figure 22).

Given the importance of β4 expression in preventing metastasis development, inducing the expression of β4 could represent a new strategy for inhibiting metastasis appearance, especially through n-3 PUFA, and particularly DHA, supplementation. Indeed, this long chain PUFA is known to have a chemosensitive effect, to increase survival of breast cancer patients with severe metastatic disease and to have no additional side effect to chemotherapy. In breast cancer patients, DHA efficacy has been shown in a Phase II Study (Bougnoux *et al*., 2009). There has been important progress in better understanding the mechanisms of action of DHA *in vitro*. Here, we highlighted that DHA enhanced β4 expression directly through promoter activation, combined with PPAR modulation, thus decreasing cancer cell invasiveness (see Figure 23).

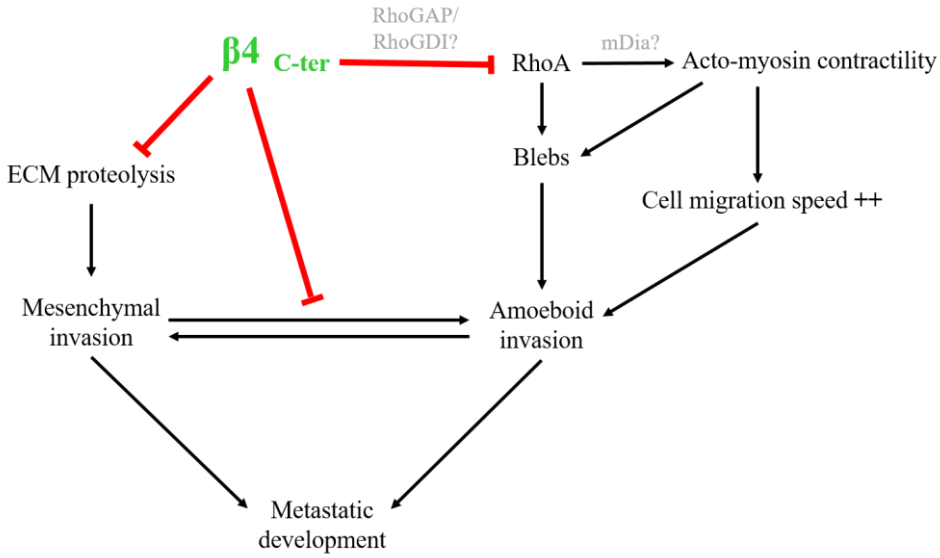

Figure 22 : Mechanism of β4-dependent regulation of cancer cell invasiveness.

Expression of β4 decreases ECM degradation and mesenchymal invasion, thus preventing metastatic development. RhoA GTPase activity, which promotes actomyosin contractility, blebs formation and enhanced cell migration speed engage amoeboid phenotype which favor metastatic development. This part is inhibited by the intracellular C-terminal domain of the β4 protein.

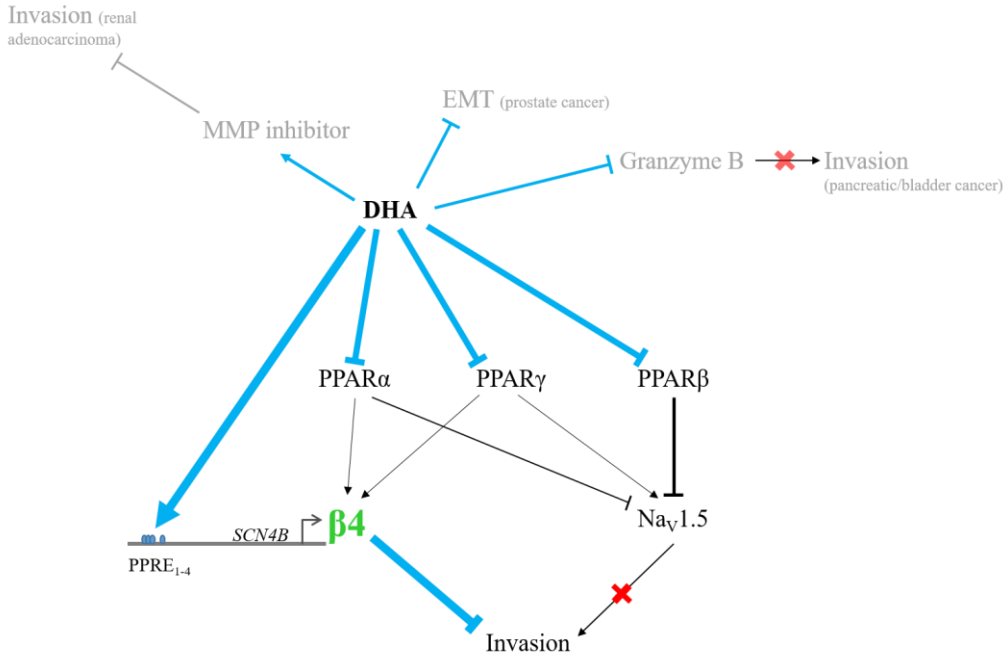

Figure 23 : Mechansims of DHA-induced inhibition of invasiveness in various cancer.

In breast cancer, DHA reduces both PPARα, PPARβ and PPARγ expression, which in turns increases β4 expression, reduces $Na_V1.5$ expression and inhibit invasiveness. DHA increases *SCN4B* promoter activity, thus enhancing β4 mRNA and protein expression. In pancreatic and bladder cancer (right corner), DHA inhibits granzyme B expression, in prostate cancer, DHA inhibits EMT and DHA reduces invasiveness of renal adenocarcinoma cells through enchanced secretion of MMP inhibitors.

In order to understand the mechanisms by which DHA and β4 regulate cell invasiveness, several parameters remain to be further investigated. Firstly, shCTL and shβ4 cells present different morphological phenotypes depending on the substrate they are seeded on (glass *vs* Matrigel™ substrate, see Figure 24). On glass, shβ4 cells had less filopodia than the shCTL cells. In contrast, when those cells were plated on Matrigel™, both shCTL and shβ4 cells had the same number of filopodia (for shCTL, twice more than on glass and for shβ4, four times more). However, there is no difference between numbers of filopodia in both cell lines on Matrigel™ substrate. Studying the cell behavior (morphology and migration parameters) on different extracellular matrices, such as collagen I or fibronectin, might be important to understand the switches between mesenchymal and amoeboid phenotype in cells which are not expressing β4. Moreover, this experiment could highlight a possible involvement of integrins in β4-dependent regulation of cell invasiveness.

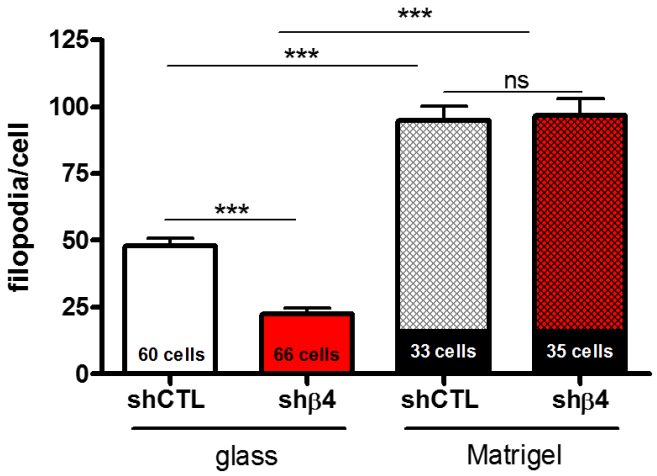

Figure 24 : MDA-MB-231shCTL and shβ4 cells exert more filopodia on a Matrigel™ substrate.
MDA-MB-231shCTL and shβ4 cells were plated on glass coverslip or Matrigel™-coated coverslips and the number of filopodia per cell was assessed manually after scanning electron microscopy analysis. ***p<0.001.

Secondly, the involvement of β4 C-terminal fragment in the inhibition of breast cancer cell invasiveness remains unclear. Since we know that BACE1 is expressed in MDA-MB-231 breast cancer cell line (see Figure 25), enzyme activity and β4 cleavage could be assessed, as the effect of secretase inhibitor on breast cancer cell invasiveness.

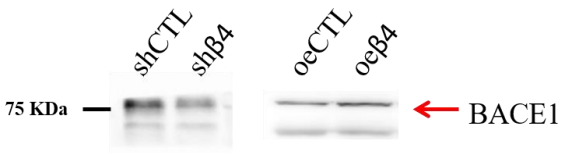

Figure 25 : BACE1 is expressed in MDA-MB-231 cell line.

Proteins from MDA-MB-231 cancer cells shCTL, shβ4 and overexpressing β4 were extracted and analysed by Western Blot. BACE1 expression was assessed using anti-human BACE1 rabbit antibody (ref 18711, immune-Biological Laboratories, Japan).

Thirdly, the modification of RhoA activity through β4 expression has to be further investigated. Indeed, our results strongly suggest that β4 and RhoA are close enough to interact and that β4 expression is inversely associated with RhoA activity. Using mass spectrometry, direct interaction of β4, especially C-terminal domain, with RhoA or RhoGTPase regulating protein preventing RhoA activation, such as RhoGDI or RhoGAP, could be investigated. A second hypothesis concerning the involvement of β4 C-terminal domain in the regulation of invasion could be investigated. The β4 protein can be cleaved by γ-secretase, releasing a C-terminal cytoplasmic soluble fragment, which could act as a blocker of RhoA activity.

It is clear that the RhoA pathway is involved in the cancer cell invasivenessmediated by the loss of β4. However, ROCK inhibition using Y27632 (10 µM) had no effect on shβ4 cell invasiveness (see Figure 26). Even more surprisingly, Y27632 inhibitor enhanced shCTL cell invasiveness but did not reduce shβ4 cell invasiveness. This suggests that in these cell lines, mDia could be involved in cell invasiveness rather than ROCK.

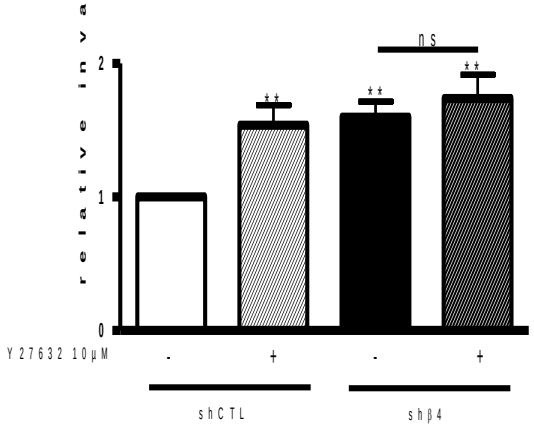

Figure 26 : ROCK inhibitor Y27632 enchances shCTL invasiveness without affecting shβ4 invasiveness.

MDA-MB-231 shCTL and shβ4 ells were pre-treated with Y27632 inhibitor (10 µM) for 2 hours before transwell invasion assay. 24 hours later, cells were fixed and nuclei were stained with DAPI, and the number of nuclei was assessed manually (n=5). **p<0.01.

It is largely known that RhoGTPase activity is modulated by phosphorylation by PKCs (Garcia-Mata *et al.*, 2011). Assessing PKCα (protein kinase C α) basal activity in MDA-MB-231shCTL and shβ4 cells might be relevant. A study had shown that inhibition of PKCα (enzastaurin or dominant negative) induces AMT in amoeboid cell line and reduces invasiveness, and activation of PKCα (PMA, Phorbol-12-Myristate-13-Acetate) induces MAT in mesenchymal cell line (Vaskovicova *et al.*, 2015). A preliminary time lapse experiment performed on shCTL and shβ4 cells indicated that PMA (PKCα activator) increased shCTL migration speed and that enzastaurin (PKCα inhibitor) decreased shβ4 migration speed (see Figure 27). This result is consistent with Vaskovicoa *et al.*, 2015, and highlight new perspective concerning β4-relative regulation of RhoGTPase.

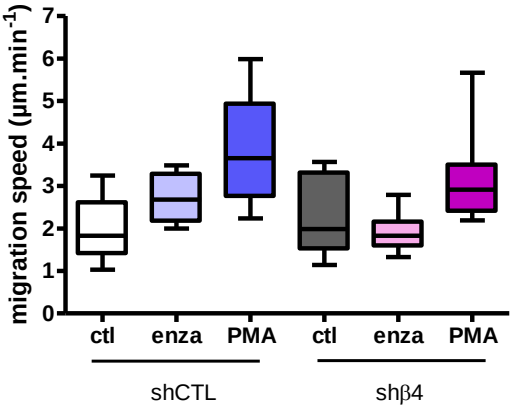

Figure 27 : Activation or inhibition of PKCα modulate MDA-MB-231 shCTL and shβ4 cell migration speed. Cells were pre-treated with enzastaurin (1 µM for 1 hour) or PMA (100 nM for 15 minutes) prior time lapse acquisition (1 picture per 2 minutes for 18 hours). PMA (PKCα activator) increased shCTL migration speed and that enzastaurin (PKCα inhibitor) decreased shβ4 migration speed.

To reinforce the strength of this study, we planned a mouse mammary fat pad experiment with MDA-MB-468luc shCTL, shβ4 or overexpressing β4 cells, which are not expressing functional $Na_V\alpha$ subunit. The next step will also consist in studying β4-dependent regulation of invasiveness in lung or colon cancer cells.

Since we planned to investigate β4-dependent regulation of cell invasiveness in several cancers, the regulation of β4 expression is likely to be similar in various solid tumours. As it has been shown that n-3 PUFA exert similar effects in both breast and colon cancer (Bougnoux *et al.*, 2010, Cockbain *et al.*, 2012), we performed preliminary experiments assessing β4 expression in MCF-7 breast and HT29 colon cancer cell lines. Preliminary data suggest that DHA increases

β4 mRNA level in HT29 colon and MCF-7 breast cancer cell lines (see Figure 28), while n-6 PUFA treatment (AA, 20:4n-6) had no effect.

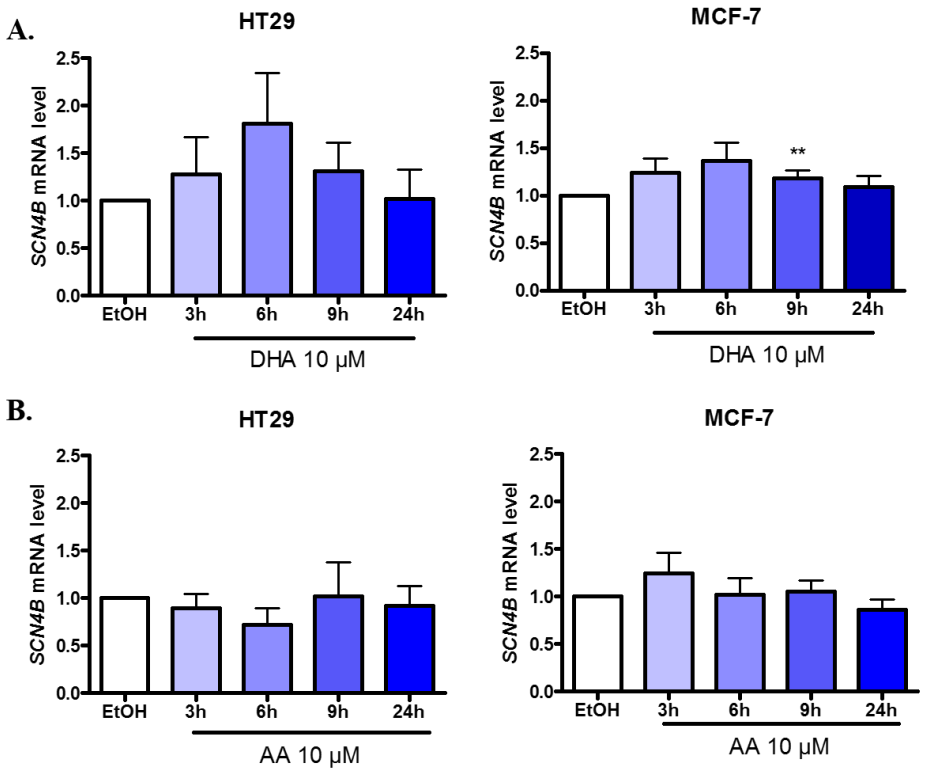

Figure 28 : DHA treatment, but not AA treatment, increases β4 expression in HT29 colon and MCF-7 breast cancer cell lines.

HT29 and MCF-7 cell lines were treated with 10 µM of DHA or AA. Total RNA was extracted after 3, 6, 9 or 24 hours of PUFA treatment and qPCR was performed after cDNA retro-transcription. Amount of β4 mRNA were compared to a control treatment (CTL, ethanol 0.01%) and normalized with *HPRT1* housekeeping gene expression. A. HT29 and MCF-7 cell lines treated with 10 µM of DHA (HT29 n=4, MCF-7 n=5). B. HT29 and MCF-7 cell lines treated with 10 µM of AA (HT29 n=4, MCF-7 n=4). **p<0.01

This study has to be continued at a promoter and a protein level. Indeed, DHA regulatory effect on *SCN4B* promoter depends on $PPRE_{1-4}$, and the activity of these did not depend on PPARα, meaning that other responsive elements could be involved in the DHA- or PPAR-dependent regulation of β4 expression.

Since PPARα is able to decrease 3489mut promoter activity, the next step consists in mutating successively the $PPRE_5$ to $PPRE_{10}$ and to measure promoter activity under PPARα overexpression. To confirm the participation of the PPRE, DNA-purified affinity assays should be performed.

In vivo, using metastatic fat pad experiment in mice, the identified DHA-induced β4 expression in breast cancer cells injected following a dietary uptake could represent a good strategy to verify the transcriptional regulation observed *in vitro*. Immunohistological analysis of β4 and $Na_V1.5$ expression at the primary site of tumor and in eventually distant sites of metastases, as well as PUFA incorporation in plasma and tissues would bring out a positive correlation between β4 expression and n-3 PUFA rate. In spite of the fact that fish oil supplementation did not affect tumor appearance in PyMT transgenic mice (Turbitt *et al.*, 2015), this model of spontaneous mammary carcinogenesis could investigate the effect of DHA supplementation on tumor growth and metastases development.

Bibliographie

Abbey, C. A. and Bayless, K. J. Matrix density alters zyxin phosphorylation, which limits peripheral process formation and extension in endothelial cells invading 3D collagen matrices. *Matrix Biol.* 2014,38: 36-47.

Abercrombie, M., Heaysman, J. E. and Pegrum, S. M. The locomotion of fibroblasts in culture. II. "RRuffling". *Exp Cell Res.* 1970,60(3): 437-444.

Abo, A., QU, J., Cammarano, M. S., Dan, C., Fritsch, A., Baud, V., Belisle, B. and Minden, A. PAK4, a novel effector for Cdc42Hs, is implicated in the reorganization of the actin cytoskeleton and in the formation of filopodia. *EMBO J.* 1998,17(22): 6527-6540.

Adachi, K., Toyota, M., Sasaki, Y., Yamashita, T., Ishida, S., Ohe-Toyota, M., Maruyama, R., Hinoda, Y., Saito, T., Imai, K., Kudo, R. and Tokino, T. Identification of SCN3B as a novel p53-inducible proapoptotic gene. *Oncogene.* 2004,23(47): 7791-7798.

Afsharimani, B., Cabot, P. J. and Parat, M. O. Effect of lysine antifibrinolytics and cyclooxygenase inhibitors on the proteolytic profile of breast cancer cells interacting with macrophages or endothelial cells. *Br J Anaesth.* 2014,113 Suppl 1: i22-31.

Ahmed, N., Maines-Bandiera, S., Quinn, M. A., Unger, W. G., Dedhar, S. and Auersperg, N. Molecular pathways regulating EGF-induced epithelio-mesenchymal transition in human ovarian surface epithelium. *Am J Physiol Cell Physiol.* 2006,290(6): C1532-1542.

Alblazi, K. M. and Siar, C. H. Cellular protrusions--lamellipodia, filopodia, invadopodia and podosomes--and their roles in progression of orofacial tumours: current understanding. *Asian Pac J Cancer Prev.* 2015,16(6): 2187-2191.

Allen, W. E., Zicha, D., Ridley, A. J. and Jones, G. E. A role for Cdc42 in macrophage chemotaxis. *J Cell Biol.* 1998,141(5): 1147-1157.

Arjonen, A., Kaukonen, R. and Ivaska, J. Filopodia and adhesion in cancer cell motility. *Cell Adh Migr.* 2011,5(5): 421-430.

Arjonen, A., Kaukonen, R., Mattila, E., Rouhi, P., Hognas, G., Sihto, H., Miller, B. W., Morton, J. P., Bucher, E., Taimen, P., Virtakoivu, R., Cao, Y., Sansom, O. J., Joensuu, H. and Ivaska, J. Mutant p53-associated myosin-X upregulation promotes breast cancer invasion and metastasis. *J Clin Invest.* 2014,124(3): 1069-1082.

Arthur, W. T., Petch, L. A. and Burridge, K. Integrin engagement suppresses RhoA activity via a c-Src-dependent mechanism. *Curr Biol.* 2000,10(12): 719-722.

Artym, V. V., Zhang, Y., Seillier-Moiseiwitsch, F., Yamada, K. M. and Mueller, S. C. Dynamic interactions of cortactin and membrane type 1 matrix metalloproteinase at invadopodia: defining the stages of invadopodia formation and function. *Cancer Res.* 2006,66(6): 3034-3043.

Aspenström, P., Fransson, A. and Saras, J. Rho GTPases have diverse effects on the organization of the actin filament system. *Biochem J.* 2004,377(Pt2): 327-337.

Attakpa, E., Hichami, A., Simonin, A. M., Sanson, E. G., Dramane, K. L. and Khan, N. A. Docosahexaenoic acid modulates the expression of T-bet and GATA-3 transcription factors, independently of PPARalpha, through suppression of MAP kinase activation. *Biochimie.* 2009,91(11-12): 1359-1365.

Azios, N. G., Krishnamoorthy, L., Harris, M., Cubano, L. A., Cammer, M. and Dharmawardhane, S. F. Estrogen and Resveratrol Regulate Rac and Cdc42 Signaling to the Actin Cytoskeleton of Metastatic Breast Cancer Cells. *Neoplasia.* 2007,9(2): 147-158.

Balcioglu, H. E., van Hoorn, H., Donato, D. M., Schmidt, T. and Danen, E. H. The integrin expression profile modulates orientation and dynamics of force transmission at cell-matrix adhesions. *J Cell Sci.* 2015,128(7): 1316-1326.

Barascu, A., Besson, P., Le Floch, O., Bougnoux, P. and Jourdan, M. L. CDK1-cyclin B1 mediates the inhibition of proliferation induced by omega-3 fatty acids in MDA-MB-231 breast cancer cells. *Int J Biochem Cell Biol.* 2006,38(2): 196-208.

Barbosa, C., Tan, Z. Y., Wang, R., Xie, W., Strong, J. A., Patel, R. R., Vasko, M. R., Zhang, J. M. and Cummins, T. R. Navbeta4 regulates fast resurgent sodium currents and excitability in sensory neurons. *Mol Pain.* 2015,11(1): 60.

Bardot, O., Aldridge, T. C., Latruffe, N. and Green, S. PPAR-RXR heterodimer activates a peroxisome proliferator response element upstream of the bifunctional enzyme gene. *Biochem Biophys Res Commun.* 1993,192(1): 37-45.

Beaty, B. T., Sharma, V. P., Bravo-Cordero, J. J., Simpson, M. A., Eddy, R. J., Koleske, A. J. and Condeelis, J. beta1 integrin regulates Arg to promote invadopodial maturation and matrix degradation. *Mol Biol Cell.* 2013,24(11): 1661-1675, S1661-1611.

Beaty, B. T., Wang, Y., Bravo-Cordero, J. J., Sharma, V. P., Miskolci, V., Hodgson, L. and Condeelis, J. Talin regulates moesin-NHE-1 recruitment to invadopodia and promotes mammary tumor metastasis. *J Cell Biol.* 2014,205(5): 737-751.

Beckham, Y., Vasquez, R. J., Stricker, J., Sayegh, K., Campillo, C. and Gardel, M. L. Arp2/3 inhibition induces amoeboid-like protrusions in MCF10A epithelial cells by reduced cytoskeletal-membrane coupling and focal adhesion assembly. *PLoS One.* 2014,9(6): e100943.

Beggs, H. E., Soriano, P. and Maness, P. F. NCAM-dependent neurite outgrowth is inhibited in neurons from Fyn-minus mice. *J Cell Biol.* 1994,127(3): 825-833.

Bereiter-Hahn, J., Luck, M., Miebach, T., Stelzer, H. K. and Voth, M. Spreading of trypsinized cells: cytoskeletal dynamics and energy requirements. *J Cell Sci.* 1990,96 (Pt 1): 171-188.

Bergamaschi, A., Tagliabue, E., Sorlie, T., Naume, B., Triulzi, T., Orlandi, R., Russnes, H. G., Nesland, J. M., Tammi, R., Auvinen, P., Kosma, V. M., Menard, S. and Borresen-Dale, A. L. Extracellular matrix signature identifies breast cancer subgroups with different clinical outcome. *J Pathol.* 2008,214(3): 357-367.

Bergert, M., Chandradoss, S. D., Desai, R. A. and Paluch, E. Cell mechanics control rapid transitions between blebs and lamellipodia during migration. *Proc Natl Acad Sci U S A.* 2012,109(36): 14434-14439.

Besson, P., Driffort, V., Bon, E., Gradek, F., Chevalier, S. and Roger, S. How do voltage-gated sodium channels enhance migration and invasiveness in cancer cells? *Biochim Biophys Acta.* 2015,1848(10 Pt B): 2493-2501.

Bianchini, F., Giannoni, E., Serni, S., Chiarugi, P. and Calorini, L. 22 : 6n-3 DHA inhibits differentiation of prostate fibroblasts into myofibroblasts and tumorigenesis. *Br J Nutr.* 2012,108(12): 2129-2137.

Blanckaert, V., Ulmann, L., Mimouni, V., Antol, J., Brancquart, L. and Chenais, B. Docosahexaenoic acid intake decreases proliferation, increases apoptosis and decreases the invasive potential of the human breast carcinoma cell line MDA-MB-231. *Int J Oncol.* 2010,36(3): 737-742.

Blouw, B., Patel, M., Iizuka, S., Abdullah, C., You, W. K., Huang, X., Li, J. L., Diaz, B., Stallcup, W. B. and Courtneidge, S. A. The invadopodia scaffold protein Tks5 is required for the growth of human breast cancer cells in vitro and in vivo. *PLoS One.* 2015,10(3): e0121003.

Blouw, B., Seals, D. F., Pass, I., Diaz, B. and Courtneidge, S. A. A role for the podosome/invadopodia scaffold protein Tks5 in tumor growth in vivo. *Eur J Cell Biol.* 2008,87(8-9): 555-567.

Bohil, A. B., Robertson, B. W. and Cheney, R. E. Myosin-X is a molecular motor that functions in filopodia formation. *Proc Natl Acad Sci U S A.* 2006,103(33): 12411-12416.

Bokoch, G. M. Biology of the p21-activated kinases. *Annu Rev Biochem.* 2003,72: 743-781.

Bonnans, C., Chou, J. and Werb, Z. Remodelling the extracellular matrix in development and disease. *Nat Rev Mol Cell Biol.* 2014,15(12): 786-801.

Bougnoux, P., Germain, E., Chajes, V., Hubert, B., Lhuillery, C., Le Floch, O., Body, G. and Calais, G. Cytotoxic drugs efficacy correlates with adipose tissue docosahexaenoic acid level in locally advanced breast carcinoma. *Br J Cancer.* 1999,79(11-12): 1765-1769.

Bougnoux, P., Hajjaji, N., Ferrasson, M. N., Giraudeau, B., Couet, C. and Le Floch, O. Improving outcome of chemotherapy of metastatic breast cancer by docosahexaenoic acid: a phase II trial. *Br J Cancer.* 2009,101(12): 1978-1985.

Bougnoux, P., Hajjaji, N., Maheo, K., Couet, C. and Chevalier, S. Fatty acids and breast cancer: sensitization to treatments and prevention of metastatic re-growth. *Prog Lipid Res.* 2010,49(1): 76-86.

Bourguignon, L. Y., Wong, G., Earle, C., Krueger, K. and Spevak, C. C. Hyaluronan-CD44 interaction promotes c-Src-mediated twist signaling, microRNA-10b expression, and RhoA/RhoC up-regulation, leading to Rho-kinase-associated cytoskeleton activation and breast tumor cell invasion. *J Biol Chem.* 2010,285(47): 36721-36735.

Bovellan, M., Fritzsche, M., Stevens, C. and Charras, G. Death-associated protein kinase (DAPK) and signal transduction: blebbing in programmed cell death. *FEBS J.* 2010,277(1): 58-65.

Boyle, S. N., Michaud, G. A., Schweitzer, B., Predki, P. F. and Koleske, A. J. A critical role for cortactin phosphorylation by Abl-family kinases in PDGF-induced dorsal-wave formation. *Curr Biol.* 2007,17(5): 445-451.

Brackenbury, W. J., Chioni, A. M., Diss, J. K. and Djamgoz, M. B. The neonatal splice variant of Nav1.5 potentiates in vitro invasive behaviour of MDA-MB-231 human breast cancer cells. *Breast Cancer Res Treat.* 2007,101(2): 149-160.

Bravo-Cordero, J. J., Magalhaes, M. A., Eddy, R. J., Hodgson, L. and Condeelis, J. Functions of cofilin in cell locomotion and invasion. *Nat Rev Mol Cell Biol.* 2013,14(7): 405-415.

Bravo-Cordero, J. J., Oser, M., Chen, X., Eddy, R., Hodgson, L. and Condeelis, J. A novel spatiotemporal RhoC activation pathway locally regulates cofilin activity at invadopodia. *Curr Biol.* 2011,21(8): 635-644.

Bray, D. and White, J. G. Cortical flow in animal cells. *Science.* 1988,239(4842): 883-888.

Brisson, L., Driffort, V., Benoist, L., Poet, M., Counillon, L., Antelmi, E., Rubino, R., Besson, P., Labbal, F., Chevalier, S., Reshkin, S. J., Gore, J. and Roger, S. NaV1.5 Na(+) channels allosterically regulate the NHE-1 exchanger and promote the activity of breast cancer cell invadopodia. *J Cell Sci.* 2013,126(Pt 21): 4835-4842.

Brisson, L., Gillet, L., Calaghan, S., Besson, P., Le Guennec, J. Y., Roger, S. and Gore, J. Na(V)1.5 enhances breast cancer cell invasiveness by increasing NHE1-dependent H(+) efflux in caveolae. *Oncogene.* 2011,30(17): 2070-2076.

Brisson, L., Reshkin, S. J., Gore, J. and Roger, S. pH regulators in invadosomal functioning: proton delivery for matrix tasting. *Eur J Cell Biol.* 2012,91(11-12): 847-860.

Brugnera, E., Haney, L., Grimsley, C., Lu, M., Walk, S. F., Tosello-Trampont, A. C., Macara, I. G., Madhani, H., Fink, G. R. and Ravichandran, K. S. Unconventional Rac-GEF activity is mediated through the Dock180-ELMO complex. *Nat Cell Biol.* 2002,4(8): 574-582.

Buccione, R., Caldieri, G. and Ayala, I. Invadopodia: specialized tumor cell structures for the focal degradation of the extracellular matrix. *Cancer Metastasis Rev.* 2009,28(1-2): 137-149.

Busco, G., Cardone, R. A., Greco, M. R., Bellizzi, A., Colella, M., Antelmi, E., Mancini, M. T., Dell'Aquila, M. E., Casavola, V., Paradiso, A. and Reshkin, S. J. NHE1 promotes invadopodial ECM proteolysis through acidification of the peri-invadopodial space. *FASEB J.* 2010,24(10): 3903-3915.

Campbell, T. M., Main, M. J. and Fitzgerald, E. M. Functional expression of the voltage-gated Na(+)-channel Nav1.7 is necessary for EGF-mediated invasion in human non-small cell lung cancer cells. *J Cell Sci.* 2013,126(Pt 21): 4939-4949.

Campellone, K. G. and Welch, M. D. A nucleator arms race: cellular control of actin assembly. *Nat Rev Mol Cell Biol.* 2010,11(4): 237-251.

Cao, W., Ma, Z., Rasenick, M. M., Yeh, S. and Yu, J. N-3 poly-unsaturated fatty acids shift estrogen signaling to inhibit human breast cancer cell growth. *PLoS One.* 2012,7(12): e52838.

Carragher, N. O., Walker, S. M., Scott Carragher, L. A., Harris, F., Sawyer, T. K., Brunton, V. G., Ozanne, B. W. and Frame, M. C. Calpain 2 and Src dependence distinguishes mesenchymal and amoeboid modes of tumour cell invasion: a link to integrin function. *Oncogene.* 2006,25(42): 5726-5740.

Cartier-Michaud, A., Malo, M., Charrière-Bertrand, C., Gadea, G., Anguille, C., Supiramaniam, A., Lesne, A., Delaplace, F., Hutzler, G., Roux, P., Lawrence, D. A. and Barlovatz-Meimon, G. Matrix-Bound PAI-1 Supports Cell Blebbing via RhoA/ROCK1 Signaling. *PLoS ONE.* 2012,7(2): e32204.

Casar, B., Rimann, I., Kato, H., Shattil, S. J., Quigley, J. P. and Deryugina, E. I. In vivo cleaved CDCP1 promotes early tumor dissemination via complexing with activated beta1 integrin and induction of FAK/PI3K/Akt motility signaling. *Oncogene.* 2014,33(2): 255-268.

Case, L. B., Baird, M. A., Shtengel, G., Campbell, S. L., Hess, H. F., Davidson, M. W. and Waterman, C. M. Molecular mechanism of vinculin activation and nanoscale spatial organization in focal adhesions. *Nat Cell Biol.* 2015,17(7): 880-892.

Catterall, W. A., Goldin, A. L., Waxman, S. G. and International Union of, P. International Union of Pharmacology. XXXIX. Compendium of voltage-gated ion channels: sodium channels. *Pharmacol Rev.* 2003,55(4): 575-578.

Cau, J. and Hall, A. Cdc42 controls the polarity of the actin and microtubule cytoskeletons through two distinct signal transduction pathways. *Journal of Cell Science.* 2005,118: 2579-2587.

Chan, K. T., Cortesio, C. L. and Huttenlocher, A. FAK alters invadopodia and focal adhesion composition and dynamics to regulate breast cancer invasion. *J Cell Biol.* 2009,185(2): 357-370.

Charras, G. and Paluch, E. Blebs lead the way: how to migrate without lamellipodia. *Nat Rev Mol Cell Biol.* 2008,9(9): 730-736.

Charras, G. T., Hu, C. K., Coughlin, M. and Mitchison, T. J. Reassembly of contractile actin cortex in cell blebs. *J Cell Biol.* 2006,175(3): 477-490.

Chen, C., Bharucha, V., Chen, Y., Westenbroek, R. E., Brown, A., Malhotra, J. D., Jones, D., Avery, C., Gillespie, P. J., 3rd, Kazen-Gillespie, K. A., Kazarinova-Noyes, K., Shrager, P., Saunders, T. L., Macdonald, R. L., Ransom, B. R., Scheuer, T., Catterall, W. A. and Isom, L. L. Reduced sodium channel density, altered voltage dependence of inactivation, and increased susceptibility to seizures in mice lacking sodium channel beta 2-subunits. *Proc Natl Acad Sci U S A.* 2002,99(26): 17072-17077.

Chen, C., Westenbroek, R. E., Xu, X., Edwards, C. A., Sorenson, D. R., Chen, Y., McEwen, D. P., O'Malley, H. A., Bharucha, V., Meadows, L. S., Knudsen, G. A., Vilaythong, A., Noebels, J. L., Saunders, T. L., Scheuer, T., Shrager, P., Catterall, W. A. and Isom, L. L. Mice lacking sodium channel beta1 subunits display defects in neuronal excitability, sodium channel expression, and nodal architecture. *J Neurosci.* 2004,24(16): 4030-4042.

Chen, W. T. Proteolytic activity of specialized surface protrusions formed at rosette contact sites of transformed cells. *J Exp Zool.* 1989,251(2): 167-185.

Chen, X. and Macara, I. G. Par-3 controls tight junction assembly through the Rac exchange factor Tiam1. *Nat Cell Biol.* 2005,7(3): 262-269.

Chen, X. F., Zhang, H. J., Wang, H. B., Zhu, J., Zhou, W. Y., Zhang, H., Zhao, M. C., Su, J. M., Gao, W., Zhang, L., Fei, K., Zhang, H. T. and Wang, H. Y. Transforming growth factor-

beta1 induces epithelial-to-mesenchymal transition in human lung cancer cells via PI3K/Akt and MEK/Erk1/2 signaling pathways. *Mol Biol Rep.* 2012,39(4): 3549-3556.

Cheng, G. Z., Chan, J., Wang, Q., Zhang, W., Sun, C. D. and Wang, L. H. Twist transcriptionally up-regulates AKT2 in breast cancer cells leading to increased migration, invasion, and resistance to paclitaxel. *Cancer Res.* 2007,67(5): 1979-1987.

Chioni, A. M., Brackenbury, W. J., Calhoun, J. D., Isom, L. L. and Djamgoz, M. B. A novel adhesion molecule in human breast cancer cells: voltage-gated Na+ channel beta1 subunit. *Int J Biochem Cell Biol.* 2009,41(5): 1216-1227.

Choi, C. K., Vicente-Manzanares, M., Zareno, J., Whitmore, L. A., Mogilner, A. and Horwitz, A. R. Actin and alpha-actinin orchestrate the assembly and maturation of nascent adhesions in a myosin II motor-independent manner. *Nat Cell Biol.* 2008,10(9): 1039-1050.

Cockbain, A. J., Toogood, G. J. and Hull, M. A. Omega-3 polyunsaturated fatty acids for the treatment and prevention of colorectal cancer. *Gut.* 2012,61(1): 135-149.

Cockbain, A. J., Volpato, M., Race, A. D., Munarini, A., Fazio, C., Belluzzi, A., Loadman, P. M., Toogood, G. J. and Hull, M. A. Anticolorectal cancer activity of the omega-3 polyunsaturated fatty acid eicosapentaenoic acid. *Gut.* 2014,63(11): 1760-1768.

Cognault, S., Jourdan, M. L., Germain, E., Pitavy, R., Morel, E., Durand, G., Bougnoux, P. and Lhuillery, C. Effect of an alpha-linolenic acid-rich diet on rat mammary tumor growth depends on the dietary oxidative status. *Nutr Cancer.* 2000,36(1): 33-41.

Colas, S., Maheo, K., Denis, F., Goupille, C., Hoinard, C., Champeroux, P., Tranquart, F. and Bougnoux, P. Sensitization by dietary docosahexaenoic acid of rat mammary carcinoma to anthracycline: a role for tumor vascularization. *Clin Cancer Res.* 2006,12(19): 5879-5886.

Coopman, P. J., Do, M. T., Thompson, E. W. and Mueller, S. C. Phagocytosis of cross-linked gelatin matrix by human breast carcinoma cells correlates with their invasive capacity. *Clin Cancer Res.* 1998,4(2): 507-515.

Corbett, B. F., Leiser, S. C., Ling, H. P., Nagy, R., Breysse, N., Zhang, X., Hazra, A., Brown, J. T., Randall, A. D., Wood, A., Pangalos, M. N., Reinhart, P. H. and Chin, J. Sodium channel cleavage is associated with aberrant neuronal activity and cognitive deficits in a mouse model of Alzheimer's disease. *J Neurosci.* 2013,33(16): 7020-7026.

Couffinhal, T., Dufourcq, P. and Duplaa, C. Beta-catenin nuclear activation: common pathway between Wnt and growth factor signaling in vascular smooth muscle cell proliferation? *Circ Res.* 2006,99(12): 1287-1289.

Cramer, L. P., Siebert, M. and Mitchison, T. J. Identification of novel graded polarity actin filament bundles in locomoting heart fibroblasts: implications for the generation of motile force. *J Cell Biol.* 1997,136(6): 1287-1305.

D'Anselmi, F., Masiello, M. G., Cucina, A., Proietti, S., Dinicola, S., Pasqualato, A., Ricci, G., Dobrowolny, G., Catizone, A., Palombo, A. and Bizzarri, M. Microenvironment promotes tumor cell reprogramming in human breast cancer cell lines. *PLoS One.* 2013,8(12): e83770.

D'Eliseo, D., Manzi, L., Merendino, N. and Velotti, F. Docosahexaenoic acid inhibits invasion of human RT112 urinary bladder and PT45 pancreatic carcinoma cells via down-modulation of granzyme B expression. *J Nutr Biochem.* 2012,23(5): 452-457.

Davis, T. H., Chen, C. and Isom, L. L. Sodium channel beta1 subunits promote neurite outgrowth in cerebellar granule neurons. *J Biol Chem.* 2004,279(49): 51424-51432.

de Toledo, M., Anguille, C., Roger, L., Roux, P. and Gadea, G. Cooperative Anti-Invasive Effect of Cdc42/Rac1 Activation and ROCK Inhibition in SW620 Colorectal Cancer Cells with Elevated Blebbing Activity. *PLoS ONE.* 2012,7(11): e48344.

Desmarais, V., Yamaguchi, H., Oser, M., Soon, L., Mouneimne, G., Sarmiento, C., Eddy, R. and Condeelis, J. N-WASP and cortactin are involved in invadopodium-dependent chemotaxis to EGF in breast tumor cells. *Cell Motil Cytoskeleton.* 2009,66(6): 303-316.

Devreotes, P. and Horwitz, A. R. Signaling Networks that Regulate Cell Migration. *Cold Spring Harb Perspect Biol.* 2015,7(8).

Diaz, D., Delgadillo, D. M., Hernandez-Gallegos, E., Ramirez-Dominguez, M. E., Hinojosa, L. M., Ortiz, C. S., Berumen, J., Camacho, J. and Gomora, J. C. Functional expression of voltage-gated sodium channels in primary cultures of human cervical cancer. *J Cell Physiol.* 2007,210(2): 469-478.

Diaz, J., Mendoza, P., Ortiz, R., Diaz, N., Leyton, L., Stupack, D., Quest, A. F. and Torres, V. A. Rab5 is required in metastatic cancer cells for Caveolin-1-enhanced Rac1 activation, migration and invasion. *J Cell Sci.* 2014,127(Pt 11): 2401-2406.

Diss, J. K., Archer, S. N., Hirano, J., Fraser, S. P. and Djamgoz, M. B. Expression profiles of voltage-gated Na(+) channel alpha-subunit genes in rat and human prostate cancer cell lines. *Prostate.* 2001,48(3): 165-178.

Diss, J. K., Fraser, S. P., Walker, M. M., Patel, A., Latchman, D. S. and Djamgoz, M. B. Beta-subunits of voltage-gated sodium channels in human prostate cancer: quantitative in vitro and in vivo analyses of mRNA expression. *Prostate Cancer Prostatic Dis.* 2008,11(4): 325-333.

Driffort, V., Gillet, L., Bon, E., Marionneau-Lambot, S., Oullier, T., Joulin, V., Collin, C., Pagès, J. C., Jourdan, M. L., Chevalier, S., Bougnoux, P., Le Guennec, J. Y., Besson, P. and Roger, S. Ranolazine inhibits NaV1.5-mediated breast cancer cell invasiveness and lung colonization. *Molecular Cancer.* 2014,13(264).

Dulong, C., Fang, Y. J., Gest, C., Zhou, M. H., Patte-Mensah, C., Mensah-Nyagan, A. G., Vannier, J. P., Lu, H., Soria, C., Cazin, L., Mei, Y. A., Varin, R. and Li, H. The small GTPase RhoA regulates the expression and function of the sodium channel Nav1.5 in breast cancer cells. *Int J Oncol.* 2013,44(2): 539-547.

Dulyaninova, N. G., House, R. P., Betapudi, V. and Bresnick, A. R. Myosin-IIA heavy-chain phosphorylation regulates the motility of MDA-MB-231 carcinoma cells. *Mol Biol Cell.* 2007,18(8): 3144-3155.

Elad, N., Volberg, T., Patla, I., Hirschfeld-Warneken, V., Grashoff, C., Spatz, J. P., Fassler, R., Geiger, B. and Medalia, O. The role of integrin-linked kinase in the molecular architecture of focal adhesions. *J Cell Sci.* 2013,126(Pt 18): 4099-4107.

Emsley, J., Knight, C. G., Farndale, R. W., Barnes, M. J. and Liddington, R. C. Structural Basis of Collagen Recognition by Integrin α2β1. *Cell.* 2000,101(1): 47-56.

Esnakula, A. K., Ricks-Santi, L., Kwagyan, J., Kanaan, Y. M., DeWitty, R. L., Wilson, L. L., Gold, B., Frederick, W. A. and Naab, T. J. Strong association of fascin expression with triple negative breast cancer and basal-like phenotype in African-American women. *J Clin Pathol.* 2014,67(2): 153-160.

Etienne-Manneville, S. Cdc42 – the centre of polarity. *Journal of Cell Science.* 2004,117: 1291-1300.

Etienne-Manneville, S. and Hall, A. Integrin-Mediated Activation of Cdc42 Controls Cell Polarity in Migrating Astrocytes through PKCzeta. *Cell.* 2001,106: 489–498.

Evangelista, M., Zigmond, S. H. and Boone, C. Mechanism of formin-induced nucleation of actin filaments. *Biochemistry.* 2003,42(2): 486-496.

Fackler, O. T. and Grosse, R. Cell motility through plasma membrane blebbing. *J Cell Biol.* 2008,181(6): 879-884.

Fahmi, A. I., Patel, M., Stevens, E. B., A.L., F., John, J. E., Lee, K., Pinnock, R., Morgan, K., Jackson, A. P. and Vandenberg, J. I. The sodium channel beta-subunit SCN3b modulates the kinetics of SCN5a and is expressed heterogeneously in sheep heart. *J Physiol.* 2001,537(Pt3): 693-700.

Fang, D., Hawke, D., Zheng, Y., Xia, Y., Meisenhelder, J., Nika, H., Mills, G. B., Kobayashi, R., Hunter, T. and Lu, Z. Phosphorylation of beta-catenin by AKT promotes beta-catenin transcriptional activity. *J Biol Chem.* 2007,282(15): 11221-11229.

Fearon, E. R. and Vogelstein, B. A genetic model for colorectal tumorigenesis. *Cell.* 1990,61(5): 759-767.

Ferré, P. The biology of peroxisome proliferator-activated receptors: relationship with lipid metabolism and insulin sensitivity. *Diabetes.* 2004,53(Suppl 1): S43-50.

Fife, C. M., McCarroll, J. A. and Kavallaris, M. Movers and shakers: cell cytoskeleton in cancer metastasis. *British Journal of Pharmacology.* 2014,171(24).

Fishkind, D. J., Cao, L. G. and Wang, Y. L. Microinjection of the catalytic fragment of myosin light chain kinase into dividing cells: effects on mitosis and cytokinesis. *J Cell Biol.* 1991,114(5): 967-975.

Fourcade, S., Savary, S., Albet, S., Gauthe, D., Gondcaille, C., Pineau, T., Bellenger, J., Bentejac, M., Holzinger, A., Berger, J. and Bugaut, M. Fibrate induction of the adrenoleukodystrophy-related gene (ABCD2): promoter analysis and role of the peroxisome proliferator-activated receptor PPARalpha. *Eur J Biochem.* 2001,268(12): 3490-3500.

Fraser, S. P., Diss, J. K., Chioni, A. M., Mycielska, M. E., Pan, H., Yamaci, R. F., Pani, F., Siwy, Z., Krasowska, M., Grzywna, Z., Brackenbury, W. J., Theodorou, D., Koyuturk, M., Kaya, H., Battaloglu, E., De Bella, M. T., Slade, M. J., Tolhurst, R., Palmieri, C., Jiang, J., Latchman, D. S., Coombes, R. C. and Djamgoz, M. B. Voltage-gated sodium channel

expression and potentiation of human breast cancer metastasis. *Clin Cancer Res.* 2005,11(15): 5381-5389.

Friedl, P. and Wolf, K. Tumour-cell invasion and migration: diversity and escape mechanisms. *Nat Rev Cancer.* 2003,3(5): 362-374.

Friedl, P. and Wolf, K. Plasticity of cell migration: a multiscale tuning model. *J Cell Biol.* 2010,188(1): 11-19.

Fritz, G., Just, I. and Kaina, B. Rho GTPases are over-expressed in human tumors. *Int. J. Cancer.* 1999,81: 682-687.

Fujiwara, K. and Pollard, T. D. Fluorescent antibody localization of myosin in the cytoplasm, cleavage furrow, and mitotic spindle of human cells. *J Cell Biol.* 1976,71(3): 848-875.

Gadea, G., Sanz-Moreno, V., Self, A., Godi, A. and Marshall, C. J. DOCK10-mediated Cdc42 activation is necessary for amoeboid invasion of melanoma cells. *Curr Biol.* 2008,18(19): 1456-1465.

Garcia-Mata, R., Boulter, E. and Burridge, K. The 'invisible hand': regulation of RHO GTPases by RHOGDIs. *Nat Rev Mol Cell Biol.* 2011,12(8): 493-504.

Gardel, M. L., Schneider, I. C., Aratyn-Schaus, Y. and Waterman, C. M. Mechanical integration of actin and adhesion dynamics in cell migration. *Annu Rev Cell Dev Biol.* 2010,26: 315-333.

Gasparski, A. N. and Beningo, K. A. Mechanoreception at the Cell Membrane: More than the Integrins. *Arch Biochem Biophys.* 2015.

Gavert, N. and Ben-Ze'ev, A. Epithelial-mesenchymal transition and the invasive potential of tumors. *Trends Mol Med.* 2008,14(5): 199-209.

Giannone, G., Dubin-Thaler, B. J., Rossier, O., Cai, Y., Chaga, O., Jiang, G., Beaver, W., Dobereiner, H. G., Freund, Y., Borisy, G. and Sheetz, M. P. Lamellipodial actin mechanically links myosin activity with adhesion-site formation. *Cell.* 2007,128(3): 561-575.

Giannoni, E., Taddei, M. L., Parri, M., Bianchini, F., Santosuosso, M., Grifantini, R., Fibbi, G., Mazzanti, B., Calorini, L. and Chiarugi, P. EphA2-mediated mesenchymal-amoeboid transition induced by endothelial progenitor cells enhances metastatic spread due to cancer-associated fibroblasts. *J Mol Med (Berl).* 2013,91(1): 103-115.

Gillet, L., Roger, S., Besson, P., Lecaille, F., Gore, J., Bougnoux, P., Lalmanach, G. and Le Guennec, J. Y. Voltage-gated Sodium Channel Activity Promotes Cysteine Cathepsin-dependent Invasiveness and Colony Growth of Human Cancer Cells. *J Biol Chem.* 2009,284(13): 8680-8691.

Goel, H. L. and Mercurio, A. M. VEGF targets the tumour cell. *Nat Rev Cancer.* 2013,13(12): 871-882.

Gomes, E. R., Jani, S. and Gundersen, G. G. Nuclear movement regulated by Cdc42, MRCK, myosin, and actin flow establishes MTOC polarization in migrating cells. *Cell.* 2005,121(3): 451-463.

Gonzalez, D. M. and Medici, D. Signaling mechanisms of the epithelial-mesenchymal transition. *Sci Signal.* 2014,7(344): re8.

Goode, B. L. and Eck, M. J. Mechanism and function of formins in the control of actin assembly. *Annu Rev Biochem.* 2007,76: 593-627.

Gould, C. M. and Courtneidge, S. A. Regulation of invadopodia by the tumor microenvironment. *Cell Adhesion & Migration.* 2014,8(3): 226-235.

Grande-Garcia, A., Echarri, A., de Rooij, J., Alderson, N. B., Waterman-Storer, C. M., Valdivielso, J. M. and del Pozo, M. A. Caveolin-1 regulates cell polarization and directional migration through Src kinase and Rho GTPases. *J Cell Biol.* 2007,177(4): 683-694.

Grieco, T. M., Malhotra, J. D., Chen, C., Isom, L. L. and Raman, I. M. Open-channel block by the cytoplasmic tail of sodium channel beta4 as a mechanism for resurgent sodium current. *Neuron.* 2005,45(2): 233-244.

Grosson, C. L. S., Cannon, S. C., Corey, D. P. and Gusella, J. F. Sequence of the voltage-gated sodium channel β1-subunit in wild-type and in quivering mice. *Molecular Brain Research.* 1996,42(2): 222-226.

Gurel, P. S., A, M., Guo, B., Shu, R., Mierke, D. F. and Higgs, H. N. Assembly and Turnover of Short Actin Filaments by the Formin INF2 and Profilin. *J Biol Chem.* 2015,290(37): 22494-22506.

Hakim, P., Brice, N., Thresher, R., Lawrence, J., Zhang, Y., Jackson, A. P., Grace, A. A. and Huang, C. L. Scn3b knockout mice exhibit abnormal sino-atrial and cardiac conduction properties. *Acta Physiol (Oxf).* 2010,198(1): 47-59.

Halfter, W., Oertle, P., Monnier, C. A., Camenzind, L., Reyes-Lua, M., Hu, H., Candiello, J., Labilloy, A., Balasubramani, M., Henrich, P. B. and Plodinec, M. New concepts in basement membrane biology. *FEBS Journal.* 2015: n/a-n/a.

Hartshorne, R. and Catterall, W. The sodium channel from rat brain : purification and subunit composition. *The Journal of Biological Chemistry.* 1984,259(3): 1667-1675.

Hashimoto, Y., Ito, T., Inoue, H., Okumura, T., Tanaka, E., Tsunoda, S., Higashiyama, M., Watanabe, G., Imamura, M. and Shimada, Y. Prognostic significance of fascin overexpression in human esophageal squamous cell carcinoma. *Clin Cancer Res.* 2005,11(7): 2597-2605.

Hashimoto, Y., Skacel, M., Lavery, I. C., Mukherjee, A. L., Casey, G. and Adams, J. C. Prognostic significance of fascin expression in advanced colorectal cancer: an immunohistochemical study of colorectal adenomas and adenocarcinomas. *BMC Cancer.* 2006,6: 241.

Havrylenko, S., Noguera, P., Abou-Ghali, M., Manzi, J., Faqir, F., Lamora, A., Guerin, C., Blanchoin, L. and Plastino, J. WAVE binds Ena/VASP for enhanced Arp2/3 complex-based actin assembly. *Mol Biol Cell.* 2015,26(1): 55-65.

Hawcroft, G., Volpato, M., Marston, G., Ingram, N., Perry, S. L., Cockbain, A. J., Race, A. D., Munarini, A., Belluzzi, A., Loadman, P. M., Coletta, P. L. and Hull, M. A. The omega-3 polyunsaturated fatty acid eicosapentaenoic acid inhibits mouse MC-26 colorectal cancer cell

liver metastasis via inhibition of PGE2-dependent cell motility. *Br J Pharmacol.* 2012,166(5): 1724-1737.

He, T. C., Chan, T. A., Vogelstein, B. and Kinzler, K. W. PPARdelta is an APC-regulated target of nonsteroidal anti-inflammatory drugs. *Cell.* 1999,99(3): 335-345.

Head, B. P., Patel, H. H. and Insel, P. A. Interaction of membrane/lipid rafts with the cytoskeleton: impact on signaling and function: membrane/lipid rafts, mediators of cytoskeletal arrangement and cell signaling. *Biochim Biophys Acta.* 2014,1838(2): 532-545.

Head, J. A., Jiang, D., Li, M., Zorn, L. J., Schaefer, E. M., Parsons, J. T. and Weed, S. A. Cortactin tyrosine phosphorylation requires Rac1 activity and association with the cortical actin cytoskeleton. *Mol Biol Cell.* 2003,14(8): 3216-3229.

Hecht, I., Bar-El, Y., Balmer, F., Natan, S., Tsarfaty, I., Schweitzer, F. and Ben-Jacob, E. Tumor invasion optimization by mesenchymal-amoeboid heterogeneity. *Sci Rep.* 2015,5: 10622.

Heinemann, S. H., Terlau, H., Stuhmer, W., Imoto, K. and Numa, S. Calcium channel characteristics conferred on the sodium channel by single mutations. *Nature.* 1992,356(6368): 441-443.

Hernandez-Plata, E., Ortiz, C. S., Marquina-Castillo, B., Medina-Martinez, I., Alfaro, A., Berumen, J., Rivera, M. and Gomora, J. C. Overexpression of NaV 1.6 channels is associated with the invasion capacity of human cervical cancer. *Int J Cancer.* 2012,130(9): 2013-2023.

Hodgkin, A. L. and Huxley, A. F. Propagation of electrical signals along giant nerve fibers. *Proc R Soc Lond B Biol Sci.* 1952,140(899): 177-183.

Hooper, S., Marshall, J. F. and Sahai, E. Tumor cell migration in three dimensions. *Methods Enzymol.* 2006,406: 625-643.

Hovanes, K., Li, T. W., Munguia, J. E., Truong, T., Milovanovic, T., Lawrence Marsh, J., Holcombe, R. F. and Waterman, M. L. Beta-catenin-sensitive isoforms of lymphoid enhancer factor-1 are selectively expressed in colon cancer. *Nat Genet.* 2001,28(1): 53-57.

Huang, B., Lu, M., Jolly, M. K., Tsarfaty, I., Onuchic, J. and Ben-Jacob, E. The three-way switch operation of Rac1/RhoA GTPase-based circuit controlling amoeboid-hybrid-mesenchymal transition. *Sci Rep.* 2014,4: 6449.

Iden, S. and Collard, J. G. Crosstalk between small GTPases and polarity proteins in cell polarization. *Nat Rev Mol Cell Biol.* 2008,9(11): 846-859.

Ishikawa, T., Takahashi, N., Ohno, S., Sakurada, H., Nakamura, K., On, Y. K., Park, J. E., Makiyama, T., Horie, M., Arimura, T., Makita, N. and Kimura, A. Novel SCN3B mutation associated with brugada syndrome affects intracellular trafficking and function of Nav1.5. *Circ J.* 2013,77(4): 959-967.

Isom, L. L., De Jongh, K. S. and Catterall, W. A. Auxiliary subunits of voltage-gated ion channels. *Neuron.* 1994,12(6): 1183-1194.

Isom, L. L., De Jongh, K. S., Patton, D. E., Reber, B. F., Offord, J., Charbonneau, H., Walsh, K., Goldin, A. L. and Catterall, W. A. Primary structure and functional expression of the beta 1 subunit of the rat brain sodium channel. *Science.* 1992,256(5058): 839-842.

Itoh, R. E., Kurokawa, K., Ohba, Y., Yoshizaki, H., Mochizuki, N. and Matsuda, M. Activation of rac and cdc42 video imaged by fluorescent resonance energy transfer-based single-molecule probes in the membrane of living cells. *Mol Cell Biol.* 2002,22(18): 6582-6591.

Iwaya, K., Norio, K. and Mukai, K. Coexpression of Arp2 and WAVE2 predicts poor outcome in invasive breast carcinoma. *Mod Pathol.* 2007,20(3): 339-343.

Jacquemet, G., Hamidi, H. and Ivaska, J. Filopodia in cell adhesion, 3D migration and cancer cell invasion. *Curr Opin Cell Biol.* 2015,36: 23-31.

Jaiswal, R., Breitsprecher, D., Collins, A., Correa, I. R., Jr., Xu, M. Q. and Goode, B. L. The formin Daam1 and fascin directly collaborate to promote filopodia formation. *Curr Biol.* 2013,23(14): 1373-1379.

Jansson, K. H., Castillo, D. G., Morris, J. W., Boggs, M. E., Czymmek, K. J., Adams, E. L., Schramm, L. P. and Sikes, R. A. Identification of beta-2 as a key cell adhesion molecule in PCa cell neurotropic behavior: a novel ex vivo and biophysical approach. *PLoS One.* 2014,9(6): e98408.

Jansson, K. H., Lynch, J. E., Lepori-Bui, N., Czymmek, K. J., Duncan, R. L. and Sikes, R. A. Overexpression of the VSSC-associated CAM, beta-2, enhances LNCaP cell metastasis associated behavior. *Prostate.* 2012,72(10): 1080-1092.

Jechlinger, M., Sommer, A., Moriggl, R., Seither, P., Kraut, N., Capodiecci, P., Donovan, M., Cordon-Cardo, C., Beug, H. and Grunert, S. Autocrine PDGFR signaling promotes mammary cancer metastasis. *J Clin Invest.* 2006,116(6): 1561-1570.

Jeganathan, S., Morrow, A., Amiri, A. and Lee, J. M. Eukaryotic elongation factor 1A2 cooperates with phosphatidylinositol-4 kinase III beta to stimulate production of filopodia through increased phosphatidylinositol-4,5 bisphosphate generation. *Mol Cell Biol.* 2008,28(14): 4549-4561.

Jelassi, B., Anchelin, M., Chamouton, J., Cayuela, M. L., Clarysse, L., Li, J., Gore, J., Jiang, L. H. and Roger, S. Anthraquinone emodin inhibits human cancer cell invasiveness by antagonizing P2X7 receptors. *Carcinogenesis.* 2013,34(7): 1487-1496.

Jiang, W., Betson, M., Mulloy, R., Foster, R., Levay, M., Ligeti, E. and Settleman, J. p190A RhoGAP is a glycogen synthase kinase-3-beta substrate required for polarized cell migration. *J Biol Chem.* 2008,283(30): 20978-20988.

Jiang, W., Watkins, G., Lane, J., Cunnick, G., Douglas-Jones, A., Mokbel, K. and Mansel, R. Prognostic Value of Rho GTPases and Rho Guanine Nucleotide Dissociation Inhibitors in Human Breast Cancers. *Clin Cancer Res.* 2003,9: 6432–6440.

Joberty, G., Petersen, C., Gao, L. and Macara, I. G. The cell-polarity protein Par6 links Par3 and atypical protein kinase C to Cdc42. *Nat Cell Biol.* 2000,2(8): 531-539.

Johnson, D., Montpetit, M. L., Stocker, P. J. and Bennett, E. S. The sialic acid component of the beta1 subunit modulates voltage-gated sodium channel function. *J Biol Chem.* 2004,279(43): 44303-44310.

Kalluri, R. and Weinberg, R. A. The basics of epithelial-mesenchymal transition. *J Clin Invest.* 2009,119(6): 1420-1428.

Kameritsch, P., Kiemer, F., Beck, H., Pohl, U. and Pogoda, K. Cx43 increases serum induced filopodia formation via activation of p21-activated protein kinase 1. *Biochim Biophys Acta.* 2015.

Kang, K. S., Wang, P., Yamabe, N., Fukui, M., Jay, T. and Zhu, B. T. Docosahexaenoic acid induces apoptosis in MCF-7 cells in vitro and in vivo via reactive oxygen species formation and caspase 8 activation. *PLoS One.* 2010,5(4): e10296.

Kardash, E., Reichman-Fried, M., Maitre, J. L., Boldajipour, B., Papusheva, E., Messerschmidt, E. M., Heisenberg, C. P. and Raz, E. A role for Rho GTPases and cell-cell adhesion in single-cell motility in vivo. *Nat Cell Biol.* 2010,12(1): 47-53; sup pp 41-11.

Katoh, Y. and Katoh, M. FGFR2-related pathogenesis and FGFR2-targeted therapeutics (Review). *Int J Mol Med.* 2009,23(3): 307-311.

Kazarinova-Noyes, K., Malhotra, J. D., McEwen, D. P., Mattei, L. N., Berglund, E. O., Ranscht, B., Levinson, S. R., Schachner, M., Shrager, P., Isom, L. L. and Xiao, Z. C. Contactin associates with Na+ channels and increases their functional expression. *J Neurosci.* 2001,21(19): 7517-7525.

Khajah, M. A., Mathew, P. M., Alam-Eldin, N. S. and Luqmani, Y. A. Bleb formation is induced by alkaline but not acidic pH in estrogen receptor silenced breast cancer cells. *Int J Oncol.* 2015,46(4): 1685-1698.

Kielar, M. L., Jeyarajah, D. R., Penfield, J. G. and Lu, C. Y. Docosahexaenoic acid decreases IRF-1 mRNA and thus inhibits activation of both the IRF-E and NFkappa d response elements of the iNOS promoter. *Transplantation.* 2000,69(10): 2131-2137.

Kim, D. Y., Carey, B. W., Wang, H., Ingano, L. A., Binshtok, A. M., Wertz, M. H., Pettingell, W. H., He, P., Lee, V. M., Woolf, C. J. and Kovacs, D. M. BACE1 regulates voltage-gated sodium channels and neuronal activity. *Nat Cell Biol.* 2007a,9(7): 755-764.

Kim, D. Y., Ingano, L. A., Carey, B. W., Pettingell, W. H. and Kovacs, D. M. Presenilin/gamma-secretase-mediated cleavage of the voltage-gated sodium channel beta2-subunit regulates cell adhesion and migration. *J Biol Chem.* 2005,280(24): 23251-23261.

Kim, D. Y., Wertz, M. H., Gautam, V., D'Avanzo, C., Bhattacharyya, R. and Kovacs, D. M. The E280A presenilin mutation reduces voltage-gated sodium channel levels in neuronal cells. *Neurodegener Dis.* 2014,13(2-3): 64-68.

Kim, H. J., Litzenburger, B. C., Cui, X., Delgado, D. A., Grabiner, B. C., Lin, X., Lewis, M. T., Gottardis, M. M., Wong, T. W., Attar, R. M., Carboni, J. M. and Lee, A. V. Constitutively active type I insulin-like growth factor receptor causes transformation and xenograft growth of immortalized mammary epithelial cells and is accompanied by an epithelial-to-mesenchymal transition mediated by NF-kappaB and snail. *Mol Cell Biol.* 2007b,27(8): 3165-3175.

Kim, S., Lee, J., Jeon, M., Nam, S. J. and Lee, J. E. Elevated TGF-beta1 and -beta2 expression accelerates the epithelial to mesenchymal transition in triple-negative breast cancer cells. *Cytokine.* 2015.

Kimura, K., Ito, M., Amano, M., Chihara, K., Fukata, Y., Nakafuku, M., Yamamori, B., Feng, J., Nakano, T., Okawa, K., Iwamatsu, A. and Kaibuchi, K. Regulation of myosin phosphatase by Rho and Rho-associated kinase (Rho-kinase). *Science.* 1996,273(5272): 245-248.

Kitzing, T. M., Wang, Y., Pertz, O., Copeland, J. W. and Grosse, R. Formin-like 2 drives amoeboid invasive cell motility downstream of RhoC. *Oncogene.* 2010,29(16): 2441-2448.

Ko, S. H., Lenkowski, P. W., Lee, H. C., Mounsey, J. P. and Patel, M. K. Modulation of Na(v)1.5 by beta1-- and beta3-subunit co-expression in mammalian cells. *Pflugers Arch.* 2005,449(4): 403-412.

Kolsch, V., Charest, P. G. and Firtel, R. A. The regulation of cell motility and chemotaxis by phospholipid signaling. *J Cell Sci.* 2008,121(Pt 5): 551-559.

Korner, A., Mudduluru, G., Manegold, C. and Allgayer, H. Enzastaurin inhibits invasion and metastasis in lung cancer by diverse molecules. *Br J Cancer.* 2010,103(6): 802-811.

Kornfeld, S., Goupille, C., Vibet, S., Chevalier, S., Pinet, A., Lebeau, J., Tranquart, F., Bougnoux, P., Martel, E., Maurin, A., Richard, S., Champeroux, P. and Maheo, K. Reducing endothelial NOS activation and interstitial fluid pressure with n-3 PUFA offset tumor chemoresistance. *Carcinogenesis.* 2012,33(2): 260-267.

Kosla, J., Paňková, D., Plachý, J., Tolde, O., Bicanová, K., Dvořák, M., Rösel, D. and Brábek, J. Metastasis of aggressive amoeboid sarcoma cells is dependent on Rho/ROCK/MLC signaling. *Cell Commun Signal.* 2013,11(51).

Krugmann, S., Jordens, I., Gevaert, K., Driessens, M., Vandekerckhove, J. and Hall, A. Cdc42 induces filopodia by promoting the formation of an IRSp53:Mena complex. *Curr Biol.* 2001,11(21).

Kuhn, S. and Geyer, M. Formins as effector proteins of Rho GTPases. *Small GTPases.* 2014,5: e29513.

Kurisaki, A., Kose, S., Yoneda, Y., Heldin, C. H. and Moustakas, A. Transforming growth factor-beta induces nuclear import of Smad3 in an importin-beta1 and Ran-dependent manner. *Mol Biol Cell.* 2001,12(4): 1079-1091.

Ladoux, B. and Nicolas, A. Physically based principles of cell adhesion mechanosensitivity in tissues. *Reports on Progress in Physics.* 2012,75(11): 116601.

Laedermann, C. J., Syam, N., Pertin, M., Decosterd, I. and Abriel, H. beta1- and beta3- voltage-gated sodium channel subunits modulate cell surface expression and glycosylation of Nav1.7 in HEK293 cells. *Front Cell Neurosci.* 2013,7: 137.

Lammermann, T. and Sixt, M. Mechanical modes of 'amoeboid' cell migration. *Curr Opin Cell Biol.* 2009,21(5): 636-644.

Laniado, M. E., Lalani, E. N., Fraser, S. P., Grimes, J. A., Bhangal, G., Djamgoz, M. B. and Abel, P. D. Expression and functional analysis of voltage-activated Na+ channels in human prostate cancer cell lines and their contribution to invasion in vitro. *Am J Pathol.* 1997,150(4): 1213-1221.

Larsson, S. C., Kumlin, M., Ingelman-Sundberg, M. and Wolk, A. Dietary long-chain n-3 fatty acids for the prevention of cancer: a review of potential mechanisms. *Am J Clin Nutr.* 2004,79(6): 935-945.

Laser-Azogui, A., Diamant-Levi, T., Israeli, S., Roytman, Y. and Tsarfaty, I. Met-induced membrane blebbing leads to amoeboid cell motility and invasion. *Oncogene.* 2014,33(14): 1788-1798.

Laukaitis, C. M., Webb, D. J., Donais, K. and Horwitz, A. F. Differential dynamics of alpha 5 Integrin, Paxillin, and alpha-actinin during formation and disassembly of adhesions in migrating cells. *J Cell Biol.* 2001,153(7): 1427-1440.

Lavelin, I., Wolfenson, H., Patla, I., Henis, Y. I., Medalia, O., Volberg, T., Livne, A., Kam, Z. and Geiger, B. Differential effect of actomyosin relaxation on the dynamic properties of focal adhesion proteins. *PLoS One.* 2013,8(9): e73549.

Lazarides, E. and Burridge, K. Alpha-actinin: immunofluorescent localization of a muscle structural protein in nonmuscle cells. *Cell.* 1975,6(3): 289-298.

Lazennec, G., Canaple, L., Saugy, D. and Wahli, W. Activation of peroxisome proliferator-activated receptors (PPARs) by their ligands and protein kinase A activators. *Mol Endocrinol.* 2000,14(12): 1962-1975.

Le Clainche, C. and Carlier, M. F. Regulation of actin assembly associated with protrusion and adhesion in cell migration. *Physiol Rev.* 2008,88(2): 489-513.

Leabu, M., Uniyal, S., Xie, J., Xu, Y. Q., Vladau, C., Morris, V. L. and Chan, B. M. Integrin alpha2beta1 modulates EGF stimulation of Rho GTPase-dependent morphological changes in adherent human rhabdomyosarcoma RD cells. *J Cell Physiol.* 2005,202(3): 754-766.

Lebensohn, A. M. and Kirschner, M. W. Activation of the WAVE complex by coincident signals controls actin assembly. *Mol Cell.* 2009,36(3): 512-524.

Lebrand, C., Dent, E. W., Strasser, G. A., Lanier, L. M., Krause, M., Svitkina, T. M., Borisy, G. G. and Gertler, F. B. Critical role of Ena/VASP proteins for filopodia formation in neurons and in function downstream of netrin-1. *Neuron.* 2004,42(1): 37-49.

Lees, J. G., Bach, C. T., Bradbury, P., Paul, A., Gunning, P. W. and O'Neill, G. M. The actin-associating protein Tm5NM1 blocks mesenchymal motility without transition to amoeboid motility. *Oncogene.* 2011,30(10): 1241-1251.

Levental, K. R., Yu, H., Kass, L., Lakins, J. N., Egeblad, M., Erler, J. T., Fong, S. F., Csiszar, K., Giaccia, A., Weninger, W., Yamauchi, M., Gasser, D. L. and Weaver, V. M. Matrix crosslinking forces tumor progression by enhancing integrin signaling. *Cell.* 2009,139(5): 891-906.

Li, A., Dawson, J. C., Forero-Vargas, M., Spence, H. J., Yu, X., Konig, I., Anderson, K. and Machesky, L. M. The actin-bundling protein fascin stabilizes actin in invadopodia and potentiates protrusive invasion. *Curr Biol.* 2010,20(4): 339-345.

Li, A., Morton, J. P., Ma, Y., Karim, S. A., Zhou, Y., Faller, W. J., Woodham, E. F., Morris, H. T., Stevenson, R. P., Juin, A., Jamieson, N. B., MacKay, C. J., Carter, C. R., Leung, H. Y., Yamashiro, S., Blyth, K., Sansom, O. J. and Machesky, L. M. Fascin is regulated by slug, promotes progression of pancreatic cancer in mice, and is associated with patient outcomes. *Gastroenterology.* 2014,146(5): 1386-1396 e1381-1317.

Lim, J. and Thiery, J. P. Epithelial-mesenchymal transitions: insights from development. *Development.* 2012,139(19): 3471-3486.

Lin, D., Edwards, A. S., Fawcett, J. P., Mbamalu, G., Scott, J. D. and Pawson, T. A mammalian PAR-3-PAR-6 complex implicated in Cdc42/Rac1 and aPKC signalling and cell polarity. *Nat Cell Biol.* 2000,2(8): 540-547.

Linder, S. Invadosomes at a glance. *J Cell Sci.* 2009,122(Pt 17): 3009-3013.

Lindsey, S. and Langhans, S. A. Crosstalk of Oncogenic Signaling Pathways during Epithelial-Mesenchymal Transition. *Front Oncol.* 2014,4: 358.

Liu, Q., Jin, Y., Wang, K., Meng, X. X., Yang, Y., Yang, Z., Zhao, Y. S., Zhao, M. Y. and Zhang, J. H. Study of the residues involved in the binding of beta1 to beta3 subunits in the sodium channel. *C R Biol.* 2014,337(2): 73-77.

Liu, Y. J., Le Berre, M., Lautenschlaeger, F., Maiuri, P., Callan-Jones, A., Heuze, M., Takaki, T., Voituriez, R. and Piel, M. Confinement and low adhesion induce fast amoeboid migration of slow mesenchymal cells. *Cell.* 2015,160(4): 659-672.

Lopez-Santiago, L. F., Meadows, L. S., Ernst, S. J., Chen, C., Malhotra, J. D., McEwen, D. P., Speelman, A., Noebels, J. L., Maier, S. K., Lopatin, A. N. and Isom, L. L. Sodium channel Scn1b null mice exhibit prolonged QT and RR intervals. *J Mol Cell Cardiol.* 2007,43(5): 636-647.

Lu, I. F., Hasio, A. C., Hu, M. C., Yang, F. M. and Su, H. M. Docosahexaenoic acid induces proteasome-dependent degradation of estrogen receptor alpha and inhibits the downstream signaling target in MCF-7 breast cancer cells. *J Nutr Biochem.* 2010,21(6): 512-517.

Lucato, C. M., Halls, M. L., Ooms, L. M., Liu, H. J., Mitchell, C. A., Whisstock, J. C. and Ellisdon, A. M. The Phosphatidylinositol (3,4,5)-Trisphosphate-dependent Rac Exchanger 1.Ras-related C3 Botulinum Toxin Substrate 1 (P-Rex1.Rac1) Complex Reveals the Basis of Rac1 Activation in Breast Cancer Cells. *J Biol Chem.* 2015,290(34): 20827-20840.

Machacek, M., Hodgson, L., Welch, C., Elliott, H., Pertz, O., Nalbant, P., Abell, A., Johnson, G. L., Hahn, K. M. and Danuser, G. Coordination of Rho GTPase activities during cell protrusion. *Nature.* 2009,461(7260): 99-103.

Mader, C. C., Oser, M., Magalhaes, M. A., Bravo-Cordero, J. J., Condeelis, J., Koleske, A. J. and Gil-Henn, H. An EGFR-Src-Arg-cortactin pathway mediates functional maturation of invadopodia and breast cancer cell invasion. *Cancer Res.* 2011,71(5): 1730-1741.

Magalhaes, M. A., Larson, D. R., Mader, C. C., Bravo-Cordero, J. J., Gil-Henn, H., Oser, M., Chen, X., Koleske, A. J. and Condeelis, J. Cortactin phosphorylation regulates cell invasion through a pH-dependent pathway. *J Cell Biol.* 2011,195(5): 903-920.

Maillard, V., Bougnoux, P., Ferrari, P., Jourdan, M. L., Pinault, M., Lavillonniere, F., Body, G., Le Floch, O. and Chajes, V. N-3 and N-6 fatty acids in breast adipose tissue and relative risk of breast cancer in a case-control study in Tours, France. *Int J Cancer.* 2002,98(1): 78-83.

Maillard, V., Hoinard, C., Arab, K., Jourdan, M. L., Bougnoux, P. and Chajes, V. Dietary beta-carotene inhibits mammary carcinogenesis in rats depending on dietary alpha-linolenic acid content. *Br J Nutr.* 2006,96(1): 18-21.

Malhotra, J. D., Kazen-Gillespie, K., Hortsch, M. and Isom, L. L. Sodium channel beta subunits mediate homophilic cell adhesion and recruit ankyrin to points of cell-cell contact. *J Biol Chem.* 2000,275(15): 11383-11388.

Malhotra, J. D., Koopmann, M. C., Kazen-Gillespie, K. A., Fettman, N., Hortsch, M. and Isom, L. L. Structural requirements for interaction of sodium channel beta 1 subunits with ankyrin. *J Biol Chem.* 2002,277(29): 26681-26688.

Malhotra, J. D., Thyagarajan, V., Chen, C. and Isom, L. L. Tyrosine-phosphorylated and nonphosphorylated sodium channel beta1 subunits are differentially localized in cardiac myocytes. *J Biol Chem.* 2004,279(39): 40748-40754.

Mandal, C. C., Ghosh-Choudhury, T., Yoneda, T., Choudhury, G. G. and Ghosh-Choudhury, N. Fish oil prevents breast cancer cell metastasis to bone. *Biochem Biophys Res Commun.* 2010,402(4): 602-607.

Mangelsdorf, D. J., Umesono, K., Kliewer, S. A., Borgmeyer, U., Ong, E. S. and Evans, R. M. A direct repeat in the cellular retinol-binding protein type II gene confers differential regulation by RXR and RAR. *Cell.* 1991,66(3): 555-561.

Manser, E., Leung, T., Salihuddin, H., Zhao, Z. S. and Lim, L. A brain serine/threonine protein kinase activated by Cdc42 and Rac1. *Nature.* 1994,367(6458): 40-46.

Manser, E., Loo, T. H., Koh, C. G., Zhao, Z. S., Chen, X. Q., Tan, L., Tan, I., Leung, T. and Lim, L. PAK kinases are directly coupled to the PIX family of nucleotide exchange factors. *Mol Cell.* 1998,1(2): 183-192.

Margheri, F., Luciani, C., Taddei, M. L., Giannoni, E., Laurenzana, A., Biagioni, A., Chillà, A., Chiarugi, P., Fibbi, G. and Del Rosso, M. The receptor for urokinase-plasminogen activator (uPAR) controls plasticity of cancer cell movement in mesenchymal and amoeboid migration style. *Oncotarget.* 2014,5(6): 1538-1553.

Maschietto, M., Girardi, S., Dal Maschio, M., Scorzeto, M. and Vassanelli, S. Sodium channel beta2 subunit promotes filopodia-like processes and expansion of the dendritic tree in developing rat hippocampal neurons. *Front Cell Neurosci.* 2013,7: 2.

McCabe, A. J., Wallace, J. M., Gilmore, W. S., McGlynn, H. and Strain, S. J. Docosahexaenoic acid reduces in vitro invasion of renal cell carcinoma by elevated levels of tissue inhibitor of metalloproteinase-1. *J Nutr Biochem.* 2005,16(1): 17-22.

Meadows, L. S., Malhotra, J., Loukas, A., Thyagarajan, V., Kazen-Gillespie, K. A., Koopman, M. C., Kriegler, S., Isom, L. L. and Ragsdale, D. S. Functional and biochemical analysis of a sodium channel beta1 subunit mutation responsible for generalized epilepsy with febrile seizures plus type 1. *J Neurosci.* 2002,22(24): 10699-10709.

Medeiros-Domingo, A., Kaku, T., Tester, D. J., Iturralde-Torres, P., Itty, A., Ye, B., Valdivia, C., Ueda, K., Canizales-Quinteros, S., Tusie-Luna, M. T., Makielski, J. C. and Ackerman, M. J. SCN4B-encoded sodium channel beta4 subunit in congenital long-QT syndrome. *Circulation.* 2007,116(2): 134-142.

Mellor, H. The role of formins in filopodia formation. *Biochim Biophys Acta.* 2010,1803(2): 191-200.

Mercier, A., Clement, R., Harnois, T., Bourmeyster, N., Faivre, J. F., Findlay, I., Chahine, M., Bois, P. and Chatelier, A. The beta1-subunit of Na(v)1.5 cardiac sodium channel is required for a dominant negative effect through alpha-alpha interaction. *PLoS One.* 2012,7(11): e48690.

Merrick, E. C., Kalmar, C. L., Snyder, S. L., Cusdin, F. S., Yu, E. J., Sando, J. J., Isakson, B. E., Jackson, A. P. and Patel, M. K. The importance of serine 161 in the sodium channel beta3 subunit for modulation of Na(V)1.2 gating. *Pflugers Arch.* 2010,460(4): 743-753.

Mishra, S., Undrovinas, N. A., Maltsev, V. A., Reznikov, V., Sabbah, H. N. and Undrovinas, A. Post-transcriptional silencing of SCN1B and SCN2B genes modulates late sodium current in cardiac myocytes from normal dogs and dogs with chronic heart failure. *Am J Physiol Heart Circ Physiol.* 2011,301(4): H1596-1605.

Miyazaki, H., Oyama, F., Wong, H. K., Kaneko, K., Sakurai, T., Tamaoka, A. and Nukina, N. BACE1 modulates filopodia-like protrusions induced by sodium channel beta4 subunit. *Biochem Biophys Res Commun.* 2007,361(1): 43-48.

Moazzam, M., Ye, L., Sun, P.-H., Kynaston, H. and Jiang, W. G. Knockdown of WAVE3 impairs HGF induced migration and invasion of prostate cancer cells. *Cancer Cell International.* 2015,15(1).

Mogilner, A. and Rubinstein, B. The physics of filopodial protrusion. *Biophys J.* 2005,89(2): 782-795.

Moran, O. and Conti, F. Skeletal muscle sodium channel is affected by an epileptogenic beta1 subunit mutation. *Biochem Biophys Res Commun.* 2001,282(1): 55-59.

Morgan, K., Stevens, E. B., Shah, B., Cox, P. J., Dixon, A. K., Lee, K., Pinnock, R. D., Hughes, J., Richardson, P. J., Mizuguchi, K. and Jackson, A. P. beta 3: an additional auxiliary subunit of the voltage-sensitive sodium channel that modulates channel gating with distinct kinetics. *Proc Natl Acad Sci U S A.* 2000,97(5): 2308-2313.

Morimura, S., Suzuki, K. and Takahashi, K. BetaPIX and GIT1 regulate HGF-induced lamellipodia formation and WAVE2 transport. *Biochem Biophys Res Commun.* 2009,382(3): 614-619.

Murillo, M. M., del Castillo, G., Sanchez, A., Fernandez, M. and Fabregat, I. Involvement of EGF receptor and c-Src in the survival signals induced by TGF-beta1 in hepatocytes. *Oncogene.* 2005,24(28): 4580-4587.

Nahm, J. H., Kim, H., Lee, H., Cho, J. Y., Choi, Y. R., Yoon, Y. S., Han, H. S. and Park, Y. N. Transforming acidic coiled-coil-containing protein 3 (TACC3) overexpression in hepatocellular carcinomas is associated with "stemness" and epithelial-mesenchymal transition-related marker expression and a poor prognosis. *Tumour Biol.* 2015.

Nalbant, P., Hodgson, L., Kraynov, V., Toutchkine, A. and Hahn, K. M. Activation of endogenous Cdc42 visualized in living cells. *Science.* 2004,305(5690): 1615-1619.

Nelson, M., Millican-Slater, R., Forrest, L. C. and Brackenbury, W. J. The sodium channel beta1 subunit mediates outgrowth of neurite-like processes on breast cancer cells and promotes tumour growth and metastasis. *Int J Cancer.* 2014,135(10): 2338-2351.

Niho, N., Takahashi, M., Kitamura, T., Shoji, Y., Itoh, M., Noda, T., Sugimura, T. and Wakabayashi, K. Concomitant suppression of hyperlipidemia and intestinal polyp formation in Apc-deficient mice by peroxisome proliferator-activated receptor ligands. *Cancer Res.* 2003,63(18): 6090-6095.

Nobes, C. D. and Hall, A. Rho, rac, and cdc42 GTPases regulate the assembly of multimolecular focal complexes associated with actin stress fibers, lamellipodia, and filopodia. *Cell.* 1995,81(1).

Nobes, C. D. and Hall, A. Rho GTPases control polarity, protrusion, and adhesion during cell movement. *J Cell Biol.* 1999,144(6): 1235-1244.

Noda, M., Suzuki, H., Numa, S. and Stuhmer, W. A single point mutation confers tetrodotoxin and saxitoxin insensitivity on the sodium channel II. *FEBS Lett.* 1989,259(1): 213-216.

Nurnberg, A., Kitzing, T. and Grosse, R. Nucleating actin for invasion. *Nat Rev Cancer.* 2011,11(3): 177-187.

O'Connor, K. and Chen, M. Dynamic functions of RhoA in tumor cell migration and invasion. *Small GTPases.* 2014,4(3): 141-147.

O'Malley, H. A. and Isom, L. L. Sodium channel beta subunits: emerging targets in channelopathies. *Annu Rev Physiol.* 2015,77: 481-504.

O'Malley, H. A., Shreiner, A. B., Chen, G. H., Huffnagle, G. B. and Isom, L. L. Loss of Na+ channel beta2 subunits is neuroprotective in a mouse model of multiple sclerosis. *Mol Cell Neurosci.* 2009,40(2): 143-155.

Omran, O. M. and Al Sheeha, M. Cytoskeletal Focal Adhesion Proteins Fascin-1 and Paxillin Are Predictors of Malignant Progression and Poor Prognosis in Human Breast Cancer. *J Environ Pathol Toxicol Oncol.* 2015,34(3): 201-212.

Orgaz, J. L., Pandya, P., Dalmeida, R., Karagiannis, P., Sanchez-Laorden, B., Viros, A., Albrengues, J., Nestle, F. O., Ridley, A. J., Gaggioli, C., Marais, R., Karagiannis, S. N. and Sanz-Moreno, V. Diverse matrix metalloproteinase functions regulate cancer amoeboid migration. *Nat Commun.* 2014,5: 4255.

Oser, M., Yamaguchi, H., Mader, C. C., Bravo-Cordero, J. J., Arias, M., Chen, X., Desmarais, V., van Rheenen, J., Koleske, A. J. and Condeelis, J. Cortactin regulates cofilin and N-WASp

activities to control the stages of invadopodium assembly and maturation. *J Cell Biol.* 2009,186(4): 571-587.

Ota, D., Kanayama, M., Matsui, Y., Ito, K., Maeda, N., Kutomi, G., Hirata, K., Torigoe, T., Sato, N., Takaoka, A., Chambers, A. F., Morimoto, J. and Uede, T. Tumor-alpha9beta1 integrin-mediated signaling induces breast cancer growth and lymphatic metastasis via the recruitment of cancer-associated fibroblasts. *J Mol Med (Berl).* 2014,92(12): 1271-1281.

Oyama, F., Miyazaki, H., Sakamoto, N., Becquet, C., Machida, Y., Kaneko, K., Uchikawa, C., Suzuki, T., Kurosawa, M., Ikeda, T., Tamaoka, A., Sakurai, T. and Nukina, N. Sodium channel beta4 subunit: down-regulation and possible involvement in neuritic degeneration in Huntington's disease transgenic mice. *J Neurochem.* 2006,98(2): 518-529.

Palamidessi, A., Frittoli, E., Garre, M., Faretta, M., Mione, M., Testa, I., Diaspro, A., Lanzetti, L., Scita, G. and Di Fiore, P. P. Endocytic trafficking of Rac is required for the spatial restriction of signaling in cell migration. *Cell.* 2008,134(1): 135-147.

Parri, M. and Chiarugi, P. Rac and Rho GTPases in cancer cell motility control. *Cell Commun Signal.* 2010,8: 23.

Parsons, J. T., Horwitz, A. R. and Schwartz, M. A. Cell adhesion: integrating cytoskeletal dynamics and cellular tension. *Nat Rev Mol Cell Biol.* 2010,11(9): 633-643.

Pasapera, A. M., Plotnikov, S. V., Fischer, R. S., Case, L. B., Egelhoff, T. T. and Waterman, C. M. Rac1-dependent phosphorylation and focal adhesion recruitment of myosin IIA regulates migration and mechanosensing. *Curr Biol.* 2015,25(2): 175-186.

Pasca di Magliano, M. and Hebrok, M. Hedgehog signalling in cancer formation and maintenance. *Nat Rev Cancer.* 2003,3(12): 903-911.

Patel, F. and Brackenbury, W. J. Dual roles of voltage-gated sodium channels in development and cancer. *Int J Dev Biol.* 2015.

Peinado, H., Quintanilla, M. and Cano, A. Transforming growth factor beta-1 induces snail transcription factor in epithelial cell lines: mechanisms for epithelial mesenchymal transitions. *J Biol Chem.* 2003,278(23): 21113-21123.

Pellegrin, S. and Mellor, H. The Rho family GTPase Rif induces filopodia through mDia2. *Curr Biol.* 2005,15(2): 129-133.

Peters, J. M., Shah, Y. M. and Gonzalez, F. J. The role of peroxisome proliferator-activated receptors in carcinogenesis and chemoprevention. *Nat Rev Cancer.* 2012,12(3): 181-195.

Petrie, R. J. and Yamada, K. M. At the leading edge of three-dimensional cell migration. *J Cell Sci.* 2012,125(Pt 24): 5917-5926.

Piedra, J., Miravet, S., Castano, J., Palmer, H. G., Heisterkamp, N., Garcia de Herreros, A. and Dunach, M. p120 Catenin-Associated Fer and Fyn Tyrosine Kinases Regulate -Catenin Tyr-142 Phosphorylation and -Catenin- -Catenin Interaction. *Molecular and Cellular Biology.* 2003,23(7): 2287-2297.

Poincloux, R., Collin, O., Lizarraga, F., Romao, M., Debray, M., Piel, M. and Chavrier, P. Contractility of the cell rear drives invasion of breast tumor cells in 3D Matrigel. *Proc Natl Acad Sci U S A.* 2011,108(5): 1943-1948.

Pollard, T. D., Blanchoin, L. and Mullins, R. D. Molecular mechanisms controlling actin filament dynamics in nonmuscle cells. *Annu Rev Biophys Biomol Struct.* 2000,29: 545-576.

Pollard, T. D. and Borisy, G. G. Cellular motility driven by assembly and disassembly of actin filaments. *Cell.* 2003,112(4): 453-465.

Ponti, A., Machacek, M., Gupton, S. L., Waterman-Storer, C. M. and Danuser, G. Two distinct actin networks drive the protrusion of migrating cells. *Science.* 2004,305(5691): 1782-1786.

Provenzano, P. P., Inman, D. R., Eliceiri, K. W. and Keely, P. J. Matrix density-induced mechanoregulation of breast cell phenotype, signaling and gene expression through a FAK-ERK linkage. *Oncogene.* 2009,28(49): 4326-4343.

Provenzano, P. P., Inman, D. R., Eliceiri, K. W., Knittel, J. G., Yan, L., Rueden, C. T., White, J. G. and Keely, P. J. Collagen density promotes mammary tumor initiation and progression. *BMC Med.* 2008,6: 11.

Qiao, X., Sun, G., Clare, J. J., Werkman, T. R. and Wadman, W. J. Properties of human brain sodium channel alpha-subunits expressed in HEK293 cells and their modulation by carbamazepine, phenytoin and lamotrigine. *Br J Pharmacol.* 2014,171(4): 1054-1067.

Qualtrough, D., Singh, K., Banu, N., Paraskeva, C. and Pignatelli, M. The actin-bundling protein fascin is overexpressed in colorectal adenomas and promotes motility in adenoma cells in vitro. *Br J Cancer.* 2009,101(7): 1124-1129.

Ratcliffe, C. F., Qu, Y., McCormick, K. A., Tibbs, V. C., Dixon, J. E., Scheuer, T. and Catterall, W. A. A sodium channel signaling complex: modulation by associated receptor protein tyrosine phosphatase beta. *Nat Neurosci.* 2000,3(5): 437-444.

Remme, C. A., Scicluna, B. P., Verkerk, A. O., Amin, A. S., van Brunschot, S., Beekman, L., Deneer, V. H., Chevalier, C., Oyama, F., Miyazaki, H., Nukina, N., Wilders, R., Escande, D., Houlgatte, R., Wilde, A. A., Tan, H. L., Veldkamp, M. W., de Bakker, J. M. and Bezzina, C. R. Genetically determined differences in sodium current characteristics modulate conduction disease severity in mice with cardiac sodium channelopathy. *Circ Res.* 2009,104(11): 1283-1292.

Ren, X. D., Kiosses, W. B., Sieg, D. J., Otey, C. A., Schlaepfer, D. D. and Schwartz, M. A. Focal adhesion kinase suppresses Rho activity to promote focal adhesion turnover. *J Cell Sci.* 2000,113 (Pt 20): 3673-3678.

Reymond, N., Im, J. H., Garg, R., Vega, F. M., Borda d'Agua, B., Riou, P., Cox, S., Valderrama, F., Muschel, R. J. and Ridley, A. J. Cdc42 promotes transendothelial migration of cancer cells through beta1 integrin. *J Cell Biol.* 2012,199(4): 653-668.

Ridley, A. J. Rho GTPases and actin dynamics in membrane protrusions and vesicle trafficking. *Trends Cell Biol.* 2006,16(10): 522-529.

Ridley, A. J. Life at the leading edge. *Cell.* 2011,145(7): 1012-1022.

Ridley, A. J., Schwartz, M. A., Burridge, K., Firtel, R. A., Ginsberg, M. H., Borisy, G., Parsons, J. T. and Horwitz, A. R. Cell migration: integrating signals from front to back. *Science.* 2003,302(5851): 1704-1709.

Riuro, H., Beltran-Alvarez, P., Tarradas, A., Selga, E., Campuzano, O., Verges, M., Pagans, S., Iglesias, A., Brugada, J., Brugada, P., Vazquez, F. M., Perez, G. J., Scornik, F. S. and Brugada, R. A missense mutation in the sodium channel beta2 subunit reveals SCN2B as a new candidate gene for Brugada syndrome. *Hum Mutat.* 2013,34(7): 961-966.

Rivera, G. M., Vasilescu, D., Papayannopoulos, V., Lim, W. A. and Mayer, B. J. A reciprocal interdependence between Nck and PI(4,5)P(2) promotes localized N-WASp-mediated actin polymerization in living cells. *Mol Cell.* 2009,36(3): 525-535.

Robertson, A. M., Bird, C. C., Waddell, A. W. and Currie, A. R. Morphological aspects of glucocorticoid-induced cell death in human lymphoblastoid cells. *J Pathol.* 1978,126(3): 181-187.

Rocken, M. Early tumor dissemination, but late metastasis: insights into tumor dormancy. *J Clin Invest.* 2010,120(6): 1800-1803.

Roger, S., Besson, P. and Le Guennec, J. Y. Involvement of a novel fast inward sodium current in the invasion capacity of a breast cancer cell line. *Biochim Biophys Acta.* 2003,1616(2): 107-111.

Roger, S., Gillet, L., Le Guennec, J. Y. and Besson, P. Voltage-gated sodium channels and cancer: is excitability their primary role? *Front Pharmacol.* 2015,6: 152.

Roger, S. and Pelegrin, P. P2X7 receptor antagonism in the treatment of cancers. *Expert Opin Investig Drugs.* 2011,20(7): 875-880.

Roger, S., Rollin, J., Barascu, A., Besson, P., Raynal, P. I., Iochmann, S., Lei, M., Bougnoux, P., Gruel, Y. and Le Guennec, J. Y. Voltage-gated sodium channels potentiate the invasive capacities of human non-small-cell lung cancer cell lines. *Int J Biochem Cell Biol.* 2007,39(4): 774-786.

Romero, S., Le Clainche, C., Didry, D., Egile, C., Pantaloni, D. and Carlier, M. F. Formin is a processive motor that requires profilin to accelerate actin assembly and associated ATP hydrolysis. *Cell.* 2004,119(3): 419-429.

Ruoslahti, E. RGD and other recognition sequences for integrins. *Annu Rev Cell Dev Biol.* 1996,12: 697-715.

Ruprecht, V., Wieser, S., Callan-Jones, A., Smutny, M., Morita, H., Sako, K., Barone, V., Ritsch-Marte, M., Sixt, M., Voituriez, R. and Heisenberg, C. P. Cortical contractility triggers a stochastic switch to fast amoeboid cell motility. *Cell.* 2015,160(4): 673-685.

Sahai, E. and Marshall, C. J. Differing modes of tumour cell invasion have distinct requirements for Rho/ROCK signalling and extracellular proteolysis. *Nat Cell Biol.* 2003,5(8): 711-719.

Sakurai-Yageta, M., Recchi, C., Le Dez, G., Sibarita, J. B., Daviet, L., Camonis, J., D'Souza-Schorey, C. and Chavrier, P. The interaction of IQGAP1 with the exocyst complex is required for tumor cell invasion downstream of Cdc42 and RhoA. *J Cell Biol.* 2008,181(6): 985-998.

Sanz-Moreno, V., Gadea, G., Ahn, J., Paterson, H., Marra, P., Pinner, S., Sahai, E. and Marshall, C. J. Rac activation and inactivation control plasticity of tumor cell movement. *Cell.* 2008,135(3): 510-523.

Schaefer, A., Reinhard, N. R. and Hordijk, P. L. Toward understanding RhoGTPase specificity: structure, function and local activation. *Small GTPases.* 2014,5(2): 6.

Schirenbeck, A., Bretschneider, T., Arasada, R., Schleicher, M. and Faix, J. The Diaphanous-related formin dDia2 is required for the formation and maintenance of filopodia. *Nat Cell Biol.* 2005,7(6): 619-625.

Schlegel, N. C., von Planta, A., Widmer, D. S., Dummer, R. and Christofori, G. PI3K signalling is required for a TGFbeta-induced epithelial-mesenchymal-like transition (EMT-like) in human melanoma cells. *Exp Dermatol.* 2015,24(1): 22-28.

Schoumacher, M., Goldman, R. D., Louvard, D. and Vignjevic, D. M. Actin, microtubules, and vimentin intermediate filaments cooperate for elongation of invadopodia. *J Cell Biol.* 2010,189(3): 541-556.

Schoumacher, M., Louvard, D. and Vignjevic, D. Cytoskeleton networks in basement membrane transmigration. *Eur J Cell Biol.* 2011,90(2-3): 93-99.

Selhuber-Unkel, C., Erdmann, T., Lopez-Garcia, M., Kessler, H., Schwarz, U. S. and Spatz, J. P. Cell adhesion strength is controlled by intermolecular spacing of adhesion receptors. *Biophys J.* 2010,98(4): 543-551.

Sells, M. A., Knaus, U. G., Bagrodia, S., Ambrose, D. M., Bokoch, G. M. and Chernoff, J. Human p21-activated kinase (Pak1) regulates actin organization in mammalian cells. *Curr Biol.* 1997,7(3): 202-210.

Shao, H., Li, S., Watkins, S. C. and Wells, A. alpha-Actinin-4 is required for amoeboid-type invasiveness of melanoma cells. *J Biol Chem.* 2014,289(47): 32717-32728.

Simopoulos, A. P. Omega-3 fatty acids and antioxidants in edible wild plants. *Biol Res.* 2004,37(2): 263-277.

Sjoblom, T., Jones, S., Wood, L. D., Parsons, D. W., Lin, J., Barber, T. D., Mandelker, D., Leary, R. J., Ptak, J., Silliman, N., Szabo, S., Buckhaults, P., Farrell, C., Meeh, P., Markowitz, S. D., Willis, J., Dawson, D., Willson, J. K., Gazdar, A. F., Hartigan, J., Wu, L., Liu, C., Parmigiani, G., Park, B. H., Bachman, K. E., Papadopoulos, N., Vogelstein, B., Kinzler, K. W. and Velculescu, V. E. The consensus coding sequences of human breast and colorectal cancers. *Science.* 2006,314(5797): 268-274.

Small, J. V. Dicing with dogma: de-branching the lamellipodium. *Trends Cell Biol.* 2010,20(11): 628-633.

Small, J. V., Stradal, T., Vignal, E. and Rottner, K. The lamellipodium: where motility begins. *Trends Cell Biol.* 2002,12(3): 112-120.

Sosa, M. S., Lopez-Haber, C., Yang, C., Wang, H., Lemmon, M. A., Busillo, J. M., Luo, J., Benovic, J. L., Klein-Szanto, A., Yagi, H., Gutkind, J. S., Parsons, R. E. and Kazanietz, M. G.

Identification of the Rac-GEF P-Rex1 as an essential mediator of ErbB signaling in breast cancer. *Mol Cell.* 2010,40(6): 877-892.

Spampanato, J., Kearney, J. A., de Haan, G., McEwen, D. P., Escayg, A., Aradi, I., MacDonald, B. T., Levin, S. I., Soltesz, I., Benna, P., Montalenti, E., Isom, L. L., Goldin, A. L. and Meisler, M. H. A novel epilepsy mutation in the sodium channel SCN1A identifies a cytoplasmic domain for beta subunit interaction. *J Neurosci.* 2004,24(44): 10022-10034.

Spratley, S. J., Bastea, L. I., Doppler, H., Mizuno, K. and Storz, P. Protein kinase D regulates cofilin activity through p21-activated kinase 4. *J Biol Chem.* 2011,286(39): 34254-34261.

Srinivasan, J., Schachner, M. and Catterall, W. A. Interaction of voltage-gated sodium channels with the extracellular matrix molecules tenascin-C and tenascin-R. *Proc Natl Acad Sci U S A.* 1998,95(26): 15753-15757.

Stern, C. D. Evolution of the mechanisms that establish the embryonic axes. *Curr Opin Genet Dev.* 2006,16(4): 413-418.

Stradal, T. E. and Scita, G. Protein complexes regulating Arp2/3-mediated actin assembly. *Curr Opin Cell Biol.* 2006,18(1): 4-10.

Sui, X., Zhu, J., Tang, H., Wang, C., Zhou, J., Han, W., Wang, X., Fang, Y., Xu, Y., Li, D., Chen, R., Ma, J., Jing, Z., Gu, X., Pan, H. and He, C. p53 controls colorectal cancer cell invasion by inhibiting the NF-κB-mediated activation of Fascin. *Oncotarget.* 2015,6(26): 22869-22879.

Sun, X. H., Flynn, D. C., Castranova, V., Millecchia, L. L., Beardsley, A. R. and Liu, J. Identification of a novel domain at the N terminus of caveolin-1 that controls rear polarization of the protein and caveolae formation. *J Biol Chem.* 2007,282(10): 7232-7241.

Svitkina, T. M., Bulanova, E. A., Chaga, O. Y., Vignjevic, D. M., Kojima, S., Vasiliev, J. M. and Borisy, G. G. Mechanism of filopodia initiation by reorganization of a dendritic network. *J Cell Biol.* 2003,160(3): 409-421.

Symons, M. and Rusk, N. Control of Vesicular Trafficking by Rho GTPases. *Current Biology.* 2003,13(10): R409-R418.

Tai, Y. L., Chu, P. Y., Lai, I. R., Wang, M. Y., Tseng, H. Y., Guan, J. L., Liou, J. Y. and Shen, T. L. An EGFR/Src-dependent beta4 integrin/FAK complex contributes to malignancy of breast cancer. *Sci Rep.* 2015,5: 16408.

Takahashi, K. and Suzuki, K. Requirement of kinesin-mediated membrane transport of WAVE2 along microtubules for lamellipodia formation promoted by hepatocyte growth factor. *Exp Cell Res.* 2008,314(11-12): 2313-2322.

Takahashi, K. and Suzuki, K. Membrane transport of WAVE2 and lamellipodia formation require Pak1 that mediates phosphorylation and recruitment of stathmin/Op18 to Pak1-WAVE2-kinesin complex. *Cell Signal.* 2009,21(5): 695-703.

Takai, M., Terai, Y., Kawaguchi, H., Ashihara, K., Fujiwara, S., Tanaka, T., Tsunetoh, S., Tanaka, Y., Sasaki, H., Kanemura, M., Tanabe, A. and Ohmichi, M. The EMT (epithelial-mesenchymal-transition)-related protein expression indicates the metastatic status and prognosis in patients with ovarian cancer. *J Ovarian Res.* 2014,7: 76.

Tammaro, P., Conti, F. and Moran, O. Modulation of sodium current in mammalian cells by an epilepsy-correlated beta 1-subunit mutation. *Biochem Biophys Res Commun.* 2002,291(4): 1095-1101.

Tan, B. H., Pundi, K. N., Van Norstrand, D. W., Valdivia, C. R., Tester, D. J., Medeiros-Domingo, A., Makielski, J. C. and Ackerman, M. J. Sudden infant death syndrome-associated mutations in the sodium channel beta subunits. *Heart Rhythm.* 2010,7(6): 771-778.

Tanaka, T., Kohno, H., Yoshitani, S., Takashima, S., Okumura, A., Murakami, A. and Hosokawa, M. Ligands for peroxisome proliferator-activated receptors alpha and gamma inhibit chemically induced colitis and formation of aberrant crypt foci in rats. *Cancer Res.* 2001,61(6): 2424-2428.

ten Berge, D., Koole, W., Fuerer, C., Fish, M., Eroglu, E. and Nusse, R. Wnt signaling mediates self-organization and axis formation in embryoid bodies. *Cell Stem Cell.* 2008,3(5): 508-518.

ten Klooster, J. P., Jaffer, Z. M., Chernoff, J. and Hordijk, P. L. Targeting and activation of Rac1 are mediated by the exchange factor beta-Pix. *J Cell Biol.* 2006,172(5): 759-769.

Teng, Y., Xu, S., Yue, W., Ma, L., Zhang, L., Zhao, X., Guo, Y., Zhang, C., Gu, M. and Wang, Y. Serological investigation of the clinical significance of fascin in non-small-cell lung cancer. *Lung Cancer.* 2013,82(2): 346-352.

Terlau, H., Heinemann, S. H., Stuhmer, W., Pusch, M., Conti, F., Imoto, K. and Numa, S. Mapping the site of block by tetrodotoxin and saxitoxin of sodium channel II. *FEBS Lett.* 1991,293(1-2): 93-96.

Thuault, S., Tan, E. J., Peinado, H., Cano, A., Heldin, C. H. and Moustakas, A. HMGA2 and Smads co-regulate SNAIL1 expression during induction of epithelial-to-mesenchymal transition. *J Biol Chem.* 2008,283(48): 33437-33446.

Tokuo, H. and Ikebe, M. Myosin X transports Mena/VASP to the tip of filopodia. *Biochem Biophys Res Commun.* 2004,319(1): 214-220.

Tokuo, H., Mabuchi, K. and Ikebe, M. The motor activity of myosin-X promotes actin fiber convergence at the cell periphery to initiate filopodia formation. *J Cell Biol.* 2007,179(2): 229-238.

Tong, J., Potts, J. F., Rochelle, J. M., Seldin, M. F. and Agnew, W. S. A single B1 subunit mapped to mouse chromosome 7 may be a common component of Na channel isoforms from brain, skeletal muscle and heart. *Biochem Biophys Res Commun.* 1993,192(2): 679-685.

Tremble, P., Chiquet-Ehrismann, R. and Werb, Z. The extracellular matrix ligands fibronectin and tenascin collaborate in regulating collagenase gene expression in fibroblasts. *Mol Biol Cell.* 1994,5(4): 439-453.

Tsai, Y. P. and Wu, K. J. Hypoxia-regulated target genes implicated in tumor metastasis. *J Biomed Sci.* 2012,19: 102.

Turbitt, W. J., Black, A. J., Collins, S. D., Meng, H., Xu, H., Washington, S., Aliaga, C., El-Bayoumy, K., Manni, A. and Rogers, C. J. Fish Oil Enhances T Cell Function and Tumor

Infiltration and Is Correlated With a Cancer Prevention Effect in HER-2/neu But Not PyMT Transgenic Mice. *Nutr Cancer.* 2015,67(6): 965-975.

Vaskovicova, K., Szabadosova, E., Cermak, V., Gandalovicova, A., Kasalova, L., Rosel, D. and Brabek, J. PKCalpha promotes the mesenchymal to amoeboid transition and increases cancer cell invasiveness. *BMC Cancer.* 2015,15(1): 326.

Vignjevic, D., Kojima, S., Aratyn, Y., Danciu, O., Svitkina, T. and Borisy, G. G. Role of fascin in filopodial protrusion. *J Cell Biol.* 2006,174(6): 863-875.

Vignjevic, D., Schoumacher, M., Gavert, N., Janssen, K. P., Jih, G., Lae, M., Louvard, D., Ben-Ze'ev, A. and Robine, S. Fascin, a novel target of beta-catenin-TCF signaling, is expressed at the invasive front of human colon cancer. *Cancer Res.* 2007,67(14): 6844-6853.

Vincent, C., Siddiqui, T. A. and Schlichter, L. C. Podosomes in migrating microglia: components and matrix degradation. *J Neuroinflammation.* 2012,9: 190.

Vincent, T., Neve, E. P., Johnson, J. R., Kukalev, A., Rojo, F., Albanell, J., Pietras, K., Virtanen, I., Philipson, L., Leopold, P. L., Crystal, R. G., de Herreros, A. G., Moustakas, A., Pettersson, R. F. and Fuxe, J. A SNAIL1-SMAD3/4 transcriptional repressor complex promotes TGF-beta mediated epithelial-mesenchymal transition. *Nat Cell Biol.* 2009,11(8): 943-950.

Wahli, W. and Michalik, L. PPARs at the crossroads of lipid signaling and inflammation. *Trends Endocrinol Metab.* 2012,23(7): 351-363.

Wallace, R. H., Wang, D. W., Singh, R., Scheffer, I. E., George, A. L. J., Phillips, H. A., Saar, K., Reis, A., Johnson, E. W., Sutherland, G. R., Berkovic, S. F. and Mulley, J. C. Febrile seizures and generalized epilepsy associated with a mutation in the Na+-channel beta1 subunit gene SCN1B. *Nature Genetics.* 1998,19(4): 366-370.

Wang, D. and Dubois, R. N. Prostaglandins and cancer. *Gut.* 2006,55(1): 115-122.

Wang, F. and Lin, S. L. Knockdown of kinesin KIF11 abrogates directed migration in response to epidermal growth factor-mediated chemotaxis. *Biochem Biophys Res Commun.* 2014,452(3): 642-648.

Wannous, R., Bon, E., Gillet, L., Chamouton, J., Weber, G., Brisson, L., Gore, J., Bougnoux, P., Besson, P., Roger, S. and Chevalier, S. Suppression of PPARbeta, and DHA treatment, inhibit NaV1.5 and NHE-1 pro-invasive activities. *Pflugers Arch.* 2015,467(6): 1249-1259.

Wannous, R., Bon, E., Maheo, K., Goupille, C., Chamouton, J., Bougnoux, P., Roger, S., Besson, P. and Chevalier, S. PPARbeta mRNA expression, reduced by n-3 PUFA diet in mammary tumor, controls breast cancer cell growth. *Biochim Biophys Acta.* 2013,1831(11): 1618-1625.

Watanabe, H., Darbar, D., Kaiser, D. W., Jiramongkolchai, K., Chopra, S., Donahue, B. S., Kannankeril, P. J. and Roden, D. M. Mutations in sodium channel beta1- and beta2-subunits associated with atrial fibrillation. *Circ Arrhythm Electrophysiol.* 2009,2(3): 268-275.

Weiger, M. C., Wang, C. C., Krajcovic, M., Melvin, A. T., Rhoden, J. J. and Haugh, J. M. Spontaneous phosphoinositide 3-kinase signaling dynamics drive spreading and random migration of fibroblasts. *J Cell Sci.* 2009,122(Pt 3): 313-323.

Wilson, C. A., Tsuchida, M. A., Allen, G. M., Barnhart, E. L., Applegate, K. T., Yam, P. T., Ji, L., Keren, K., Danuser, G. and Theriot, J. A. Myosin II contributes to cell-scale actin network treadmilling through network disassembly. *Nature.* 2010,465(7296): 373-377.

Wolf, K., Mazo, I., Leung, H., Engelke, K., von Andrian, U. H., Deryugina, E. I., Strongin, A. Y., Brocker, E. B. and Friedl, P. Compensation mechanism in tumor cell migration: mesenchymal-amoeboid transition after blocking of pericellular proteolysis. *J Cell Biol.* 2003,160(2): 267-277.

Wolfenson, H., Bershadsky, A., Henis, Y. I. and Geiger, B. Actomyosin-generated tension controls the molecular kinetics of focal adhesions. *J Cell Sci.* 2011,124(Pt 9): 1425-1432.

Wolven, A., Okamura, H., Rosenblatt, Y. and Resh, M. D. Palmitoylation of p59fyn is reversible and sufficient for plasma membrane association. *Mol Biol Cell.* 1997,8(6): 1159-1173.

Wong, H. K., Sakurai, T., Oyama, F., Kaneko, K., Wada, K., Miyazaki, H., Kurosawa, M., De Strooper, B., Saftig, P. and Nukina, N. beta Subunits of voltage-gated sodium channels are novel substrates of beta-site amyloid precursor protein-cleaving enzyme (BACE1) and gamma-secretase. *J Biol Chem.* 2005,280(24): 23009-23017.

Wozniak, M. A., Modzelewska, K., Kwong, L. and Keely, P. J. Focal adhesion regulation of cell behavior. *Biochim Biophys Acta.* 2004,1692(2-3): 103-119.

Wyckoff, J. B., Pinner, S. E., Gschmeissner, S., Condeelis, J. S. and Sahai, E. ROCK- and myosin-dependent matrix deformation enables protease-independent tumor-cell invasion in vivo. *Curr Biol.* 2006,16(15): 1515-1523.

Xu, H. E., Lambert, M. H., Montana, V. G., Parks, D. J., Blanchard, S. G., Brown, P. J., Sternbach, D. D., Lehmann, J. M., Wisely, G. B., Willson, T. M., Kliewer, S. A. and Milburn, M. V. Molecular Recognition of Fatty Acids by Peroxisome Proliferator–Activated Receptors. *Molecular Cell.* 1999,3: 397–403.

Xu, L., Chen, Y. G. and Massague, J. The nuclear import function of Smad2 is masked by SARA and unmasked by TGFbeta-dependent phosphorylation. *Nat Cell Biol.* 2000,2(8): 559-562.

Xue, C., Wyckoff, J., Liang, F., Sidani, M., Violini, S., Tsai, K. L., Zhang, Z. Y., Sahai, E., Condeelis, J. and Segall, J. E. Epidermal growth factor receptor overexpression results in increased tumor cell motility in vivo coordinately with enhanced intravasation and metastasis. *Cancer Res.* 2006,66(1): 192-197.

Xue, M., Wang, Q., Zhao, J., Dong, L., Ge, Y., Hou, L., Liu, Y. and Zheng, Z. Docosahexaenoic acid inhibited the Wnt/beta-catenin pathway and suppressed breast cancer cells in vitro and in vivo. *J Nutr Biochem.* 2014,25(2): 104-110.

Yamamoto, H., Sutoh, M., Hatakeyama, S., Hashimoto, Y., Yoneyama, T., Koie, T., Saitoh, H., Yamaya, K., Funyu, T., Nakamura, T., Ohyama, C. and Tsuboi, S. Requirement for FBP17 in invadopodia formation by invasive bladder tumor cells. *J Urol.* 2011,185(5): 1930-1938.

Yang, C., Czech, L., Gerboth, S., Kojima, S., Scita, G. and Svitkina, T. Novel roles of formin mDia2 in lamellipodia and filopodia formation in motile cells. *PLoS Biol.* 2007,5(11): e317.

Yang, M. and Brackenbury, W. J. Membrane potential and cancer progression. *Front Physiol.* 2013,4: 185.

Yang, M., Kozminski, D. J., Wold, L. A., Modak, R., Calhoun, J. D., Isom, L. L. and Brackenbury, W. J. Therapeutic potential for phenytoin: targeting Na(v)1.5 sodium channels to reduce migration and invasion in metastatic breast cancer. *Breast Cancer Res Treat.* 2012,134(2): 603-615.

Yao, X., Chen, X., Cottonham, C. and Xu, L. Preferential utilization of Imp7/8 in nuclear import of Smads. *J Biol Chem.* 2008,283(33): 22867-22874.

Yoshinaga, M., Taki, K., Somada, S., Sakiyama, Y., Kubo, N., Kaku, T., Tsuruta, S., Kusumoto, T., Sakai, H., Nakamura, K., Takayanagi, R. and Muto, Y. The expression of both peroxisome proliferator-activated receptor delta and cyclooxygenase-2 in tissues is associated with poor prognosis in colorectal cancer patients. *Dig Dis Sci.* 2011,56(4): 1194-1200.

Yu, F. H., Westenbroek, R. E., Silos-Santiago, I., McCormick, K. A., Lawson, D., Ge, P., Ferriera, H., Lilly, J., DiStefano, P. S., Catterall, W. A., Scheuer, T. and Curtis, R. Sodium channel beta4, a new disulfide-linked auxiliary subunit with similarity to beta2. *J Neurosci.* 2003,23(20): 7577-7585.

Yuan, H., Lu, J., Xiao, J., Upadhyay, G., Umans, R., Kallakury, B., Yin, Y., Fant, M. E., Kopelovich, L. and Glazer, R. I. PPARdelta induces estrogen receptor-positive mammary neoplasia through an inflammatory and metabolic phenotype linked to mTOR activation. *Cancer Res.* 2013,73(14): 4349-4361.

Zaidel-Bar, R., Ballestrem, C., Kam, Y. and Geiger, B. Early molecular events in the assembly of matrix adhesions at the leading edge of migrating cells. *J Cell Sci.* 2003,116(Pt 22): 4605-4613.

Zaidel-Bar, R., Itzkovitz, S., Ma'ayan, A., Ivengar, R. and Geiger, B. Functional atlas of the integrin adhesome. *Nat Cell Biol.* 2007a,9(8): 858-867.

Zaidel-Bar, R., Milo, R., Kam, Z. and Geiger, B. A paxillin tyrosine phosphorylation switch regulates the assembly and form of cell-matrix adhesions. *J Cell Sci.* 2007b,120(Pt 1): 137-148.

Zamir, E. and Geiger, B. Molecular complexity and dynamics of cell-matrix adhesions. *J Cell Sci.* 2001,114(Pt 20): 3583-3590.

Zhang, H., Berg, J. S., Li, Z., Wang, Y., Lang, P., Sousa, A. D., Bhaskar, A., Cheney, R. E. and Stromblad, S. Myosin-X provides a motor-based link between integrins and the cytoskeleton. *Nat Cell Biol.* 2004,6(6): 523-531.

Zhang, M. M., Wilson, M. J., Azam, L., Gajewiak, J., Rivier, J. E., Bulaj, G., Olivera, B. M. and Yoshikami, D. Co-expression of Na(V)beta subunits alters the kinetics of inhibition of voltage-gated sodium channels by pore-blocking mu-conotoxins. *Br J Pharmacol.* 2013,168(7): 1597-1610.

Zhang, Y. Q., Wei, X. L., Liang, Y. K., Chen, W. L., Zhang, F., Bai, J. W., Qiu, S. Q., Du, C. W., Huang, W. H. and Zhang, G. J. Over-Expressed Twist Associates with Markers of Epithelial Mesenchymal Transition and Predicts Poor Prognosis in Breast Cancers via ERK and Akt Activation. *PLoS One.* 2015,10(8): e0135851.

Zhang, Z. N., Li, Q., Liu, C., Wang, H. B., Wang, Q. and Bao, L. The voltage-gated Na+ channel Nav1.8 contains an ER-retention/retrieval signal antagonized by the beta3 subunit. *J Cell Sci.* 2008,121(Pt 19): 3243-3252.

Annexes

Annexe 1 : Formations suivies

2012-2015 : doctorante contractuelle à activité complémentaire d'enseignement

Avril 2015 : Stage au sein du laboratoire « Telomerase and Aging group » du Dr Maria-Luisa Cayuela à Murcia, Espagne. Apprentissage de la technique de colonisation métastatique dans des embryons de poisson zèbre.

Annexe 2 : Publications non intégrées à la thèse

Wannous R, **Bon E**, Mahéo K, Goupille C, Chamouton J, Bougnoux P, Roger S, Besson P, Chevalier S. *PPARβ mRNA expression, reduced by n-3 PUFA diet in mammary tumor, controls breast cancer cell growth*. Biochim Biophys Acta. 2013 Nov;1831(11):1618-25

Driffort V, Gillet L, **Bon E**, Marionneau-Lambot S, Oullier T, Joulin V, Collin C, Pagès JC, Jourdan ML, Chevalier S, Bougnoux P, Le Guennec JY, Besson P, Roger S. *Ranolazine inhibits Na$_V$1.5-mediated breast cancer cell invasiveness and lung colonization.* Mol Cancer. 2014 Dec 11;13(1):264.

Wannous R, **Bon E**, Gillet L, Chamouton J, Weber G, Brisson L, Goré J, Bougnoux P, Besson P, Roger S, Chevalier S. *Suppression of PPARβ, and DHA treatment, inhibit NaV1.5 and NHE-1 pro-invasive activities.* Pflugers Arch. 2014 Jul 15. (2015) 467:1249-1259.

Greco MR, **Bon E**, Rubino R, Casavola V, Ciaccia L, Cayueal ML, Marionneau-Lambot S, Ouiller T, Fromont-Hankard G, Guibon R, Roger S, Reshkin SJ, Cardone RA. *NHERF1 controls in vitro and in vivo breast cancer metastatic phenotypical switches through the phosphorylation of Serines 279 and 301*. En préparation.

Les articles précédemment cités n'ont pas été intégrés à cette thèse, malgré ma participation à leur réalisation. Les articles Wannous *et al*, 2013, 2015 font l'objet principal de la thèse de Ramez Wannous (2014). L'article Driffort *et al*, 2014 fait l'objet principal de la thèse de Virginie Driffort (2014).

L'article Wannous *et al*, 2013 met en évidence l'importance de PPARβ dans la régulation de la des cellules cancéreuses mammaires par le DHA et dans le contrôle de l'expression de PPARα et PPARγ. Pour cet article, j'ai réalisé la quantification par qPCR de l'expression des ARNm PPARα, PPARβ et PPARγ, extraits à partir des tumeurs mammaires de rates.

L'article Driffort *et al*, 2014 montre l'importance du canal sodique $Na_V1.5$ dans l'invasivité cellulaire *in vivo,* et plus particulièrement au cours de la colonisation métastatique pulmonaire. Cet article met en évidence une nouvelle stratégie de régulation de l'activité du canal $Na_V1.5$, par des inhibiteurs pharmacologiques utilisés chez des patients, c'est le cas ici dans le traitement d'angines de poitrine. Pour cet article, j'ai mesuré l'activité luciférase des lignées cellulaires traitées avec la Ranolazine ou le solvant contrôle.

L'article Wannous *et al*, 2015 montre la régulation de l'invasivité des cellules cancéreuses mammaires dépendante de l'activité du canal sodique $Na_V1.5$ par PPARβ et par le DHA. Pour cet article, j'ai réalisé les expériences d'invasivité cellulaire des cellules MDA-MB-231 dans lesquelles PPARβ a été surexprimé de façon transitoire. J'ai également réalisé des expériences de gène rapporteur sur l'activité du promoteur du gène *SCN5A*, dont les résultats n'ont pas été intégrés à l'article.

Biochimica et Biophysica Acta 1831 (2013) 1618–1625

Contents lists available at ScienceDirect

Biochimica et Biophysica Acta

journal homepage: www.elsevier.com/locate/bbalip

PPARβ mRNA expression, reduced by n−3 PUFA diet in mammary tumor, controls breast cancer cell growth

Ramez Wannous [a], Emeline Bon [a], Karine Mahéo [a], Caroline Goupille [a,b], Julie Chamouton [a], Philippe Bougnoux [a,b], Sébastien Roger [a], Pierre Besson [a], Stephan Chevalier [a,c,*]

[a] Inserm UMR1069 "Nutrition, Croissance et Cancer", Faculté de Médecine, Université François Rabelais de Tours, France
[b] Hôpital Bretonneau, CHU de Tours, France
[c] Département de Biochimie, Faculté de Sciences Pharmaceutiques, Université François Rabelais de Tours, France

ARTICLE INFO

Article history:
Received 2 April 2013
Received in revised form 15 July 2013
Accepted 17 July 2013
Available online 30 July 2013

Keywords:
PPAR
MDA-MB-231
MCF-7
Breast tumor
DHA
n−3 PUFA

ABSTRACT

The effect of numerous anticancer drugs on breast cancer cell lines and rodent mammary tumors can be enhanced by a treatment with long-chain n−3 polyunsaturated fatty acids (n−3 PUFA) such as docosahexaenoic acid (DHA, 22:6n−3) which is a natural ligand of peroxisome proliferator-activated receptors (PPAR). In order to identify the PPAR regulating breast cancer cell growth, we tested the impact of siRNA, selected to suppress PPARα, PPARβ or PPARγ mRNA in MDA-MB-231 and MCF-7 breast cancer cell lines. The siPPARβ was the most effective to inhibit breast cancer cell growth in both cell lines. Using PPARα, PPARβ and PPARγ pharmacological antagonists, we showed that PPARβ regulated DHA-induced inhibition of growth in MDA-MB-231 and MCF-7 cells. In addition, the expressions of all 3 PPAR mRNA were co-regulated in both cell lines, upon treatments with siRNA or PPAR antagonists. PPAR mRNA expression was also examined in the NitrosoMethylUrea (NMU)-induced rat mammary tumor model. The expressions of PPARα and PPARβ mRNAs were correlated in the control group but not in the n−3 PUFA group in which the expression of PPARβ mRNA was reduced. Although PPARα expression was also increased in the n−3 PUFA-enriched diet group under docetaxel treatment, it is only the expression of PPARβ mRNA that correlated with the regression of mammary tumors: those that most regressed displayed the lowest PPARβ mRNA expression. Altogether, these data identify PPARβ as an important player capable of modulating other PPAR mRNA expressions, under DHA diet, for inhibiting breast cancer cell growth and mammary tumor growth.

1. Introduction

Long-chain n−3 polyunsaturated fatty acids (PUFA), and docosahexaenoic acid (DHA, 22:6n−3) in particular, can be used to sensitize breast cancer cell lines and mammary tumors to anticancer drugs [1]. In a phase II study carried on breast cancer patients with severe metastatic disease, a diet enriched in n−3 PUFA increased survival and chemotherapy efficacy [2,3]. In human breast cancer cell lines, DHA potentiated the effects of anticancer drugs such as anthracyclines [4–8] or taxanes [9,10]. The molecular effects of DHA are multiple and since it is a natural ligand of peroxisome proliferator-activated receptors (PPAR) [11–13], we hypothesized that PUFA might chemosensitize breast cancer cell lines and mammary tumors through the activation of PPAR.

PPAR comprises a family of 3 nuclear receptors (PPARα, PPARβ and PPARγ) acting as transcription factors for many genes regulating cell metabolism when stimulated with lipids or pharmacological agonists [14]. The involvement of PPAR in breast cancer has been mostly investigated using synthetic pharmacological PPAR agonists. PPARα agonists such as fibrates stimulated proliferation of both MCF-7 (estrogen receptor (ER) positive) and MDA-MB-231 (ER negative) breast cancer cell lines [15] whereas PPARγ agonists such as glitazones were anti-proliferative in MCF-7 cells [16]. PPARβ agonist (GW501516) was initially reported to stimulate proliferation of MCF-7 cells but not that of MDA-MB-231 cells [17]. Other authors reported that PPARβ agonists (GW501516 and GW0742) only modestly inhibited proliferation of MCF-7 (human) and C20 (mouse) mammary gland cancer cell lines [18,19] while a PPARβ antagonist (GSK3787) had no effect in MCF-7 cells [20]. In addition, the PPARβ agonist GW0742 induced apoptosis in the C20 mouse mammary gland cancer cell line [19]. PPARβ mRNA was significantly less expressed in MCF-7 cells than in MDA-MB-231 cells [21] and differences observed between laboratories for MCF-7 cell response to PPARβ ligands might be related to fluctuating basal level of expression of PPARβ depending on cell culture conditions [22].

In the absence of additional chemotherapy, n−3 PUFA (30–50 μM), but not oleic acid (18:1n−9), were sufficient to reduce proliferation of MDA-MB-231 cells, by slowing down their progression into mitosis

* Corresponding author at: INSERM UMR1069, "Nutrition, Croissance et Cancer", Université François-Rabelais, Faculté de Médecine, 10 Bd Tonnellé, F-37032 TOURS Cedex, France. Tel./fax: +33 2 47 36 62 26.
E-mail address: stephan.chevalier@univ-tours.fr (S. Chevalier).

1388-1981/$ – see front matter © 2013 Elsevier B.V. All rights reserved.
http://dx.doi.org/10.1016/j.bbalip.2013.07.010

[23], and by inducing apoptosis in MDA-MB-231 and MCF-7 human cell lines [23,24]. In mice bearing MDA-MB-231 cell xenografts, 2% n−3 PUFA in the diet (representing 40% of total lipids in a formula containing 5% fat) decreased tumor growth rate in the absence of chemotherapy [5]. Recently, Jiang et al. [25] also showed a much higher proportion of n−3 PUFA (4.6% in the diet, representing 87% of total dietary lipids in a formula containing 5.3% fat) limited mammary tumor incidence and tumor mass in the NitrosoMethylUrea (NMU)-induced rat model of breast cancer. This was accompanied by a reduced protein level for PPARβ and increased level for PPARγ in tumors while PPARα expression remained stable [25]. Our objectives were therefore i) to determine the relative involvement of the 3 PPAR in regulating DHA-induced reduction of growth in MDA-MB-231 and MCF-7 cell lines and ii) to identify the changes in PPAR expression associated to mammary tumor regression in NMU-induced rats chemosensitized to taxane (docetaxel) treatment by 3.5% of n−3 PUFA diet (representing 23% of total dietary lipids in a formula containing 15% fat) which is nutritionally compatible with a human diet.

2. Materials and methods

2.1. Reagents

Pharmacological antagonists GW6471 [26], GSK0660 [27] and T007 0907 [28] for PPARα, PPARβ and PPARγ, respectively, agonist for PPARβ (GW0742) and docosahexaenoic acid (DHA, 22:6n−3), were purchased Sigma-Aldrich (Saint Quentin Fallavier, France), and dissolved in 100% ethanol. DHA was used as methyl ester (50 μM), as previously described [23]. SiRNA (sc-37007 for siCTL, sc-36307 for PPARα, sc-36305 for PPARβ, sc-29455 for PPARγ) were purchased from Tebu-Bio (Le Perray en Yvelines, France).

2.2. Cell cultures and treatments

The human breast carcinoma cell lines MCF-7 and MDA-MB-231, from the American Type Culture Collection (LGC Promochem, Molsheim, France), were routinely cultured in Dulbecco's Modified Eagle's Medium (DMEM; Cambrex Bio Science, Emerainville, France) supplemented with 5% fetal calf serum (Invitrogen Life Technologies, Cergy Pontoise, France) at 37 °C in a humidified CO_2 incubator. Prior to reaching confluence, cells were trypsinized with a 0.05% trypsin/0.53 mM EDTA solution and resuspended in fresh growth medium before plating onto a new growth surface. Cells were seeded at 20,000 cells/well in 24-well plates at day 0. At day 1, 24 h after seeding, cells were treated with DHA, PPAR antagonists or combinations of those as indicated in the figure legends. Cells were collected after 24 h of treatment for RNA extraction or after 3 days of treatment for growth assessment with the tetrazomium salt [3-(4,5-dimethylthiazol-2-yl)-2,5-diphenyltetrazolium bromide] assay as described previously [23]. For siRNA testing, cells were transfected using Lipofectamine RNAi max (Invitrogen, Illkirch, France) in suspension with 4 nM siRNA according to manufacturer's instructions before seeding at $5 \times 10^3/cm^2$ in 24-well plates. MTT assay was performed at the time specified in the figure legends. RNA was extracted 48 h after seeding.

2.3. RNA extraction, reverse transcription and Q-PCR

Total RNA from cultured cells was extracted using NucleoSpin ®RNA II Columns (Macherey-Nagel, Hoerdt, France). Total RNA from rat tumor samples was extracted with TRIzol® reagent (Invitrogen, Illkirch, France). Both RNAs from MDA-MB-231 cells and rat tumors were reverse-transcribed with a RT kit ("Ready-to-go" GE Healthcare, Vélizy, France) in the presence of random hexamers $pd(N)_6$ 5′-Phosphate (Invitrogen, Illkirch, France). Quantitative (real time) PCR experiments were performed in duplicate as already described [29] with MyiQ thermocycler (Biorad, Marne-la-coquette, France) using Platinum® SYBR® Green qPCR SuperMix-UDG kit (Invitrogen, Illkirch, France). For rat tumors, PPAR mRNA expression was expressed relatively to Rpl13a mRNA expression as ΔCt (CT: cycle threshold value; Ct PPAR-CT Rpl13a). In the figures, we attributed a value of 1 arbitrary unit (au) to 1ΔCt. For MDA-MB-231 cells, PPAR mRNA amount was expressed relatively to HPRT mRNA expression and control condition as relative quantity $Q = 2^{-\Delta\Delta Ct}$.

2.4. Transactivation assays

MDA-MB-231 cells were transfected with Lipofectamine 2000 (Invitrogen) following manufacturer's protocol. 24 h prior transfection, 1.5×10^5 cells per well were seeded in a 24-well plate. Cells were transfected with a mixture of plasmid DNA containing 30 ng of the reporter vector pCMVβ-galactosidase (Clontech) to standardize the transactivation assay, 250 ng $PPRE_3$-TK-Luc, the reporter luciferase vector containing three copies of PPRE consensus upstream the Tyrosine Kinase (TK) promotor [30]. These two vectors were cotranfected with 50 ng of PPARβ expression plasmid (pSG5-PPARβ) or corresponding empty vector (pSG5). Six hours post-transfection, the culture medium was replaced by complete medium and cells were treated with PPARβ agonist (GW0742, 0.1 μM), PPARβ antagonist (GSK0660, 1 μM), DHA 50 μM or combinations of those as indicated in Fig. 3. Luc and β-galactosidase activities were measured 48 h post-transfection using Luciferase Assay System (Promega) according to the manufacturer's recommendations. Luc activity was set at 100% in the condition with no treatment and no overexpression of PPARβ. For each condition, transactivation assays were repeated at least three times.

2.5. Statistical analysis

GraphPad Prism4 was used for all statistical analysis. Statistical significance was determined using the analysis of *t*-test followed by a Mann–Whitney test. P values of <0.05 were considered statistically significant.

3. Results and discussion

3.1. Suppression of individual PPAR mRNA decreased cell growth and increased expression of the other two PPAR mRNA

In order to identify which PPAR regulate(s) breast cancer cell growth, we tested the effect of 3 siRNAs selected to suppress each of the 3 PPAR mRNAs in both MDA-MB-231 and MCF-7 cells cultured in the absence of added PPAR agonist or antagonist. SiPPARα, siPPARβ and siPPARγ reduced the expression of PPARα mRNA by 81% ($p < 0.001$), PPARβ mRNA by 84% ($p < 0.001$) and PPARγ mRNA by 89% ($p < 0.001$), respectively (Fig. 1a). In addition, the reduced expression of each of the PPAR mRNA stimulated the expression of the other two PPAR. SiPPARα stimulated the expression of PPARβ (+52%; $p < 0.01$) and PPARγ (+59%; $p < 0.001$) mRNA. SiPPARβ stimulated the expression of PPARα (+45%; $p < 0.05$) and PPARγ (+51%; $p < 0.001$) mRNA. SiPPARγ stimulated the expression of PPARα (+11%; $p < 0.001$) and PPARβ (+29%; $p < 0.01$) mRNA (Fig. 1a). Therefore, the expression of each PPAR mRNA was dependent on the expression of the other PPAR in MDA-MB-231 cells.

MDA-MB-231 cell growth was reduced by 9% with siPPARβ ($p < 0.01$) 48 h after transfection compared to siCTL (Fig. 1b). At 72 h, it was reduced by 33% with siPPARβ, 23% with siPPARα and 20% with siPPARγ. At 96 h, this reduction ($p < 0.01$) extended to 45% with siPPARβ, 33% with siPPARα and 27% with siPPARγ (Fig. 1b). Co-transfection of any combination of two PPAR siRNAs did not further reduce cell growth (data not shown), suggesting that the inhibition of growth by a particular siPPAR was not compensated by the induced overexpression of the other two PPAR mRNAs.

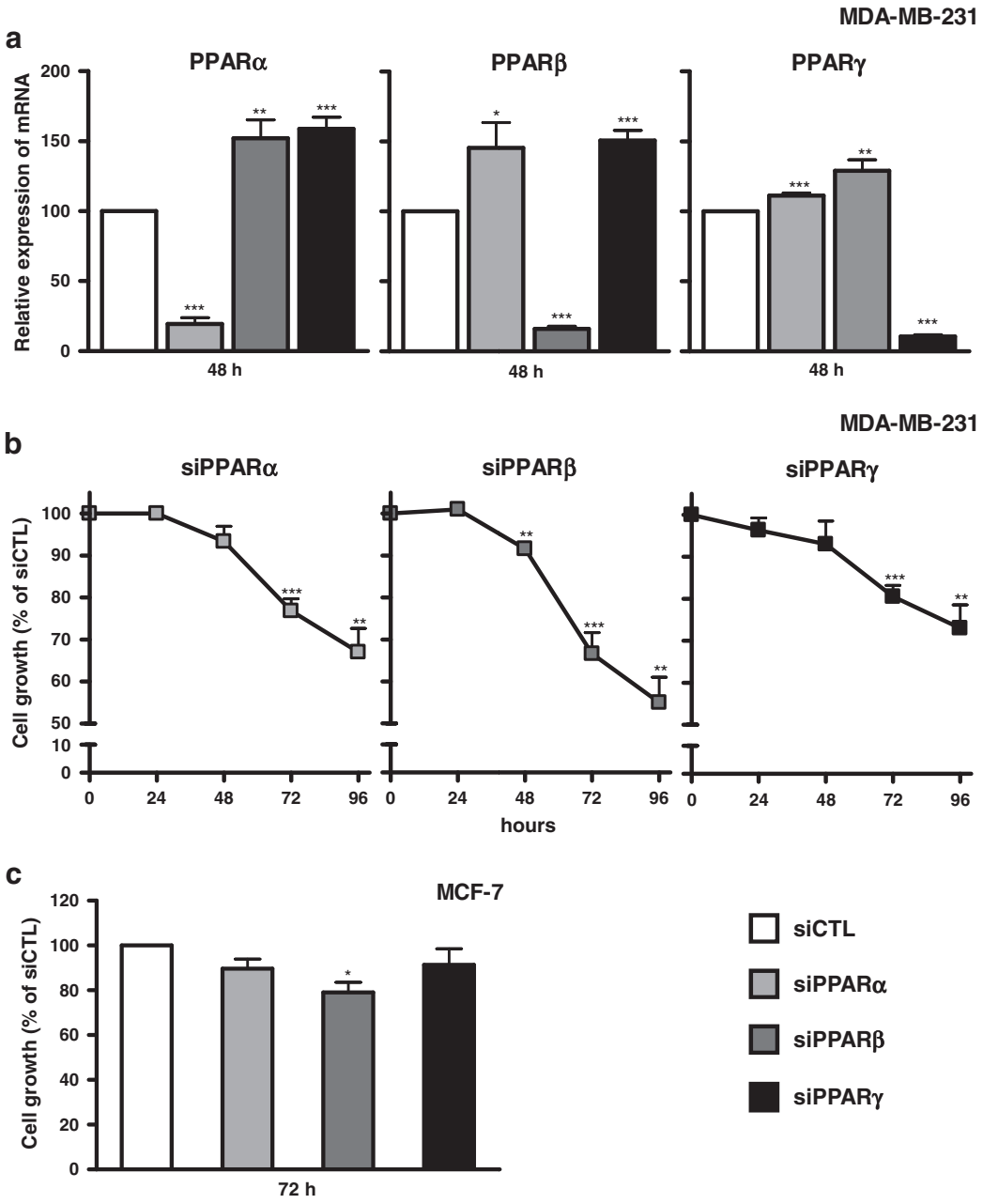

Fig. 1. Suppression of an individual PPAR mRNA led to decreased cell growth and increased expression of the other two PPAR mRNAs. (a) MDA-MB-231 cells were transfected with siRNA directed against PPARα (siPPARα), PPARβ (siPPARβ), PPARγ (siPPARγ) or scramble siRNA used as a control (siCTL). PPARα (left), PPARβ (middle) and PPARγ (right) mRNA relative expressions were assessed by RT-qPCR 48 h after transfection with siRNA directed against PPARα ($n = 3$) or PPARβ ($n = 4$) or PPARγ ($n = 3$) vs. control ($n = 4$). PPAR mRNA amount was expressed, relatively to HPRT1 mRNA expression and control condition, as relative quantity $Q = 2^{-\Delta\Delta Ct}$. (b) Cells were cultured for 24 ($n = 3$ individual cell culture experiments), 48 ($n = 3$), 72 ($n = 6$) and 96 h ($n = 3$) prior to MTT assay. (c) MCF-7 cells, transfected with each individual siRNA, were cultured for 72 h ($n = 3$) prior to MTT assay. Statistically different from siCTL condition at: $^{***}p < 0.001$ $^{**}p < 0.01$ or $^{*}p < 0.05$.

MCF-7 cell growth was also tested 72 h after siRNA treatments. While suppressing PPARγ or PPARα mRNA had no statistically significant effect, siPPARβ inhibited MCF-7 cell growth by 21% ($p < 0.05$) (Fig. 1c). Although PPARα and PPARγ were involved in regulating cell growth in MDA-MB-231 cells, only siPPARβ was efficient in reducing growth in both cell lines. Next, we hypothesized that PPARβ might be involved in modulating DHA-induced inhibition of breast cancer cell growth.

3.2. PPARβ antagonist prevented both DHA-induced reduction of cell growth and DHA-induced inhibition of PPAR mRNA expression

A 3-day treatment with 50 μM DHA methyl ester reduced MDA-MB-231 cell growth by 43% ($p < 0.001$) (Fig. 2a, CTL) as expected [23]. In similar conditions, DHA methyl ester supplementation led to a four-fold increase of DHA content in membrane phospholipids [23]. PPARα, PPARβ and PPARγ antagonists, respectively GW6471 (Antag. α) [26], GSK0660 (Antag. β) [27] and T0070907 (Antag. γ) [28], were used at the highest doses (Fig. 2a) that were not cytotoxic in our culture conditions (data not shown). PPARβ antagonist reversed the anti-proliferative effect of DHA up to 90% ($p < 0.01$) of the control (Fig. 2a, Antag. β) while PPARα and PPARγ antagonists did not. Consistent with this, the combined use of PPARβ and PPARα antagonists, or PPARβ and PPARγ antagonists, reversed the anti-proliferative effect of DHA up to 88% ($p < 0.05$) and 87% ($p < 0.05$) of the control, respectively (Fig. 2a), the combined use of PPARα and PPARγ antagonists did not. This indicated that PPARβ was involved in DHA-induced regulation of

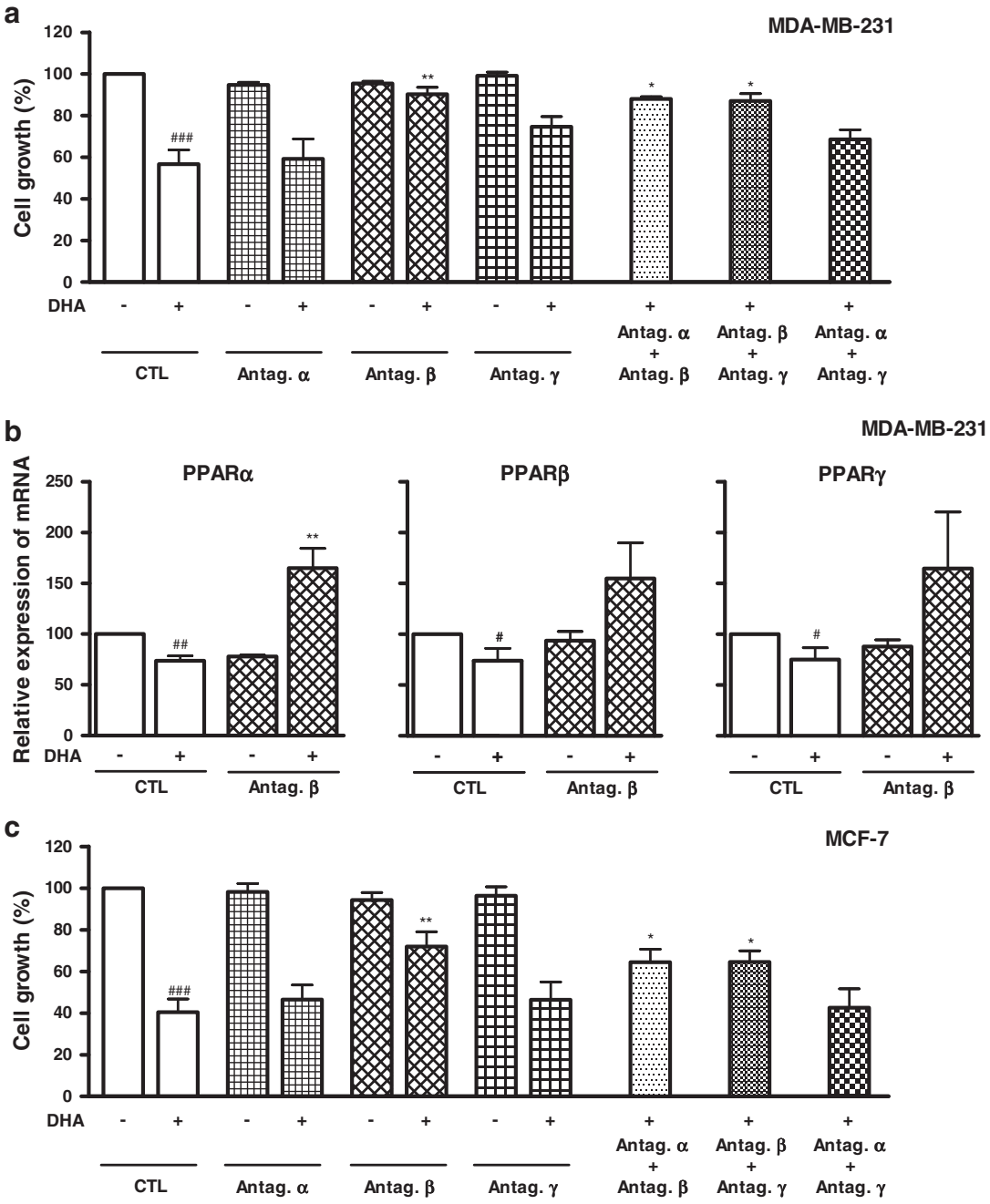

Fig. 2. PPARβ antagonist prevented both DHA-induced reduction of cell growth and DHA-induced inhibition of PPAR mRNA expression. (a) MDA-MB-231 cells were treated with either DHA (50 μM; n = 7), PPARα antagonist (GW6471, Antag. α; 0.5 μM), PPARβ antagonist (GSK0660, Antag. β; 1 μM), PPARγ antagonist (T0070907, Antag. γ; 1 μM) (n = 5) or combinations of those (n = 3) or ethanol as solvent control (CTL) for 3 days. Cell growth was assessed by MTT assay. (b) PPARα (left), PPARβ (middle) and PPARγ (right) mRNA relative expression in MDA-MB-231 cells after 24 h of supplementation with DHA (50 μM), PPARβ antagonist (Antag. β, 1 μM), or combination of both, or ethanol (as solvent control, CTL) (n = 3 except for PPARβ mRNA expression: n = 4). (c) MCF-7 cells were treated (n = 3) with either DHA (50 μM), PPARα antagonist (Antag. α; 0.5 μM), PPARβ antagonist (Antag. β; 1 μM), PPARγ antagonist (Antag. γ; 1 μM) or combination of DHA with antagonist or ethanol as solvent control (CTL) for 3 days prior to MTT assay (n = 3). Statistically different from DHA-supplemented (CTL condition) at: $^{**}p < 0.01$ or $^{*}p < 0.05$ (except for DHA-supplemented compared to "no DHA" in CTL condition: ### $p < 0.001$ or ## $p < 0.01$ or # $p < 0.05$).

breast cancer cell growth. However, PPARβ pharmacological agonists (GW501516 and GW0742) used individually or in combination were not sufficient to reduce cell growth (data not shown), probably reflecting the limitation of an agonist response compared to DHA response.

The effect of DHA on the expression of PPAR mRNA in the absence or presence of PPARβ antagonist was also investigated in MDA-MB-231 cells. All 3 PPAR mRNA expressions were decreased (−26% for PPARα, $p < 0.01$; −26% for PPARβ, $p < 0.05$ and −25% for PPARγ, $p < 0.05$) (Fig. 2b) within 24 h of DHA exposure that led to the inhibition of cell growth after 3 days of treatment (Fig. 2a). It is worth mentioning that not all mRNA examined were down-regulated in these experimental conditions. For example, the amount of GPx1 mRNA, as well as HPRT1 mRNA used as control in RT-qPCR, was stable after DHA treatment as previously published [31]. PPARβ antagonist itself did not modify the expression of any of the PPAR mRNA (Fig. 2b). Fig. 2b shows that the DHA–PPARβ antagonist co-treatment increased PPARα (+65%; $p < 0.01$), as well as PPARβ and PPARγ mRNAs (not statistically significant), which would be consistent with the hypothesis of an indirect mechanism of regulation of PPAR mRNA expression [32,33].

Similarly to MDA-MB-231 cells, a 3-day treatment with 50 μM DHA reduced MCF-7 cell growth by 59% ($p < 0.001$) (Fig. 2c). PPARα, PPARβ

and PPARγ antagonists were used at the highest non-cytotoxic doses. PPARα and PPARγ antagonists did not prevent the anti-proliferative effect of DHA whereas the PPARβ antagonist reversed the anti-proliferative effect of DHA up to 72% ($p < 0.01$) of the control (Fig. 2c). Whereas the combined use of PPARα and PPARγ antagonists did not prevent the DHA-induced reduction of cell growth, the combined use of PPARβ and PPARα antagonists, or PPARβ and PPARγ antagonists, in MCF-7 cells reversed the anti-proliferative effect of DHA up to 64% ($p < 0.05$) and 65% ($p < 0.05$) of the control, respectively (Fig. 2a). Data obtained with siRNA and antagonists indicate that PPARβ regulates DHA-induced inhibition of growth in both MDA-MB-231 and MCF-7 cells.

3.3. PPARβ is an active transcription factor in MDA-MB-231 breast cancer cells

In order to determine if endogenous PPARβ was active in MDA-MB-231 breast cancer cells, in DHA treatment conditions, transactivation assays were performed with a luciferase (Luc) reporter vector containing three copies of PPRE consensus sequence upstream of a tyrosine kinase promoter [30]. Luc activity of the $PPRE_3$-TK-Luc vector was increased by 147% ($p < 0.001$) with PPARβ agonist (Ag. β) and inhibited by 26% with PPARβ antagonist (Antag. β; $p < 0.05$) (Fig. 3a). In MCF-7 cells, Palkar et al. [20] also showed that the PPARβ-induced transcription of target gene ANGPTL4 was increased with the PPARβ agonist GW0742 and repressed by the PPARβ antagonist GSK3787.

In the condition of endogenously expressed PPAR in MDA-MB-231, DHA treatment (50 μM) slightly, but not significantly, increased Luc activity of the $PPRE_3$-TK-Luc vector, compared to control (CTL). DHA had no apparent effect on PPARβ antagonist Luc activity and it slightly limited the PPARβ agonist effect ($p < 0.05$), consistent with a weak agonist effect of n−3 PUFA on the overall transcriptional activity of endogenous PPAR [34]. In the condition of overexpressed PPARβ, Luc activity was increased by 767% ($p < 0.001$) with PPARβ agonist and inhibited by 64% with PPARβ antagonist ($p < 0.001$) (Fig. 3b). DHA induced a statistically significant agonist activity (+96%, $p < 0.05$) which was abolished by the PPARβ antagonist (−71% of DHA treatment, $p < 0.01$). Finally, the DHA effect was not cumulative with that of the PPARβ agonist (Fig. 3b), suggesting that the DHA and PPARβ agonist effects overlap in this gene reporter assay.

Altogether, our in vitro data show that DHA displays weak PPARβ agonist properties, inhibiting breast cancer cell growth and mRNA expression of all three PPAR. Those effects were counteracted by the PPARβ antagonist. Therefore, PPARβ can be regarded as an important player in modulating DHA-induced inhibition of cell growth. This also supports the proposal that PPARβ is a gateway receptor capable of modulating other PPAR mRNA expression [32].

3.4. PPARβ mRNA expression in the NitrosoMethylUrea (NMU)-induced mammary tumor rat model is correlated with n−3 PUFA diet-induced tumor size regression after docetaxel treatment

The involvement of PPARβ expression changes in regulating DHA-induced inhibition of breast cancer cell growth was tested in the NMU-induced mammary tumor model. Such an in vivo model, expressing constituents of tumor stroma including functional vessels, is considered to be representative of human breast tumors [35]. We further analyzed 36 tumors from a larger study previously performed to characterize how n−3 PUFA counteracted tumor chemoresistance to a taxane (docetaxel) by restoring a functional vascularization [29]. In this study, female Sprague–Dawley rats were separated, after the initiation of carcinogenesis, into a control diet group or into an n−3 PUFA diet group. The latter was fed with a diet containing 2.5% DHA and 1% EPA (eicosapentaenoic acid, 20:5n−3) which, in the absence of anticancer drug treatment, did not alter mammary tumor growth. Tumor sizes were measured weekly during the whole experiment and when tumors reached 2 cm^2, half of the rats of both groups were treated with docetaxel for 6 weeks. At the end of this study, there was a 2.5-fold increase of n−3 PUFA content in total tumor phospholipids in the n−3 PUFA group compared to control group [29]. The total n−3 PUFA incorporation was increased in the phospholipids of tumor tissues of the n−3 PUFA diet group (from 1.99% to 5.05%). This was mostly due to DHA which represented 1.74% in the phospholipids of tumor tissues of the control diet group and which increased to 2.94% in the n−3 PUFA diet group, to EPA which increased from 0.03% in the control diet group to 1.06% in the n−3 PUFA diet group, and to docosapentaenoic acid (22:5n−3) which increased from 0.18% in the control diet group to 1.00% in the n−3 PUFA diet group. Concurrently, total n−6 PUFA were less incorporated in the phospholipids of tumor tissues of the n−3 PUFA diet group (from 24.38% to 18.18%), mostly due to arachidonic acid (20:4n−6) which was reduced from 17.11% in the phospholipids of tumor tissues of the control diet group to 11.27% in the n−3 PUFA diet group. The total monounsaturated fatty acids in the phospholipids of

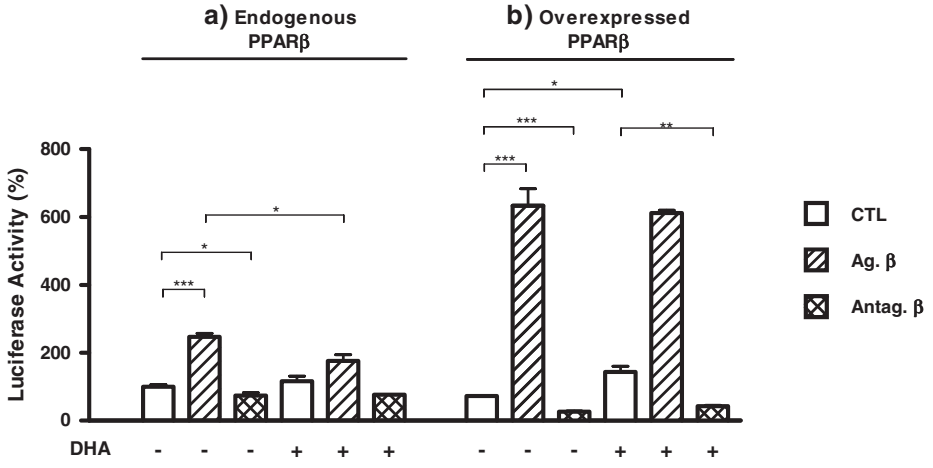

Fig. 3. PPARβ is an active transcription factor in MDA-MB-231 breast cancer cells. Transactivation assays were performed in MDA-MB-231 cells with $PPRE_3$-TK-Luc reporter vector. The expression vector for PPARβ (pSG5-PPARβ, 50 ng) (b: overexpressed PPARβ) or corresponding empty vector pSG5 (Stratagene) used for control experiments (a: endogenous PPARβ) were transfected. Six hours post-transfection, the culture medium was replaced by complete medium and cells were treated by PPARβ agonist (Ag. β, 0.1 μM), PPARβ antagonist (Antag. β, 1 μM), DHA 50 μM or combinations of those. Values are means of at least three independent experiments. Statistically significant differences between conditions at: ***$p < 0.001$ or **$p < 0.01$ or *$p < 0.05$.

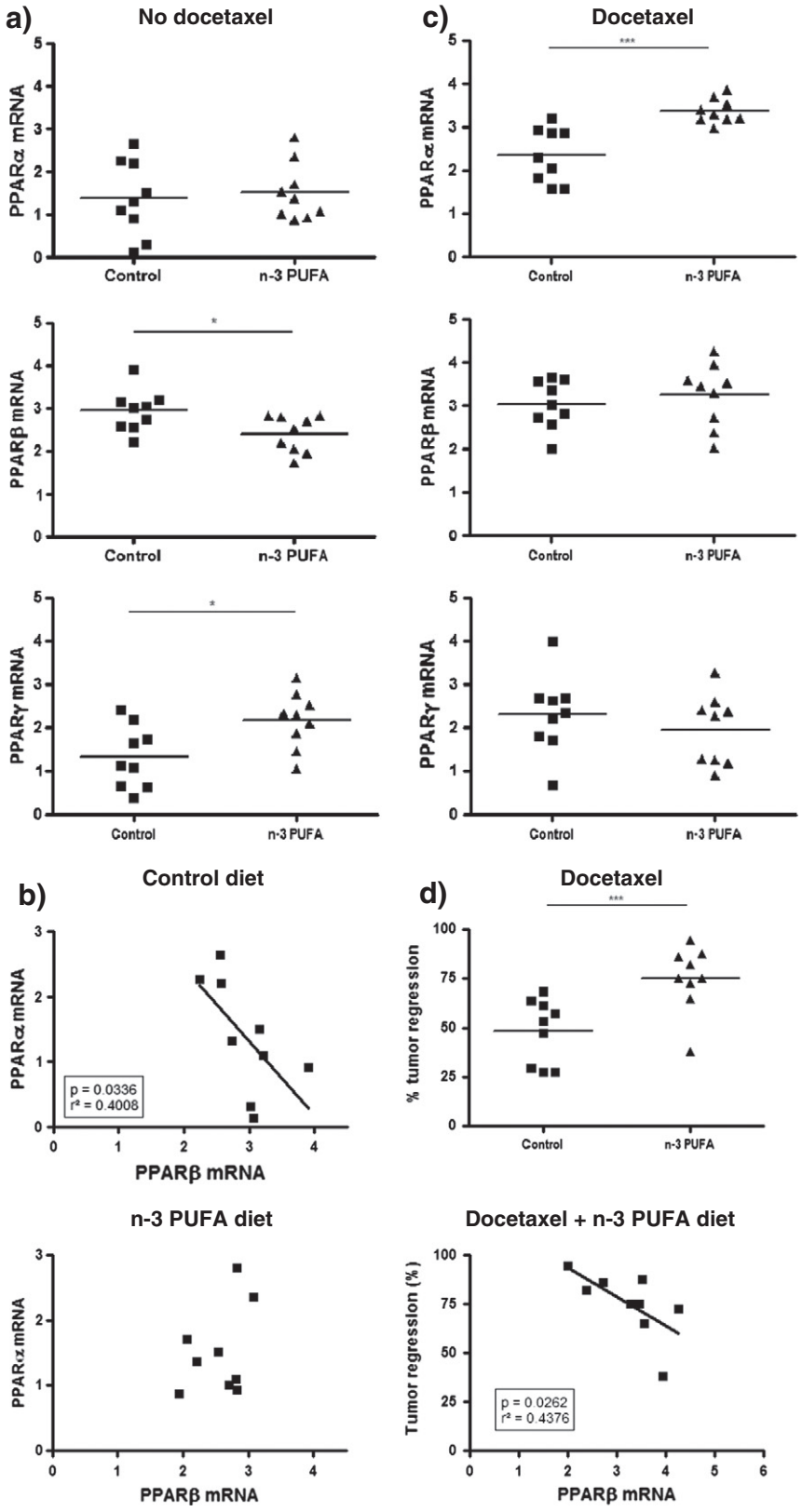

Fig. 4. PPAR mRNA expression in the NitrosoMethylUrea (NMU)-induced mammary tumor rat model and correlation with n−3 PUFA diet-induced regression in tumor size after docetaxel treatment. Female rats with induced mammary carcinogenesis were separated into a control diet group (n = 18) or n−3 PUFA diet group (n = 18; 3.5% n−3 PUFA in the diet). When tumors reached 2 cm^2, half of the rats of both groups were treated once a week with docetaxel for 6 weeks (2 groups of 9 rats) and total RNA were extracted from tumors at the end of the study (a) PPARα (top), PPARβ (middle) and PPARγ (bottom) mRNA relative expression in rat mammary tumors after exposure to control diet (n = 9, left) or n−3 PUFA diet (n = 9, right) in the absence of docetaxel treatment. (b) Correlation between the expression of PPARβ mRNA and PPARα mRNA in rat mammary tumors after exposure to control diet (top; $p < 0.05$; n = 9) or n−3 PUFA diet (bottom; ns; n = 9). (c) PPARα (top), PPARβ (middle) and PPARγ (bottom) mRNA relative expression after exposure to n−3 PUFA diet (n = 9), vs control diet (n = 9), after docetaxel treatment. (d) Percentage of tumor regression under docetaxel treatment in control vs n−3 PUFA diet groups (top). Correlation between the expression of PPARβ mRNA and n−3 PUFA-induced regression of mammary tumor size upon docetaxel treatment (bottom) ($p < 0.05$; n = 9). Statistically different from control condition at: $^{***}p < 0.001$ or $^{**}p < 0.01$ or $^{*}p < 0.05$.

tumor tissues represented 22.19% in the control diet group and 25.07% in the n−3 PUFA diet group, mostly due to oleic acid (18:1n−9) which increased from 13.88% in the phospholipids of tumor tissues of the control diet group to 16.64% in the n−3 PUFA diet group [29]. In these diet conditions, n−3 PUFA represented 3.5% of the diet but only 23% of total lipid content in the diet in a formula containing 15% fat, which makes it an acceptable recommendation for a human diet. This is strikingly different from the study performed by Thompson's group [25,36] in which mammary tumor incidence and tumor mass were reduced in NMU-induced rat model under a diet with a higher proportion of n−3 PUFA (4.6% of n−3 PUFA representing 87% of total dietary lipids in a formula containing 5.3% fat) even without any anticancer drug treatment.

Although tumor growth was similar in both dietary groups (control and n−3 PUFA) in the absence of docetaxel treatment (data not shown, [29]) the expression of PPARβ decreased significantly ($p < 0.05$) in the n−3 PUFA diet group compared to control diet group (Fig. 4a, middle panel) while the expression of PPARγ ($p < 0.05$) increased (Fig. 4a, bottom). When testing the potential correlation between the expression of PPAR in the 4 diet/treatment groups, the only statistically significant correlation ($p = 0.0336$; $r^2 = 0.4008$) that was found was between the mRNA expression of PPARα and PPARβ in the control diet group (Fig. 4b top). This correlation vanished in the n−3 PUFA diet group (Fig. 4b bottom) for which PPARβ mRNA expression was reduced (Fig. 4a, middle) while PPARα mRNA expression remained unchanged (Fig. 4a, top). This transcriptional effect of the n−3 PUFA diet on PPAR mRNA expression in rat mammary tumors was consistent with changes in PPAR protein expression observed by Jiang et al. [25].

Then, we examined the changes in PPAR mRNA expression in treatment conditions inducing tumor size regression. In the n−3 PUFA diet group, docetaxel treatment induced 75.2% of tumor regression, which was significantly greater than in the control diet group ($p < 0.001$) (Fig. 4d top). In the control diet groups, docetaxel which has not been reported as a nuclear receptor ligand or modulator, unexpectedly increased the expression of PPARα ($p < 0.01$) and PPARγ mRNA ($p < 0.01$) but the level of PPARβ remained unchanged (Fig. 4c compared to 4a). Such effects of docetaxel itself on PPARα or PPARγ mRNA expression were not detected in vitro (data not shown). In rats, the expression of PPARα was even further induced under docetaxel treatment in the n−3 PUFA diet group ($p < 0.001$) (Fig. 4c top). Since there was no correlation between changes in expression of PPARα and PPARγ and tumor size regression under docetaxel therapy in both diet groups, those changes probably reflect an in vivo adaptation to chemotherapy not related to tumor regression. Most importantly, there was a statistically significant correlation ($p = 0.0262$; $r^2 = 0.4376$) between tumor regression and the level of expression of PPARβ mRNA in rat mammary tumor in the n−3 PUFA diet group treated with docetaxel (Fig. 4d bottom). Tumors that regressed most, under docetaxel treatment and n−3 PUFA diet, displayed the lowest level of PPARβ mRNA expression.

3.5. Conclusion

Taken together, these in vitro and in vivo studies outlined a key role of PPARβ: its expression was reduced by n−3 PUFA diet in mammary tumor and DHA in human breast cancer cells, it modulated other PPAR mRNA expression and it inhibited breast cancer cell growth, as well as mammary tumor growth.

Acknowledgements

The authors would like to thank Sophie Vibet, Isabelle Domingo and the UTTIL platform of Tours' Hospital for technical help. This work was supported by the “Region Centre” (Fellowships of Emeline Bon and Julie Chamouton), the “Ligue Nationale Contre le Cancer” (committees of Charente, Indre et Loire, Mayenne and Morbihan) and Tours' Hospital oncology association ACORT (fellowship of Ramez Wannous).

References

[1] P. Bougnoux, N. Hajjaji, K. Maheo, C. Couet, S. Chevalier, Fatty acids and breast cancer: sensitization to treatments and prevention of metastatic re-growth, Prog. Lipid Res. 49 (2010) 76–86.
[2] P. Bougnoux, N. Hajjaji, M.N. Ferrasson, B. Giraudeau, C. Couet, O. Le Floch, Improving outcome of chemotherapy of metastatic breast cancer by docosahexaenoic acid: a phase II trial, Br. J. Cancer 101 (2009) 1978–1985.
[3] N. Hajjaji, P. Bougnoux, Selective sensitization of tumors to chemotherapy by marine-derived lipids: a review, Cancer Treat. Rev. 39 (5) (Aug 2013) 473–488.
[4] E. Germain, V. Chajes, S. Cognault, C. Lhuillery, P. Bougnoux, Enhancement of doxorubicin cytotoxicity by polyunsaturated fatty acids in the human breast tumor cell line MDA-MB-231: relationship to lipid peroxidation, International journal of cancer, Int. J. Cancer 75 (1998) 578–583.
[5] W.E. Hardman, C.P. Avula, G. Fernandes, I.L. Cameron, Three percent dietary fish oil concentrate increased efficacy of doxorubicin against MDA-MB 231 breast cancer xenografts, Clin. Cancer Res. 7 (2001) 2041–2049.
[6] K. Maheo, S. Vibet, J.P. Steghens, C. Dartigeas, M. Lehman, P. Bougnoux, J. Gore, Differential sensitization of cancer cells to doxorubicin by DHA: a role for lipoperoxidation, Free Radic, Biol. Med. 39 (2005) 742–751.
[7] S. Vibet, K. Maheo, J. Gore, P. Dubois, P. Bougnoux, I. Chourpa, Differential subcellular distribution of mitoxantrone in relation to chemosensitization in two human breast cancer cell lines, Drug Metab. Dispos. 35 (2007) 822–828.
[8] S. Chevalier, C. Goupille, K. Mahéo, I. Domingo, C. Dussiau, B. Renoux, P. Bougnoux, S. Papot, Dietary docosahexaenoic acid proposed to sensitize breast tumors to locally delivered drug, Clin. Lipidol. 5 (2010) 233–243.
[9] J.A. Menendez, R. Lupu, R. Colomer, Exogenous supplementation with omega-3 polyunsaturated fatty acid docosahexaenoic acid (DHA; 22:6n−3) synergistically enhances taxane cytotoxicity and downregulates Her-2/neu (c-erbB-2) oncogene expression in human breast cancer cells, Eur. J. Cancer Prev. 14 (2005) 263–270.
[10] G. Calviello, S. Serini, E. Piccioni, G. Pessina, Antineoplastic effects of n−3 polyunsaturated fatty acids in combination with drugs and radiotherapy: preventive and therapeutic strategies, Nutr. Cancer 61 (2009) 287–301.
[11] B.M. Forman, J. Chen, R.M. Evans, Hypolipidemic drugs, polyunsaturated fatty acids, and eicosanoids are ligands for peroxisome proliferator-activated receptors alpha and delta, Proc. Natl. Acad. Sci. U.S.A. 94 (1997) 4312–4317.
[12] H.E. Xu, M.H. Lambert, V.G. Montana, D.J. Parks, S.G. Blanchard, P.J. Brown, D.D. Sternbach, J.M. Lehmann, G.B. Wisely, T.M. Willson, S.A. Kliewer, M.V. Milburn, Molecular recognition of fatty acids by peroxisome proliferator-activated receptors, Mol. Cell. 3 (1999) 397–403.
[13] W. Wahli, L. Michalik, PPARs at the crossroads of lipid signaling and inflammation, Trends Endocrinol. Metab. 23 (2012) 351–363.
[14] J.M. Peters, Y.M. Shah, F.J. Gonzalez, The role of peroxisome proliferator-activated receptors in carcinogenesis and chemoprevention, Nat. Rev. Cancer 12 (2012) 181–195.
[15] K.M. Suchanek, F.J. May, J.A. Robinson, W.J. Lee, N.A. Holman, G.R. Monteith, S.J. Roberts-Thomson, Peroxisome proliferator-activated receptor alpha in the human breast cancer cell lines MCF-7 and MDA-MB-231, Mol. Carcinog. 34 (2002) 165–171.
[16] K.Y. Kim, S.S. Kim, H.G. Cheon, Differential anti-proliferative actions of peroxisome proliferator-activated receptor-gamma agonists in MCF-7 breast cancer cells, Biochem. Pharmacol. 72 (2006) 530–540.
[17] R.L. Stephen, M.C. Gustafsson, M. Jarvis, R. Tatoud, B.R. Marshall, D. Knight, E. Ehrenborg, A.L. Harris, C.R. Wolf, C.N. Palmer, Activation of peroxisome proliferator-activated receptor delta stimulates the proliferation of human breast and prostate cancer cell lines, Cancer Res. 64 (2004) 3162–3170.
[18] E.E. Girroir, H.E. Hollingshead, A.N. Billin, T.M. Willson, G.P. Robertson, A.K. Sharma, S. Amin, F.J. Gonzalez, J.M. Peters, Peroxisome proliferator-activated receptor-beta/delta (PPARbeta/delta) ligands inhibit growth of UACC903 and MCF7 human cancer cell lines, Toxicology 243 (2008) 236–243.
[19] J.E. Foreman, A.K. Sharma, S. Amin, F.J. Gonzalez, J.M. Peters, Ligand activation of peroxisome proliferator-activated receptor-beta/delta (PPARbeta/delta) inhibits cell growth in a mouse mammary gland cancer cell line, Cancer Lett. 288 (2010) 219–225.
[20] P.S. Palkar, M.G. Borland, S. Naruhn, C.H. Ferry, C. Lee, U.H. Sk, A.K. Sharma, S. Amin, I.A. Murray, C.R. Anderson, G.H. Perdew, F.J. Gonzalez, R. Muller, J.M. Peters, Cellular and pharmacological selectivity of the peroxisome proliferator-activated receptor-beta/delta antagonist GSK3787, Mol. Pharmacol. 78 (2010) 419–430.
[21] K.M. Suchanek, F.J. May, W.J. Lee, N.A. Holman, S.J. Roberts-Thomson, Peroxisome proliferator-activated receptor beta expression in human breast epithelial cell lines of tumorigenic and non-tumorigenic origin, Int. J. Biochem. Cell Biol. 34 (2002) 1051–1058.
[22] J.M. Peters, F.J. Gonzalez, Sorting out the functional role(s) of peroxisome proliferator-activated receptor-beta/delta (PPARbeta/delta) in cell proliferation and cancer, Biochim. Biophys. Acta 1796 (2009) 230–241.
[23] A. Barascu, P. Besson, O. Le Floch, P. Bougnoux, M.L. Jourdan, CDK1-cyclin B1 mediates the inhibition of proliferation induced by omega-3 fatty acids in MDA-MB-231 breast cancer cells, Int. J. Biochem. Cell Biol. 38 (2006) 196–208.
[24] K.S. Kang, P. Wang, N. Yamabe, M. Fukui, T. Jay, B.T. Zhu, Docosahexaenoic acid induces apoptosis in MCF-7 cells in vitro and in vivo via reactive oxygen species formation and caspase 8 activation, PLoS One 5 (2010) e10296.
[25] W. Jiang, Z. Zhu, J.N. McGinley, K. El Bayoumy, A. Manni, H.J. Thompson, Identification of a molecular signature underlying inhibition of mammary carcinoma growth by dietary N−3 fatty acids, Cancer Res. 72 (2012) 3795–3806.
[26] H.E. Xu, T.B. Stanley, V.G. Montana, M.H. Lambert, B.G. Shearer, J.E. Cobb, D.D. McKee, C.M. Galardi, K.D. Plunket, R.T. Nolte, D.J. Parks, J.T. Moore, S.A. Kliewer, T.M. Willson,

J.B. Stimmel, Structural basis for antagonist-mediated recruitment of nuclear co-repressors by PPARalpha, Nature 415 (2002) 813–817.
[27] B.G. Shearer, D.J. Steger, J.M. Way, T.B. Stanley, D.C. Lobe, D.A. Grillot, M.A. Iannone, M.A. Lazar, T.M. Willson, A.N. Billin, Identification and characterization of a selective peroxisome proliferator-activated receptor beta/delta (NR1C2) antagonist, Mol. Endocrinol. 22 (2008) 523–529.
[28] G. Lee, F. Elwood, J. McNally, J. Weiszmann, M. Lindstrom, K. Amaral, M. Nakamura, S. Miao, P. Cao, R.M. Learned, J.L. Chen, Y. Li, T0070907, a selective ligand for peroxisome proliferator-activated receptor gamma, functions as an antagonist of biochemical and cellular activities, J. Biol. Chem. 277 (2002) 19649–19657.
[29] S. Kornfeld, C. Goupille, S. Vibet, S. Chevalier, A. Pinet, J. Lebeau, F. Tranquart, P. Bougnoux, E. Martel, A. Maurin, S. Richard, P. Champeroux, K. Maheo, Reducing endothelial NOS activation and interstitial fluid pressure with n−3 PUFA offset tumor chemoresistance, Carcinogenesis 33 (2012) 260–267.
[30] D.J. Mangelsdorf, K. Umesono, S.A. Kliewer, U. Borgmeyer, E.S. Ong, R.M. Evans, A direct repeat in the cellular retinol-binding protein type II gene confers differential regulation by RXR and RAR, Cell 66 (1991) 555–561.
[31] S. Vibet, C. Goupille, P. Bougnoux, J.P. Steghens, J. Gore, K. Maheo, Sensitization by docosahexaenoic acid (DHA) of breast cancer cells to anthracyclines through loss of glutathione peroxidase (GPx1) response, Free Radic. Biol. Med. 44 (2008) 1483–1491.
[32] Y. Shi, M. Hon, R.M. Evans, The peroxisome proliferator-activated receptor delta, an integrator of transcriptional repression and nuclear receptor signaling, Proc. Natl. Acad. Sci. U.S.A. 99 (2002) 2613–2618.
[33] M.G. Borland, C. Khozoie, P.P. Albrecht, B. Zhu, C. Lee, T.S. Lahoti, F.J. Gonzalez, J.M. Peters, Stable over-expression of PPARbeta/delta and PPARgamma to examine receptor signaling in human HaCaT keratinocytes, Cell. Signal. 23 (2011) 2039–2050.
[34] M. Rieck, W. Meissner, S. Ries, S. Muller-Brusselbach, R. Muller, Ligand-mediated regulation of peroxisome proliferator-activated receptor (PPAR) beta/delta: a comparative analysis of PPAR-selective agonists and all-trans retinoic acid, Mol. Pharmacol. 74 (2008) 1269–1277.
[35] S. Colas, K. Maheo, F. Denis, C. Goupille, C. Hoinard, P. Champeroux, F. Tranquart, P. Bougnoux, Sensitization by dietary docosahexaenoic acid of rat mammary carcinoma to anthracycline: a role for tumor vascularization, Clin. Cancer Res. 12 (2006) 5879–5886.
[36] Z. Zhu, W. Jiang, J.N. McGinley, B. Prokopczyk, J.P. Richie Jr., K. El Bayoumy, A. Manni, H.J. Thompson, Mammary gland density predicts the cancer inhibitory activity of the N−3 to N−6 ratio of dietary fat, Cancer Prev. Res. 4 (2011) 1675–1685.

MOLECULAR CANCER

SHORT COMMUNICATION Open Access

Ranolazine inhibits $Na_V1.5$-mediated breast cancer cell invasiveness and lung colonization

Virginie Driffort[1], Ludovic Gillet[1], Emeline Bon[1], Séverine Marionneau-Lambot[2], Thibauld Oullier[2], Virginie Joulin[3], Christine Collin[4], Jean-Christophe Pagès[4,5], Marie-Lise Jourdan[1,4], Stéphan Chevalier[1,6], Philippe Bougnoux[1,4], Jean-Yves Le Guennec[7], Pierre Besson[1,6*†] and Sébastien Roger[1,8*†]

Abstract

Background: $Na_V1.5$ voltage-gated sodium channels are abnormally expressed in breast tumours and their expression level is associated with metastatic occurrence and patients' death. In breast cancer cells, $Na_V1.5$ activity promotes the proteolytic degradation of the extracellular matrix and enhances cell invasiveness.

Findings: In this study, we showed that the extinction of $Na_V1.5$ expression in human breast cancer cells almost completely abrogated lung colonisation in immunodepressed mice (NMRI nude). Furthermore, we demonstrated that ranolazine (50 μM) inhibited $Na_V1.5$ currents in breast cancer cells and reduced $Na_V1.5$-related cancer cell invasiveness *in vitro*. *In vivo*, the injection of ranolazine (50 mg/kg/day) significantly reduced lung colonisation by $Na_V1.5$-expressing human breast cancer cells.

Conclusions: Taken together, our results demonstrate the importance of $Na_V1.5$ in the metastatic colonisation of organs by breast cancer cells and indicate that small molecules interfering with Na_V activity, such as ranolazine, may represent powerful pharmacological tools to inhibit metastatic development and improve cancer treatments.

Keywords: $Na_V1.5$ voltage-gated sodium channels, Cancer cell invasiveness, Ranolazine, Metastases

Findings

Breast cancer is the primary cause of death by cancer in women worldwide and patients mostly die because of metastases appearance and development [1] which rely in part on the ability of cancer cells to degrade and migrate through extracellular matrices (ECM). Currently, there is no treatment for specifically inhibiting metastases development. Voltage-gated sodium channels (Na_V) are essential for action potential firing and as such are characteristic of excitable cells [2]. However, different Na_V isoforms have been found in non-excitable epithelial human cancer biopsies and cells, such as in breast [3,4], lung [5-7], prostate [8], cervix [9], ovarian [10,11] and colon cancer [12], and their function, through persistent currents at the membrane potential, enhances degradation of ECM [5,13-15]. Notably, the $Na_V1.5$ isoform is abnormally expressed in breast cancer biopsies, while it is not in non-cancerous mammary tissues [14], and its level of expression is associated with lymph node invasion, the development of metastases and a reduced survival of patients [3,16,17]. In cancer cells, it is expressed as a neonatal splice variant showing a 7-amino acid substitution in the segments S3 and S4 of the domain I (DI-S3-S4) of the protein compared to the adult variant that shows a particular pharmacology [18] and was proposed to serve as a metastatic marker [16]. $Na_V1.5$ is functional at the plasma membrane of highly invasive breast cancer cells [3,16,17], and its activity maintains a pro-invasive phenotype [15], related to "mesenchymal migration" [19]. Indeed, while the complete mechanism involved is not yet elucidated, $Na_V1.5$ activity was shown *i)* to control Src kinase activity, cortactin phosphorylation (Y421) and the subsequent polymerisation of actin filaments, *ii)* to increase the activity of the Na^+/H^+ exchanger type 1 (NHE-1), thus enhancing the efflux of protons and the proteolytic activity of extracellularly-released acidic cysteine cathepsins B and S [13,20]. Altogether, these results indicated that $Na_V1.5$ promotes

* Correspondence: pierre.besson@univ-tours.fr; sebastien.roger@univ-tours.fr
†Equal contributors
[1]Inserm UMR1069, Nutrition, Croissance et Cancer, Université François-Rabelais de Tours, 10 Boulevard Tonnellé, Tours 37032, France
Full list of author information is available at the end of the article

the invadopodial activity of breast cancer cells and the invasion of the surrounding ECM [15]. Molecules reducing its activity, such as tetrodotoxin, reduce cancer cell invasiveness *in vitro* [3,14,18]. Correlatively, molecules that increase its activity, such as veratridine, enhance ECM invasion [13]. However, to the best of our knowledge, the importance of $Na_V1.5$ expression, and the relevance for its pharmacological inhibition, on the metastatic organ colonisation by breast cancer cells have never been reported so far. Ranolazine is an antiarrhythmic drug indicated for the treatment of chronic angina that was approved by the Food and Drug Administration (FDA) in 2006. While it is proposed to have several pharmacological actions, its best characterized one is the selective inhibition of late sodium currents [21]. This leads to a steeper Na^+ gradient which, by increasing the activity of the Na^+/Ca^{2+} exchanger (NCX), reduces calcium overload, and improves ventricular relaxation in pathological conditions associated with cardiac ischemia [22].

In this study we investigated how $Na_V1.5$ expression in human breast cancer cells affected metastatic colonisation of organs in immunodepressed mice, and whether its pharmacological inhibition by ranolazine reduced cancer cell invasiveness both *in vitro* and *in vivo*.

Highly invasive MDA-MB-231 human breast cancer cells express mRNA for $Na_V1.5$, $Na_V1.6$ and $Na_V1.7$ channels [16], but only $Na_V1.5$ channels are functional at the plasma membrane and are giving rise to transient inward sodium currents (INa) under voltage-clamp procedures [13] (see Additional file 1: Material and methods). INa-voltage (INa-V) protocols were performed using the whole-cell configuration of the patch clamp technique from MDA-MB-231-Luc cells modified to stably express a null-target small hairpin RNA (shCTL). The INa-V relationship, obtained from a holding potential of −100 mV, indicated a threshold of activation around −60 mV and maximal current of −12.1 ± 2.2 pA/pF at a voltage of −10 mV (Figure 1A). The acute application of ranolazine

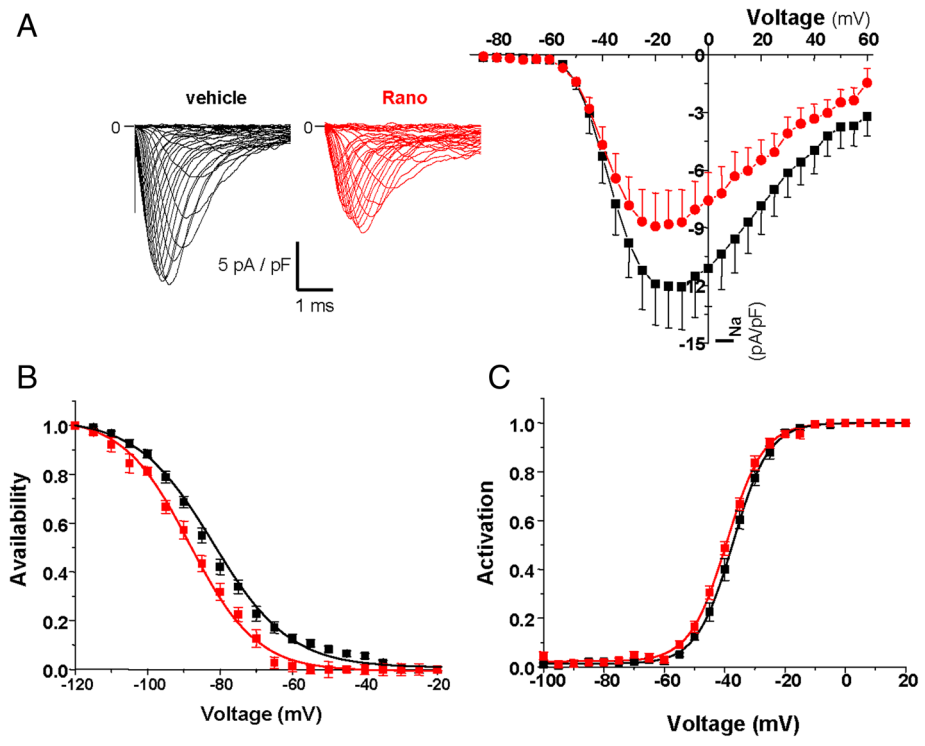

Figure 1 Ranolazine inhibits sodium current in human breast cancer cells. Sodium currents (INa) from MDA-MB-231 breast cancer cells stably expressing null target shRNA (shCTL) were studied in voltage-clamp mode with the whole-cell configuration of the patch clamp technique. **A**, Left, representative INa-voltage traces obtained from one cell before (vehicle) and after 50 μM ranolazine treatment (Rano). Right, mean ± s.e.m. steady-state INa-voltage relationships obtained from cancer cells before and after incubation with 50 μM ranolazine (n = 12 cells) from a holding potential of −100 mV. There is as statistical difference between the two conditions for voltages ranging from −35 to +40 mV ($p < 0.001$, Wilcoxon test). **B**, Availability-voltage relationships obtained in presence (red trace) or not (vehicle, black trace) of 50 μM ranolazine. There is a significant leftward shift of the availability-voltage relationship in presence of ranolazine ($p < 0.001$). The half (1/2)-inactivation voltage was shifted from −84.1 ± 1.4 mV to −90.3 ± 1.7 mV in absence and presence of ranolazine, respectively. **C**, Activation-voltage relationships obtained in presence (red trace) or not (vehicle, black trace) of 50 μM ranolazine. There is a significant leftward shift of the activation-voltage relationship in presence of ranolazine, and the 1/2-activation voltage was shifted from −37.1 ± 1.0 mV to −39.2 ± 0.6 mV in absence and presence of ranolazine, respectively. ($p < 0.01$, Wilcoxon test).

(50 μM) significantly reduced the maximal amplitude to −8.7 ± 1.7 pA/pF ($p < 0.001$). This decrease in the maximal current amplitude was associated with a significant leftward shift of the availability-voltage relationship (Figure 1B). The half (1/2)-inactivation voltage was shifted from −84.1 ± 1.4 mV to −90.3 ± 1.7 mV ($p < 0.001$) in absence and presence of ranolazine, respectively. The activation-voltage relationship was significantly modified (Figure 1C), and the 1/2-activation voltage was shifted from −37.1 ± 1.0 mV to −39.2 ± 0.6 mV ($p < 0.01$). Therefore, ranolazine reduced efficiently the activity of the neonatal $Na_V1.5$ isoform expressed in human breast cancer cells. This isoform is the only one to be functional in breast cancer cells [13,16] and we selected a population of cells stably expressing a small hairpin RNA targeting its expression ($shNa_V1.5$) after lentiviral transduction. This led to a significant 89 ± 1% decrease of $Na_V1.5$ mRNA expression (Figure 2A), resulting in the complete disappearance of sodium currents in almost all cancer cells (Figure 2B), with no effect on cell viability (Figure 2C). Before assessing the effect of ranolazine in reducing cancer cell invasiveness, we addressed a possible cytotoxic effect of its application. Figure 2D indicates that ranolazine, incubated for 5 days in a range of concentration from 0.1 to 100 μM had no effect on cell viability. It was then used at 50 μM in the 24 h invasion experiment with Matrigel™-coated filters (Figure 2E). In shCTL cells, cell invasiveness was reduced by 35 ± 4% with

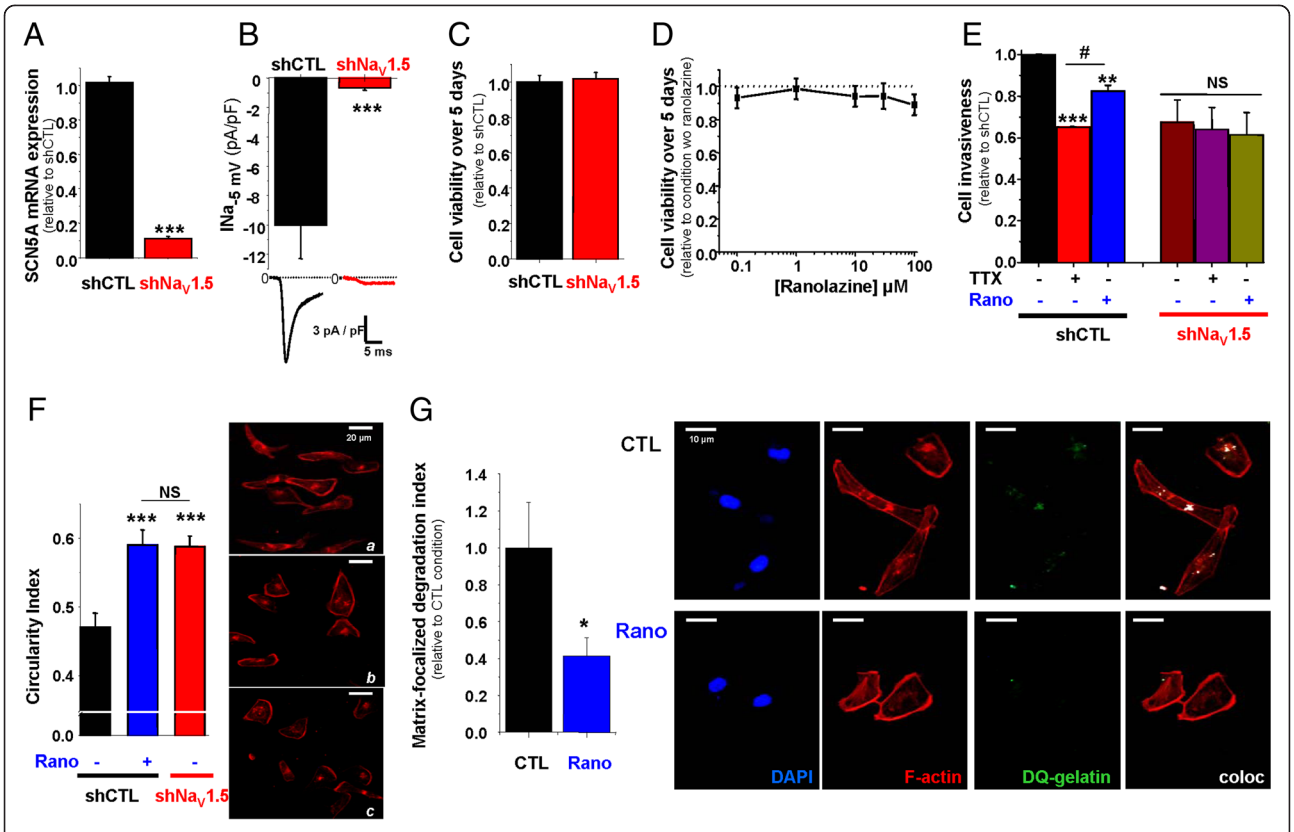

Figure 2 Ranolazine inhibits the $Na_V1.5$-mediated breast cancer cell invasiveness *in vitro*. **A**, *SCN5A* mRNA expression assessed by real-time qPCR in shCTL and $shNa_V1.5$ cells (n = 10 separate experiments) and compared with a Mann–Whitney test. **B**, Mean ± s.e.m. peak INa recorded in 23 shCTL cells and in 20 $shNa_V1.5$ cells under a depolarization from −100 to −5 mV (Mann–Whitney test). Representative currents are shown underneath. **C**, shCTL and $shNa_V1.5$ cell growth and viability after 5 days, expressed relative to the shCTL cell line (n = 3 independent experiments). **D**, Cell viability of shCTL after 5 days of growth in presence of increasing concentrations of ranolazine, from 0.1 to 100 μM, and expressed relative to the control condition without ranolazine (vehicle). **E**, Effect of 30 μM tetrodotoxin (TTX) or 50 μM ranolazine (Rano) on shCTL and $shNa_V1.5$ human breast cancer cell invasiveness (Kruskal-wallis analysis followed by a Dunn's test). **F**, shCTL and $shNa_V1.5$ cells were cultured for 24 h on a Matrigel™-composed matrix treated with 50 μM ranolazine (Rano) or not. F-actin cytoskeleton was stained with phalloidin-AlexaFluor594. A cell circularity index was calculated using ImageJ© software (n = 138–238 cells analysed, Mann–Whitney test). **G**, shCTL cells were cultured on a Matrigel™-composed matrix containing DQ-Gelatin® for 24 h in presence or not of 50 μM ranolazine. A "Matrix-Focalized-degradation activity index" was calculated as being the number of pixels corresponding to the co-localization of F-actin condensation areas (F-actin cytoskeleton was stained with phalloidin-Alexa594) and focal spots of DQ-gelatin proteolysis (coloc) (7). Results are expressed relative to the control condition (CTL, N = 534 cells) without ranolazine (Rano, N = 375 cells) and compared using Mann–Whitney test. Representative pictures are shown on the left. Statistical significance is indicated as: *p <0.05; **p < 0.01 and ***p < 0.001. NS stands for not statistically different.

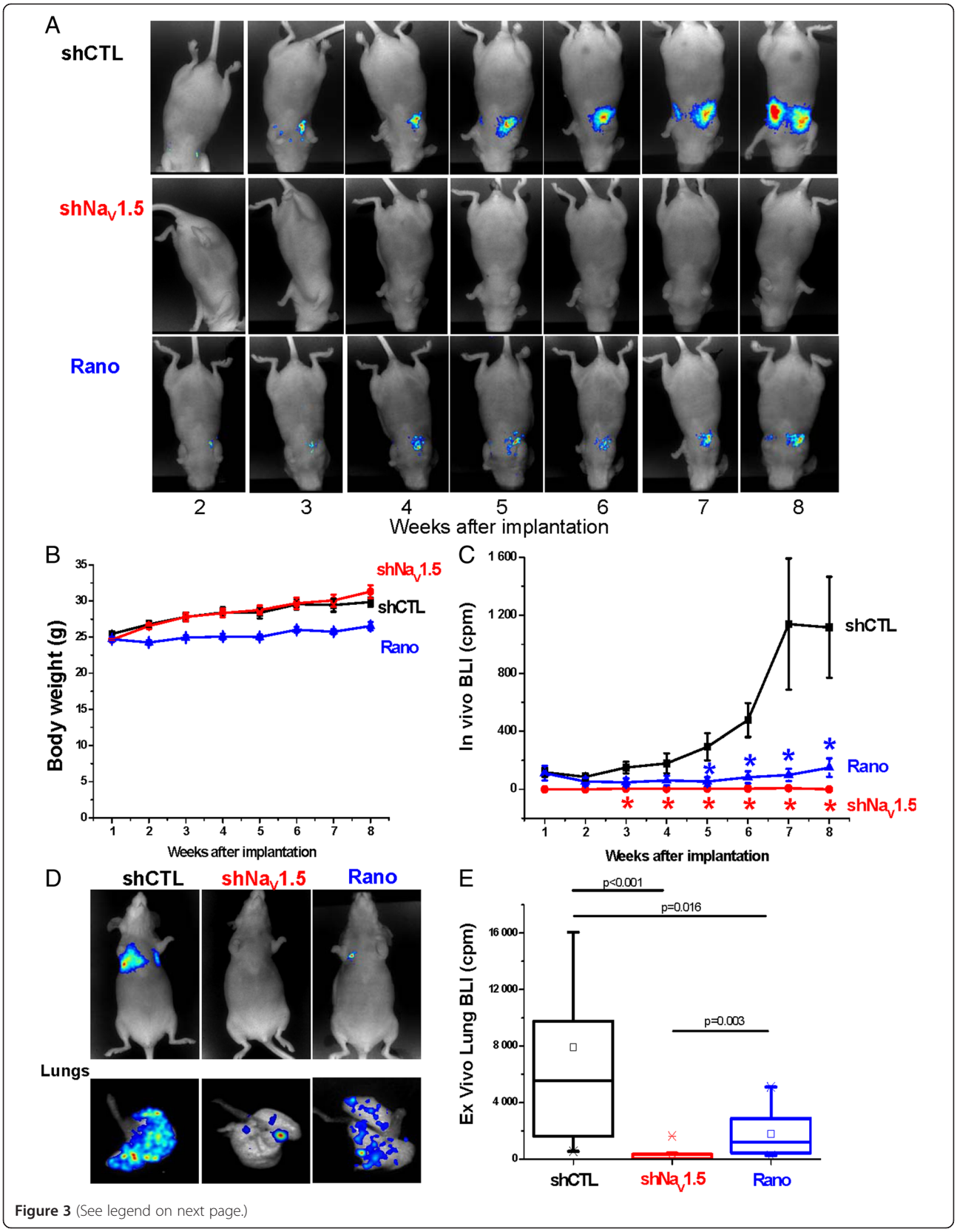

Figure 3 (See legend on next page.)

(See figure on previous page.)
Figure 3 $Na_V1.5$ suppression, or ranolazine treatment, inhibit metastatic lung colonisation by breast cancer cells. A, Representative bioluminescent imaging (BLI) measurement performed in the same NMRI nude mouse per condition from week 2 to week 8 after cancer cell injection. Mice were injected with shCTL MDA-MB-231-Luc cells (shCTL), or with $shNa_V1.5$ MDA-MB-231-Luc cells ($shNa_V1.5$) or with shCTL MDA-MB-231-Luc cells and treated (5 days/week) with ranolazine (50 mg/kg) (Rano) or vehicle (shCTL, $shNa_V1.5$). **B**, Evolution of mice body weight during the experiments in the same conditions than in A. **C**, Mean *in vivo* BLI value (expressed in cpm) as a function of time recorded in the whole body of mice coming from the three groups indicated previously (shCTL, n = 18; $shNa_V1.5$, n = 12; Rano, n = 8) (Statistical significance is indicated as: *p <0.05, Kruskal-Wallis analysis followed by Dunn's test). **D**, Representative BLI at completion of the study (8^{th} week after cells injection), in whole animals and *ex vivo* after lung isolation. **E**, BLI quantification of excised lungs. Box plots indicate the first quartile, the median, and the third quartile, squares indicate the mean (shCTL, n = 18; $shNa_V1.5$, n = 12; Rano, n = 8) (Kruskal-Wallis analysis followed by Dunn's test).

the total inhibition of $Na_V1.5$ currents with 30 μM tetrodotoxin (TTX), and by 18 ± 3% with ranolazine. In comparison to shCTL cells, $shNa_V1.5$ cancer cells, which do not express $Na_V1.5$, had a reduced invasiveness of 33 ± 10%. In $shNa_V1.5$ cells, both TTX and ranolazine were ineffective to further reduce cell invasiveness, suggesting that ranolazine was specific in inhibiting $Na_V1.5$-related invasion. $Na_V1.5$ expression and activity was recently shown to control the acquisition of a pro-invasive phenotype, by maintaining a spindle-shape morphology and by controlling the ECM proteolysis by MDA-MB-231 cancer cells [15]. We found that ranolazine increased the circularity of shCTL cells, thus decreasing the pro-invasive morphology, to the same extent as the complete extinction of $Na_V1.5$ expression (Figure 2F). Furthermore, ranolazine reduced the focal ECM degradative activity of shCTL cells by 58.6 ± 10.0% (Figure 2G). This activity, which is related to the invadopodial activity, was monitored as being the release of fluorescence from DQ-gelatin at focal sites of F-actin polymerisation as previously described [15].

Because $Na_V1.5$ was proposed to promote metastases development from breast tumours, we assessed the importance of its expression in human breast cancer cells for the colonisation of organs. ShCTL or $shNa_V1.5$ cells, both expressing the luciferase gene, were injected in the tail vein of NMRI nude mice. A third experimental group was set with mice injected with shCTL cells and receiving a daily intraperitoneal injection of ranolazine (50 mg/Kg – 5 days per week). The colonisation of mice organs by human cancer cells was followed *in vivo*, every week for a total duration of 8 weeks, by bioluminescent imaging (BLI) after luciferin injection (Figure 3A). There was no statistical difference in the evolution of animal body weights between the three groups (Figure 3B). BLI performed in living animals indicated that shCTL cells, which express $Na_V1.5$, strongly colonised and developed into the chest area (which was the case for 17 out of 18 mice). In contrast, $shNa_V1.5$ cells led to a very weak signal (1/12 mice) or no signal at all (11/12 mice) in the chest area. Ranolazine, which inhibited $Na_V1.5$ currents (Figure 1), significantly reduced total BLI signal in mice injected with shCTL cells. *In vitro*, ranolazine treatment did not interfere with luciferase activity in shCTL cells (Additional file 2: Figure S1) indicating that the BLI signal recorded was indeed strongly correlated with the abundance of cancer cells in mice organs. In this experimental group, BLI signal was recorded in 5 out of 8 mice (Figure 3C). At completion of the study, mice were sacrificed and isolated organs (lungs, brain, liver, bones from rachis/ribs and legs) were analysed *ex vivo*. In the shCTL group, all mice showed lung colonisation (18/18) and a small proportion also had bioluminescent signal in rachis and ribs (2/18) and in leg bones (2/18). In the $shNa_V1.5$ group, 7 mice out of 12 had lung colonisation and one (1/12) had bioluminescent signal in rachis and ribs. In the ranolazine group, although 8/8 mice presented lung colonisation, bioluminescence was dramatically reduced by 77 ± 8%, at a level similar to the experimental suppression of $Na_V1.5$ (inhibition of lung BLI by 97 ± 2%) (Figure 3D, 3E). In the ranolazine group, mice did not show BLI signal in other organs.

While it is now well-established that Na_V channels are anomalously expressed in several epithelial tumours and are associated with metastasis occurrence and patient mortality [12,16,17,23], the consequence of their expression on metastatic organ colonisation was not demonstrated so far. To our knowledge, this study is the first to clearly establish a link between $Na_V1.5$ expression in human breast cancer cells and the colonisation of lungs *in vivo*. Furthermore, this study using ranolazine, a drug that is clinically used, shows that the pharmacological inhibition of Na_V channels could be effective in reducing metastatic colonisation with no apparent toxic effect. In conclusion, this study opens a new therapeutical concept for the management of cancer disease. Inhibitors of Na_V channels, already approved for other clinical use such as antiarrhythmics, anticonvulsants [17] or anaesthetics [24], or new molecules that are even more effective in blocking neonatal variants, could be of high interest in the prevention and/or reduction of metastatic spreading of cancer cells at the diagnosis of the primary tumour.

Additional files

Additional file 1: Materials and methods.

Additional file 2: Figure S1. MDA-MB-231-shCTL cells expressing luciferase gene were seeded at different densities then treated for 24h with Ranolazine (50 μM, red circles) or not (black squares).

Abbreviations

BLI: Bioluminescent imaging; ECM: Extracellular matrix; INa: Sodium currents; Na_V: Voltage-gated sodium channels; TTX: Tetrodotoxin.

Competing interests

The authors declare that they have no competing interests.

Authors' contributions

VD, LG and EB performed *in vitro* experiments. VD, SM-L and TO performed *in vivo* experiments. VD, CC, VJ, J-CP. and M-LJ designed, produced shRNA, and participated to the selection of cell lines, SC, PB, and J-YLG contributed to the design of the study. Data were conceived, analyzed and interpreted by VD, PB and SR Overall supervision of the study was performed by PB and SR Paper was written by PB and SR, read and corrected by all authors. All authors read and approved the final manuscript.

Acknowledgements

This work was supported by "Ministère de la Recherche et des Technologies", Inserm, "Ligue Nationale Contre le Cancer", Région Centre (grant "Na_VMetarget" and LIPIDS project of ARD2020-Biomedicaments) and "Association CANCEN". We thank I. Domingo and C. Le Roy for technical and administrative assistance. We thank Prof. W.J. Brouillette (University of Alabama, USA) for helpful comments about the manuscript.

Author details

[1]Inserm UMR1069, Nutrition, Croissance et Cancer, Université François-Rabelais de Tours, 10 Boulevard Tonnellé, Tours 37032, France. [2]Cancéropôle du Grand Ouest, Nantes, France. [3]Inserm U1009, Institut Gustave Roussy, Villejuif, France. [4]CHRU de Tours, Tours, France. [5]Inserm, U966, Université François-Rabelais de Tours, Tours, France. [6]UFR Sciences Pharmaceutiques, Université François-Rabelais de Tours, Tours, France. [7]Inserm U1046, Université de Montpellier-1, Université de Montpellier-2, Montpellier, France. [8]UFR Sciences et Techniques, Département de Physiologie Animale, Université François-Rabelais de Tours, Tours, France.

Received: 28 August 2014 Accepted: 3 December 2014
Published: 11 December 2014

References

1. Parkin DM, Bray F, Ferlay J, Pisani P: **Global cancer statistics, 2002.** *CA Cancer J Clin* 2005, **55:**74–108.
2. Catterall WA: **Voltage-gated sodium channels at 60: structure, function, and pathophysiology.** *J Physiol* 2012.
3. Roger S, Besson P, Le Guennec JY: **Involvement of a novel fast inward sodium current in the invasion capacity of a breast cancer cell line.** *Biochim Biophys Acta* 2003, **1616:**107–111.
4. Brackenbury WJ, Chioni AM, Diss JK, Djamgoz MB: **The neonatal splice variant of Nav1.5 potentiates in vitro invasive behaviour of MDA-MB-231 human breast cancer cells.** *Breast Cancer Res Treat* 2007, **101:**149–160.
5. Roger S, Rollin J, Barascu A, Besson P, Raynal PI, Iochmann S, Lei M, Bougnoux P, Gruel Y, Le Guennec JY: **Voltage-gated sodium channels potentiate the invasive capacities of human non-small-cell lung cancer cell lines.** *Int J Biochem Cell Biol* 2007, **39:**774–786.
6. Pancrazio JJ, Viglione MP, Tabbara IA, Kim YI: **Voltage-dependent ion channels in small-cell lung cancer cells.** *Cancer Res* 1989, **49:**5901–5906.
7. Onganer PU, Djamgoz MB: **Small-cell lung cancer (Human): potentiation of endocytic membrane activity by voltage-gated Na(+) channel expression in vitro.** *J Membr Biol* 2005, **204:**67–75.
8. Diss JK, Stewart D, Pani F, Foster CS, Walker MM, Patel A, Djamgoz MB: **A potential novel marker for human prostate cancer: voltage-gated sodium channel expression in vivo.** *Prostate Cancer Prostatic Dis* 2005, **8**(3):266–273.
9. Hernandez-Plata E, Ortiz CS, Marquina-Castillo B, Medina-Martinez I, Alfaro A, Berumen J, Rivera M, Gomora JC: **Overexpression of NaV 1.6 channels is associated with the invasion capacity of human cervical cancer.** *Int J Cancer* 2012, **130:**2013–2023.
10. Gao R, Shen Y, Cai J, Lei M, Wang Z: **Expression of voltage-gated sodium channel alpha subunit in human ovarian cancer.** *Oncol Rep* 2010, **23:**1293–1299.
11. Frede J, Fraser SP, Oskay-Ozcelik G, Hong Y, Ioana Braicu E, Sehouli J, Gabra H, Djamgoz MB: **Ovarian cancer: Ion channel and aquaporin expression as novel targets of clinical potential.** *Eur J Cancer* 2013, **49:**2331–2344.
12. House CD, Vaske CJ, Schwartz AM, Obias V, Frank B, Luu T, Sarvazyan N, Irby R, Strausberg RL, Hales TG, Stuart JM, Lee NH: **Voltage-gated Na + channel SCN5A is a key regulator of a gene transcriptional network that controls colon cancer invasion.** *Cancer Res* 2010, **70:**6957–6967.
13. Gillet L, Roger S, Besson P, Lecaille F, Gore J, Bougnoux P, Lalmanach G, Le Guennec JY: **Voltage-gated sodium channel activity promotes cysteine cathepsin-dependent invasiveness and colony growth of human cancer cells.** *J Biol Chem* 2009, **284:**8680–8691.
14. Roger S, Potier M, Vandier C, Besson P, Le Guennec JY: **Voltage-gated sodium channels: new targets in cancer therapy?** *Curr Pharm Des* 2006, **12:**3681–3695.
15. Brisson L, Driffort V, Benoist L, Poet M, Counillon L, Antelmi E, Rubino R, Besson P, Labbal F, Chevalier S, Reshkin SJ, Gore J, Roger S: **NaV1.5 Na + channels allosterically regulate the NHE-1 exchanger and promote the activity of breast cancer cell invadopodia.** *J Cell Sci* 2013, **126:**4835–4842.
16. Fraser SP, Diss JK, Chioni AM, Mycielska ME, Pan H, Yamaci RF, Pani F, Siwy Z, Krasowska M, Grzywna Z, Brackenbury WJ, Theodorou D, Koyutürk M, Kaya H, Battaloglu E, De Bella MT, Slade MJ, Tolhurst R, Palmieri C, Jiang J, Latchman DS, Coombes RC, Djamgoz MB: **Voltage-gated sodium channel expression and potentiation of human breast cancer metastasis.** *Clin Cancer Res* 2005, **11:**5381–5389.
17. Yang M, Kozminski DJ, Wold LA, Modak R, Calhoun JD, Isom LL, Brackenbury WJ: **Therapeutic potential for phenytoin: targeting Na(v)1.5 sodium channels to reduce migration and invasion in metastatic breast cancer.** *Breast Cancer Res Treat* 2012, **134**(2):603–615.
18. Roger S, Guennec JY, Besson P: **Particular sensitivity to calcium channel blockers of the fast inward voltage-dependent sodium current involved in the invasive properties of a metastastic breast cancer cell line.** *Br J Pharmacol* 2004, **141:**610–615.
19. Friedl P, Alexander S: **Cancer invasion and the microenvironment: plasticity and reciprocity.** *Cell* 2011, **147:**992–1009.
20. Brisson L, Gillet L, Calaghan S, Besson P, Le Guennec JY, Roger S, Gore J: **Na(V)1.5 enhances breast cancer cell invasiveness by increasing NHE1-dependent H(+) efflux in caveolae.** *Oncogene* 2011, **30:**2070–2076.
21. Antzelevitch C, Belardinelli L, Zygmunt AC, Burashnikov A, Di Diego JM, Fish JM, Cordeiro JM, Thomas G: **Electrophysiological effects of ranolazine, a novel antianginal agent with antiarrhythmic properties.** *Circulation* 2004, **110:**904–910.
22. Fraser H, Belardinelli L, Wang L, Light PE, McVeigh JJ, Clanachan AS: **Ranolazine decreases diastolic calcium accumulation caused by ATX-II or ischemia in rat hearts.** *J Mol Cell Cardiol* 2006, **41:**1031–1038.
23. Diaz D, Delgadillo DM, Hernandez-Gallegos E, Ramirez-Dominguez ME, Hinojosa LM, Ortiz CS, Berumen J, Camacho J, Gomora JC: **Functional expression of voltage-gated sodium channels in primary cultures of human cervical cancer.** *J Cell Physiol* 2007, **210:**469–478.
24. Baptista-Hon DT, Robertson FM, Robertson GB, Owen SJ, Rogers GW, Lydon EL, Lee NH, Hales TG: **Potent inhibition by ropivacaine of metastatic colon cancer SW620 cell invasion and NaV1.5 channel function.** *Br J Anaesth* 2014, **113**(Suppl 1):i39–i48.

doi:10.1186/1476-4598-13-264
Cite this article as: Driffort *et al.*: Ranolazine inhibits $Na_V1.5$-mediated breast cancer cell invasiveness and lung colonization. *Molecular Cancer* 2014 **13**:264.

Pflugers Arch - Eur J Physiol
DOI 10.1007/s00424-014-1573-4

Suppression of PPARβ, and DHA treatment, inhibit $Na_V1.5$ and NHE-1 pro-invasive activities

Ramez Wannous · Emeline Bon · Ludovic Gillet · Julie Chamouton · Günther Weber · Lucie Brisson · Jacques Goré · Philippe Bougnoux · Pierre Besson · Sébastien Roger · Stephan Chevalier

Received: 15 April 2014 / Revised: 10 June 2014 / Accepted: 1 July 2014

Abstract Peroxisome proliferator-activated receptor β (PPARβ) and $Na_V1.5$ voltage-gated sodium channels have independently been shown to regulate human breast cancer cell invasiveness. The n-3 polyunsaturated docosahexaenoic acid (DHA, 22:6n-3), a natural ligand of PPAR, is effective in increasing survival and chemotherapy efficacy in breast cancer patient with metastasis. DHA reduces breast cancer cell invasiveness and it also inhibits PPARβ expression. We have shown previously that $Na_V1.5$ promotes MDA-MB-231 breast cancer cells invasiveness by potentiating the activity of Na^+/H^+ exchanger type 1 (NHE-1), the major regulator of H^+ efflux in these cells. We report here that DHA inhibited $Na_V1.5$ current and NHE-1 activity in human breast cancer cells, and in turn reduced $Na_V1.5$-dependent cancer cell invasiveness. For the first time, we show that antagonizing PPARβ, or inhibiting its expression, reduced $Na_V1.5$ mRNA and protein expression and $Na_V1.5$ current, as well as NHE-1 activity and cell invasiveness. Consistent with these results, the DHA-induced reduction of both $Na_V1.5$ expression and NHE-1 activity was abolished in cancer cells knocked-down for the expression of PPARβ (shPPARβ). This demonstrates a direct link between the inhibition of PPARβ expression and the inhibition of Nav1.5/NHE-1 activities and breast cancer cell invasiveness. This study provides new mechanistic data advocating for the use of natural fatty acids such as DHA to block the development of breast cancer metastases.

Keywords PPARβ · $Na_V1.5$ · NHE-1 · DHA · n-3 PUFA · MDA-MB-231

Introduction

The effect of anticancer drugs on breast cancer cell lines and rodent mammary tumors can be enhanced by a treatment with long-chain n-3 polyunsaturated fatty acids (n-3 PUFA) such as docosahexaenoic acid (DHA, 22:6n-3) or eicosapentaenoic acid (EPA, 20:5n-3) [8, 21]. A diet enriched in those n-3 PUFA increased survival and chemotherapy efficacy in breast cancer patients with severe metastatic disease [7]. In fact, supplementations of the diets or culture media with DHA were sufficient to reduce rodent mammary tumor growth [25], human breast cancer cell growth [4, 42], cell migration [24], and invasiveness [5, 29]. DHA is a natural ligand of peroxisome proliferator-activated receptors (PPAR) [17, 30, 41, 45]. DHA-induced inhibition of cell growth can be abrogated by an antagonist of peroxisome proliferator-activated receptor β (PPARβ) [42], suggesting that DHA modulates the expression of PPARβ target genes. PPARβ (also known as PPARδ or PPARβ/δ), as the other two PPAR (PPARα and PPARγ), binds to the PPAR response element (PPRE) in promoters of

Electronic supplementary material The online version of this article (doi:10.1007/s00424-014-1573-4) contains supplementary material, which is available to authorized users.

R. Wannous · E. Bon · J. Chamouton · G. Weber · J. Goré · P. Bougnoux · P. Besson · S. Roger · S. Chevalier
Inserm UMR1069 "Nutrition, Croissance et Cancer", Faculté de Médecine, Université François Rabelais de Tours, Paris, France

L. Gillet
Department of Clinical Research, Ion Channel Research Group, University of Bern, 3010 Bern, Switzerland

L. Brisson
Institut de Recherche Expérimentale et Clinique (IREC), Université catholique de Louvain, Brussels, Belgium

P. Bougnoux
Hôpital Bretonneau, CHU de Tours, Paris, France

S. Chevalier (✉)
Laboratoire de Biochimie, Faculté de Sciences Pharmaceutiques, Université François Rabelais de Tours, Paris, France
e-mail: stephan.chevalier@univ-tours.fr

Published online: 15 July 2014

numerous genes regulating cell survival, metabolism, or inflammation [32].

Many potential target genes involved in DHA [25] or PPARβ responses [2, 49] have been described in genome-wide type of studies performed in mammary tumor models and *SCN5A*, coding for $Na_V1.5$ voltage-gated sodium channel, is of particular interest for several reasons. Firstly, in HEK293 cells stably transfected with human adult *SCN5A* splice variant ($aNa_V1.5$), both $Na_V1.5$-related peak currents and veratridine-induced late currents are reduced by DHA or EPA in acute treatments, but not by monounsaturated fatty acid oleic acid (OA, 18:1n-9) or the saturated fatty acids stearic acid and palmitic acid [33, 44]. Secondly, *SCN5A* is abnormally highly expressed as a neonatal splice variant $nNa_V1.5$ [18] in breast cancer tissues and in highly invasive MDA-MB-231 breast cancer cells, and it is associated with the development of metastases [9, 18, 46]. Thirdly, we have shown previously that $nNa_V1.5$ is functional in highly invasive human breast cancer cells, such as MDA-MB-231 cells, but not in non-cancer or in weakly invasive cancer cells [35]. Its activity increases cell invasiveness through perimembrane acidification and subsequent degradation of the extracellular matrix (ECM) by cysteine cathepsins [10, 11, 19]. Furthermore, $Na_V1.5$ interacts with and potentiates the ubiquitous Na^+/H^+ exchanger type 1 (NHE-1, the major regulator of H^+ efflux in MDA-MB-231 cells) activity in plasma membrane rafts in focal ECM degradation sites corresponding to caveolin-1-containing invadopodia [10, 11]. Small interfering RNA (siRNA) targeting $Na_V1.5$ also reduces NHE-1 activity and cancer cell invasiveness [10]. Finally, Isbilen et al. (2006) reported that a 48 h treatment with 0.5 μM DHA inhibits $Na_V1.5$ messenger RNA (mRNA) and protein expression as well as MDA-MB-231 cell migration [24], but the potential effect of DHA or PPARβ on $Na_V1.5$ current and NHE-1 activity in breast cancer cells have not been investigated so far.

The objectives of the present study were to investigate if PPARβ mediates the effect of DHA on breast cancer cell invasiveness and if such anti-invasive effect of DHA is caused by PPARβ-dependent inhibition of $Na_V1.5$ expression and/or channel activity, and/or NHE-1 dependent H^+ efflux.

Materials and methods

Reagents

PPARβ antagonist GSK0660 [37] dissolved in 100 % DMSO, docosahexaenoic acid methyl ester or ethyl ester (DHA; 22:6n-3), oleic acid methyl ester (OA; 18:9n-1), DHA sodium salt, and $Na_V1.5$ antibodies (S0819) were from Sigma-Aldrich (Saint Quentin Fallavier, France). Fatty acids were purified by thin layer chromatography in our laboratory prior to using for cell culture (long-term treatment) or patch-clamp experiments (short-term and acute treatment). Fatty acids were therefore highly pure and devoid of oxidized derivatives. Fatty acids methyl or ethyl esters were dissolved in 100 % ethanol and sodium salts dissolved in patch-clamp physiological saline solution buffered at pH 7.4. Fatty acids were assayed by gas chromatography prior to making desired concentration of working solution. SiRNA (sc-37007 for siCTL and sc-36305 for siPPARβ), shCTL (sc-108080), shPPARβ (sc-36305-V), PPARβ antibodies (sc-7197), and puromycin dihydrochloride (sc-108071) were from Tebu-Bio (Le Perray en Yvelines, France). TTX was purchased from Latoxan (Valence, France) and was prepared in pH-buffered physiological saline solution at pH 7.4. Matrigel™ matrix and DQ-Gelatin® were from Invitrogen (Illkirch, France).

Cell culture and treatments

The human breast carcinoma cell line MDA-MB-231 (American Type Culture Collection, Promochem, France) was cultured in Dulbecco's Modified Eagle's Medium (DMEM; Cambrex BioScience, France) supplemented with 5 % fetal calf serum (Invitrogen, France). Cell growth was assessed with the tetrazolium salt [3-(4,5-dimethylthiazol-2-yl)-2,5-diphenyltetrazolium bromide] assay as described previously [4, 42]. MDA-MB-231 cells were transduced with lentiviral particles coding for a short hairpin shRNA designed to knock down PPARβ expression (shPPARβ), or shCTL, and cells permanently expressing shPPARβ, or shCTL, were selected with puromycin dihydrochloride as described previously [10].

RNA extraction, PCR, and western blotting

Total RNA were extracted using NucleoSpin ®RNA II Columns (Macherey-Nagel, Hoerdt, France) and reverse-transcribed with a RT kit in the presence of random hexamers pd (N) 6 50-Phosphate (RevertAid First Stand cDNA Synthesis Kit, Thermo Scientific, France). Quantitative (real time) PCR experiments were performed in duplicate with MyiQ thermocycler (Biorad, Marne-la-coquette, France) using SYBR® Primex Ex Taq ™ kit (Takara Bio Ing, France). PPARβ, $Na_V1.5$, and NHE-1 mRNA relative expressions were assessed by RTqPCR, and mRNA amounts were expressed relatively to HPRT1 mRNA expression and control condition as relative quantity $Q=2^{-\Delta\Delta Ct}$ as previously described [11, 19, 42]. Western blotting was performed as previously described [11].

Electrophysiology

Patch pipettes were pulled from borosilicate glass to a resistance of 4–6 MΩ, and currents were recorded using an Axopatch 200B amplifier (Axon Instrument, Foster City,

USA). Cell capacitance and series resistance were electronically compensated by approximately 60 %. Na^+ currents (I_{Na}) were studied as already described [19], and amplitudes were expressed as current density (pA/pF). The physiological saline solution (PSS) had the following composition (in mM): NaCl 140, KCl 4, $MgCl_2$ 1, $CaCl_2$ 2, D-Glucose 11.1, and 4-(2-hydroxyethyl)-1- piperazine ethanesulfonic acid (HEPES) 10, adjusted to pH 7.4. The intra pipette solution had the following composition (in mM): K-Glutamate 125, KCl 20, $CaCl_2$ 0.37, $MgCl_2$ 1, Mg-ATP 1, EGTA 1, and HEPES 10, adjusted to pH 7.2.

Membrane fractionation and measurement of DHA enrichment in cell membrane phospholipids

Plasma membranes were fractionated to isolate raft versus non-raft fractions as previously described [11, 12] after extraction in 500 mM Na_2CO_3 (pH 11) containing 0.5 mM EDTA and 1 % protease inhibitor cocktail (Sigma-Aldrich). Cells were scrapped then sonicated. Two milliliters homogenate were mixed with an equal volume of 90 % sucrose in MES-buffered saline solution (25 mM MES, 150 mM NaCl, 2 mM EDTA, and pH 6.5) to form a 45 % sucrose solution. A discontinuous sucrose gradient was created by layering onto this a further 4 mL each of 35 and 5 % sucrose solutions (MES-buffered saline with 250 mM Na_2CO_3). Gradients were centrifuged for 17 h at 280,000×*g* at 4 °C, after which raft and non-raft membrane fractions were collected. The fatty acid composition of membrane phospholipids was assessed as previously described [4]. Briefly, lipids were extracted following the Bligh and Dyer method [6]. Total phospholipids were purified by thin layer chromatography and transmethylated with a solution of 14 % boron trifluoride in methanol to produce fatty acid methyl esters. Fatty acid methyl esters were separated, identified, and quantified by gas chromatography. The DHA content in membrane phospholipids was expressed as mol% (mole per 100 mole total fatty acids).

Migration and in vitro invasion assay

Cell migration and invasiveness were analyzed as previously described [19] in 24-well plates receiving cell culture inserts of polyethylene terephthalate membranes of 8-μm pore size, covered (invasion), or not (migration), with a film of Matrigel™ matrix. Inserts for migration (ref. 353097) and invasion (ref. 354480) assays were from BD biosciences (France).

Measurement of intracellular pH recovery

Cells were incubated for 30 min at 37 °C in Hank's medium (Sigma-Aldrich, France) containing 2 mM BCECF-AM (2′,7′-bis-(2-carboxyethyl)-5-(6)-carboxyfluorescein; excitation 503/440 nm; emission 530 nm). H^+ efflux was measured as previously described [20]: Cells acidified with NH_4Cl pulse-wash were resuspended in a sodium-free solution. The subsequent addition of 130 mM NaCl (indicated by the arrow) in shCTL or shPPARβ cells generated H^+ effluxes mostly (≥90 %) attributed to NHE-1 [11]. The relative H^+ effluxes were determined in shCTL or shPPARβ after 5 days of treatment with solvent control (CTL) or DHA.

Epifluorescence imaging

Gelatinolytic activity was assessed by culturing cells for 24 h on a planar Matrigel™ matrix (Invitrogen, France) containing 25 μg/mL DQ-Gelatin® (Thermo Fischer Scientific, France). Epifluorescence microscopy was performed with a Nikon TI-S microscope and analysed using both NIS-BR software (Nikon, France) and ImageJ© software 1.38I (http://rsbweb.nih.gov/ij) as previously described [19].

Transfection and transactivation assays

SiRNA (4 nM), expression vector for PPARβ (pSG5-PPARβ, 50 ng; overexpressed PPARβ), or corresponding empty vector pSG5 (Stratagene) used as control expression vector (CTL) were transfected using Lipofectamine RNAi max (Invitrogen, Illkirch, France) 48 h prior to migration, invasion, DQ-gelatin tests, or RNA extraction as previously described [42].

Statistical analysis

GraphPad Prism4 was used for all statistical analyses. Data of patch-clamp are displayed as mean±standard error of the mean (n=number of cells/experiments). Statistical significance at $*p<0.05$, $**p<0.01$, and $***p<0.001$ was determined using a Mann–Whitney test.

Results

DHA reduced $nNa_V1.5$ current and $nNa_V1.5$-dependent cell invasiveness

DHA inhibits $nNa_V1.5$ expression and breast cancer cell migration [24] as well as $Na_V1.5$ sodium currents from $aNa_V1.5$ channels overexpressed in HEK293 [33, 44]. However, the potential effects of DHA on $nNa_V1.5$ current in breast cancer cell and $nNa_V1.5$-dependent cell invasiveness have not been reported so far. We initially tested by patch-clamp the effect of acute DHA treatments on $nNa_V1.5$-dependent currents elicited by depolarizing pulses in MDA-MB-231 cells. Such currents are involved in MDA-MB-231 breast cancer cell

invasiveness [19]. As shown on Fig. 1a and b, DHA (10 μM) brought under the form of a methyl ester had no significant effect on peak sodium currents as compared to a control condition (CTL) containing the same final volume of the vehicle (0.1 % ethanol). Other forms of DHA (ethyl ester and sodium salt) and higher concentrations of all three forms up to 30 μM were also tested but had no further effects (data not shown). These results obtained in cancer cells endogenously expressing $nNa_V1.5$ differ from currents recorded from aNaV1.5 channels overexpressed in HEK293 [33, 44].

We then tested whether the $nNa_V1.5$ activity (I_{Na} inward sodium current measured under depolarizing steps from a holding potential of −100) was modified by a 7 days treatment with DHA (1 μM) or oleic acid (OA, 18:1n-9; 1 μM) used as a fatty acid control (Fig. 1c). Dose-dependent analyses of DHA effects on MDA-MB-231 cells have previously been published [4, 5, 29] and doses ≤1 μM reduced $Na_V1.5$ expression [24], but not cell proliferation (n=11) (Fig. 1f). Although cell migration was previously reported to be reduced by DHA (0.5 μM) [24], this was not the case in our previous studies [10, 19, 35] and in our experimental conditions (n=9) (Fig. 1g). Oleic acid did not alter cell growth (Fig. 1f), migration (Fig. 1g), or invasiveness (Fig. 1h). I_{Na} was reduced from −14.7 to −6.5 pA/pF when cells were grown with DHA (1 μM; p<0.05; n=9), but not with oleic acid (ns; n=10), proving the inhibition of $Na_V1.5$ activity by DHA in MDA-MB-231 cells (Fig. 1c). Activation-voltage and availability-voltage relationships of I_{Na} currents were studied as previously indicated [19]. There was no difference between the activation-voltage relationships in the three conditions tested: The 1/2-activation voltages ($V_{1/2}$-activation) were −32.5±1.6; −31.8±1.5; and −31.9±1.9 for conditions CTL, OA, and DHA, respectively (Fig. 1d). In comparison, the availability-voltage relationship of I_{Na} in the DHA treatment was shifted rightward with a $V_{1/2}$-inactivation of −59.2±3.4 mV (p<0.05) compared to the CTL ($V_{½}$-inactivation, −68.3±2.1 mV) or OA ($V_{1/2}$-inactivation, −67.7±2.1 mV) conditions (Fig. 1d). These results showed that the incorporation of DHA into membrane phospholipids, in both raft and non-raft membrane fractions (Fig. 1e), unexpectedly changed the availability properties of the $nNa_V1.5$ channel, i.e., a slight increase in the window current between −60 and −10 mV. They also suggested that the main effect of DHA was a reduction of the total number of channels expressed at the plasma membrane, possibly due to a transcriptional regulation of *SCN5A*.

Treatments with DHA for 7 days and tetrodotoxin (TTX, 30 μM), a potent inhibitor of $nNa_V1.5$ [19], for 24 h inhibited invasiveness by 19.2±4.0 and 23.1±8.9 %, respectively (p<0.05; n=9) (Fig. 1h). Furthermore, there was no cumulative effect of the DHA + TTX co-treatment (−28.1±4.7 %, n=9) (Fig. 1h), suggesting that the $nNa_V1.5$-dependent part of invasiveness can be inhibited by DHA.

Fig. 1 Chronic DHA treatment reduced $nNa_V1.5$ current and $nNa_V1.5$-dependent cell invasiveness. **a** Representative traces of whole-cell recordings and associated **b** I_{Na} -voltage relationships, obtained by eliciting depolarizing pulses from a holding potential of −100 mV to voltage steps ranging from −90 to +60 mV (10 mV increments) from MDA-MB-231 cancer cells submitted to an acute (20 min) application of DHA (10 μM, n=8) and compared to a control condition (CTL, containing the same final volume of the vehicle ethanol, n=7). **c** Ethanol (solvent CTL, n=16), oleic acid (OA, 1 μM, n=10), or DHA (1 μM, n=9) were applied once a day, and media were changed every day for 7 days prior to measuring $nNa_V1.5$ currents (I_{Na}) in the whole-cell configuration of patch-clamp in voltage-clamp mode [19]. I_{Na}-voltage relationships, in the three conditions tested, are shown. **d** Activation-voltage and availability-voltage relationships of I_{Na} currents were studied as previously indicated [19]. There was no difference between the activation-voltage relationships in the three conditions tested (round symbols) ($V_{1/2}$-activation were −32.5±1.6; −31.8±1.5; and −31.9±1.9 for conditions CTL, OA, and DHA, respectively). The availability-voltage relationship of I_{Na} in the DHA treatment was shifted rightward ($V_{1/2}$-inactivation, −59.2±3.4 mV, p<0.05) compared to the CTL ($V_{1/2}$-inactivation, −68.3±2.1 mV) or OA ($V_{1/2}$-inactivation, −67.7±2.1 mV) conditions (square symbols). **e** The DHA content in phospholipids extracted from raft and non-raft membrane fractions of MDA-MB-231 cells submitted to a 7-day-long treatment with DHA 1 μM (DHA) was quantified and compared to a control treatment (CTL, ethanol) and expressed as the percentage of total fatty acids in phospholipids (n=3). **f** MDA-MB-231 cells were treated with increasing concentrations of OA (n=4) and DHA (up to 100 μM, n=11) and cell growth was measured by MTT assay [42]. **g** Cell migration (n=9) or **h** cell invasiveness (n=9) were evaluated after treatment with TTX (30 μM), OA (1 μM), DHA (1 μM), or combination of DHA with TTX. Statistical significance at *p<0.05 (compared to cells treated with solvent control, CTL) was determined using Mann–Whitney test

PPARβ displayed a pro-invasive effect

We hypothesized that such an effect of DHA might be regulated by PPARβ which was also previously reported to intervene in the invasiveness, but not in the migration of breast cancer cells [1]. PPARβ is significantly expressed in MDA-MB-231 cells [48] and DHA reduces its mRNA expression [42]. We used siRNA transient transfection to determine the involvement of PPARβ in breast cancer cell invasiveness. SiPPARβ reduced by 84±1.9 % the expression of PPARβ mRNA (p<0.001; n=4) compared to siCTL (Fig. 2a, top) in experimental conditions for which cell proliferation remained unaffected [42]. MDA-MB-231 cell migration also remained unaffected by siPPARβ (n=4; ns) (Fig. 2b, top), which is consistent with the recent results obtained with pharmacological ligands of PPARβ [1]. Cell invasiveness was significantly reduced by 47±6.2 % with siPPARβ (n=4; p<0.01) compared to siCTL (Fig. 2a, middle). In addition, siPPARβ reduced by 41±7.5 % the release of the fluorescent product characteristic of DQ-gelatin® proteolytic cleavage (Fig. 2b, middle) compared to siCTL, confirming weaker ECM degradation and invasion capabilities upon suppression of PPARβ mRNA. Overexpression of functional PPARβ, performed as previously described [42], increased cell invasiveness by 223 ±28.2 % (p<0.01, n=3) (Fig. 2b, bottom). A PPARβ

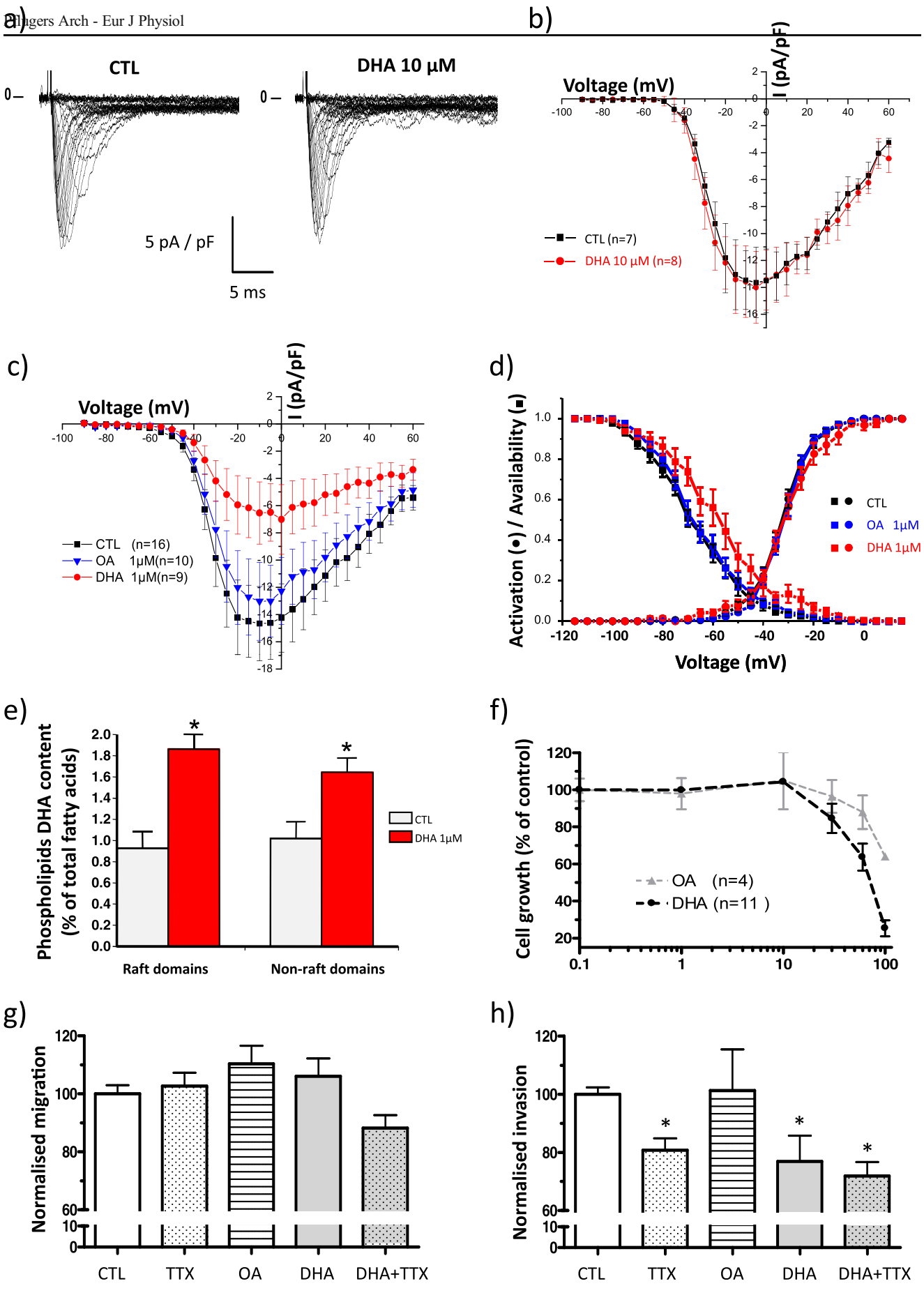
a)
CTL
DHA 10 µM
0
0
5 pA / pF
5 ms
b)
Voltage (mV)
I (pA/pF)
CTL (n=7)
DHA 10 µM (n=8)
c)
Voltage (mV)
I (pA/pF)
CTL (n=16)
OA 1µM(n=10)
DHA 1µM(n=9)
d)
Activation (•) / Availability (■)
Voltage (mV)
CTL
OA 1µM
DHA 1µM
e)
Phospholipids DHA content (% of total fatty acids)
CTL
DHA 1µM
Raft domains
Non-raft domains
f)
Cell growth (% of control)
OA (n=4)
DHA (n=11)
g)
Normalised migration
CTL
TTX
OA
DHA
DHA+TTX
h)
Normalised invasion
CTL
TTX
OA
DHA
DHA+TTX

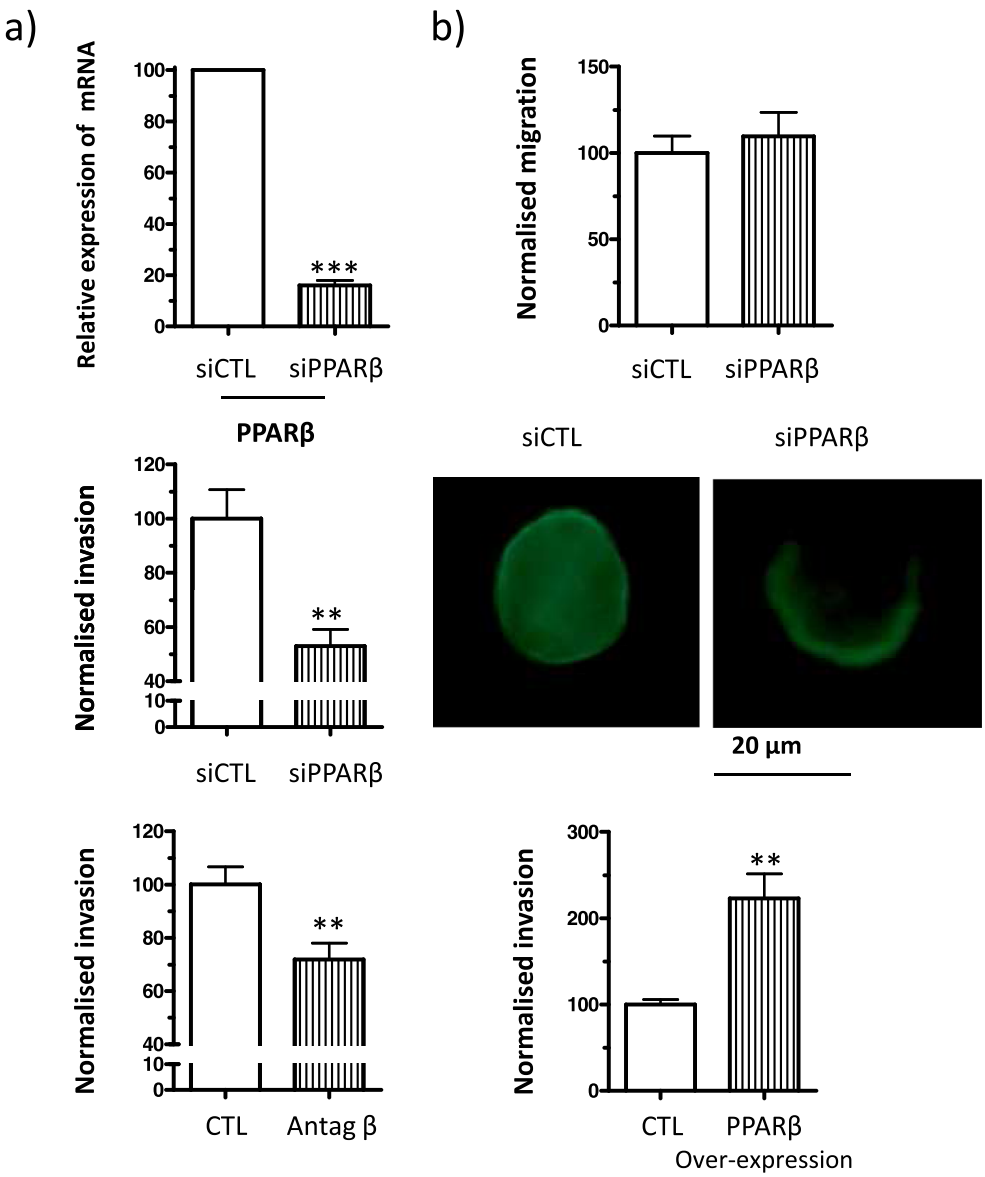

Fig. 2 Pro-invasive effects of PPARβ. **a** MDA-MB-231 cells were transfected (n=4) with siRNA directed against PPARβ (siPPARβ) or scramble siRNA (siCTL), 48 h prior to RNA extraction, migration, invasion, or DQ-gelatin tests. PPARβ mRNA expression (*top panel*) was assessed by RTqPCR and expressed relatively to HPRT1 mRNA expression and control condition (100 %) as relative quantity $Q=2^{-\Delta\Delta Ct}$. Cell invasiveness was evaluated after siRNA transfection (*middle panel*; n=4) or after treatment with PPARβ antagonist (1 μM; Antag β, *bottom panel*; n=3). **b** After siRNA transfection, cell migration (*top panel*; n=4) and proteolytic cleavage of DQ gelatin® (*middle panel* representative of three individual experiments) were evaluated, as well as cell invasiveness (*bottom panel*) after transfection (n=3) of expression vector for PPARβ (overexpressed PPARβ) or corresponding empty vector (CTL) [42]. Statistically different from cells treated with solvent control (CTL) or cells transfected with siCTL or empty vector at $^{**}p<0.01$ or $^{***}p<0.001$

antagonist (GSK0660 [37] previously used at the non-cytotoxic dose of 1 μM [42], Antag β) also reduced cell invasiveness by 28.2±6.2 % ($p<0.01$, n=3) (Fig. 2a, bottom), confirming the pro-invasive effect of PPARβ.

Reduction of PPARβ mRNA expression reduced both nNa$_V$1.5 expression and function

We examined whether reduction of PPARβ-dependent invasiveness involved regulation of nNa$_V$1.5 and NHE-1 expressions in MDA-MB-231 cells transfected transiently with siPPARβ or expressing permanently a shPPARβ. ShPPARβ suppressed the expression of PPARβ mRNA by 60.5±4.7 % ($p<0.001$, n=10, data not shown). Western blotting confirmed the inhibition of PPARβ expression with siPPARβ (Fig. 3a, top) and shPPARβ (Fig. 3b, top). In addition to reducing Na$_V$1.5 protein levels (Fig. 3a, top), siPPARβ led to a decrease in the expression of Na$_V$1.5 mRNA by 28.9± 6.8 % ($p<0.001$; n=9) (Fig. 3a, middle) but not that of NHE-1 mRNA (Fig. 3a, bottom). Similarly, shPPARβ reduced the expression of nNa$_V$1.5 mRNA by 51.4± 3.8 % ($p<0.01$; n=9) (Fig. 3b, middle) and nNa$_V$1.5 proteins (Fig. 3b, top). Not surprisingly, shPPARβ did not reduce the expression of NHE-1 mRNA (Fig. 3b, bottom) and this is consistent with our previous work showing that siNa$_V$1.5 reduced NHE-1 efficacy without altering NHE-1 expression [11].

Analyses of I_{Na}-voltage relationships indicated that silencing PPARβ reduced the amplitude of nNaV1.5-mediated sodium currents (Fig. 3c, top), while no effect was observed on both activation- and availability-

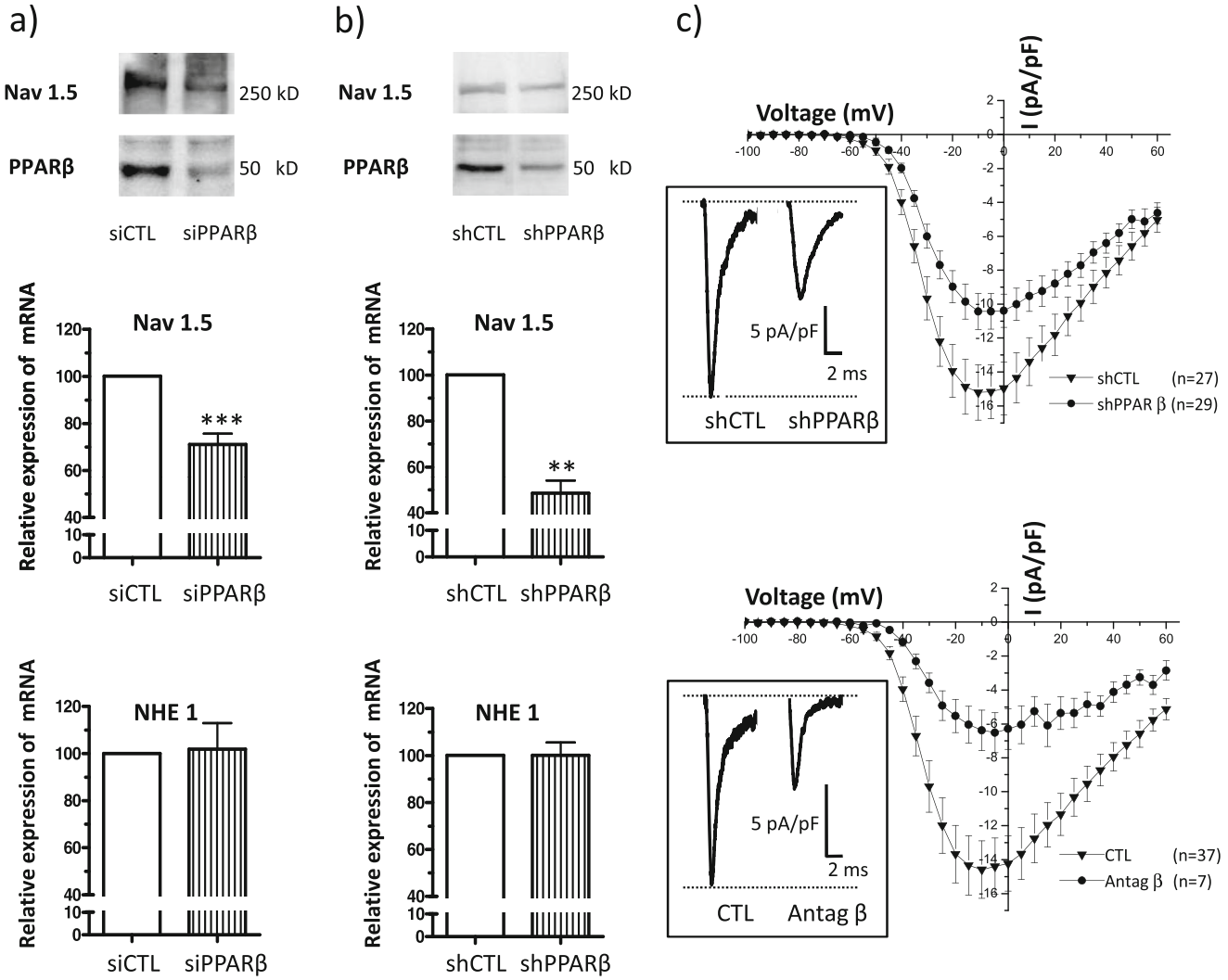

Fig. 3 Reduction of PPARβ mRNA expression led to the decrease of $Na_V1.5$ mRNA expression and $Na_V1.5$ current density (I_{Na}). **a** MDA-MB-231 cells were transfected with siPPARβ or siCTL (n=9). **b** Cells were transduced for permanent expression of shPPARβ or shCTL. Western blots with PPARβ and $Na_V1.5$ antibodies are representative of at least three individual experiments and $Na_V1.5$ and NHE-1 mRNA relative expressions were assessed by RTqPCR (n=9) as previously described [11, 19, 42]. **c** I_{Na}-voltage relationships were compared by patch-clamp in shPPARβ (n=29) versus shCTL (n=27) cells, and in shCTL cells treated with PPARβ antagonist GSK0660 (1 μM) for 5 days (Antag β; n=7) versus shCTL cells treated with solvent control (CTL; n=37). Insets, representative I_{Na} currents recorded for a voltage step from −100 to −5 mV. Statistically different from cells treated with solvent control (CTL), cells transfected with siCTL or shCTL at $^{**}p<0.01$ or $^{***}p<0.001$

voltage relationships (Supplementary Fig. S1). Indeed, I_{Na}, measured for a depolarizing step from −100 to −5 mV, was reduced from −15.5 pA/pF in shCTL cells (n=27) to −10.4 pA/pF in shPPARβ cells ($p<0.05$; n=29) (Fig. 3c, top) indicating a reduction of $nNa_V1.5$ activity at the plasma membrane of shPPARβ cells due to a reduction in $nNa_V1.5$ gene expression. Similarly, I_{Na} was also reduced in shCTL cells from −14.6 pA/pF (n=37 for CTL treatment) to −6.5 pA/pF with the PPARβ antagonist treatment ($p<0.05$; n=7; Fig. 3c, bottom). Taken together, these results show for the first time that inhibition of PPARβ reduced $nNa_V1.5$ functionality in breast cancer cells.

DHA, or reduction of PPARβ expression, reduced H^+ efflux

We hypothesized that H^+ efflux, mainly dependent on NHE-1 and regulated by $nNa_V1.5$ activity in the highly invasive MDA-MB-231 cells [10, 11], might be altered by treatments with the anti-invasive DHA (Fig. 1) and/or suppression of the pro-invasive PPARβ (Fig. 2), which both reduced $nNa_V1.5$ expression [24] (Fig. 3) and $nNa_V1.5$ currents (Fig. 1). Proton effluxes were assessed in shCTL and shPPARβ cells that were acidified by NH_4Cl pulse-wash then resuspended in a sodium-free solution. The subsequent addition of 130 mM NaCl generated H^+ effluxes and was used as a control condition.

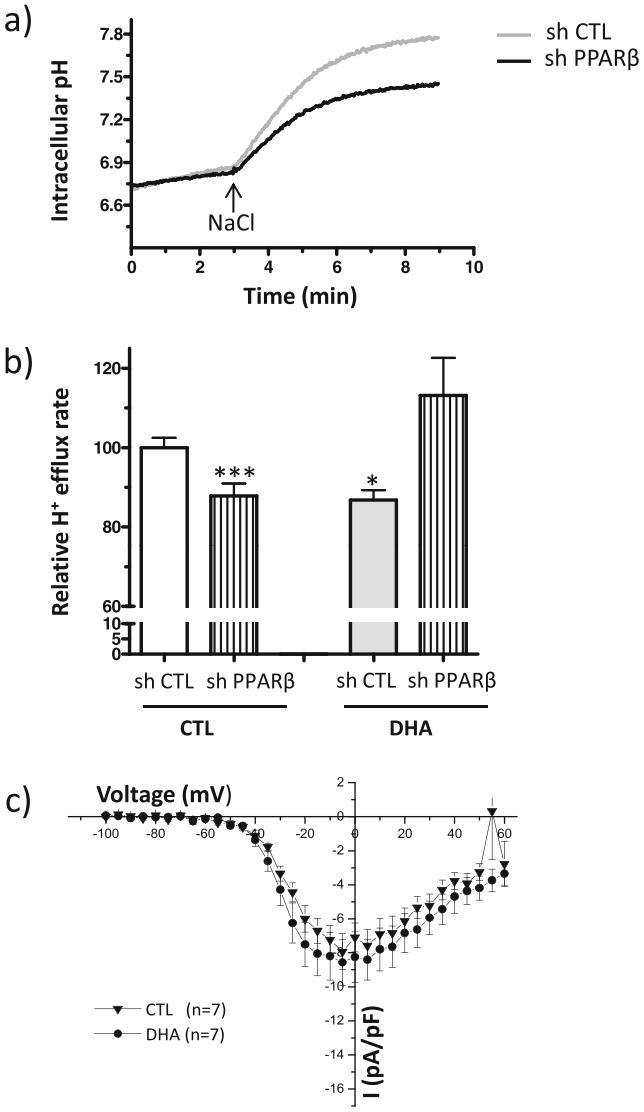

Fig. 4 DHA reduced NHE-1 activity similarly to suppression of PPARβ. **a** Cells acidified with NH_4Cl pulse-wash were resuspended in a sodium-free solution and subsequent addition of 130 mM NaCl (indicated by the arrow) in shCTL or shPPARβ cells generated H^+ effluxes attributed to NHE-1 [11]. **b** The relative H^+ effluxes were determined in shCTL or shPPARβ after a 5-day treatment with solvent control (CTL; n=7) or DHA (1 μM; n=4). **c** I_{Na}-voltage relationships were compared by patch-clamp in shPPARβ cells treated with solvent control (CTL; n=7) or DHA (1 μM; n=7). Statistically different from cells transfected with shCTL and treated with solvent control (CTL) at *p<0.05 or ***p<0.001

The NHEs inhibitor EIPA (5-N-ethyl-N-isopropyl amiloride, 10 μM), used as an internal experiment control, reduced H^+ effluxes by ~90 % (data not shown). Silencing PPARβ (shPPARβ) led to a 12.2±3.2 % reduction of H^+ efflux compared with the control condition (shCTL) (p<0,001, n=7; Fig. 4a, b). This is comparable to the reported reduction (19±8.0 %) of H^+ efflux obtained with si$Na_V1.5$ [11]. In similar experimental conditions, siNHE-1 reduced H^+ efflux by ~65 % without modifying $Na_V1.5$ expression or I_{Na}-voltage relationship [11]. We concluded that shPPARβ efficiently reduced NHE-1-dependent H^+ efflux by inhibiting the activity of $Na_V1.5$ channels.

DHA (1 μM) treatment reduced H^+ efflux in shCTL cells by 13.2±2.5 % (p<0.05; n=3; Fig. 4b), which is also comparable to si$Na_V1.5$ [11] or shPPARβ without DHA treatment (Fig. 4b). This reduction of H^+ efflux by DHA was abolished in shPPARβ cells (p<0.05, n=4; Fig. 4b). Furthermore, the reduction of n$Na_V1.5$ current by DHA (from −14.7 to −6.5 pA/pF; Fig. 1a) was no longer present in shPPARβ cells treated with DHA (−8.56 pA/pF; n=7) (Fig. 4c), compared to solvent control (−7.93 pA/pF; n=7) (Fig. 4c), proving that PPARβ is necessary for DHA to reduce n$Na_V1.5$ activity and H^+ efflux. These data show for the first time that, in the process of ECM invasion by breast cancer cells, H^+ efflux is a downstream target of DHA and PPARβ, through the regulation of $Na_V1.5$ expression and subsequent activity.

Discussion

In this study, performed in the highly invasive MDA-MB-231 breast cancer cells endogenously expressing n$Na_V1.5$ channels, we show for the first time that PPARβ suppression (performed by PPARβ antagonist or RNA interference) inhibits n$Na_V1.5$ channel expression and activity, as well as subsequent NHE-1-dependent H^+ efflux and ECM degradation, eventually leading to the reduction of breast cancer cells invasiveness. These data demonstrate that H^+ efflux is a downstream target of DHA and PPARβ through the regulation of $Na_V1.5$ expression and subsequent activity. We also show that DHA chronic treatment, but not the acute application, which suppresses PPAR mRNA expression [42], also inhibits n$Na_V1.5$ current and NHE-1 activity in breast cancer cells. This extends significantly the previous study showing that DHA inhibited n$Na_V1.5$ expression in breast cancer cells [24].

Several studies suggested that qualitative and quantitative changes in total dietary fat intake can positively impact breast cancer outcome, irrespective of genomic alterations that are the hallmarks of the disease [14]. DHA and EPA have emerged owing to their potential to increase cancer treatment efficacy without additional side effects [8, 13, 21]. Indeed, mammary tumor growth in different rodent models can be consistently reduced by DHA and/or EPA [22, 25, 28]. In a phase II study carried on breast cancer patients with severe metastatic disease, a diet enriched in those n-3 PUFA increased survival and chemotherapy efficacy [7]. Randomized double-blind phase III studies, including ours, testing DHA supplementation in breast cancer patients under chemotherapy are currently being conducted (ClinicalTrials.gov identifiers: NCT01849250 and NCT01548534), hence the necessity to better understand its

mechanisms of action. DHA treatment inhibits breast cancer cell growth in vitro and invasiveness in vitro and in vivo but its effects are multiple and at least at two different levels [8, 13]. DHA is a ligand of the nuclear receptors PPAR [17, 30, 41, 45], modulating the expression of numerous genes [2, 49], and DHA can modify the activity of transmembrane proteins by incorporating into cell membrane phospholipids of proliferating cancer cells (Fig. 1e) and in tumor tissues [15, 16]. In this study, we found that DHA chronic treatments were responsible for an inhibition of *SCN5A* mRNA and protein expression, and a decrease in $nNa_V1.5$ protein levels at the plasma membrane. As a consequence of this decrease, the invasiveness is significantly reduced, and this prevails over an expected increase in invasiveness due to the slight rightward shift observed in the steady-state availability-voltage relationship (Fig. 1d).

Our results are in apparent contradiction with the studies which showed an acute effect of DHA or EPA on $Na_V1.5$ currents in HEK293 cells overexpressing the adult splice variant of *SCN5A* [33, 44] and which suggested a direct interaction of n-3 PUFAs with a single amino acid residue N406 located in the segment 6 of domain I (DIS6) of the protein [43]. However, in those studies, currents were analyzed from adult splice variants of the *SCN5A* gene. In breast tumors, as well as in MDA-MB-231 breast cancer cells, the SCN5A gene is expressed under a neonatal splice variant [18] with a substitution of 7-amino acid in the segments 3 and 4 of domain I (DI-S3-S4) of the protein [31]. This change in the peptidic sequence of domain I might interfere with PUFAs binding to the channel and be responsible for these discrepancies.

Since using pharmacological inhibitors for the direct inhibition of $Na_V1.5$ channels would greatly interfere with nervous and cardiac functions, reducing the mRNA expression of its neonatal splice variant in invasive cancer cells with DHA, through PPARβ, might become an important alternative pathway to block breast cancer cell invasiveness. The nuclear receptor PPAR are the transcription factors binding to PPRE in promoters of the genes they regulate [32]. Although *SCN5A* promoter has not been studied in cancer cells, two regions displaying promoter activity for *SCN5A* in cardiac cells have been described: a 4.0 kb sequence in the region of exon 1 [36, 47] and a 1.5 kb sequence upstream of exon 2 [36], the latter containing a 400 bp transcriptional regulatory sequence, named CNS28 [3]. The 4.0 kb sequence in the region of exon 1 and the 1.5 kb sequence in the region of exon 2 contain 10 and 7 putative PPRE, respectively (data not shown). These putative PPRE suggest that transcription of $Na_V1.5$ might be regulated by PPAR, and in turn potentially inhibited by DHA treatment, although testing this hypothesis in breast cancer cells is beyond the scope of the present study. It is worth noting that the NHE-1 gene (*SLC9A1*) has two PPRE motifs in its promoter region [40] and that PPARγ agonists (glitazones) reduced its expression in breast cancer cell lines and in breast tumor tissues [26].

Our data showing that DHA treatment inhibits $nNa_V1.5$ current, and NHE-1 activity (and breast cancer cell invasiveness as reported by others [5, 29]) agrees with, and extend, Isbilen et al. (2006) published work showing that DHA inhibited $nNa_V1.5$ mRNA and protein expression [24]. However, we did not observe that cell migration was reduced by DHA. This discrepancy might be due to differences in the experimental approaches: for example, Isbilen et al. (2006) used 12-μm pore size membranes for migration assays while we used 8-μm pore size. Isbilen et al. (2006) used DHA in Na^+ salt solubilized in cell culture medium (0.5 μM) and filtered while we used DHA methyl ester, purified by thin layer chromatography, quantified by gas chromatography [4], dissolved in 100 % ethanol, and used at 1 μM in cell culture medium. In our conditions, we measured that DHA was efficiently incorporated in membrane phospholipids. In addition, we never observed any effect of TTX on cancer cell migration in our experimental conditions [10, 19, 34, 35]. Furthermore, the absence of difference in cell migration under DHA methyl ester treatment is consistent with the absence of change in cell migration under siPPARβ, which is itself consistent with recent results obtained with pharmacological ligands of PPARβ [1]. However, it is worth noting that PPARβ regulates migration of keratinocytes [39] and vascular smooth muscle cells [27]. It is, therefore, possible that a better understanding of the molecular effectors of PPARβ in cell migration, under comparable experimental conditions, might shed some light on the apparent discrepancy obtained by DHA on breast cancer cell migration.

Conclusion

On the one hand, DHA treatment displays a weak agonist property in PPARβ reporter gene assay and DHA-induced inhibition of MDA-MB-231 growth can be abolished by a PPARβ antagonist [42], consistent with the proposal [48] that PPARβ agonists might be used in breast cancer. On the other hand, DHA displays anti-inflammatory effects [23] and inhibits the expression of PPARβ [42] which has been reported to be pro-inflammatory in a breast cancer context [49]. This would advocate for the use of a PPARβ inverse agonist or antagonist [1, 38]. The present study suggests that underexpressing $nNa_V1.5$ or PPARβ in breast cancer cells would greatly reduce metastases development, and that DHA treatment should even amplify this effect. Although further experimental work is obviously required to fully understand the role (s) of PPARβ and select its appropriate pharmacological ligand in cancer cells, our study shows for the first time that PPARβ is necessary for DHA to reduce $nNa_V1.5$ activity and H^+ efflux and that reducing $nNa_V1.5$/NHE-1 activities in

invasive cancer cells with natural n-3 PUFA, such as DHA, might become a relevant strategy to block metastasis. We conclude that this in vitro study provides with a direct link between DHA, PPARβ, $Na_V1.5$ current, and NHE-1 pro-invasive activities in breast cancer cells expressing endogenously $Na_V1.5$ channels.

Acknowledgments The authors thank Isabelle Domingo and the UTTIL platform of Tours' Hospital for technical help. This work was supported by the "Région Centre" of FRANCE (fellowships of Emeline Bon and Julie Chamouton; LIPIDS project of ARD2020 Biomédicaments), the "Ligue Nationale Contre le Cancer" (committees of Charente, Indre et Loire, Mayenne and Morbihan), the Association "CANCEN" and Tours' Hospital oncology association ACORT (fellowship of Ramez Wannous).

References

1. Adhikary T, Brandt DT, Kaddatz K, Stockert J, Naruhn S, Meissner W, Finkernagel F, Obert J, Lieber S, Scharfe M, Jarek M, Toth PM, Scheer F, Diederich WE, Reinartz S, Grosse R, Muller-Brusselbach S, Muller R (2013) Inverse PPARbeta/delta agonists suppress oncogenic signaling to the ANGPTL4 gene and inhibit cancer cell invasion. Oncogene 32:5241–5252. doi:10.1038/onc.2012.549
2. Adhikary T, Kaddatz K, Finkernagel F, Schonbauer A, Meissner W, Scharfe M, Jarek M, Blocker H, Muller-Brusselbach S, Muller R (2011) Genomewide analyses define different modes of transcriptional regulation by peroxisome proliferator-activated receptor-beta/delta (PPARbeta/delta). PLoS One 6(1):e16344. doi:10.1371/journal.pone.0016344
3. Atack TC, Stroud DM, Watanabe H, Yang T, Hall L, Hipkens SB, Lowe JS, Leake B, Magnuson MA, Yang P, Roden DM (2011) Informatic and functional approaches to identifying a regulatory region for the cardiac sodium channel. Circ Res 109:38–46. doi:10.1161/CIRCRESAHA.110.235630
4. Barascu A, Besson P, Le Floch O, Bougnoux P, Jourdan ML (2006) CDK1-cyclin B1 mediates the inhibition of proliferation induced by omega-3 fatty acids in MDA-MB-231 breast cancer cells. Int J Biochem Cell Biol 38:196–208. doi:10.1016/j.biocel.2005.08.015
5. Blanckaert VU, L. Mimouni, V. Antol, J. Brancquart, L. Chénais, B (2010) Docosahexaenoic acid intake decreases proliferation, increases apoptosis and decreases the invasive potential of the human breast carcinoma cell line MDA-MB-231. Int J Oncol 36. doi:10.3892/ijo_00000549
6. Bligh EG, Dyer WJ (1959) A rapid method of total lipid extraction and purification. Can J Biochem Phys 37:911–917
7. Bougnoux P, Hajjaji N, Ferrasson MN, Giraudeau B, Couet C, Le Floch O (2009) Improving outcome of chemotherapy of metastatic breast cancer by docosahexaenoic acid: a phase II trial. Brit J Cancer 101:1978–1985. doi:10.1038/sj.bjc.6605441
8. Bougnoux P, Hajjaji N, Maheo K, Couet C, Chevalier S (2010) Fatty acids and breast cancer: sensitization to treatments and prevention of metastatic re-growth. Prog Lipid Res 49:76–86. doi:10.1016/j.plipres.2009.08.003
9. Brackenbury WJ (2012) Voltage-gated sodium channels and metastatic disease. Channels 6:352–361. doi:10.4161/chan.21910
10. Brisson L, Driffort V, Benoist L, Poet M, Counillon L, Antelmi E, Rubino R, Besson P, Labbal F, Chevalier S, Reshkin SJ, Gore J, Roger S (2013) NaV1.5 Na (+) channels allosterically regulate the NHE-1 exchanger and promote the activity of breast cancer cell invadopodia. J Cell Sci 126:4835–4842. doi:10.1242/jcs.123901
11. Brisson L, Gillet L, Calaghan S, Besson P, Le Guennec JY, Roger S, Gore J (2011) Na (V) 1.5 enhances breast cancer cell invasiveness by increasing NHE1-dependent H (+) efflux in caveolae. Oncogene 30:2070–2076. doi:10.1038/onc.2010.574
12. Calaghan S, Kozera L, White E (2008) Compartmentalisation of cAMP-dependent signalling by caveolae in the adult cardiac myocyte. J Mol Cell Cardiol 45:88–92. doi:10.1016/j.yjmcc.2008.04.004
13. Chevalier S, Goupille C, Mahéo K, Domingo I, Dussiau C, Renoux B, Bougnoux P, Papot S (2010) Dietary docosahexaenoic acid proposed to sensitize breast tumors to locally delivered drug. Clin Lipidol 5:233–243. doi:10.2217/clp.10.12
14. Chlebowski RT, Blackburn GL, Thomson CA, Nixon DW, Shapiro A, Hoy MK, Goodman MT, Giuliano AE, Karanja N, McAndrew P, Hudis C, Butler J, Merkel D, Kristal A, Caan B, Michaelson R, Vinciguerra V, Del Prete S, Winkler M, Hall R, Simon M, Winters BL, Elashoff RM (2006) Dietary fat reduction and breast cancer outcome: Interim efficacy results from the Women's Intervention Nutrition Study. J Nat Cancer Inst 98:1767–1776. doi:10.1093/jnci/djj494
15. Colas S, Germain E, Arab K, Maheo K, Goupille C, Bougnoux P (2005) Alpha-tocopherol suppresses mammary tumor sensitivity to anthracyclines in fish oil-fed rats. Nutr Cancer 51:178–183. doi:10.1207/s15327914nc5102_8
16. Colas S, Paon L, Denis F, Prat M, Louisot P, Hoinard C, Le Floch O, Ogilvie G, Bougnoux P (2004) Enhanced radiosensitivity of rat autochthonous mammary tumors by dietary docosahexaenoic acid. Int J Cancer 109:449–454. doi:10.1002/ijc.11725
17. Forman BM, Chen J, Evans RM (1997) Hypolipidemic drugs, polyunsaturated fatty acids, and eicosanoids are ligands for peroxisome proliferator-activated receptors alpha and delta. Proc Natl Acad Sci U S A 94:4312–4317
18. Fraser SP, Diss JK, Chioni AM, Mycielska ME, Pan H, Yamaci RF, Pani F, Siwy Z, Krasowska M, Grzywna Z, Brackenbury WJ, Theodorou D, Koyuturk M, Kaya H, Battaloglu E, De Bella MT, Slade MJ, Tolhurst R, Palmieri C, Jiang J, Latchman DS, Coombes RC, Djamgoz MB (2005) Voltage-gated sodium channel expression and potentiation of human breast cancer metastasis. Clin Cancer Res 11:5381–5389. doi:10.1158/1078-0432.CCR-05-0327
19. Gillet L, Roger S, Besson P, Lecaille F, Gore J, Bougnoux P, Lalmanach G, Le Guennec JY (2009) Voltage-gated sodium channel activity promotes cysteine Cathepsin-dependent invasiveness and colony growth of human cancer cells. J Biol Chem 284:8680–8691. doi:10.1074/jbc.M806891200
20. Gore J, Besson P, Hoinard C, Bougnoux P (1994) Na-W antiporter activity in relation to membrane fatty acid composition and cell proliferation. Am J Physiol 266:110–120
21. Hajjaji N, Bougnoux P (2012) Selective sensitization of tumors to chemotherapy by marine-derived lipids: a review. Cancer Treat Rev 39:473–488. doi:10.1016/j.ctrv.2012.07.001
22. Hardman WE, Avula CP, Fernandes G, Cameron IL (2001) Three percent dietary fish oil concentrate increased efficacy of doxorubicin against MDA-MB 231 breast cancer xenografts. Clin Cancer Res 7:2041–2049
23. Im DS (2012) Omega-3 fatty acids in anti-inflammation (pro-resolution) and GPCRs. Prog Lipid Res 51:232–237. doi:10.1016/j.plipres.2012.02.003
24. Isbilen B, Fraser SP, Djamgoz MB (2006) Docosahexaenoic acid (omega-3) blocks voltage-gated sodium channel activity and migration of MDA-MB-231 human breast cancer cells. Int J Biochem Cell Biol 38:2173–2182. doi:10.1016/j.biocel.2006.06.014
25. Jiang W, Zhu Z, McGinley JN, El Bayoumy K, Manni A, Thompson HJ (2012) Identification of a molecular signature underlying inhibition of mammary carcinoma growth by dietary N-3 fatty acids. Cancer Res 72:3795–3806. doi:10.1158/0008-5472.CAN-12-1047

26. Kumar AP, Quake AL, Chang MK, Zhou T, Lim KS, Singh R, Hewitt RE, Salto-Tellez M, Pervaiz S, Clement MV (2009) Repression of NHE1 expression by PPARgamma activation is a potential new approach for specific inhibition of the growth of tumor cells in vitro and in vivo. Cancer Res 69:8636–8644. doi:10.1158/0008-5472.CAN-09-0219
27. Lim HJ, Lee S, Park JH, Lee KS, Choi HE, Chung KS, Lee HH, Park HY (2009) PPAR delta agonist L-165041 inhibits rat vascular smooth muscle cell proliferation and migration via inhibition of cell cycle. Atherosclerosis 202:446–454. doi:10.1016/j.atherosclerosis.2008.05.023
28. Maheo K, Vibet S, Steghens JP, Dartigeas C, Lehman M, Bougnoux P, Gore J (2005) Differential sensitization of cancer cells to doxorubicin by DHA: a role for lipoperoxidation. Free Rad Biol Med 39:742–751. doi:10.1016/j.freeradbiomed.2005.04.023
29. Mandal CC, Ghosh-Choudhury T, Yoneda T, Choudhury GG, Ghosh-Choudhury N (2010) Fish oil prevents breast cancer cell metastasis to bone. Biochem Biophys Res Comm 402:602–607. doi:10.1016/j.bbrc.2010.10.063
30. Moraes LA, Piqueras L, Bishop-Bailey D (2006) Peroxisome proliferator-activated receptors and inflammation. Pharmacol Therap 110:371–385. doi:10.1016/j.pharmthera.2005.08.007
31. Onkal R, Djamgoz MB (2009) Molecular pharmacology of voltage-gated sodium channel expression in metastatic disease: Clinical potential of neonatal Nav1.5 in breast cancer. Eur J Pharmacol 625:206–219. doi:10.1016/j.ejphar.2009.08.040
32. Peters JM, Shah YM, Gonzalez FJ (2012) The role of peroxisome proliferator-activated receptors in carcinogenesis and chemoprevention. Nature Rev Cancer 12:181–195. doi:10.1038/nrc3214
33. Pignier C, Revenaz C, Rauly-Lestienne I, Cussac D, Delhon A, Gardette J, Le Grand B (2007) Direct protective effects of polyunsaturated fatty acids, DHA and EPA, against activation of cardiac late sodium current: a mechanism for ischemia selectivity. Basic Res Cardiol 102:553–564. doi:10.1007/s00395-007-0676-x
34. Roger S, Rollin J, Barascu A, Besson P, Raynal PI, Iochmann S, Lei M, Bougnoux P, Gruel Y, Le Guennec JY (2007) Voltage-gated sodium channels potentiate the invasive capacities of human non-small-cell lung cancer cell lines. Int J Biochem Cell Biol 39:774–786. doi:10.1016/j.biocel.2006.12.007
35. Roger S, Besson P, Le Guennec JY (2003) Involvement of a novel fast inward sodium current in the invasion capacity of a breast cancer cell line. Biochem Biophys Acta 1616:107–111. doi:10.1016/j.bbamem.2003.07.001
36. Shang LL, Dudley SC Jr (2005) Tandem promoters and developmentally regulated 5′- and 3′-mRNA untranslated regions of the mouse Scn5a cardiac sodium channel. J Biol Chem 280:933–940. doi:10.1074/jbc.M409977200
37. Shearer BG, Steger DJ, Way JM, Stanley TB, Lobe DC, Grillot DA, Iannone MA, Lazar MA, Willson TM, Billin AN (2008) Identification and characterization of a selective peroxisome proliferator-activated receptor beta/delta (NR1C2) antagonist. Mol Endocrinol 22:523–529. doi:10.1210/me.2007-0190
38. Stephen RL, Gustafsson MC, Jarvis M, Tatoud R, Marshall BR, Knight D, Ehrenborg E, Harris AL, Wolf CR, Palmer CN (2004) Activation of peroxisome proliferator-activated receptor delta stimulates the proliferation of human breast and prostate cancer cell lines. Cancer Res 64:3162–3170. doi:10.1158/0008-5472.CAN-03-2760
39. Tan NS, Icre G, Montagner A, Bordier-ten-Heggeler B, Wahli W, Michalik L (2007) The nuclear hormone receptor peroxisome proliferator-activated receptor beta/delta potentiates cell chemotactism, polarization, and migration. Mol Cell Biol 27:7161–7175. doi:10.1128/MCB.00436-07
40. Venkatachalam G, Kumar AP, Yue LS, Pervaiz S, Clement MV, Sakharkar MK (2009) Computational identification and experimental validation of PPRE motifs in NHE1 and MnSOD genes of human. BMC genomics 10 Suppl 3:S5. doi:10.1186/1471-2164-10-S3-S5
41. Wahli W, Michalik L (2012) PPARs at the crossroads of lipid signaling and inflammation. Trends Endocrinol Metab 23:351–363. doi:10.1016/j.tem.2012.05.001
42. Wannous R, Bon E, Maheo K, Goupille C, Chamouton J, Bougnoux P, Roger S, Besson P, Chevalier S (2013) PPARbeta mRNA expression, reduced by n-3 PUFA diet in mammary tumor, controls breast cancer cell growth. Biochem Biophys Acta 1831:1618–1625. doi:10.1016/j.bbalip.2013.07.010
43. Xiao YF, Ke Q, Wang SY, Auktor K, Yang Y, Wang GK, Morgan JP, Leaf A (2001) Single point mutations affect fatty acid block of human myocardial sodium channel alpha subunit Na+channels. Proc Natl Acad Sci U S A 98:3606–3611. doi:10.1073/pnas.061003798
44. Xiao YF, Ma L, Wang SY, Josephson ME, Wang GK, Morgan JP, Leaf A (2006) Potent block of inactivation-deficient Na+channels by n-3 polyunsaturated fatty acids. Am J Physiol Cell Physiol 290:C362–370. doi:10.1152/ajpcell.00296.2005
45. Xu HE, Lambert MH, Montana VG, Parks DJ, Blanchard SG, Brown PJ, Sternbach DD, Lehmann JM, Wisely GB, Willson TM, Kliewer SA, Milburn MV (1999) Molecular recognition of fatty acids by peroxisome proliferator-activated receptors. Mol Cell 3:397–403. doi:10.1016/S1097-2765(00)80467-0
46. Yang M, Kozminski DJ, Wold LA, Modak R, Calhoun JD, Isom LL, Brackenbury WJ (2012) Therapeutic potential for phenytoin: Targeting Na (v) 1.5 sodium channels to reduce migration and invasion in metastatic breast cancer. Breast Cancer Res Treat 134:603–615. doi:10.1007/s10549-012-2102-9
47. Yang P, Kupershmidt S, Roden DM (2004) Cloning and initial characterization of the human cardiac sodium channel (SCN5A) promoter. Cardiovasc Res 61:56–65. doi:10.1016/j.cardiores.2003.09.030
48. Yao PL, Morales JL, Zhu B, Kang BH, Gonzalez FJ, Peters JM (2014) Activation of peroxisome proliferator-activated receptor-beta/delta (PPAR-beta/delta) inhibits human breast cancer cell line tumorigenicity. Mol Cancer Therap 13:1008–1017. doi:10.1158/1535-7163.MCT-13-0836
49. Yuan H, Lu J, Xiao J, Upadhyay G, Umans R, Kallakury B, Yin Y, Fant ME, Kopelovich L, Glazer RI (2013) PPARdelta induces estrogen receptor-positive mammary neoplasia through an inflammatory and metabolic phenotype linked to mTOR activation. Cancer Res 73:4349–4361. doi:10.1158/0008-5472.CAN-13-0322

Emeline BON

Implication de la sous-unité β4 des canaux sodiques dépendants du voltage dans l'invasivité des cellules cancéreuses mammaires et régulation de son expression par l'acide docosahexaènoïque

Résumé

La perte de l'expression de la sous-unité β4 des canaux sodiques dépendants du voltage Na_V dans les tumeurs mammaires est associée à un grade cancéreux élevé et au développement des métastases. L'extinction de son expression dans les cellules MDA-MB-231 augmente de plus de deux fois leur invasivité. Au cours de cette thèse, nous avons montré que la sous-expression de β4 favorise la transition mésenchymato-amoeboïde et augmente l'invasion cancéreuse indépendante de Na_V. Cette transition se caractérise par l'acquisition d'une morphologie plus arrondie, par la présence de blebs à la surface cellulaire et par une augmentation de l'activité RhoA-GTPase. Cette transition est inhibée par la surexpression du domaine intracellulaire C-terminal de la sous-unité β4. L'expression de β4 peut être augmentée par un apport en acide docosahexaènoïque (22:6n-3), qui augmente l'activité du promoteur de son gène *SCN4B*. Le DHA augmente également l'expression de β4 en modulant l'expression des récepteurs nucléaires PPAR, sensibles aux lipides.

Mots clefs : β4, métastases, invasion, transition mésenchymato-amoeboïde, DHA, PPAR

Résumé en anglais

The loss of voltage gated sodium channel Na_Vβ4 subunit expression in breast cancer biopsies is associated with high grade tumors and metastatic development. The inhibition of β4 expression in MDA-MB-231 breast cancer cells enhanced their invasiveness by two fold. During this thesis, we have shown that β4 underexpression promotes mesenchymal-amoeboid transition and increases Na_V-independent invasion. This transition is characterized by rounded morphology, the presence of blebs at the cell surface and an increased RhoAGTPase activity. This transition is inhibited by β4 C-terminal intracellular domain overexpression. Expression of β4 can be enhanced by a DHA supplementation that increases the encoding *SCN4B* promoter activity. DHA also increases β4 expression through the modulation of PPARs lipid-sensitive nuclear receptors expression.

Key words: β4, metastasis, invasiveness, mesenchymal-amoeboid transition, DHA, PPAR